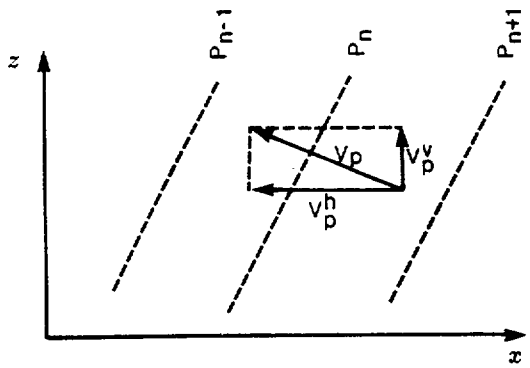

HYDRAULIC HEAD GRADIENT.
V_P - VELOCITY

+

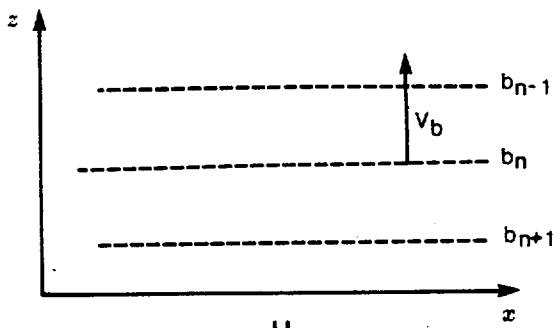

BUOYANCY GRADIENT.
V_b - VELOCITY

||

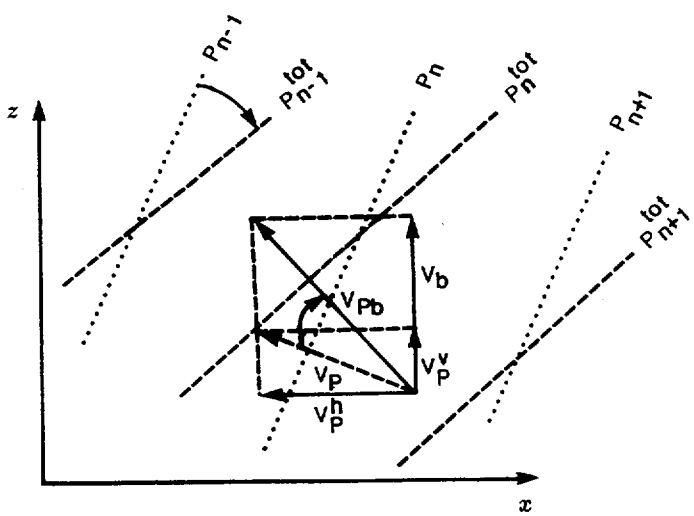

TOTAL HYDRAULIC GRADIENT.
V_{Pb} - VELOCITY

Total hydraulic gradient combines buoyancy and hydraulic head gradient.

890 8030304

~~[illegible]~~ - part 4

plate 3.4.2.-1

GOVERNING EQUATIONS

CONSERVATION OF FLUID MASS:

$$\phi\rho^f(c^f + c^r)p_{,t} - \phi\rho^f\beta T_{,t} - (\rho^f \frac{k}{\mu} ij(p_{,j} - \rho^f g_j))_{,i} = 0; \quad \text{AND}$$

CONSERVATION OF THERMAL ENERGY:

$$((\rho C)^* T)_{,t} - (\lambda^* T_{,i})_{,i} + (\rho^f C^f (\frac{k}{\mu} ij(p_{,j} - \rho^f g_j))T)_{,i} = 0.$$

EQUATIONS OF STATE

$$\rho^f = \rho^f(p, T), \quad \mu^f = \mu^f(p, T).$$

NOTE: FOR EXPLANATION OF SYMBOLS USED SEE PLATE 3.4.2-4.

Mathematical model for a simultaneous flow of heat and fluid. From Thunvik and Braester, 1982.

CONSERVATION OF FLUID MASS:

$$< \phi\rho^f (c^f + c^r) p_{,t} , \Psi_I > - < \phi\rho^f \beta T_{,t} , \Psi_I > - < (\rho^f \frac{k}{\mu} ij(p_{,j} - \rho^f g_j))_{,i} , \Psi_I >= 0: \quad \text{AND}$$

CONSERVATION OF THERMAL ENERGY:

$$< ((\rho C)^* T)_{,t}, \Psi_I > - < (\lambda^* T_{,i})_{,i} , \Psi_I > + < (\rho^f C^f (\frac{k}{\mu} ij(p_{,j} - \rho^f g_j)) T)_{,i} , \Psi_I >= 0$$

NOTE: FOR EXPLANATION OF SYMBOLS USED SEE PLATE 3.4.2-4.

Governing equations in the Galerkin finite element method. From Thunvik and Braester, 1982.

Symbol	Description
c	compressibility
C	specific heat capacity
g	acceleration of gravity
k	permeability
p	pressure
Q	heat flow rate
t	time
T	temperature
x_i	Cartesian coordinate
β	coefficient of thermal volume expansion of the fluid
λ	thermal conductivity
μ	dynamic viscosity
ϕ	porosity
Ψ	basis function

$$\langle f(x), g(x) \rangle = \int_V f(x)g(x)\, dv, \text{ inner product}$$

superscripts

f	fluid
r	rock
*	equivalent medium

subscripts

i,j	indices used for Cartesian tensor notation, repeated indices indicate summation over these indices (i=j=1,2,3)
	$p_{,t}$ partial time derivative of p
	$p_{,j}$ gradient of p
I	node index

Explanation of symbols used on Plate 3.4.2-2 and 3.4.2-3.

R_{ah} - RAYLEIGH NUMBER FOR A HORIZONTAL LAYER OF FLUID;

R_{act} - CRITICAL RAYLEIGH NUMBER FOR LONG TUBES;

R_{ap} - RAYLEIGH NUMBER FOR A FLUID IN HORIZONTAL LAYER OF POROUS MATERIAL;

R_{apc} - CRITICAL RAYLEIGH NUMBER FOR A FLUID IN HORIZONTAL LAYER OF POROUS MATERIAL;

R^2 - D'ARCY - RAYLEIGH NUMBER;

R_1^2 - FLOW MODIFIED D'ARCY - RAYLEIGH NUMBER;

R_c^1 - CRITICAL RAYLEIGH NUMBER FOR FLUID IN VERTICAL POROUS CHANNEL WITH "WEAK" THROUGH-FLOW;

R_{ac} - CRITICAL RAYLEIGH NUMBER FOR FLUID IN FAULTS AND FRACTURES;

R_a - IN-SITU RAYLEIGH NUMBER FOR FLUID IN FAULTS AND FRACTURES;

a - FAULT APERTURE OR WIDTH OF PERMEABLE FAULT ZONE;

G - GEOTHERMAL OR VERTICAL TEMPERATURE GRADIENT;

g - ACCELERATION OF GRAVITY;

k - PERMEABILITY OF POROUS OR FRACTURED MEDIUM;

L - THICKNESS OF HORIZONTAL LAYER OF POROUS MATERIAL;

T - TEMPERATURE;

ΔT - TEMPERATURE DIFFERENCE;

c_f - SPECIFIC HEAT OF FLUID;

α - COEFFICIENT OF THERMAL EXPANSION FOR FLUID;

β - COEFFICIENT OF VISCOSITY VARIATION;

ρf - FLUID DENSITY;

μ - FLUID VISCOSITY;

ν - FLUID KINEMETIC VISCOSITY;

λf - FLUID THERMAL DIFFUSIVITY;

λm - MEDIUM THERMAL DIFFUSIVITY;

γ - DIMENSIONLESS THROUGH-FLOW STRENGTH;

w_0 - THROUGH-FLOW VELOCITY

Explanation of mathematical notations used in Section 3.4.3.

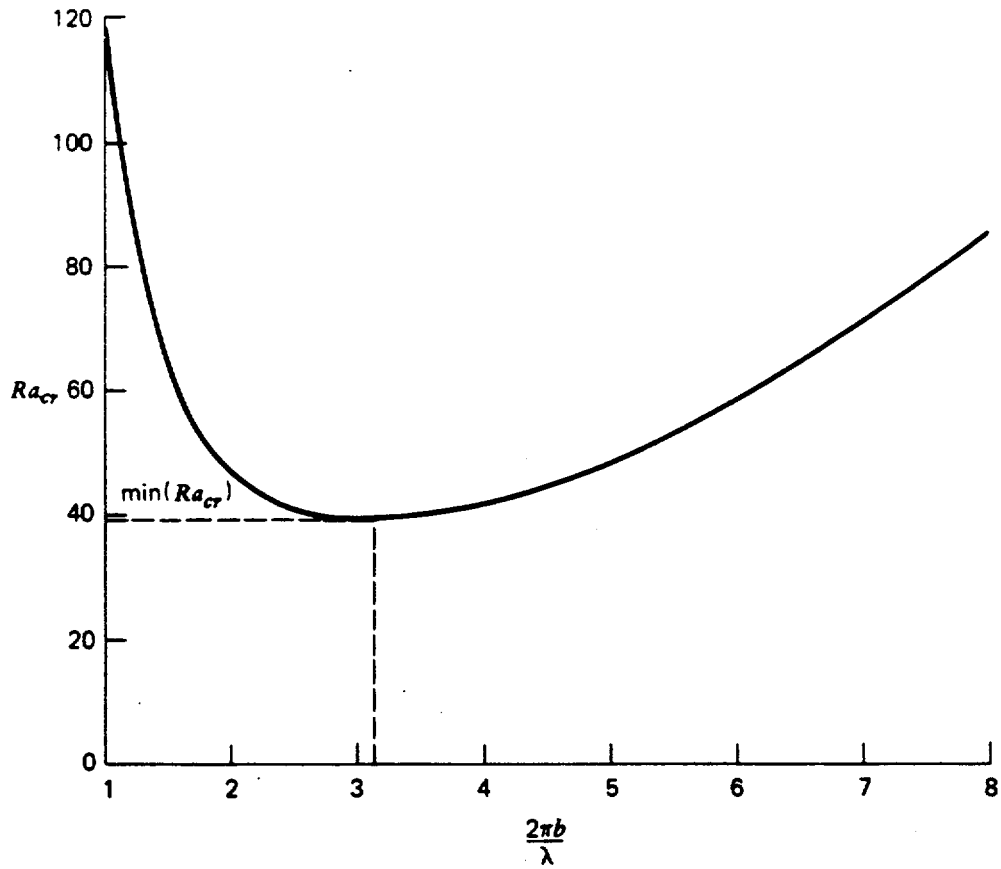

a) STABILITY LIMITS (RAYLEIGH NUMBER Ra_{cr}) FOR THE ONSET OF CONVECTION IN A POROUS MATERIAL AS A FUNCTION OF THE WAVELENGTH PARAMETER $\frac{2\pi b}{\lambda}$.

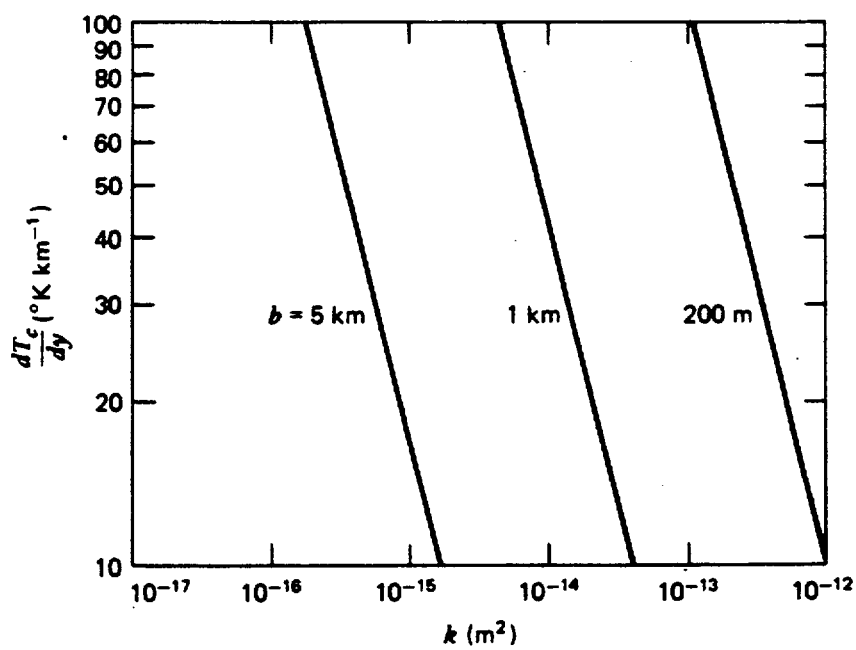

b) THE THERMAL GRADIENT REQUIRED FOR CONVECTION IN A POROUS MATERIAL AS A FUNCTION OF THE PERMEABILITY OF THE LAYER FOR DIFFERENT LAYER THICKNESSES.

Requirements for the onset of thermal convection in a porous medium. From Turcotte and Schubert, 1982.

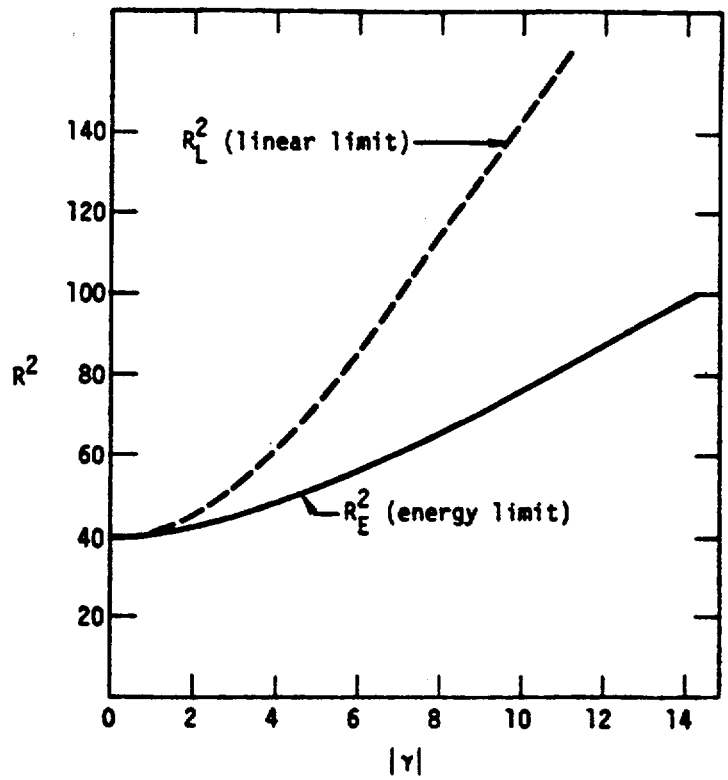

a) STABILITY LIMITS (THE D'ARCY - RAYLEIGH NUMBER R^2) FOR THE ONSET OF CONVECTION IN A POROUS MEDIUM WITH THE THROUGH-FLOW AS A FUNCTION OF DIMENSIONLESS FLOW STRENGTH PARAMETER. FROM HOMSY AND SHERWOOD, 1976.

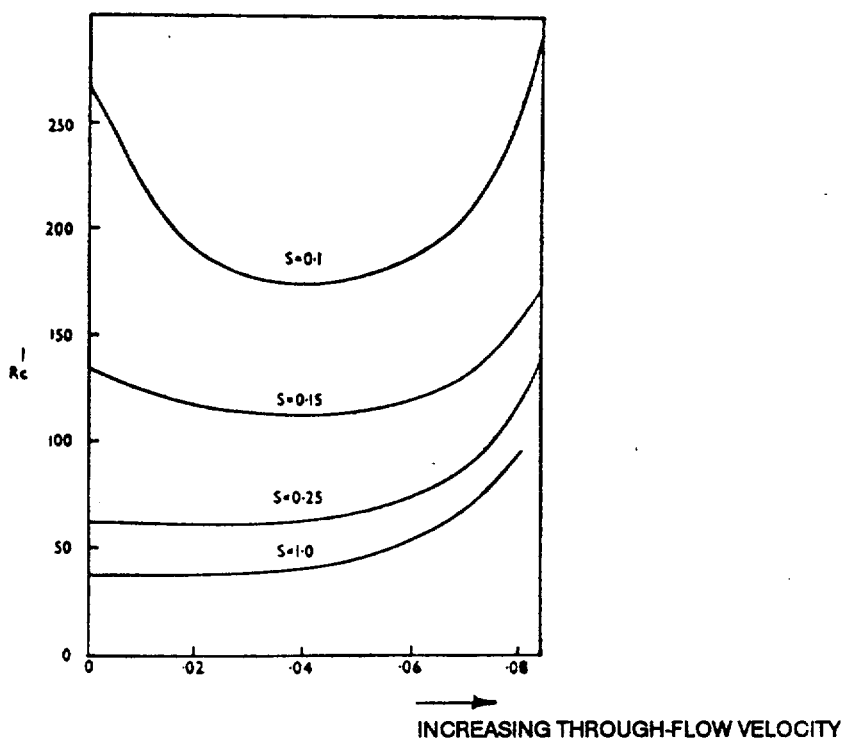

b) STABILITY LIMITS FOR THE ONSET OF CONVECTION, IN A POROUS CHANNEL WITH LOW INTENSITY THROUGH-FLOW, AS A FUNCTION OF THE ASPECT RATIO(S) AND OF THE THROUGH-FLOW VELOCITY. FROM SUTTON, 1970.

Requirements for the onset of thermal convection in a porous medium with consideration of through-flow.

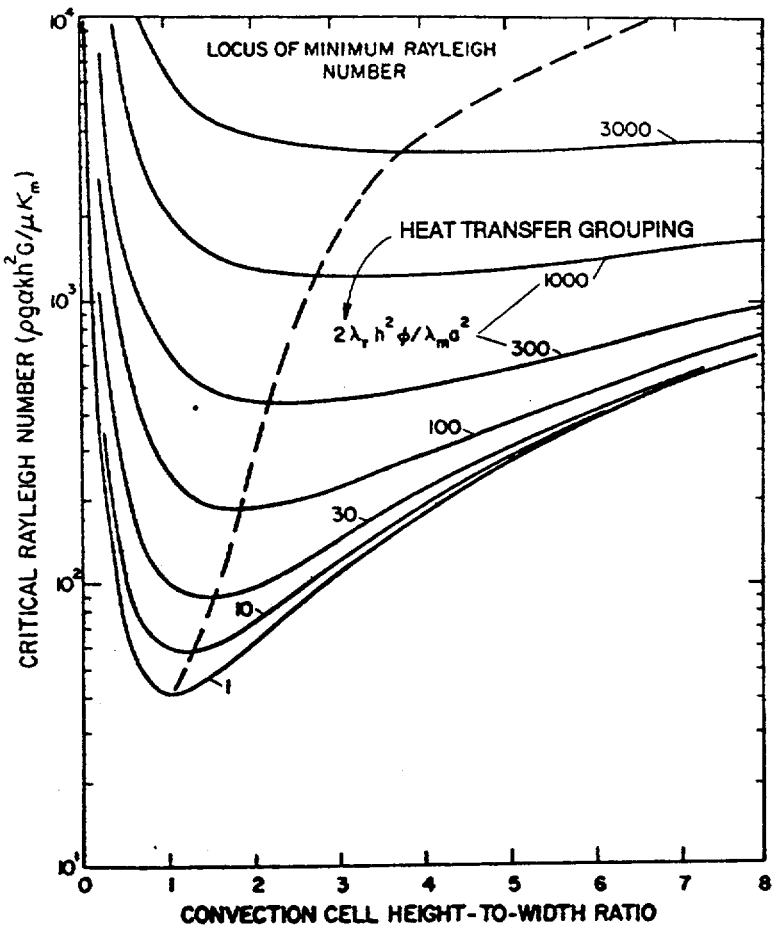

The stability limit (the critical Rayleigh number at neutral stability) for the onset of thermal convection in faults and fractures as a function of the aspect ratio and the heat transfer grouping. From Murphy, 1979.

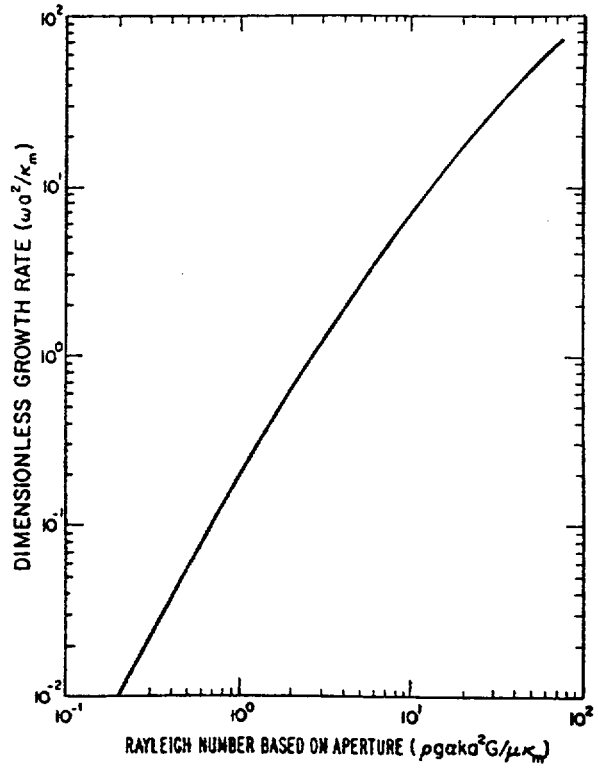

a) DEPENDENCE OF THE PERTURBATION GROWTH RATE UPON THE IN-SITU RAYLEIGH NUMBER.

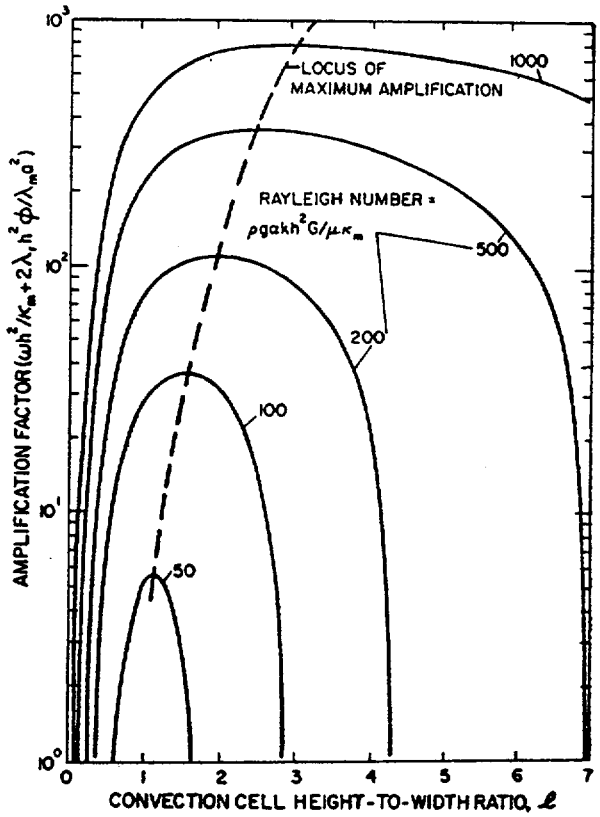

b) DEPENDENCE OF THE PERTURBATION GROWTH RATE UPON THE IN-SITU RAYLEIGH NUMBER AND THE ASPECT RATIO.

The perturbation growth rate for convection in fractures. From Murphy, 1979.

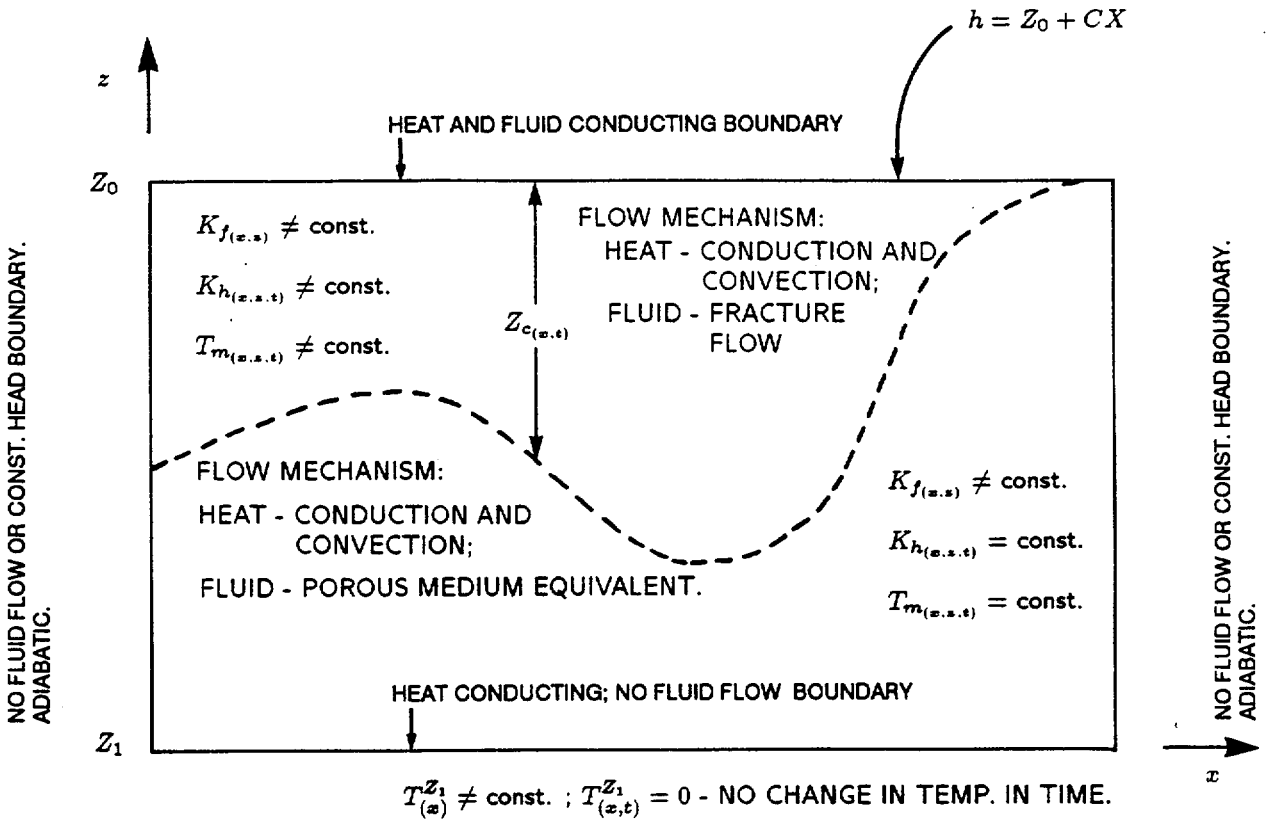

$T^{Z_1}_{(x)} \neq$ const. ; $T^{Z_1}_{(x,t)} = 0$ - NO CHANGE IN TEMP. IN TIME.

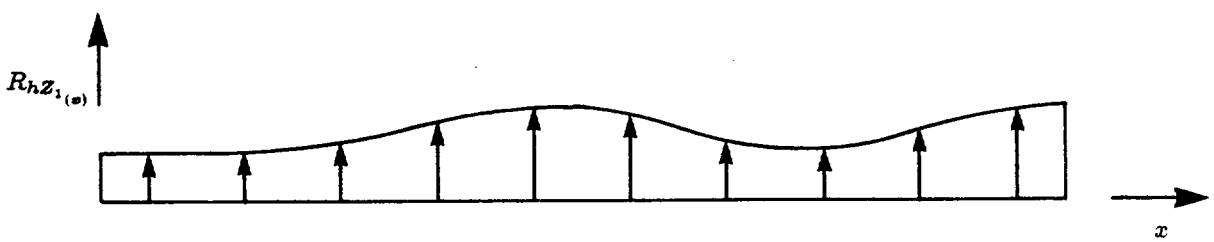

$R_{hZ_{1_{(x)}}} \neq$ const. CHANGE IN HEAT FLUX IN SPACE

$R_{hZ_{1_{(x,t)}}} =$ const. NO CHANGE IN HEAT FLUX IN TIME

DEPTH OF CONVECTION IN FRACTURES

$Z_{c_{(x,t)}} \neq$ const.

$$Z_{c_{(x,t)}} = f\left(K_{f_{(x,z)}}; T_{Z_{c(x)}} - T_{Z_{0(x)}}\right)$$

COMPOSITE TEMPERATURE

$T_{m_{(x,z,t)}} \neq$ const. $\qquad T_{m_{(x,z,t)}} = f\left(R_{hZ_{1_{(x)}}}; Z_{c_{(x,t)}}; K_{h_{(x,z)}}\right)$

TEMPERATURE GRADIENTS

$\partial^2 T_{m_{(x,z,t)}}/\partial x(\partial y)\partial t \neq 0$ $\qquad$ above $Z_{c_{(x,t)}}$

$\partial^2 T_{m_{(x,z,t)}}/\partial x(\partial y)\partial t = 0$ $\qquad$ below $Z_{c_{(x,t)}}$

Conceptual model of a flow system in fractured medium and influenced by terrestrial heat.

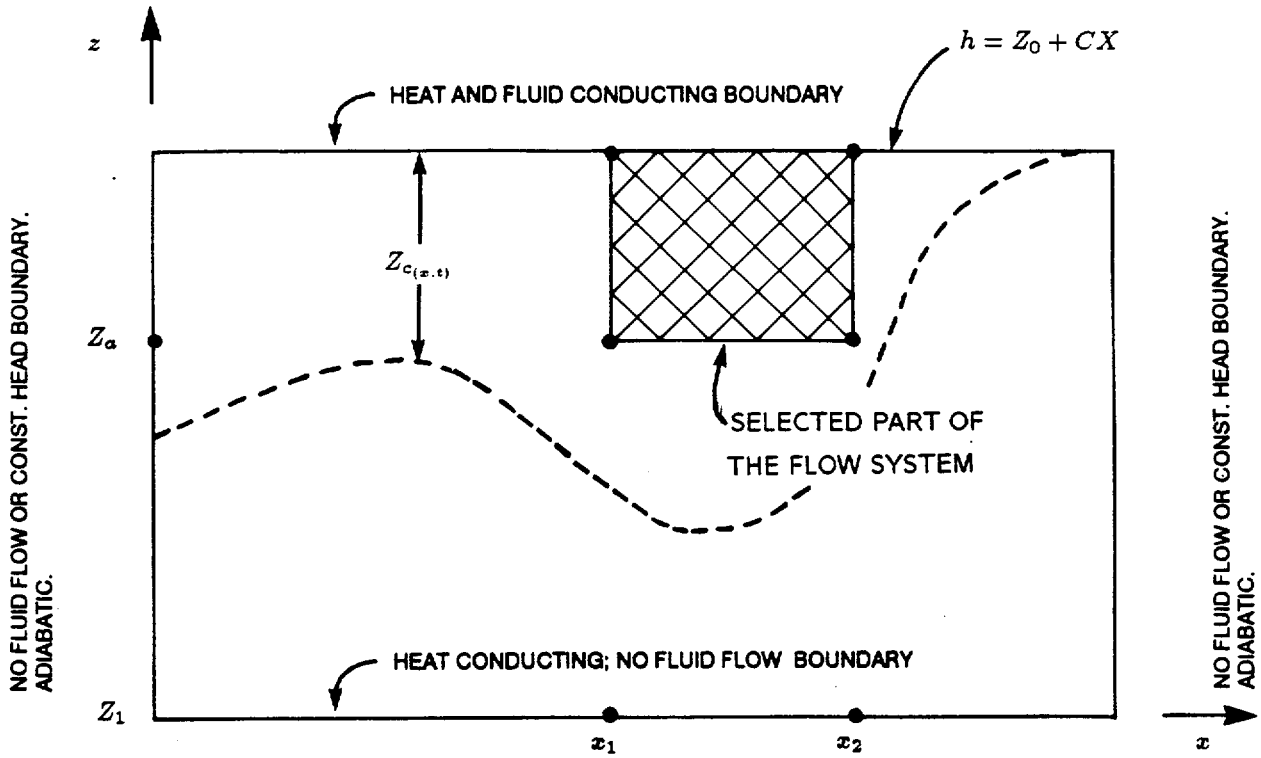

$T^{Z_1}_{(x)} \neq$ const; $\quad T^{Z_1}_{(x,t)} =$ const.

ASSUMED INITIAL BOUNDARY CONDITIONS.

UPSTREAM VERTICAL BOUNDARY - $\partial q^{uin}_{f(h)_{(x,t)}} / \partial z(\partial t) = 0$

DOWNSTREAM VERTICAL BOUNDARY - $\partial q^{din}_{f(h)_{(x,t)}} / \partial z(\partial t) = 0$

LOWER HORIZONTAL BOUNDARY - $\partial q^{in}_{f(h)Za_{(x,t)}} / \partial x(\partial t) = 0$

INITIAL AMOUNT OF FLUID IN TRANSIT.

$$\partial Q^{in}_{tr_{(t)}} / \partial t = 0$$

Location of a selected part of the flow system considered on Plates 3.4.4-3 through 3.4.4-6

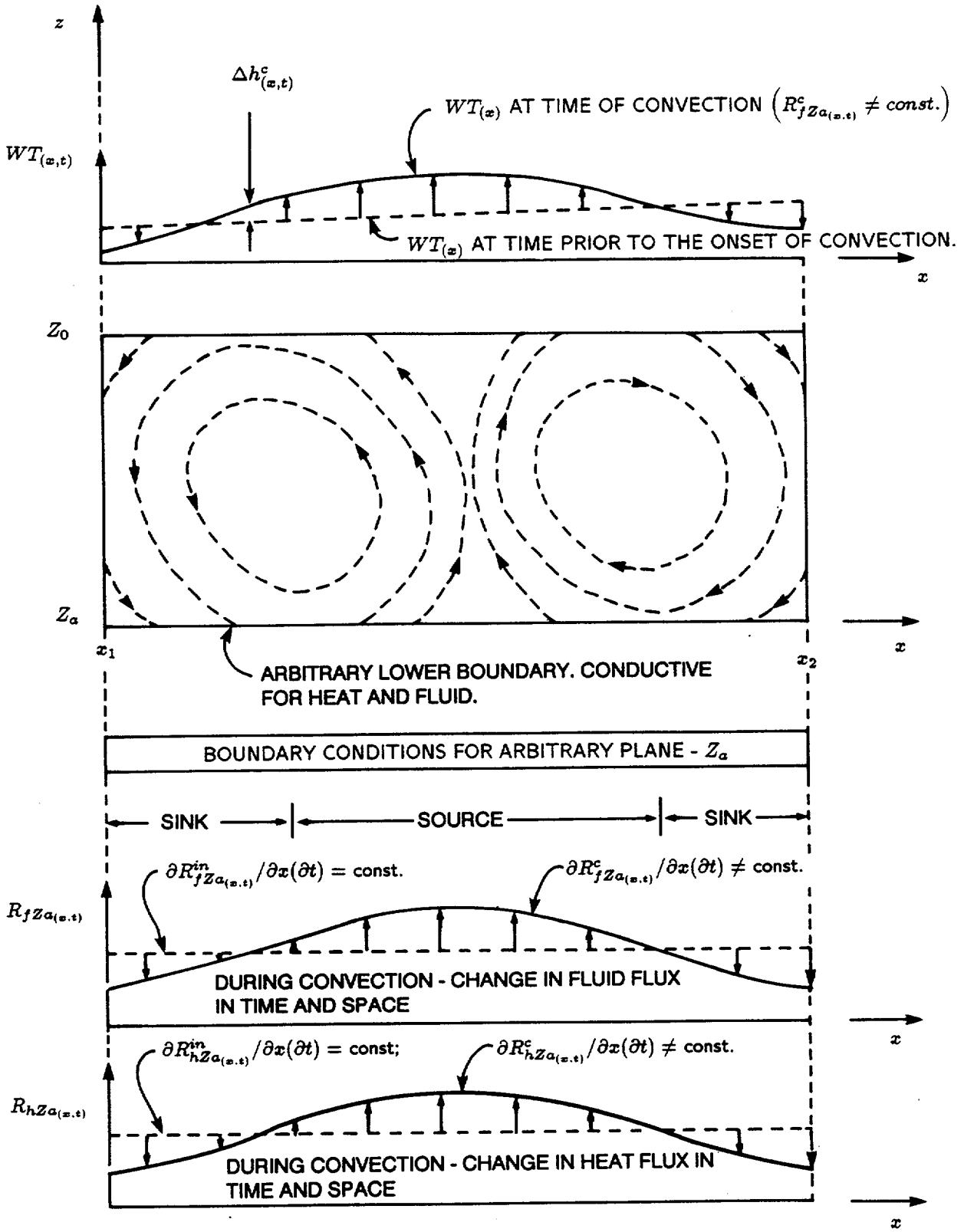

Change in boundary conditions for an arbitrary plane -Z_a caused by convection of fluids in the selected part of the flow system.

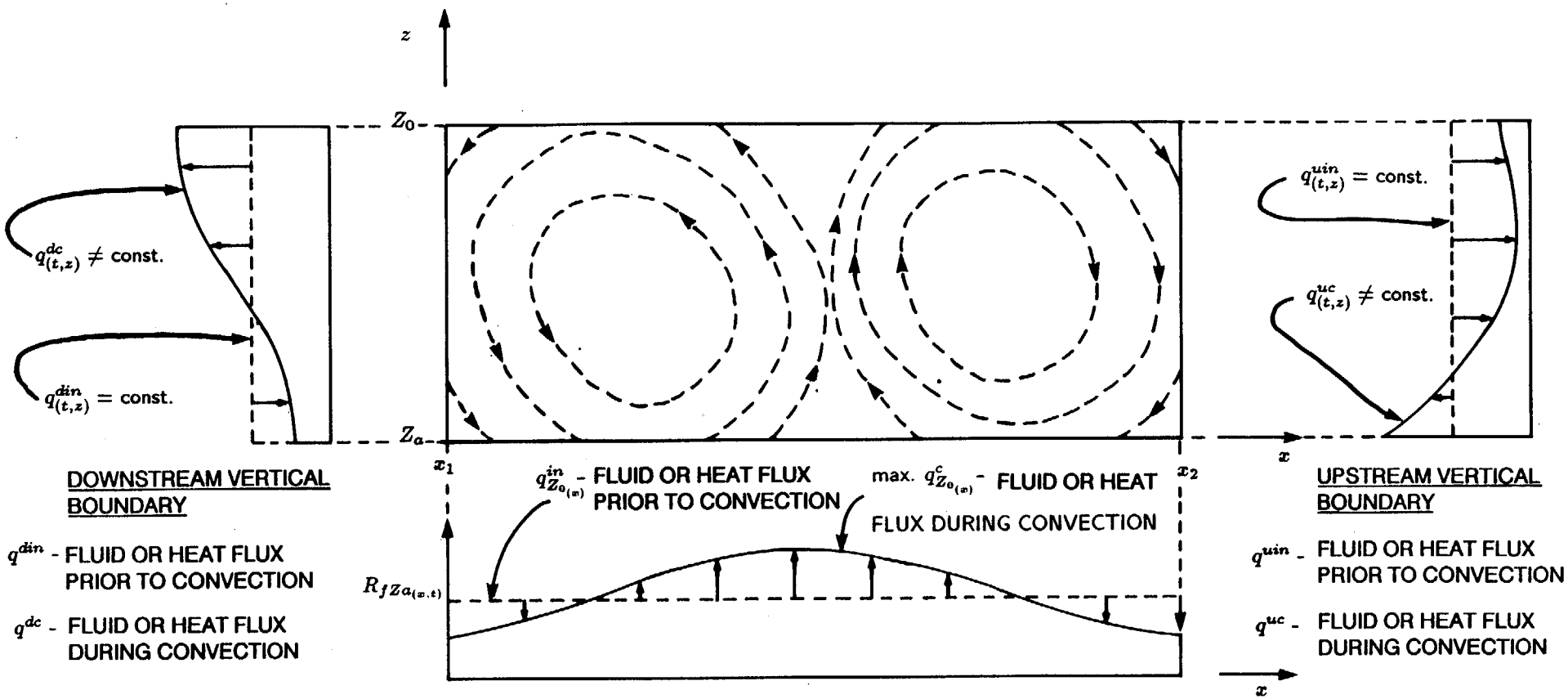

PRIOR TO CONVECTION:

$$q^{din}_{(t,z)} = q^{uin}_{(t,z)} = \text{const.} \ ; \text{ and } q^{in}_{Z_{0(x)}} = \text{const.} \longrightarrow Q^{in}_{tr} = \text{const.}$$

AMOUNT OF WATER IN TRANSIT PRIOR TO THE ONSET OF CONVECTION

DURING CONVECTION:

$$q^{din}_{(t,z)} \neq q^{uin}_{(t,z)} \neq \text{const.} \ ; \text{ and } q^{c}_{Z_{0(t,x)}} \neq \text{const.} \longrightarrow Q^{c}_{tr} \neq \text{const. and } Q^{c}_{tr} > Q^{in}_{tr}$$

Amount of fluid in transit (storage) through the selected part of the flow system prior and during convection.

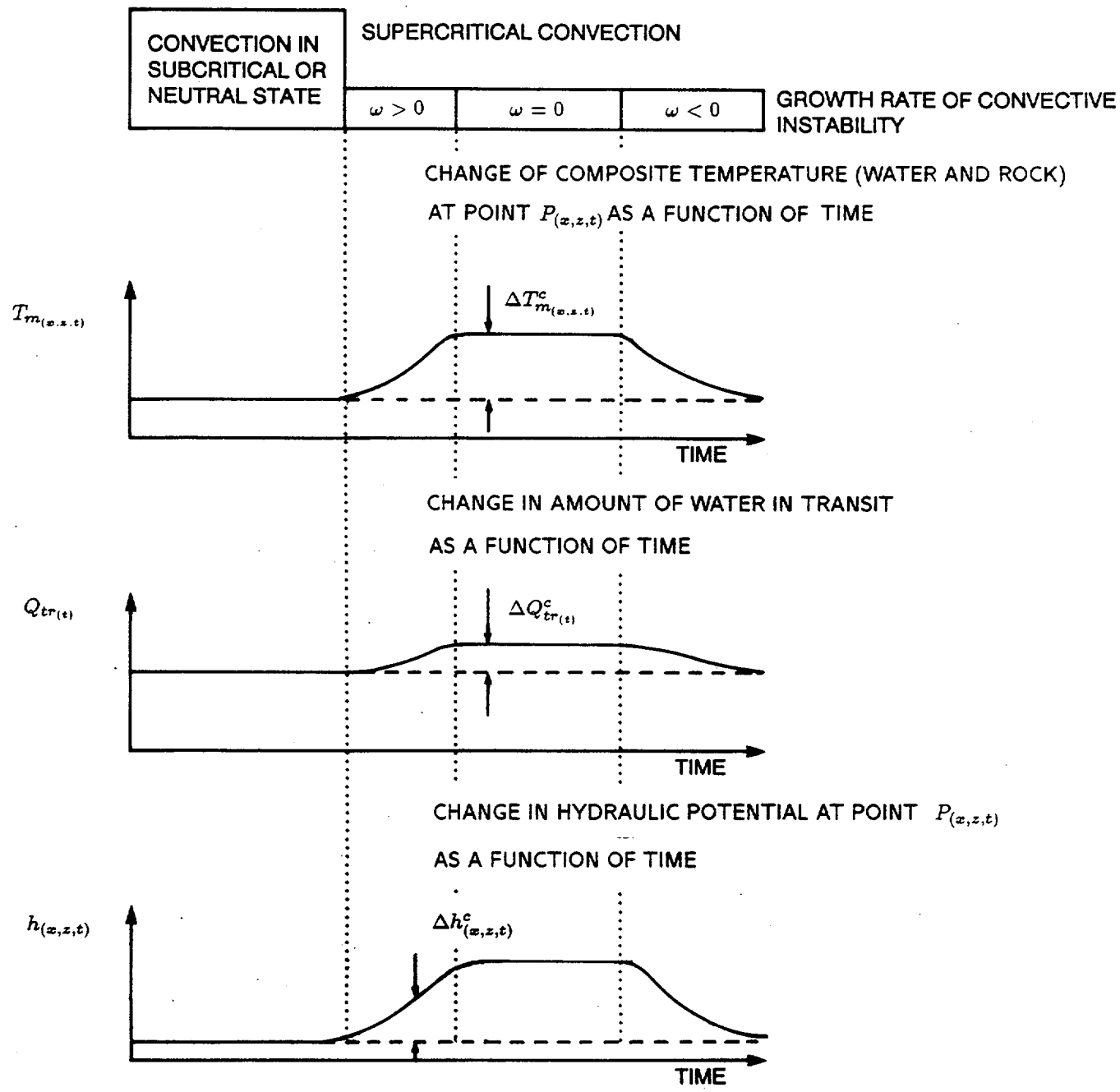

Changes introduced into the selected part of the flow system by thermal convection.

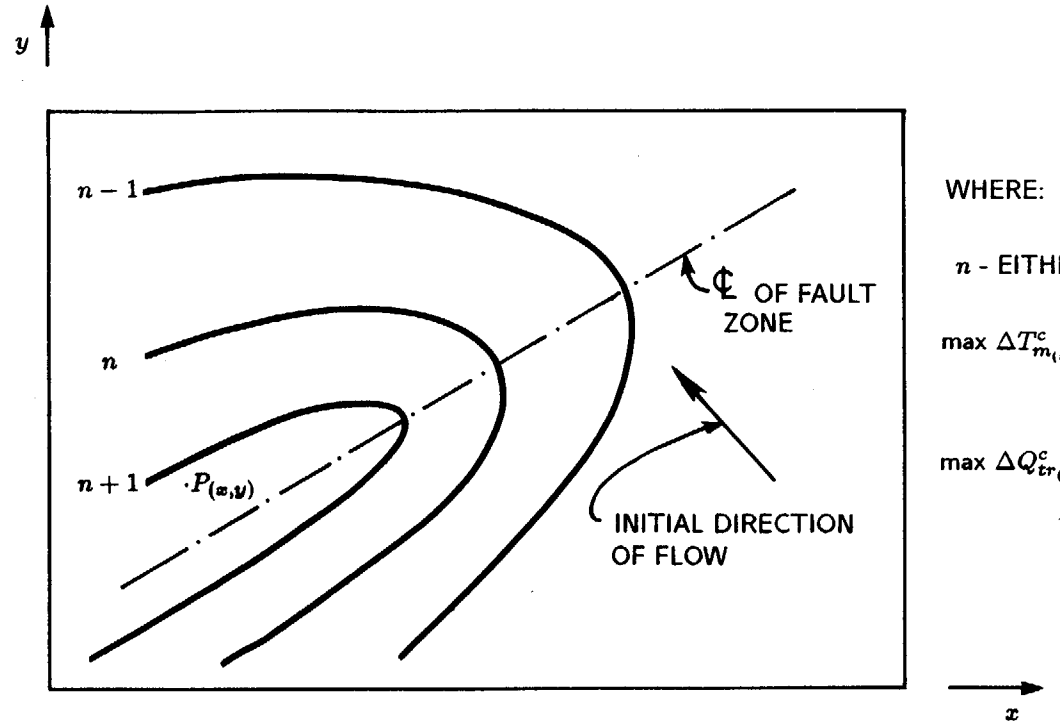

WHERE:

n - EITHER max $\Delta T^c_{m_{(x,y)}}$ or max $\Delta Q^c_{tr_{(x,y)}}$

max $\Delta T^c_{m_{(x,y)}}$ - MAXIMUM AVERAGE CHANGE IN TEMPERATURE FOR POINT $P_{(x,y)}$

max $\Delta Q^c_{tr_{(x,y)}}$ - MAXIMUM AVERAGE CHANGE IN AMOUNT OF FLUID IN TRANSIT FOR POINT $P_{(x,y)}$

$$\text{max } \Delta h^c_{(x,y)} = \text{max } \Delta h^{cb}_{(x,y)} + \text{max } \Delta h^{ch}_{(x,y)}$$

$$\text{max } \Delta h^{cb}_{(x,y)} = \alpha \cdot \text{max } T^c_{m_{(x,y)}} \cdot D$$

$$\text{max } \Delta h^{ch}_{(x,y)} = \text{max } Q^c_{tr}/Q^{in}_{tr} \cdot \Delta h^{in}_{(x,y)}$$

max $\Delta h^c_{(x,y)}$ - MAX. RISE OF WATER TABLE AT POINT $P_{(x,y)}$;

max $\Delta h^{cb}_{(x,y)}$ - MAX. BUOYANCY COMPONENT;

max $\Delta h^{ch}_{(x,y)}$ - MAX. HYDRAULIC HEAD COMPONENT;

α - COEFFICIENT OF THERMAL EXPANSION $= 3.85 \cdot 10^{-4}$ PER ^0C ;

D - DEPTH OF CONVECTION INSTABILITY

max Q^c_{tr}/Q^{in}_{tr} - RATIO OF MAXIMUM AVERAGE AMOUNT OF FLUID IN TRANSIT DURING CONVECTION TO INITIAL AMOUNT OF FLUID IN TRANSIT.

$\Delta h^{in}_{(x,y)} = i_{in} \cdot L$

L - SHORTEST DISTANCE BETWEEN $P_{(x,y)}$ AND A POINT DOWNSTREAM FOR WHICH $Q^c_{(tr)} = Q^{in}_{tr}$

i_{in} - INITIAL HYDRAULIC GRADIENT ALONG DISTANCE L.

Maximum rise of water table at $P_{(x,y)}$ caused by thermal convection.

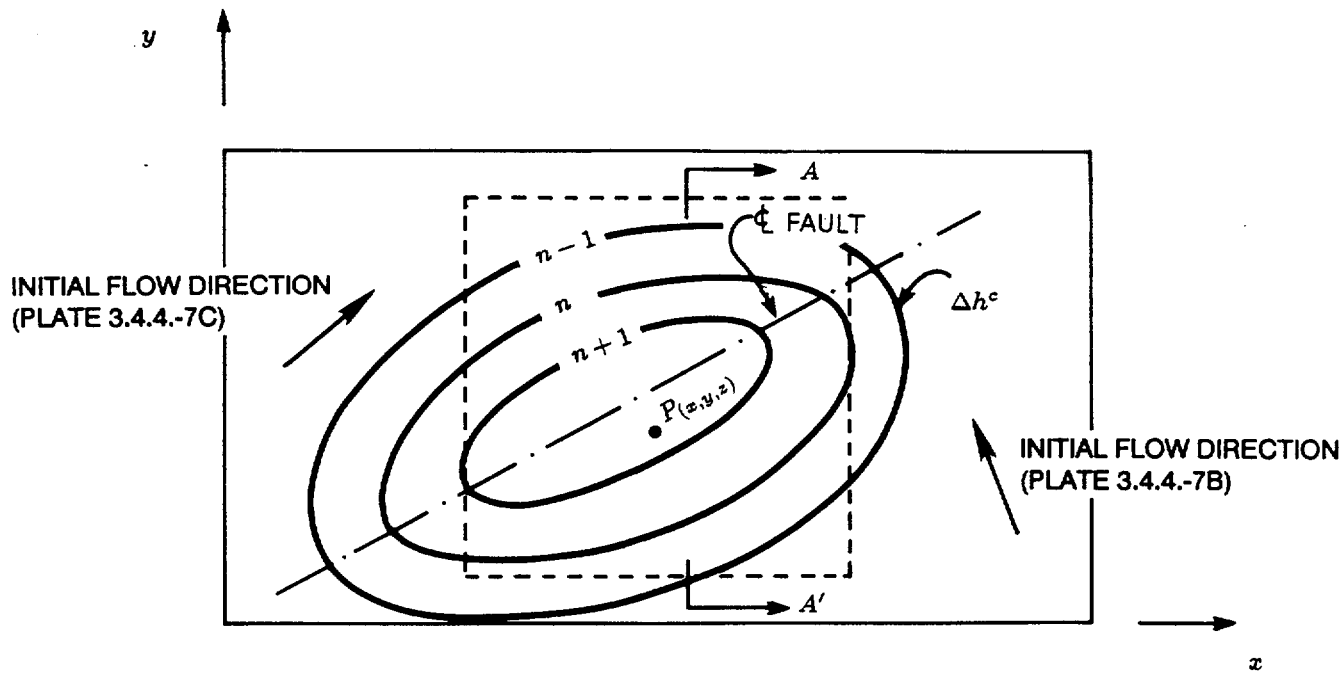

PLAN VIEW OF CHANGES IN HYDRAULIC HEAD CAUSED BY CONVECTION.

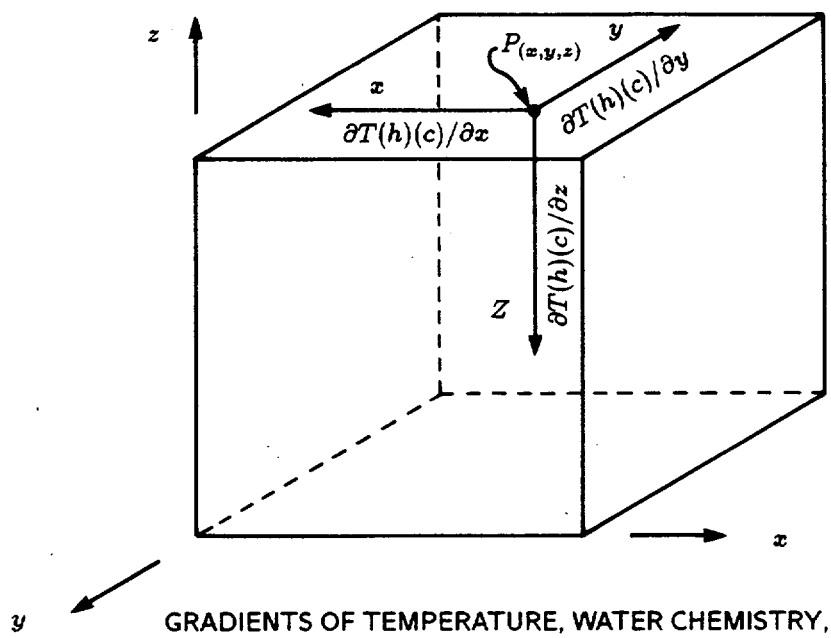

GRADIENTS OF TEMPERATURE, WATER CHEMISTRY,
AND HYDRAULIC HEAD INTRODUCED BY CONVECTION.

Changes introduced into flow field by thermal convection.

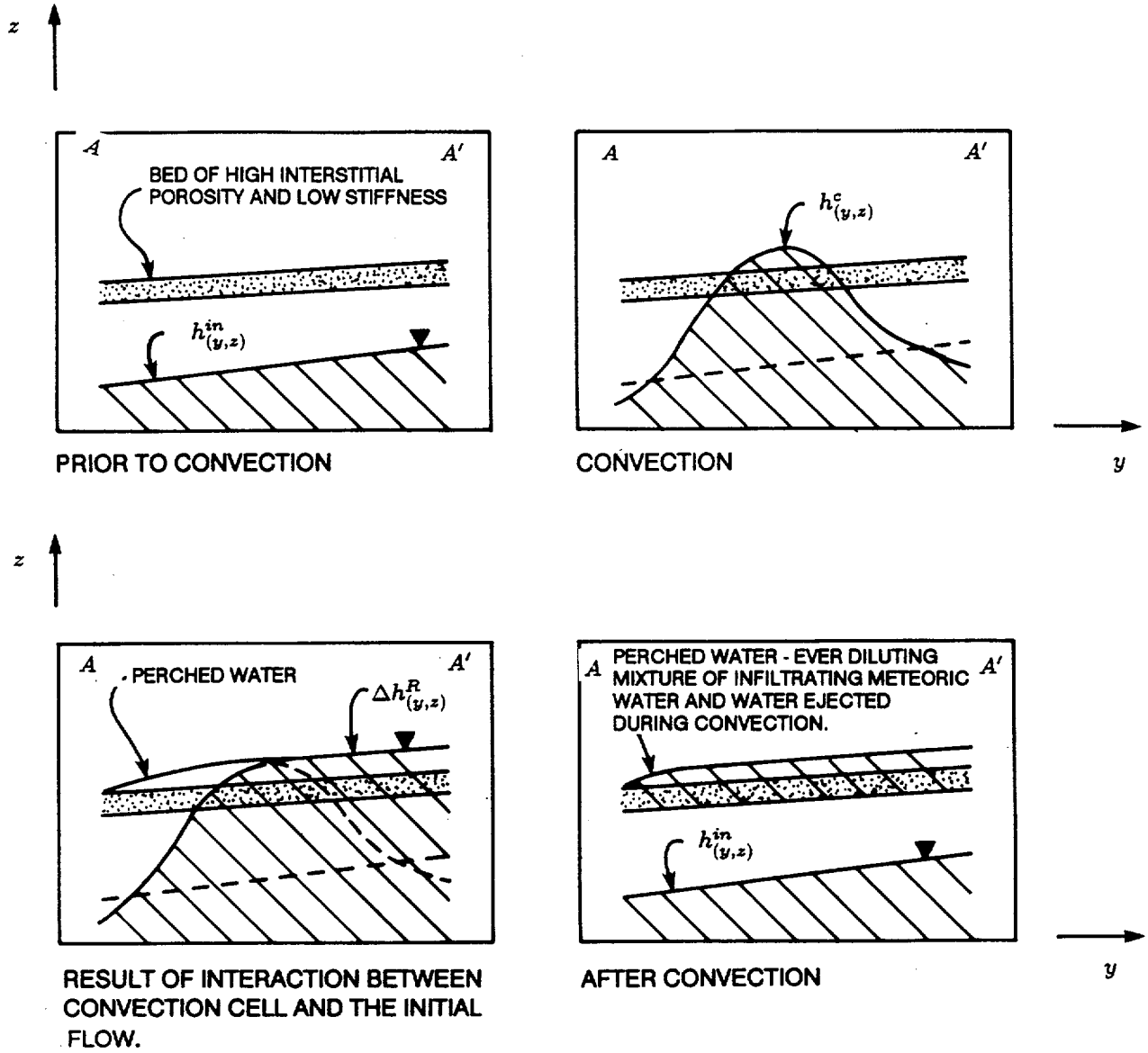

INITIAL FLOW DIRECTION ⊥ TO LONG AXES OF THE CONVECTION CELL.

Changes introduced into flow field by thermal convection - formation of perched waters.

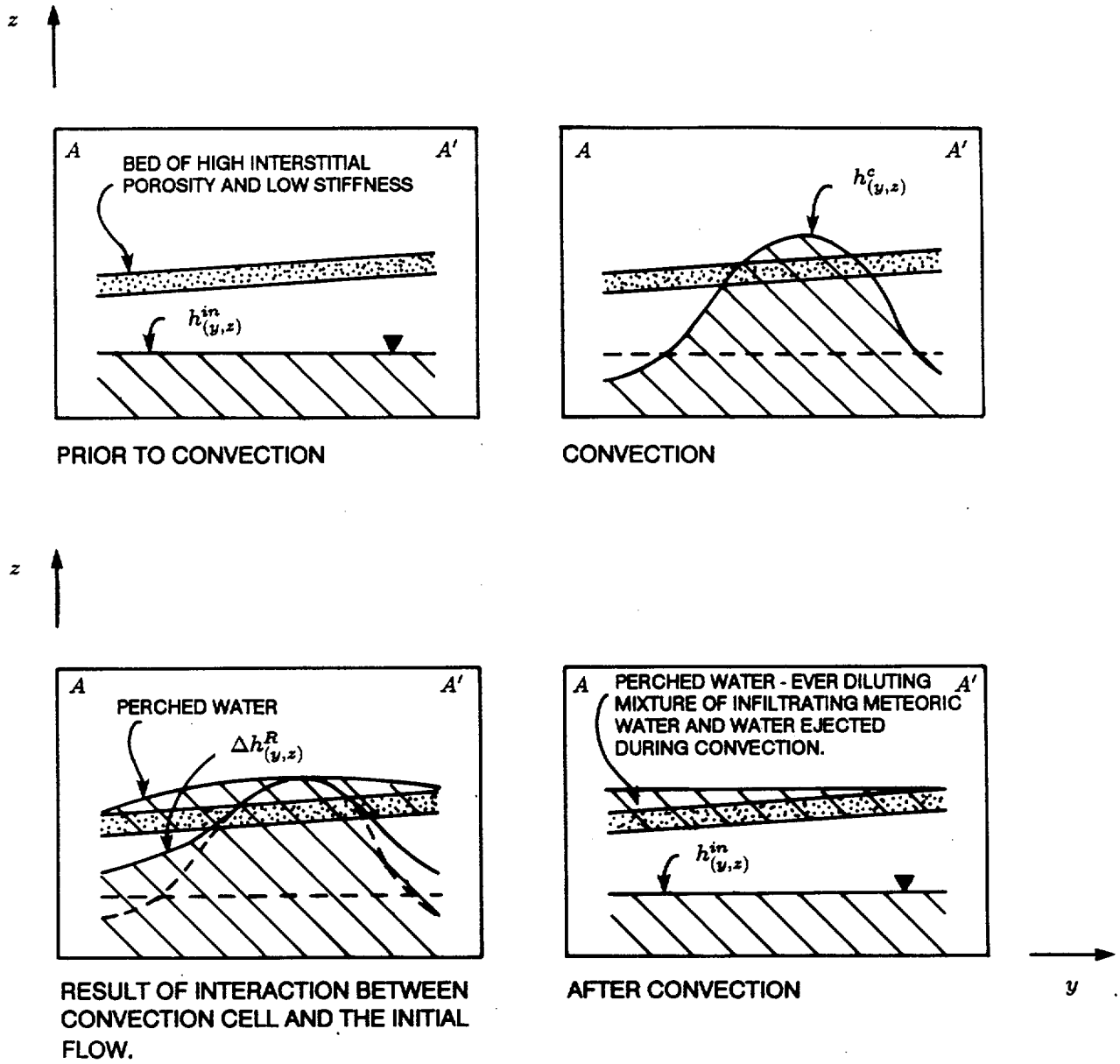

INITIAL FLOW DIRECTION || TO LONG AXIS OF THE CONVECTION CELL.

Changes introduced into flow field by thermal convection - formation of perched waters.

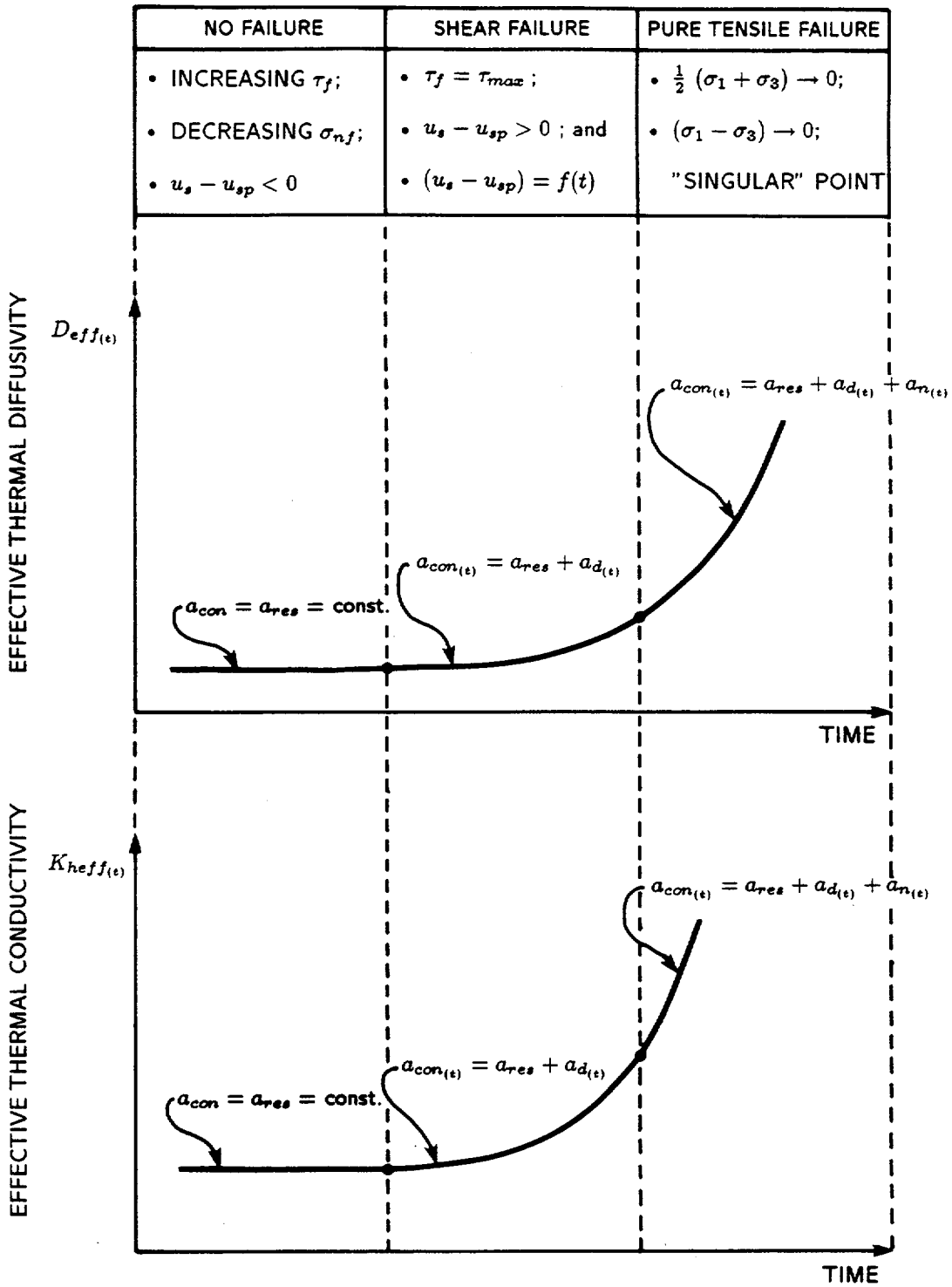

Time-dependence of thermal properties (K_h and D) around a segment of a deforming fracature at a const. depth.

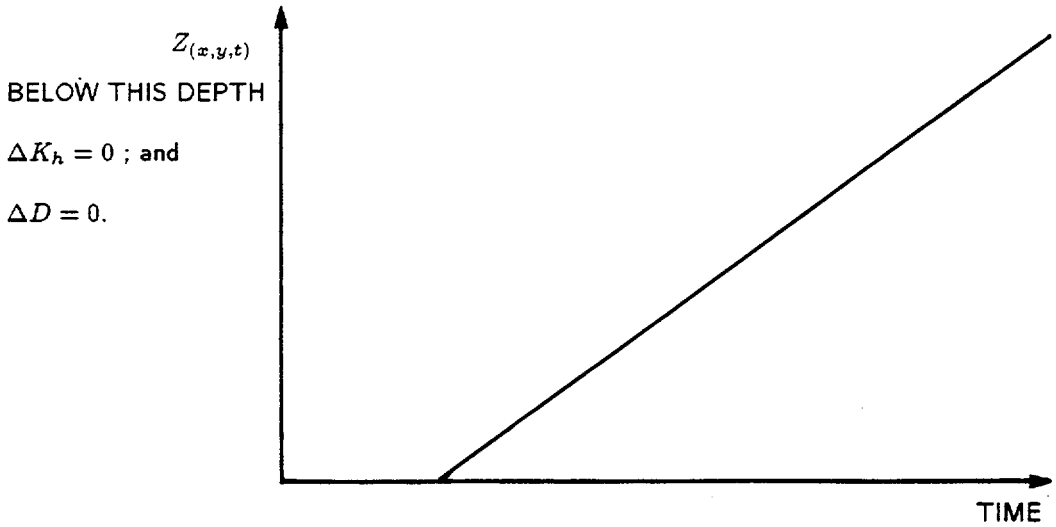

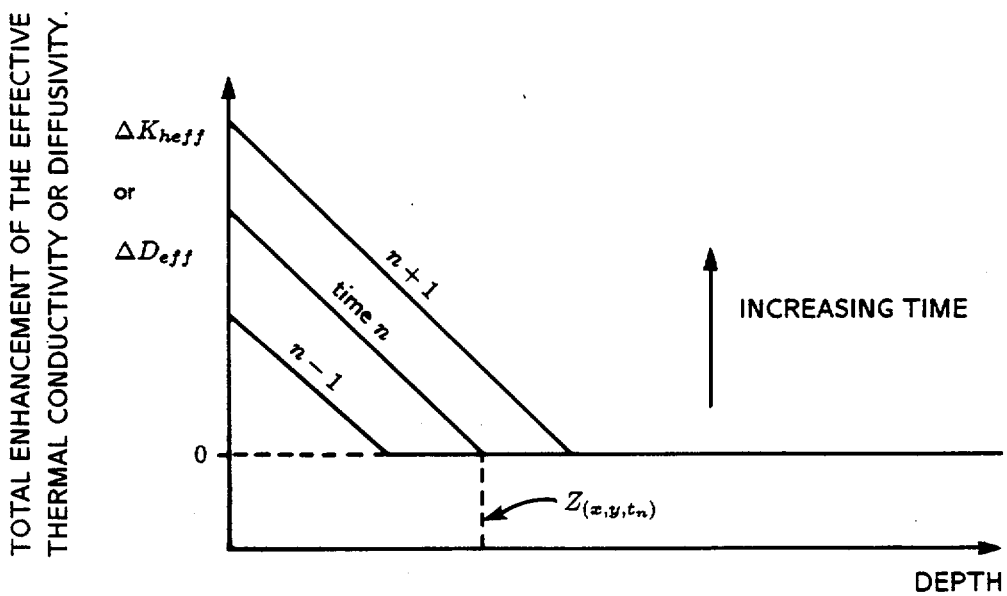

Time-dependence of the vertical extent of the in situ stress enhancement of thermal properties ($K_h and D$) and time-dependence of the value of this enhancement.

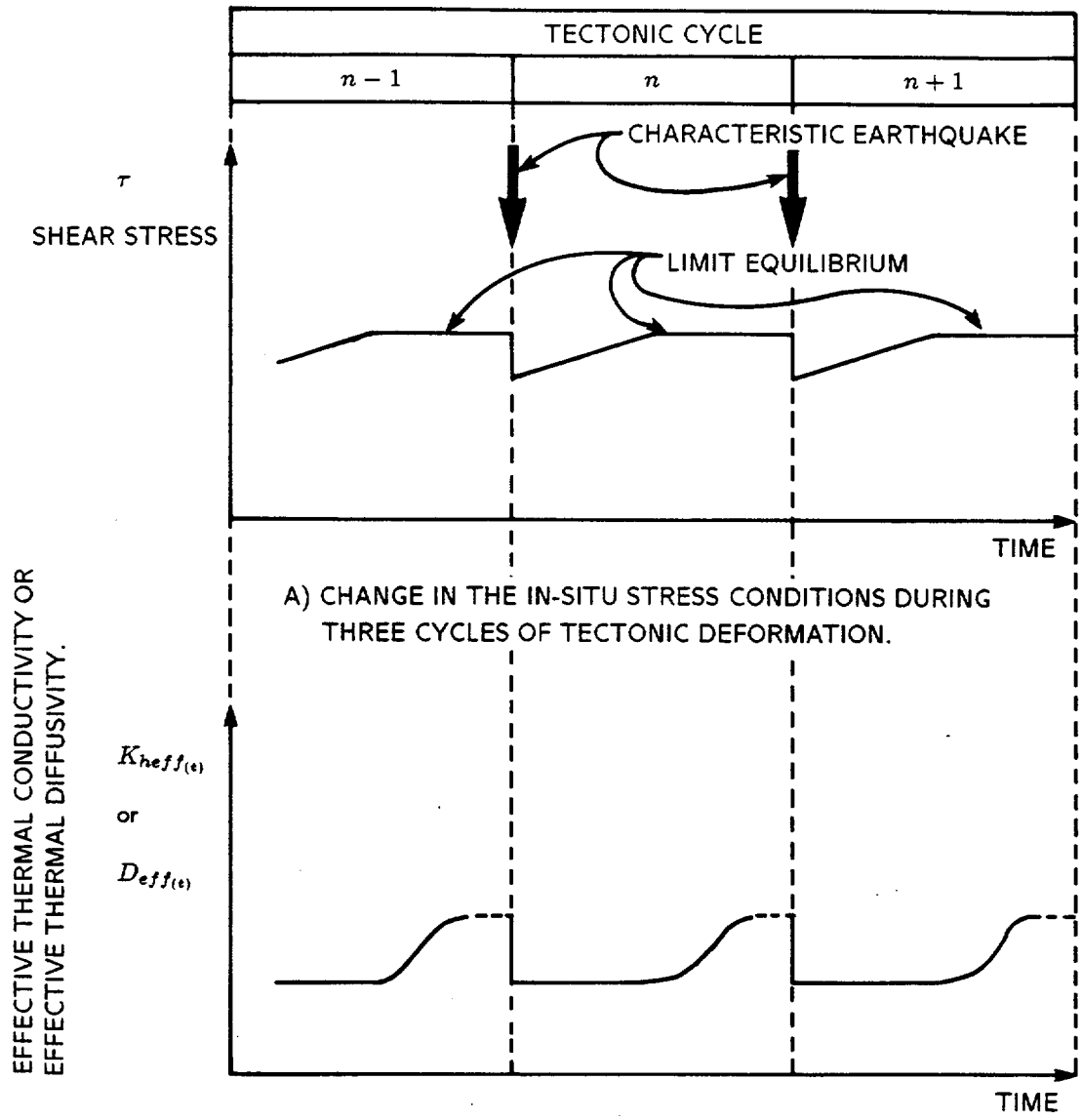

Schematic representation of changes in: a) the in situ stress conditions; and b) the thermal properties. A cyclically deforming fractured medium, near the ground surface.

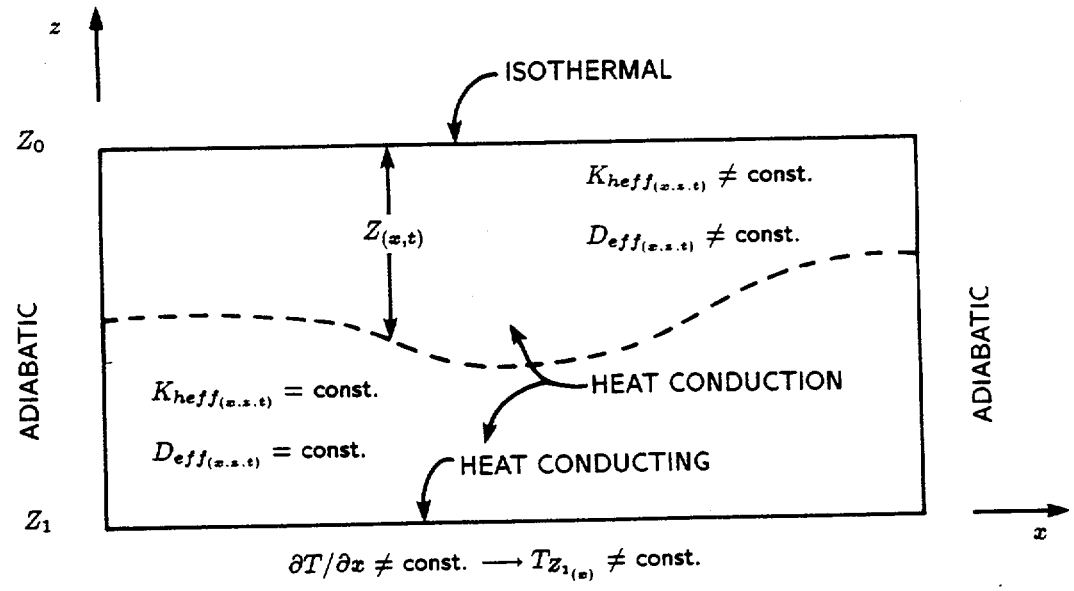

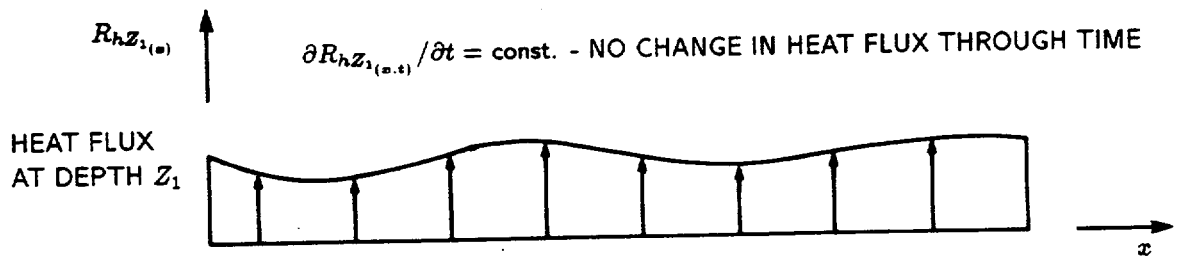

$[\sigma;\tau] = f(t)$

$Z_{(x,t)} = f([\sigma;\tau])$

$K_{heff_{(x,z,t)}} = f([\sigma;\tau])$

$D_{eff_{(x,z,t)}} = f([\sigma;\tau])$

$K_{h_{(x,z)}} \neq$ const.

$D_{(x,z)} \neq$ const.

Conceptual model of a "simple" flow of heat through a deforming fractured medium.

GEOTHERMAL FIELD DEVELOPED IN THE DEFORMING FRACTUARY MEDIUM WITH $R_{h_{z_{1(x,t)}}}$ = const. HAS THE FOLOWING CHARACTERISTICS.

THREE DIMENSIONS	TWO DIMENSIONS	ONE DIMENSION
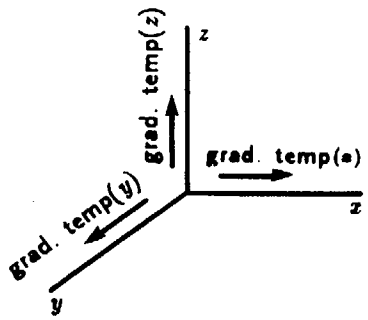 $\frac{\partial^2 temp}{\partial x \partial t} \neq 0 \neq$ const; $\frac{\partial^2 temp}{\partial y \partial t}; \neq 0 \neq$ const. ; and $\frac{\partial^2 temp}{\partial z \partial t} \neq 0 \neq$ const.	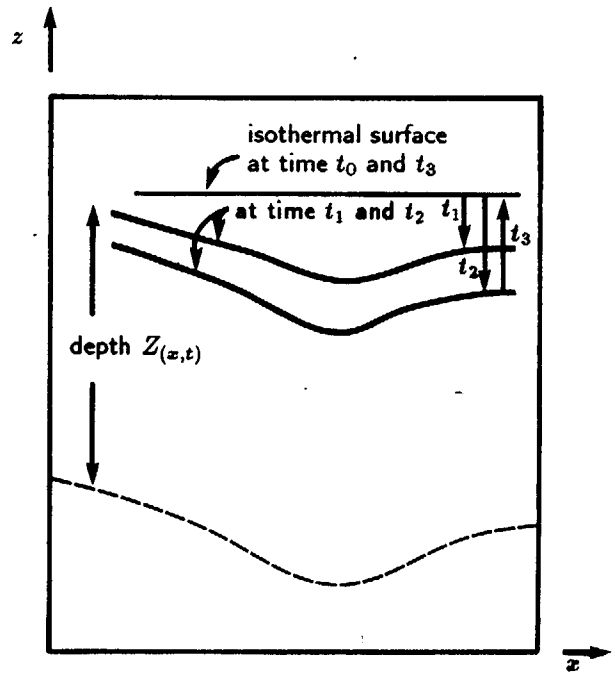	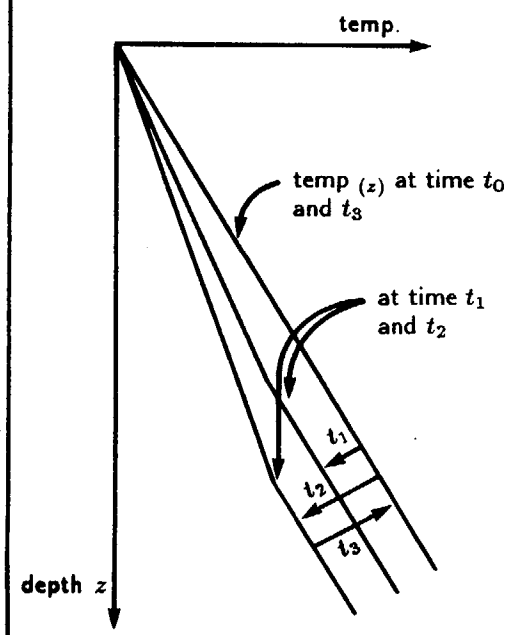

Main characteristics of the geothermal field developed in a deforming fractured medium.

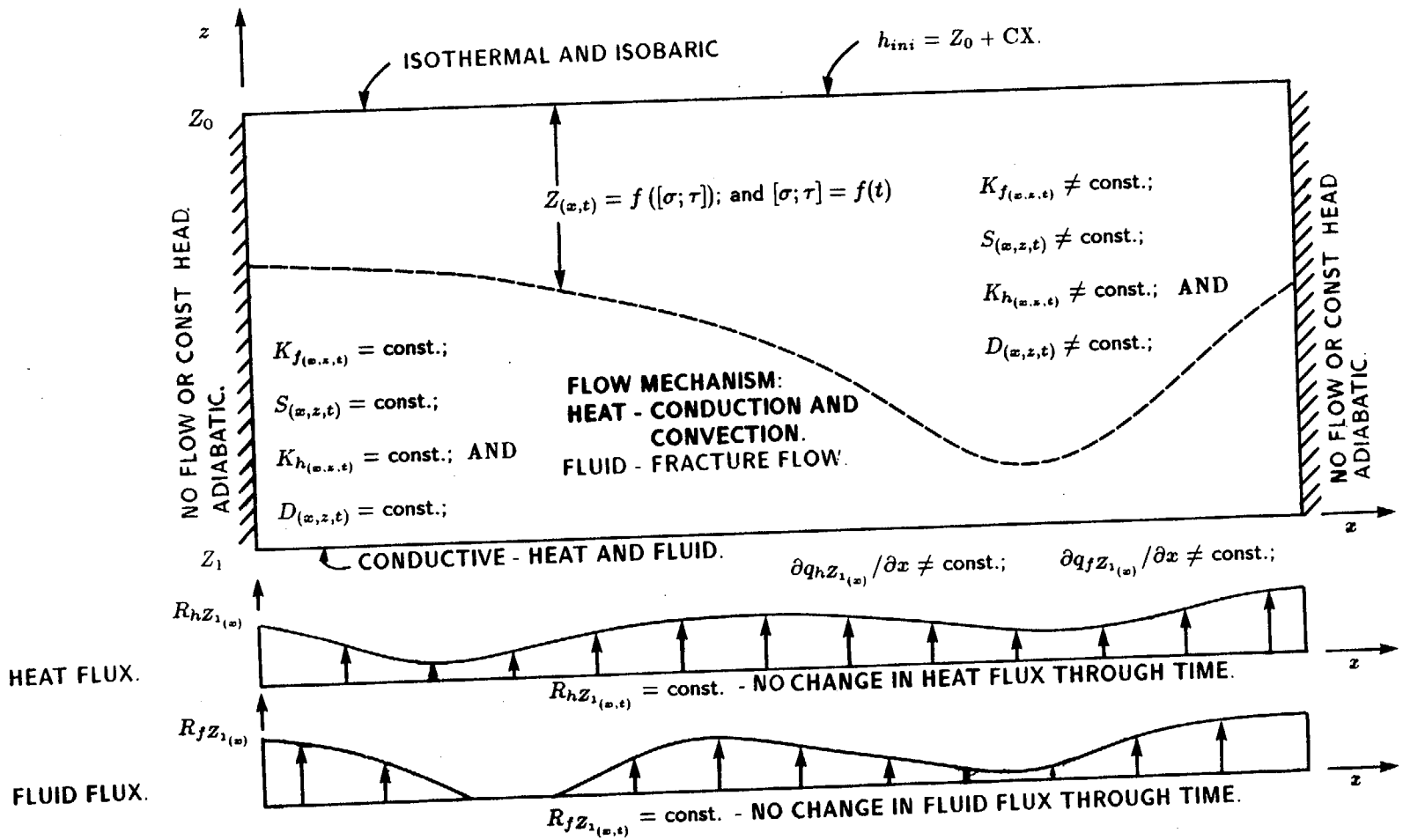

Conceptual model of a heat-fluid coupled groundwater system developed in a deforming fractured medium.

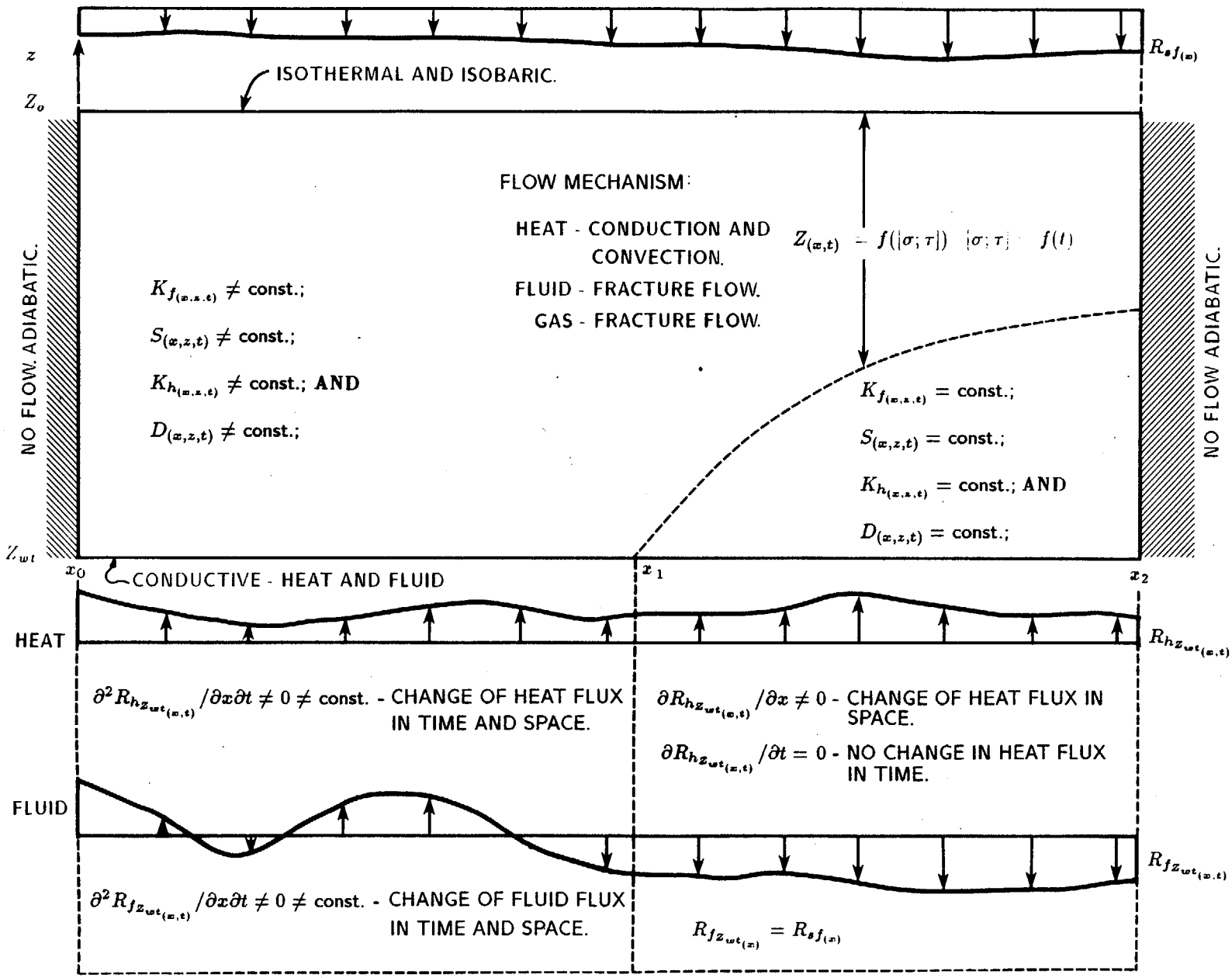

Conceptual model of flow in the vadose zone of the coupled heat-fluid flow field developed in a deforming fractured medium.

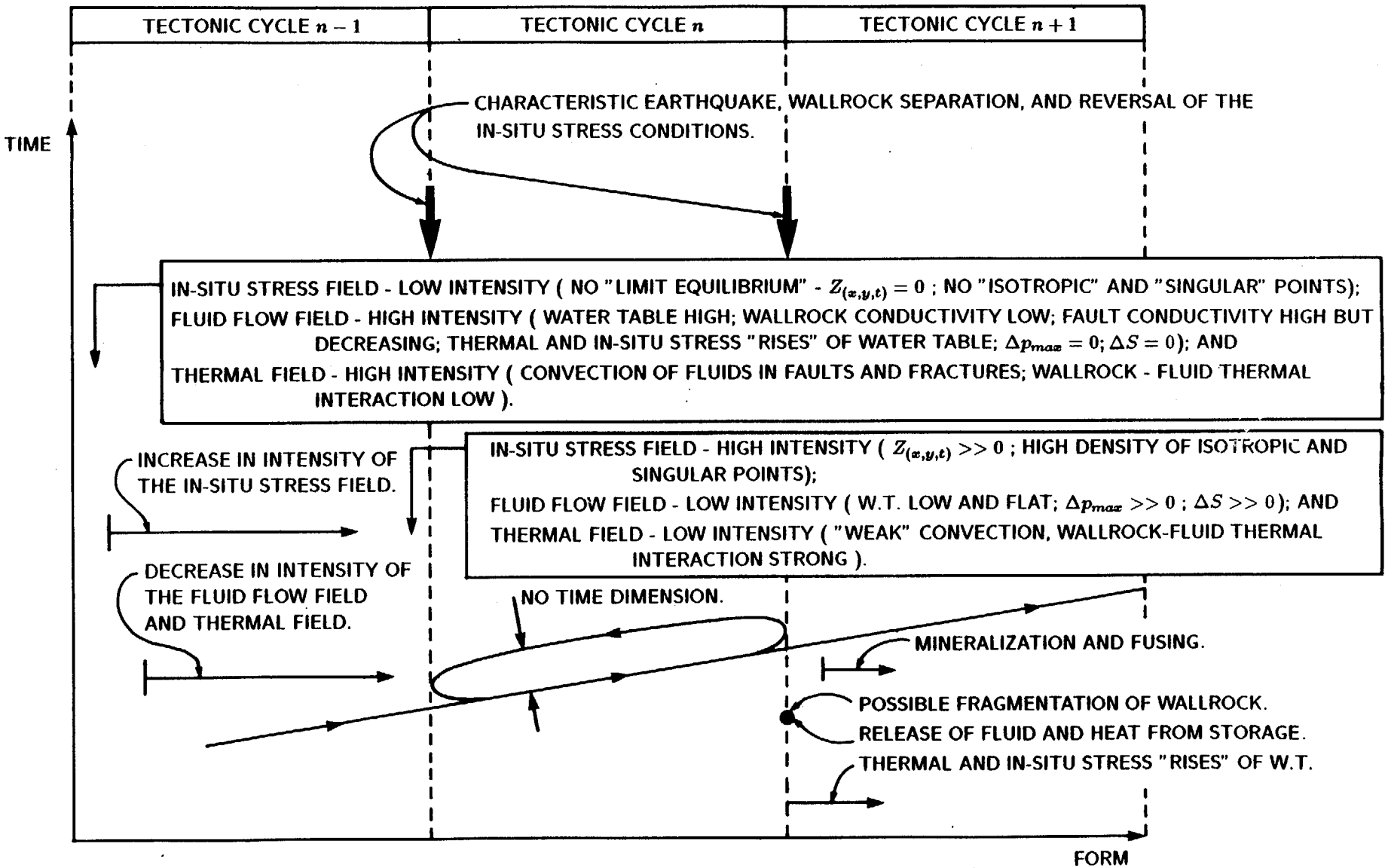

Evolution of the coupled heat-fluid flow system developed in a deforming fractured medium and operating near the ground surface.

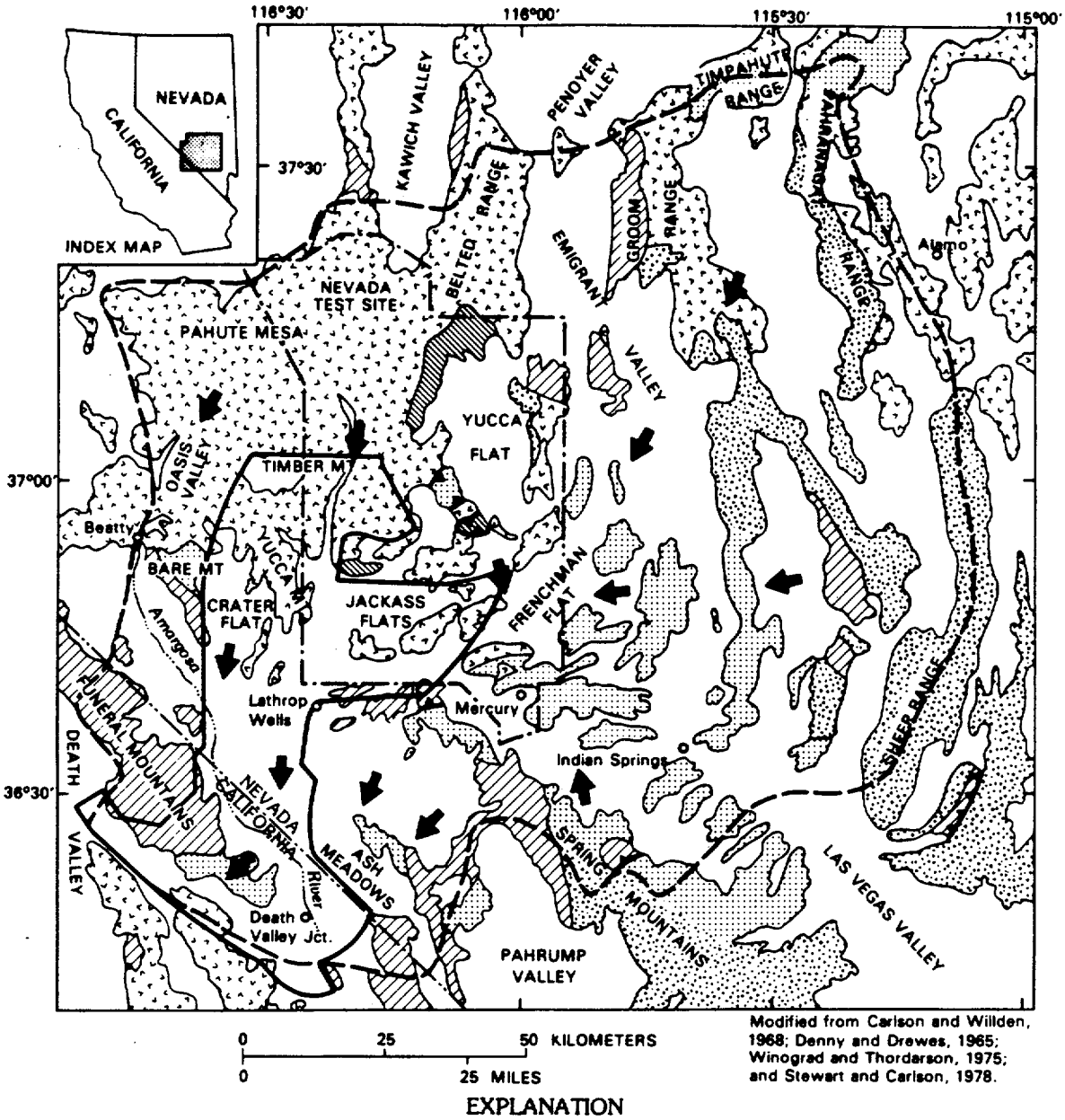

Location of the Death Valley groundwater system. From Czarnecki and Waddell, 1984.

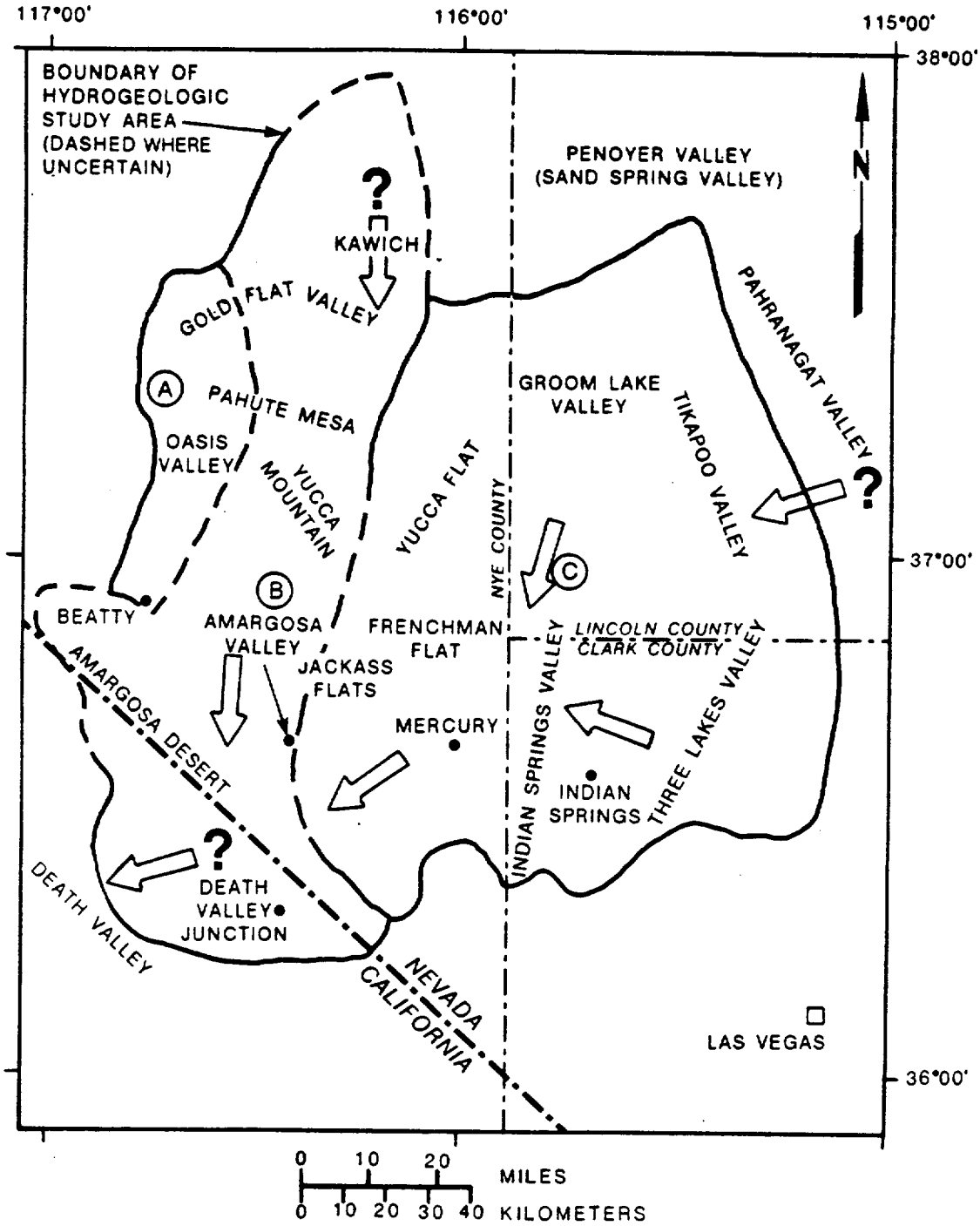

GENERAL DIRECTION OF REGIONAL GROUND-WATER FLOW (QUESTION MARK INDICATES UNCERTAINTY)

A. OASIS VALLEY SUBBASIN
B. ALKALI FLAT-FURNACE CREEK RANCH SUBBASIN
C. ASH MEADOWS SUBBASIN

Subdivision of the Death Valley groundwater system. Modified from Winograd and Thordarson, 1975; Waddell, 1982; and Waddell, et al., 1984.

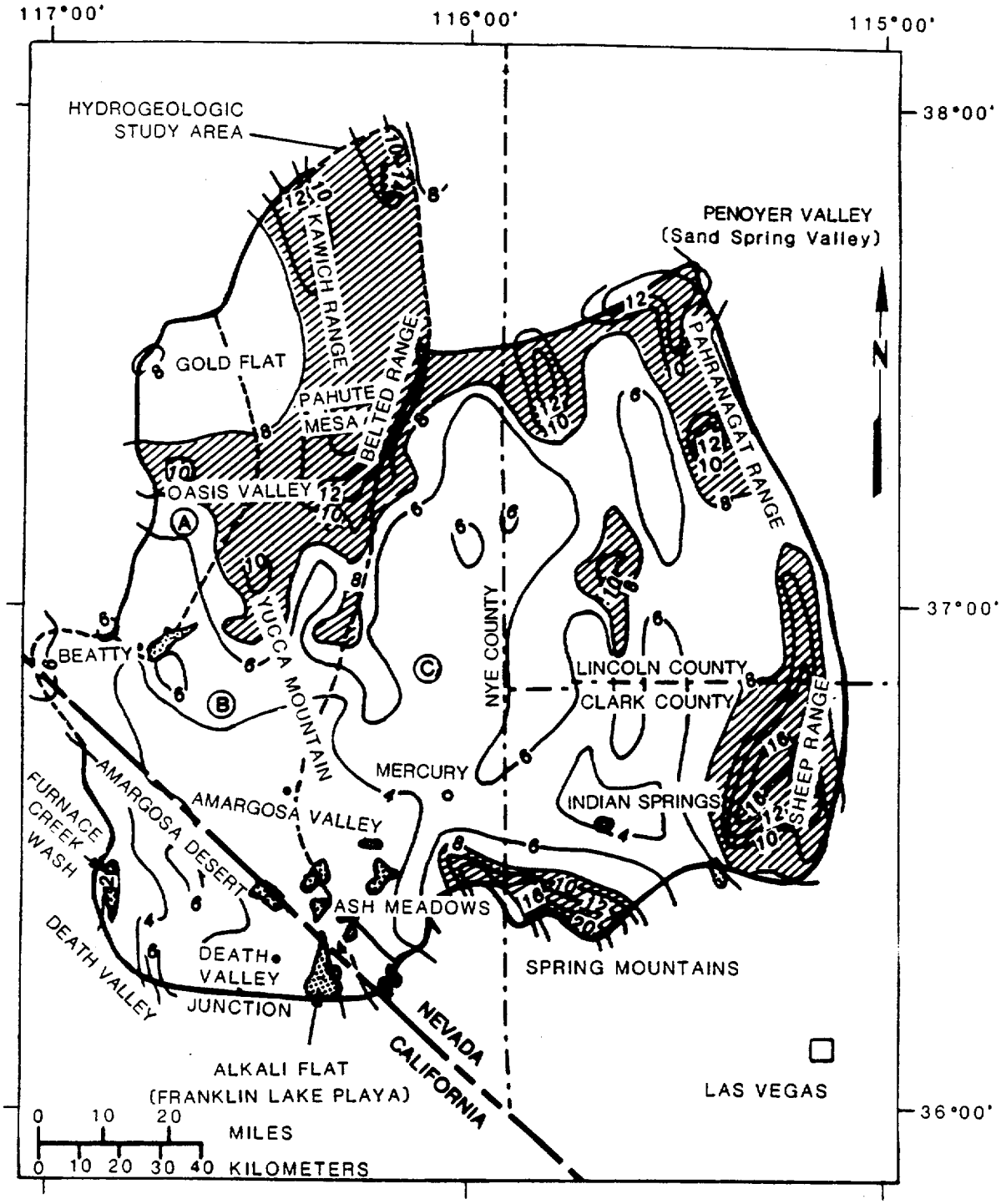

RECHARGE AREAS

DISCHARGE AREAS

BOUNDARY OF HYDROGEOLOGIC STUDY AREA; DASHED WHERE UNCERTAIN

SUBBASIN BOUNDARY

(A) OASIS VALLEY SUBBASIN

(B) ALKALI FLAT-FURNACE CREEK RANCH SUBBASIN

(C) ASH MEADOWS SUBBASIN

LINE OF EQUAL AVERAGE ANNUAL PRECIPITATION, IN INCHES

Subdivision of the Death Valley groundwater system. Modified from Winograd and Thordarson, 1975; Waddell, 1982; and Waddell, et al., 1984.

Well No.	Stratigraphic Unit	Number of Samples	Saturated Matrix Hydraulic Conductivity [m/d]	Source
J-13	Topopah Spring	5	$2x10^{-4}$ $-3x10^{-7}$	Thordarson, 1983.
UE-25 a#1	Topopah Spring	24	$5x10^{-4}$ $-7x10^{-7}$	Anderson, 1981.
UE-25 a#1	Calico Hills	6	$3x10^{-4}$ $-4x10^{-6}$	Anderson, 1981.
UE-25 a#1	Prow Pass Member of Crater Flat Tuff	12	$1x10^{-3}$ $-2x10^{-5}$	Anderson, 1981.
UE-25 a#1	Bullfrog Member of Crater Flat Tuff	3	$1x10^{-3}$ $-2x10^{-4}$	Anderson, 1981.
UE-25 b#1	Topopah Spring	1	$8x10^{-7}$	Lahoud et al., 1984.
USW G-4	Prow Pass Member of Crater Flat Tuff	18	$1x10^{-3}$ $-6x10^{-7}$	Peters et al., 1984.
USW G-4	Bullfrog Member of Crater Flat Tuff	6	$2x10^{-4}$ $-5x10^{-4}$	Peters et al., 1984.
USW H-1	Prow Pass Member of Crater Flat Tuff	3	$1x10^{-4}$ $-6x10^{-5}$	Rush et al., 1984.
USW H-1	Bullfrog Member of Crater Flat Tuff	9	$1x10^{-3}$ $-3x10^{-5}$	Rush et al., 1984.
USW H-1	Tram Member of Crater Flat Tuff	9	$4x10^{-4}$ $-4x10^{-6}$	Rush et al., 1984.
USW H-1	Lithic Ridge Tuff	2	$3x10^{-4}$ $-6x10^{-5}$	Rush et al., 1984.

Results of laboratory measurements of the saturated matrix hydraulic conductivity. Tuff "pile" - Yucca Mountain.

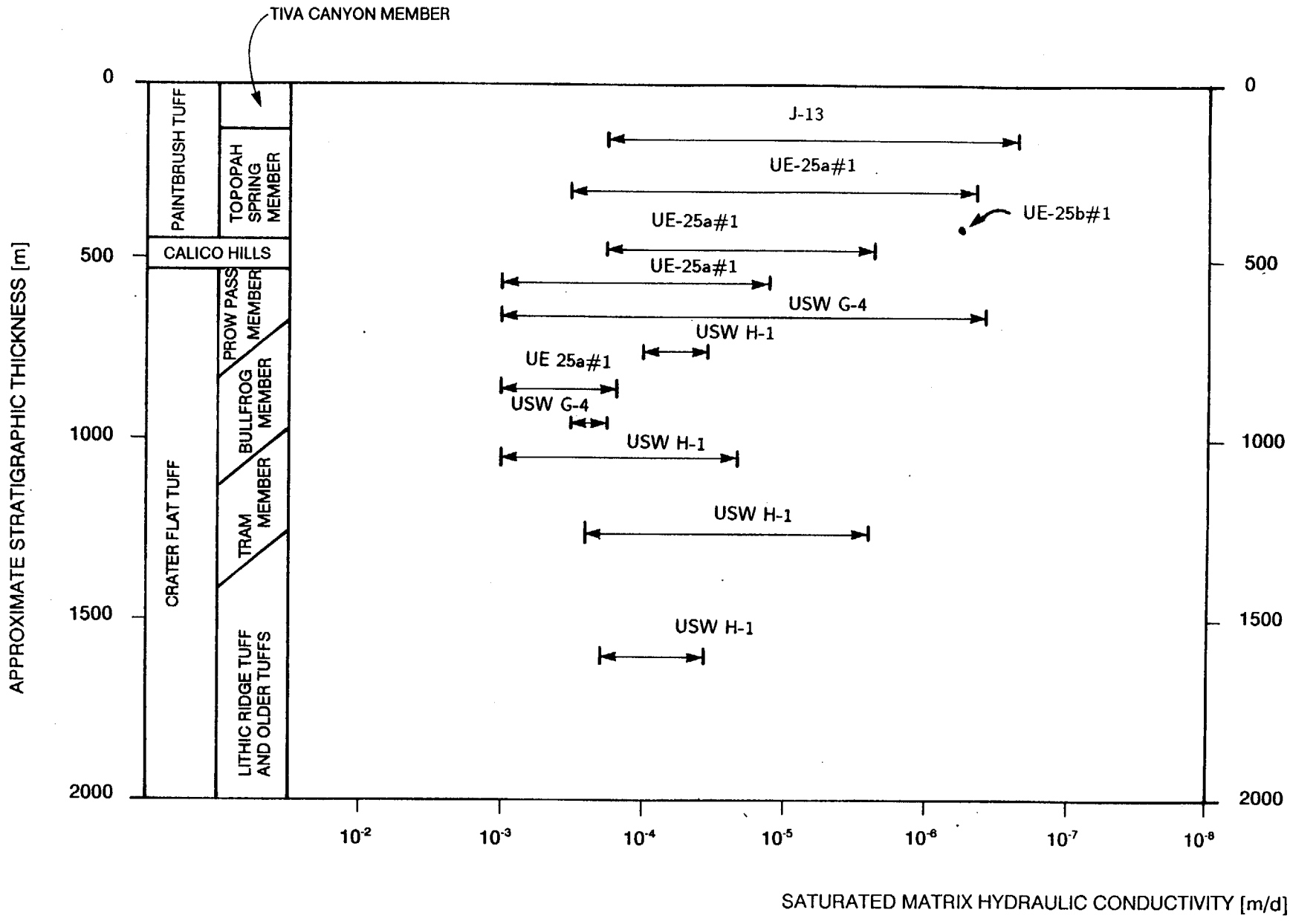

Laboratory values of saturated matrix hydraulic conductivity as a function of stratigraphic depth. Tuff "pile" - Yucca Mountain.

Well No.	Stratigraphic Unit	Thickness (m)	Transmissivity (m^2/d)			Average Hydraulic Conductivity (m/d)	Source
			Specific Capacity	Drawdown Curve	Recovery Curve		
79-69a	Carrara Formation	49	$1x10^4$			204	Winograd and Thordarson, 1975.
79-69	Carrara Formation	34	75			2.2	Winograd and Thordarson, 1975.
67-73	Bonanza King Formation	86	100	250	660	1.16	Winograd and Thordarson, 1975.
67-68	Bonanza King Formation	117	75	490	1100	0.64	Winograd and Thordarson, 1975.
66-75	Nopah Formation	224	50	140	330	0.22	Winograd and Thordarson, 1975.
88-66	Pogonip Group	266	9	16	66	0.03	Winograd and Thordarson, 1975.
75-73	Pogonip Group	229	7	47		0.03	Winograd and Thordarson, 1975.
73-66	Silurian Dolomite	80	740			9.25	Winograd and Thordarson, 1975.
87-62	Devil's Gate Limestone	172	12			0.07	Winograd and Thordarson, 1975.
84-68d	Devonian Dolomite	62	9			0.14	Winograd and Thordarson, 1975.

Pumping test data for carbonate aquifers at the Nevada Test Site and vicinity.

Well No.	Stratigraphic Unit	Thickness (m)	Transmissivity (m^2/d)			Average Hydraulic Conductivity (m/d)	Source
			Specific Capacity	Drawdown Curve	Recovery Curve		
81-67	Bedded Tuff of Piapi Canyon Group	35	12	16	26	0.34	Winograd and Thordarson, 1975.
90-74	Bedded Tuff of Piapi Canyon Group	55	2			0.04	Winograd and Thordarson, 1975.
90-75	Bedded Tuff of Piapi Canyon Group	59	5			0.08	Winograd and Thordarson, 1975.
75-58	Topopah Spring	45	1240			27.5	Winograd and Thordarson, 1975.
74-57	Topopah Spring	161	500	850		3.1	Winograd and Thordarson, 1975.
81-69	Topopah Spring	51	2.5		0.6	0.04	Winograd and Thordarson, 1975.
74-61	Basalt of Kiwi Mesa	34	50	350		1.47	Winograd and Thordarson, 1975.
J-13	Topopah Spring	167	120			0.7	Thordarson, 1983.
USW VH-1	Paintbrush Tuff - Crater Flat Tuff	579	2000			3.45	Thordarson and Howells, 1987.
USW H-4	Paintbrush Tuff - Crater Flat Tuff	700			790	1.1	Whitfield et al, 1975.

Pumping test data for tuff "pile" at the Nevada Test Site and vicinity.

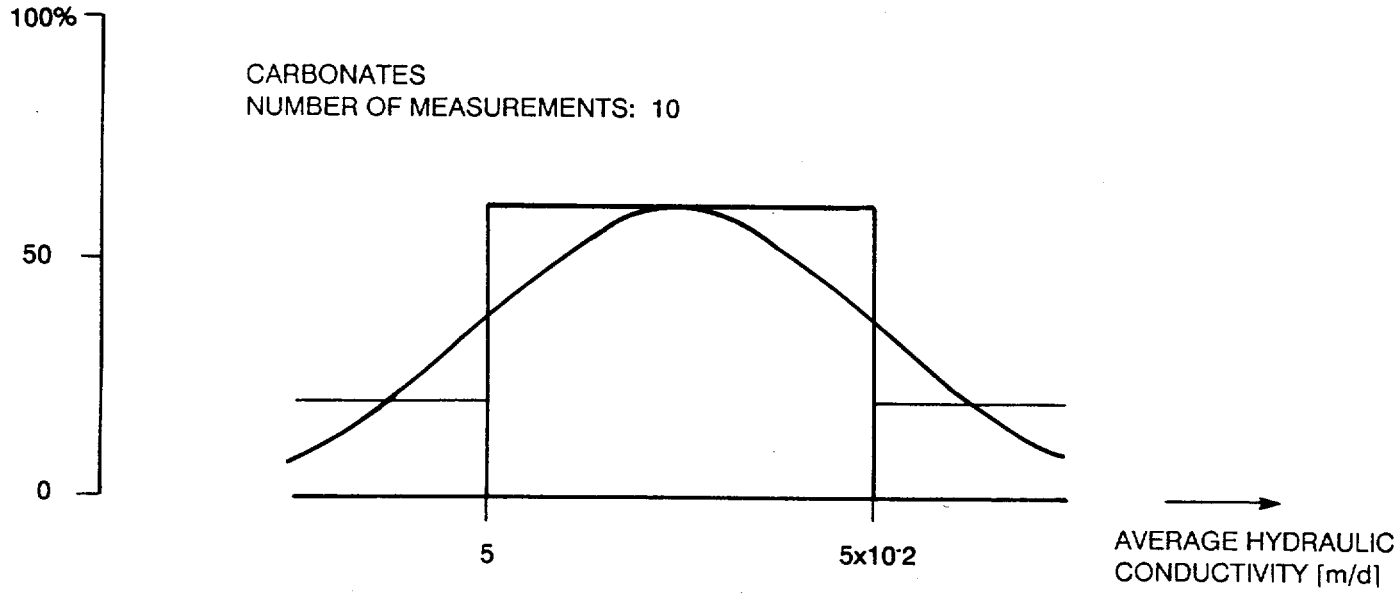

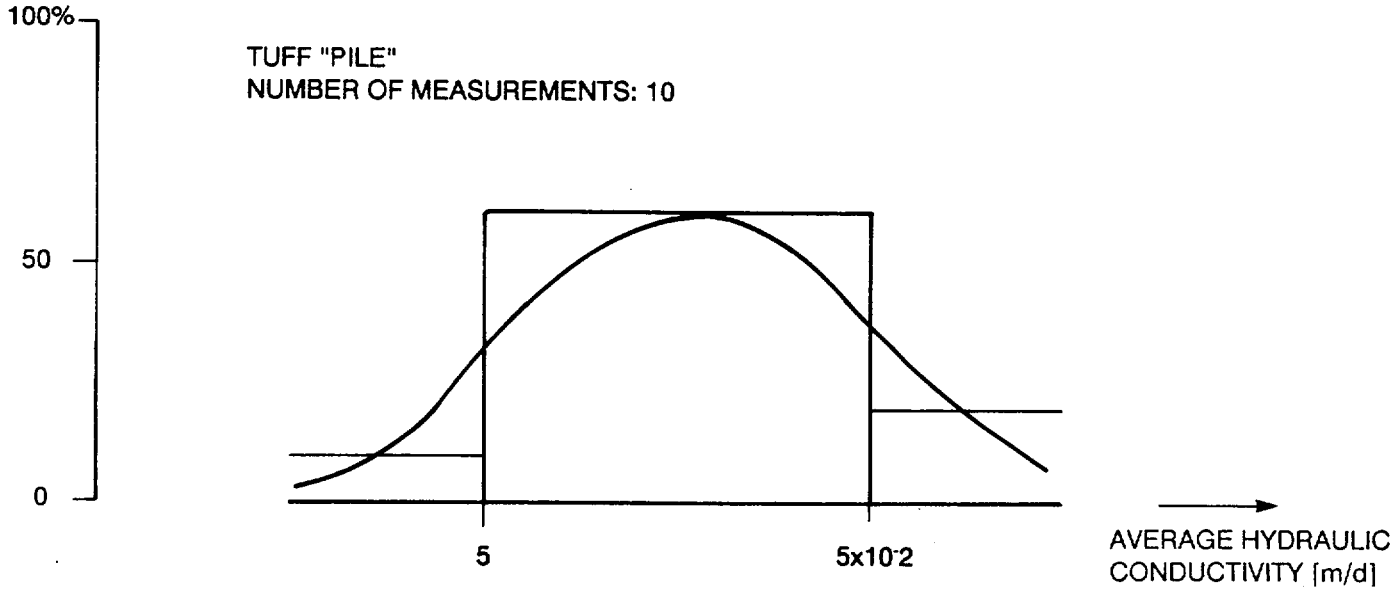

Comparison of values of hydraulic conductivity in carbonates with values of hydraulic conductivity in tuff "pile". All conductivity data are based on pumping tests.

Elevation (m)	Depth (m)	Stratigraphic Section	Interval Tested	Thickness (m)	Transmissivity (m^2/d)	Average Hydraulic Conductivity (m/d)	Source
			Injection Test				
1302	1829	0-459. Paintbrush 0-29. Tiva 29-459. Topopah 459-566. Calico Hills. 566-1829. Crater Flat 566-707. Prow Pass 707-832. Bullfrog 832-1235. Tram. 1235-1829. Lithic Ridge and older tuffs.	687-697	10	$1x10^{-1}$	10^{-2}	Rush et al., 1984.
			811-926	115	$5x10^{-3}$	$4x10^{-5}$	
			926-1200	274	$<2x10^{-3}$	$<7x10^{-6}$	
			1200-1407	207	$<2x10^{-3}$	$<1x10^{-5}$	
			1407-1621	214	$8x10^{-4}$	$4x10^{-6}$	
			1621-1829	208	$2x10^{-4}$	$1x10^{-6}$	
			Pumping Test				
			572-597	25	74	3	
			597-616	19	18	1	
			616-652	36	40	1	
			652-653	1	18	18	

Well H-1 - Hydraulic conductivity data based on Cooper-Bredehoeft injection tests and pumping tests.

Elevation (m)	Depth (m)	Stratigraphic Section	Interval Tested	Thickness (m)	Transmissivity (m^2/d)	Average Hydraulic Conductivity (m/d)	Source
			Pumping Test Continued				
			653-688	35	<1	$<3x10^{-2}$	
			687-694	7	$1x10^{-1}$	$1x10^{-2}$	
			694-736	42	$<1x10^{-2}$	$<2x10^{-4}$	
			736-741	5	$6x10^{-1}$	$1x10^{-1}$	
			741-758	17	$2x10^{-1}$	$1x10^{-2}$	
			758-792	34	$1x10^{-2}$	$3x10^{-4}$	
			792-811	19	$<3x10^{-3}$	$<2x10^{-4}$	

Well H-1 - Hydraulic conductivity data based on Cooper-Bredehoeft injection tests and pumping tests.

Elevation (m)	Depth (m)	Stratigraphic Section	Interval Tested	Thickness (m)	Transmissivity (m^2/d)	Average Hydraulic Conductivity (m/d)	Source
1483	1219	0-424. Paintbrush 0-120. Tiva 120-424. Topopah 424-453. Calico Hills. 453-1219. Crater Flat 453-580. Prow Pass 580-755. Bullfrog 755-1109. Tram 1109-1209. Lithic Ridge Tuff.	Injection Test				Thordarson, et al.,1985
			792-850	58	1.2	$2x10^{-2}$	
			851-917	66	$2x10^{-2}$	$3x10^{-4}$	
			911-972	61	av. $4.5x10^{-2}$	$7.3x10^{-4}$	
			1063-1124	61	av. $6.5x10^{-2}$	$1x10^{-3}$	
			1126-1219	93	$1x10^{-2}$	$1x10^{-4}$	
			Pumping Test				
			754-1219	465	$5x10^{-1}$	$1x10^{-3}$	
			822-1219	397	1.0	$2.5x10^{-3}$	
			Swabbing				
			729-1219	427	1.1	$2.5x10^{-3}$	
			1063-1124	61	$1x10^{-1}$	$1.6x10^{-3}$	

Well H-3 - Hydraulic conductivity data based on Cooper-Bredehoeft injection tests, pumping tests, and swabbing tests.

Elevation (m)	Depth (m)	Stratigraphic Section	Interval Tested	Thickness (m)	Transmissivity (m^2/d)	Average Hydraulic Conductivity (m/d)	Source
			Pumping Test				
1249	1219	0-400. Paintbrush 0-62. Tiva 62-400. Topopah 400-496. Calico Hills 496-1219. Crater Flat 496-693. Prow Pass 693-812. Bullfrog 812-1164. Tram 1164-1219. Lithic Ridge Tuff.	561-584	23.5	11.5	0.49	Whitfield et al., 1985.
			623-639	16.0	18.6	1.16	
			643-669	21.0	6.9	.33	
			680-707	27	1.1	$4x10^{-2}$	
			707-733	26	55.8	2.15	
			779-785	6	8.2	1.37	
			785-805	20	10.4	.52	
			820-834	14	5.7	.41	
			834-852	18	3.4	.19	
			863-876	13	18.6	1.43	

Well H-4 - Hydraulic conductivity data based on pumping tests.

Elevation (m)	Depth (m)	Stratigraphic Section	Interval Tested	Thickness (m)	Transmissivity (m^2/d)	Average Hydraulic Conductivity (m/d)	Source
			Pumping Test Continued				
			876-881	5	1.2	.24	
			881-892	11	2.3	.12	
			892-905	13	19.8	1.52	
			911-922	11	11.6	1.05	
			922-928	6	1.2	.20	
			957-1003	46	1.4	$3x10^{-2}$	
			1181-1194	13	20.4	1.57	
			1194-1213	19	1.3	$7x10^{-2}$	
			1213-1219	6	1.6	.27	

Well H-4 - Hydraulic conductivity data based on pumping tests.

Elevation (m)	Depth (m)	Stratigraphic Section	Interval Tested	Thickness (m)	Transmissivity (m^2/d)	Average Hydraulic Conductivity (m/d)	Source
			Injection Test				
1302	1220	0-419. Paintbrush 70-79. Tiva 79-419. Topopah 419-458. Calico Hills 458-1220. Crater Flat 458-678. Prow Pass 678-874. Bullfrog 874-1130. Tram 1130-1220. Lithic Ridge Tuff.	581-607	26	$3x10^{-1}$	$1x10^{-2}$	Craig and Reed, 1987.
			606-640	34	>5	$>1.5x10^{-1}$	
			649-683	34	$2x10^{-2}$	$6x10^{-4}$	
			686-753	67	$2x10^{-1}$	$3x10^{-3}$	
			753-787	34	>5	$>1.5x10^{-1}$	
			804-838	34	$1x10^{-1}$	$4x10^{-3}$	
			835-869	34	$2x10^{-1}$	$5x10^{-3}$	
			1118-1152	34	$<3x10^{-3}$	$<5x10^{-5}$	
			1155-1220	65	$3x10^{-3}$	$5x10^{-5}$	
			Pumping Test				
			581-607	26	14	$5x10^{-1}$	
			606-640	34	140	4	

Well H-6 - Hydraulic conductivity data based on Cooper-Bredehoeft injection tests and pumping tests.

Elevation (m)	Depth (m)	Stratigraphic Section	Interval Tested	Thickness (m)	Transmissivity (m^2/d)	Average Hydraulic Conductivity (m/d)	Source
			Pumping Test Continued				
			649-683		No Flow		
			686-753		No Flow		
			753-787	34	75	2.2	
			804-838		No Flow		
			835-869		No Flow		
			871-1220		No Flow		

Well H-6 - Hydraulic conductivity data based on Cooper-Bredehoeft injection tests and pumping tests.

Elevation (m)	Depth (m)	Stratigraphic Section	Interval Tested	Thickness (m)	Transmissivity (m^2/d)	Average Hydraulic Conductivity (m/d)	Source
			Injection Test				
1200	1220	45.7-422. Paintbrush 45.7-83.8. Tiva 83.8-422. Topopah 422-570. Calico Hills 570-1220. Crater Flat 570-720. Prow Pass 720-878. Bullfrog 878-1207. Tram 1207-1220. Lithic Ridge Tuff.	504-544	40	1.4	3.5×10^{-2}	Lahoud et al., 1984.
			581-621	40	37	9.2×10^{-1}	
			621-661	40	2.1	5.3×10^{-2}	
			703-743	40	.18	4.6×10^{-3}	
			743-783	40	9.9×10^{-2}	2.5×10^{-3}	
			779-819	40	39	9.9×10^{-1}	
			820-860	40	13	3.3×10^{-1}	
			1006-1220	214	2.1×10^{-2}	9.8×10^{-5}	
			Pumping Test				
			471-1220	749	340	4.5×10^{-1}	

Well UE-25b#1 - Hydraulic conductivity data based on Cooper-Bredehoeft injection tests and pumping tests.

Elevation (m)	Depth (m)	Stratigraphic Section	Interval Tested	Thickness (m)	Transmissivity (m^2/d)	Average Hydraulic Conductivity (m/d)	Source
			Injection Test				
1113	1805	0-52. Timber Mtn. Tuff 52-381. Paintbrush Tuff 52-81. Tiva 81-381. Topopah 381-422. Calico Hills 422-1244 Crater Flat Tuff 422-548. Prow Pass 548-690. Bullfrog 690-873. Tram 873-1244. Lithic Ridge Tuff 1244-1805. Lone Mtn. Dolomite and Roberts Mtn. Formation.	384-500	116	1	8.6×10^{-3}	Craig and Robison, 1984.
			500-550	50	0.1	2×10^{-3}	
			550-600	50	2.8	5.6×10^{-2}	
			600-650	50	4	8×10^{-2}	
			640-690	50	1.1	2.2×10^{-3}	
			690-740	50	.2	4×10^{-3}	
			739-789	50	1.1	2.2×10^{-3}	
			764-834	70	.6	8.5×10^{-3}	
			834-904	70	.8	1.1×10^{-2}	
			904-974	70	.9	1.2×10^{-2}	

Well UE-25p#1 - Hydraulic conductivity data based on Cooper-Bredehoeft injection tests and pumping tests.

Elevation (m)	Depth (m)	Stratigraphic Section	Interval Tested	Thickness (m)	Transmissivity (m^2/d)	Average Hydraulic Conductivity (m/d)	Source
			Injection Test Continued				
			974-1044	70	4	$5.7x10^{-2}$	
			1044-1114	70	>5	$>7.1x10^{-2}$	
			1110-1180	70	0.1	$1.4x10^{-3}$	
			1183-1301	118	1	$8.4x10^{-3}$	
			1341-1381	40	>5	$>1.2x10^{-1}$	
			1381-1421	40	>5	$>1.2x10^{-1}$	
			1423-1463	40	>5	$>1.2x10^{-1}$	
			1463-1509	46	>5	$>1.08x10^{-1}$	
			1509-1555	46	>5	$>1.01x10^{-1}$	
			1558-1805	247	>5	$>2x10^{-2}$	

Well UE-25p#1 - Hydraulic conductivity data based on Cooper-Bredehoeft injection tests and pumping tests.

Elevation (m)	Depth (m)	Stratigraphic Section	Interval Tested	Thickness (m)	Transmissivity (m^2/d)	Average Hydraulic Conductivity (m/d)	Source
			Pumping Test				
			384-500	116	14	$1.2x10^{-1}$	
			550-600	50	0.5	$1x10^{-2}$	
			600-650	50	0.5	$1x10^{-2}$	
			640-690	50	.3	$6x10^{-3}$	
			974-1044	70	.5	$7x10^{-3}$	
			1044-1114	70	1.5	$2.1x10^{-2}$	
			1180-1301	121	7	$5.8x10^{-2}$	
			1341-1381	40	72	1.8	
			1381-1421	40	10	$2.5x10^{-1}$	
			1423-1463	40	4	$1x10^{-1}$	

Well UE-25p#1 - Hydraulic conductivity data based on Cooper-Bredehoeft injection tests and pumping tests.

Elevation (m)	Depth (m)	Stratigraphic Section	Interval Tested	Thickness (m)	Transmissivity (m^2/d)	Average Hydraulic Conductivity (m/d)	Source
			Pumping Test Continued				
			1463-1509	46	2	4.3×10^{-2}	
			1509-1555	46	13	2.8×10^{-1}	
			1554-1600	46	1	2×10^{-2}	
			1597-1643	46	1	2×10^{-2}	
			1643-1689	46	1	2×10^{-2}	
			1689-1735	46	1	2×10^{-2}	
			1735-1781	46	1	2×10^{-2}	
			1781-1805	26	2	7.6×10^{-2}	

Well UE-25p#1 - Hydraulic conductivity data based on Cooper-Bredehoeft injection tests and pumping tests.

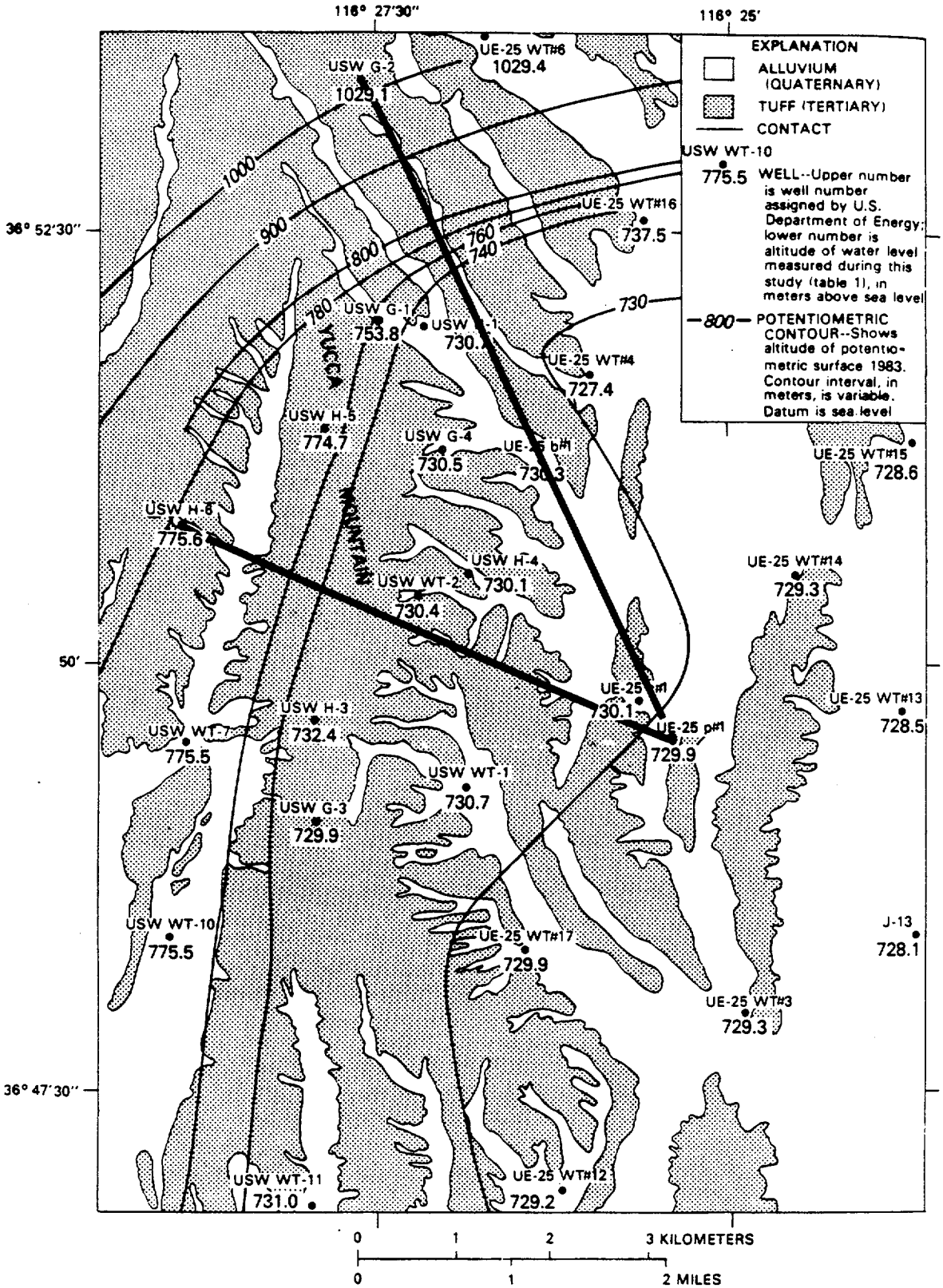

Location map for hydraulic conductivity cross-sections. Modified from Robison, 1984.

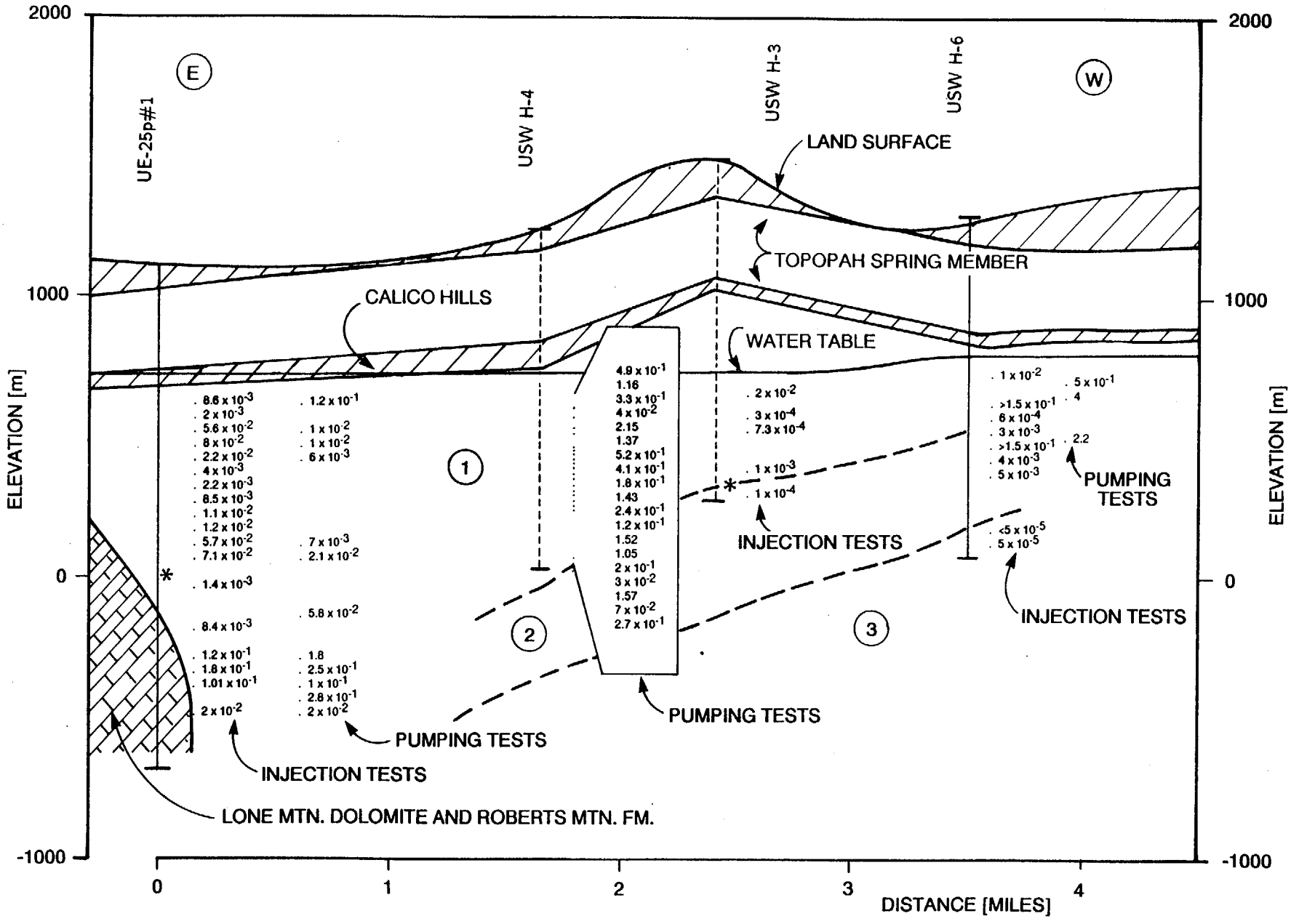

Hydraulic conductivity structure. E-W cross-section. Yucca Mountain.

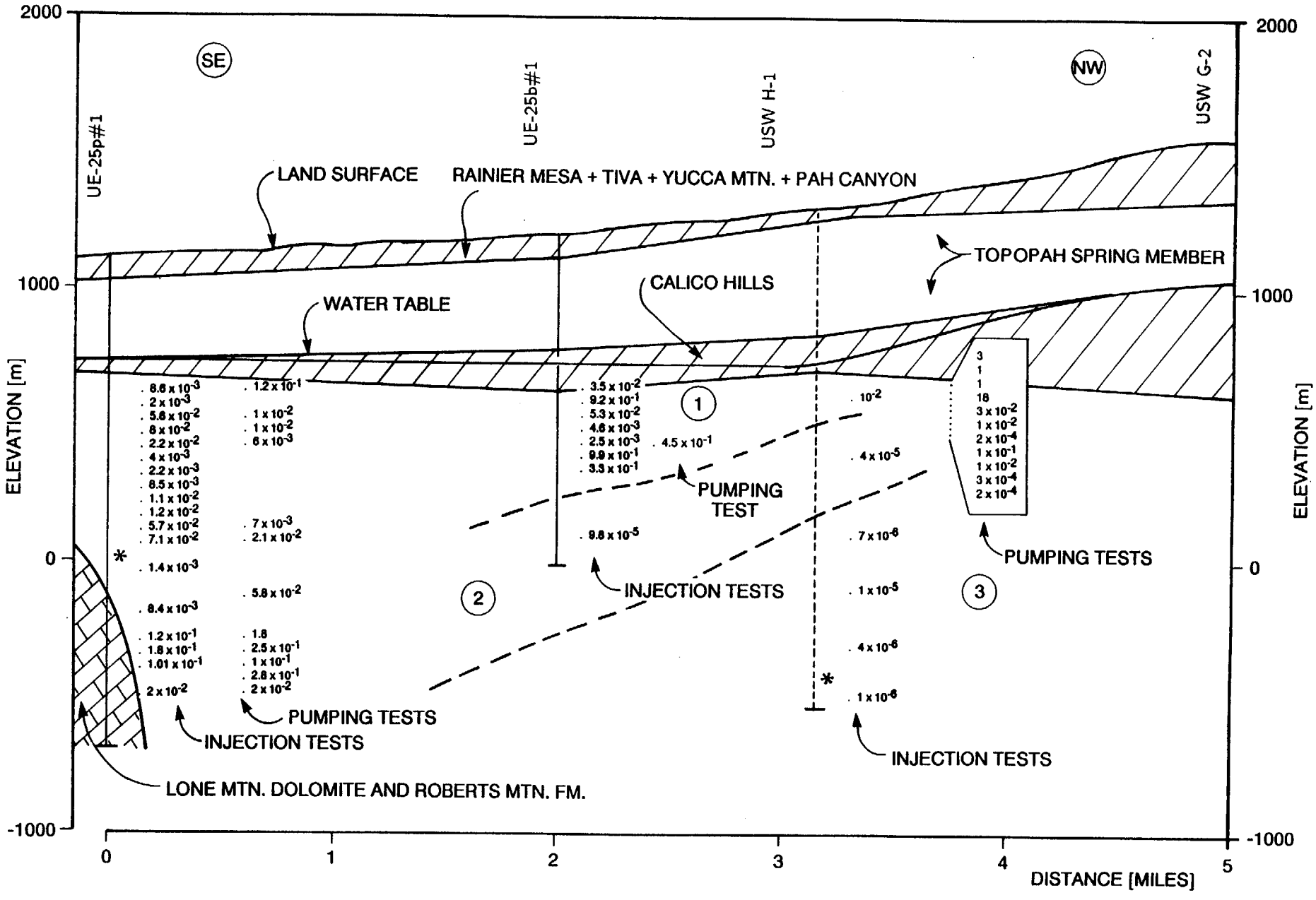

Hydraulic conductivity structure. NW-SE cross-section. Yucca Mountain.

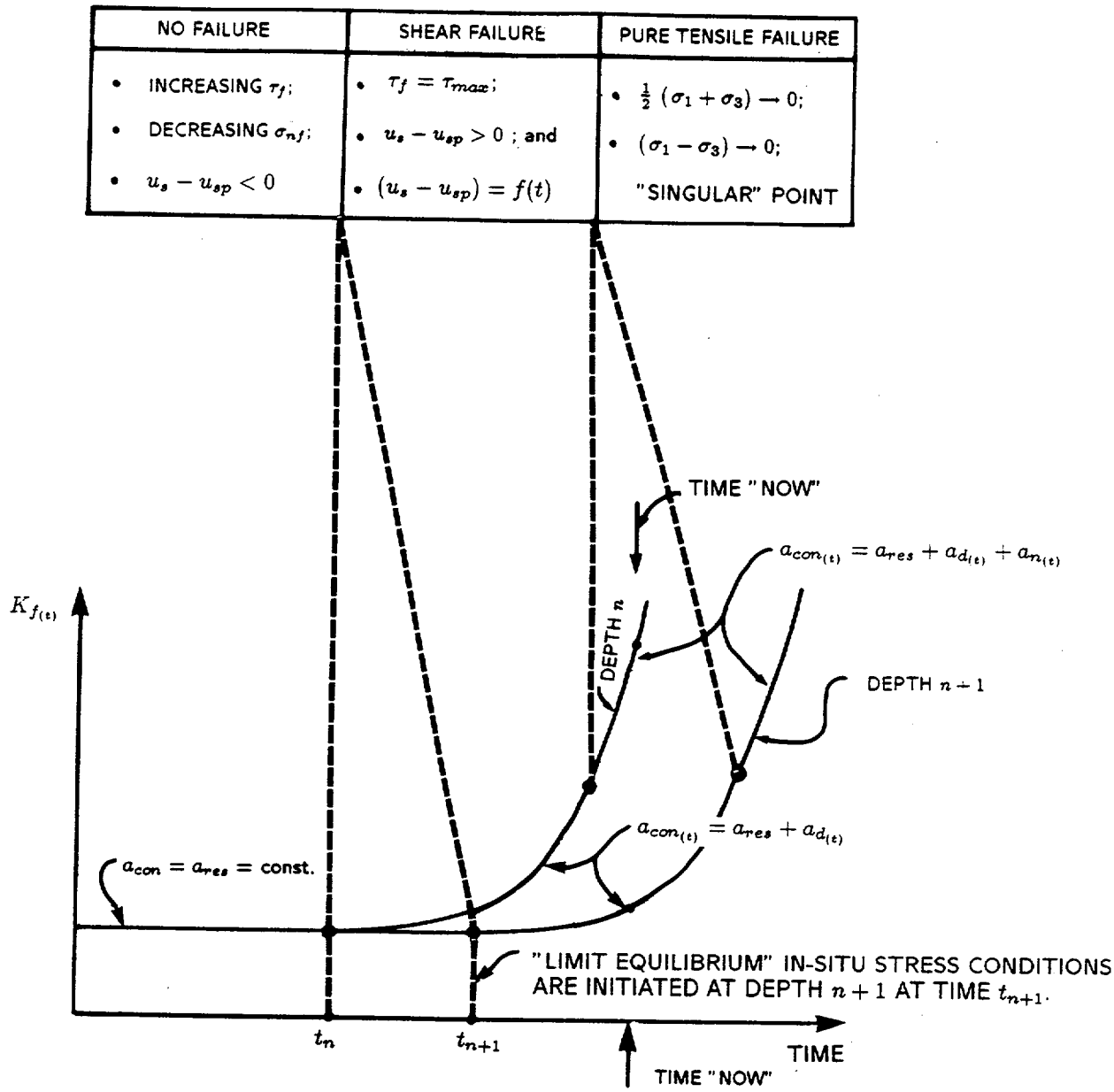

LAYER 1	$K > 10^{-2}$ m/d	H-1 ABOVE 700m; H-3 ABOVE 850m; H-4 ENTIRE DEPTH; UE-25p#1 ABOVE 500m; UE-25b#1 ABOVE 700m.
LAYER 2	$10^{-5} \leq K \leq 10^{-2}$ m/d	H-1 700m-800m; H-3 850m-BOTTOM; UE-25p#1 700m-1244m UE-25b#1 700m-1000m.
LAYER 3	$K < 10^{-5}$ m/d	H-1 800m-BOTTOM; USW H-6 800m-BOTTOM; UE-25b#1 1000m-BOTTOM

Conceptual understanding of the "three" layer hydraulic conductivity structure at Yucca Mountain.

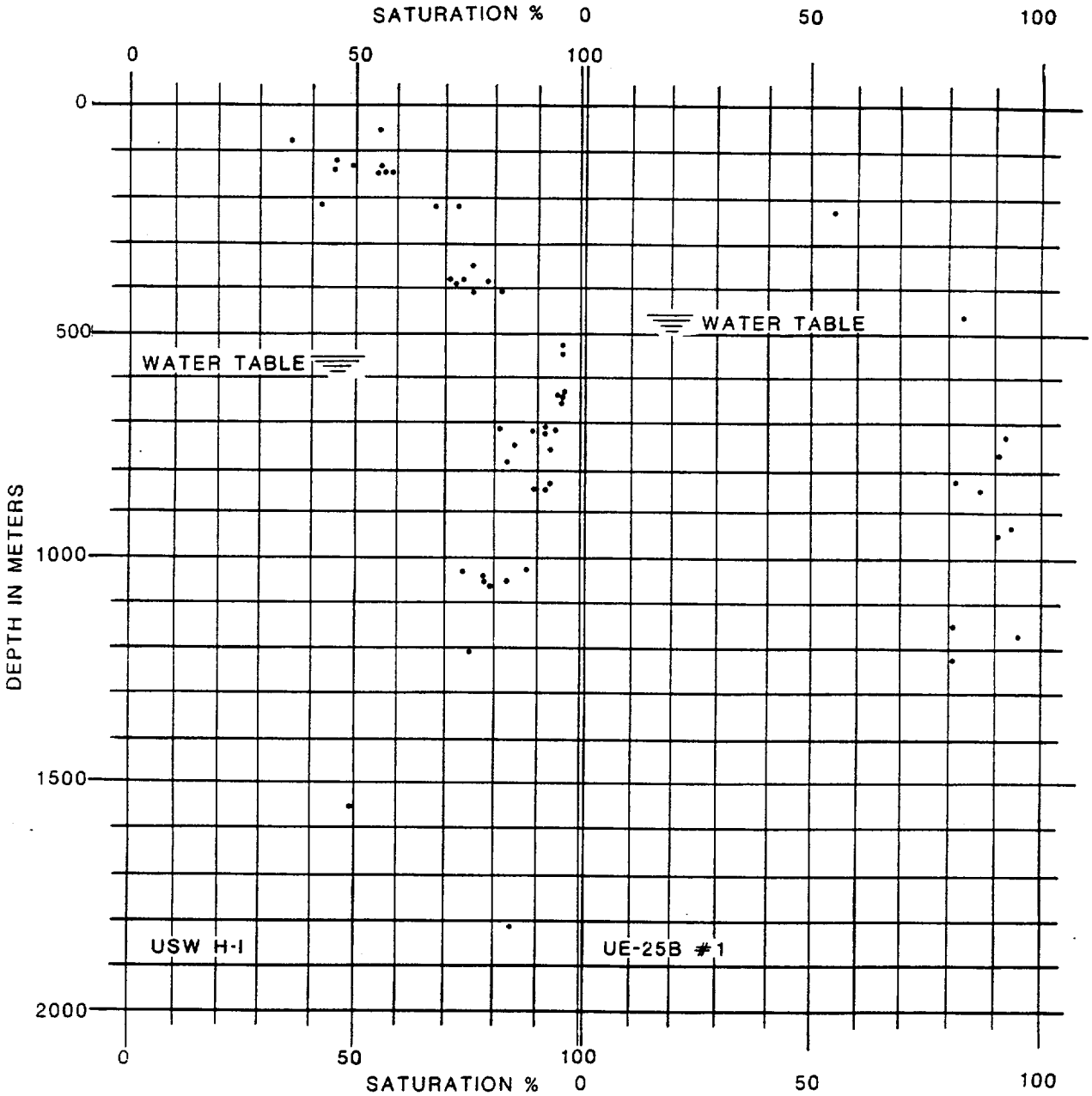

Degree of saturation above and below water table. From Lahoud et al., 1984; Rush et al., 1983.

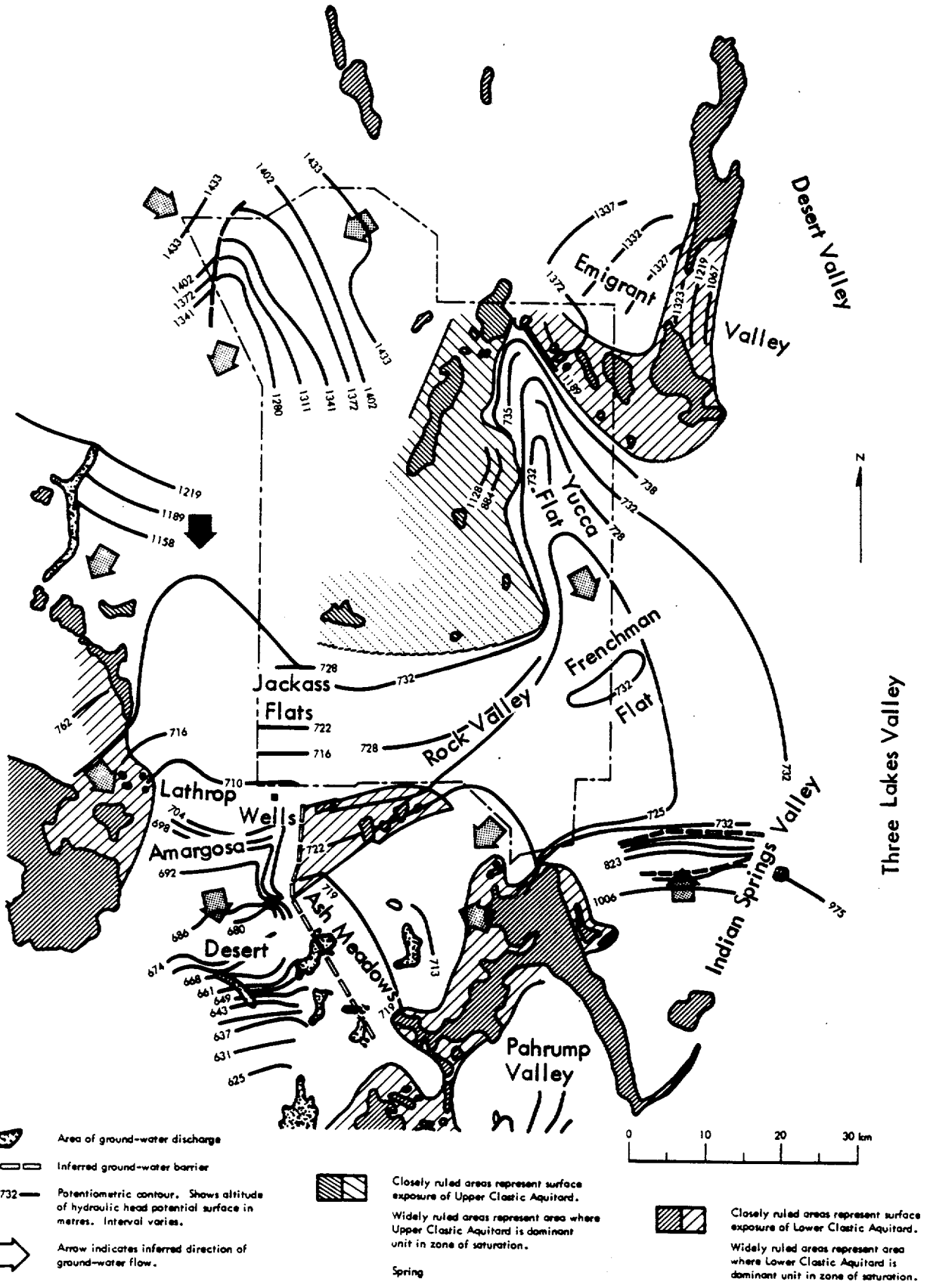

Configuration of the water table in the Death Valley groundwater system. From Winograd and Thordarson, 1975.

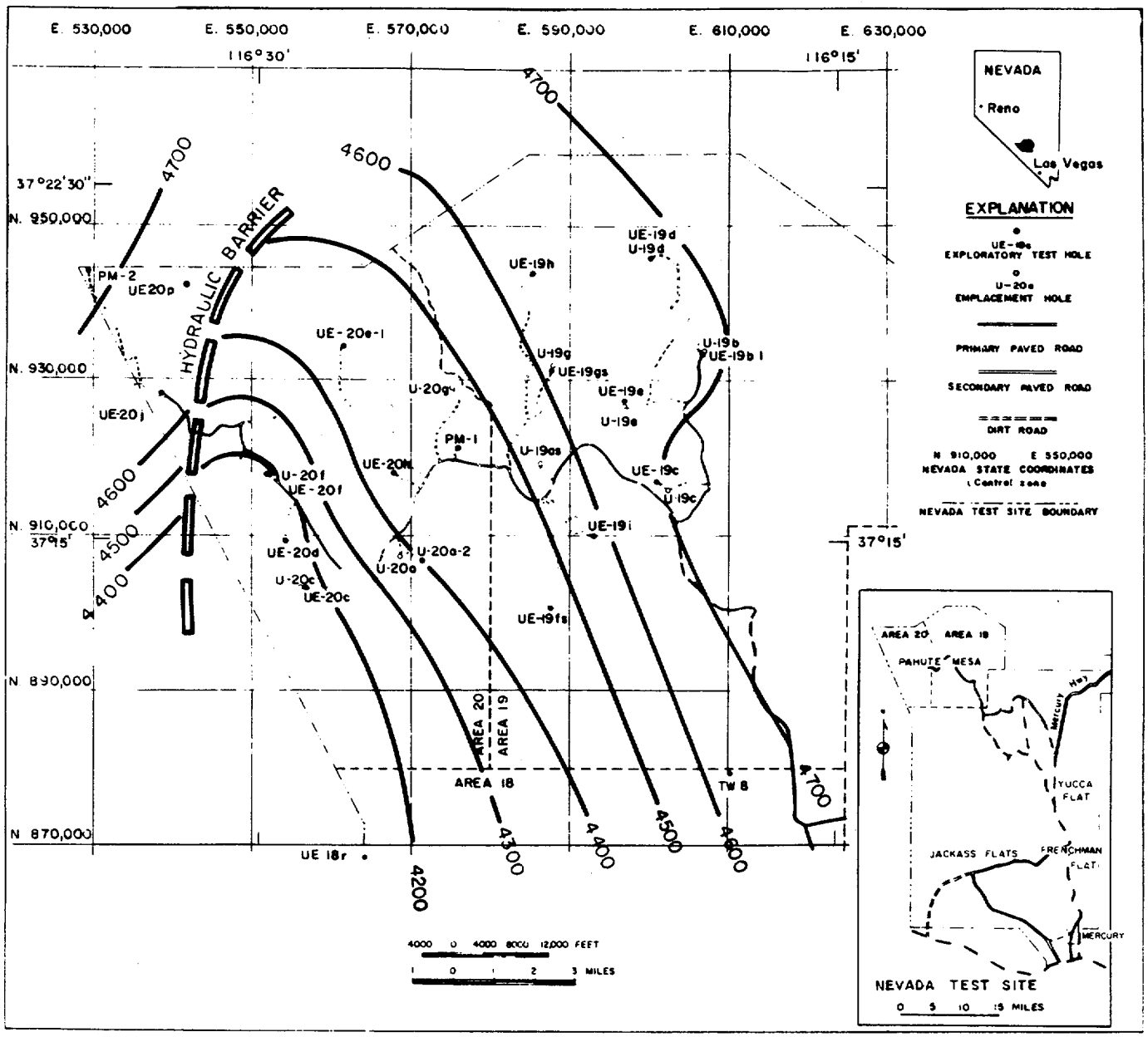

Configuration of water table in Pahute Mesa (recharge area of the Death Valley groundwater system). From Corchary and Dinwiddie, 1976.

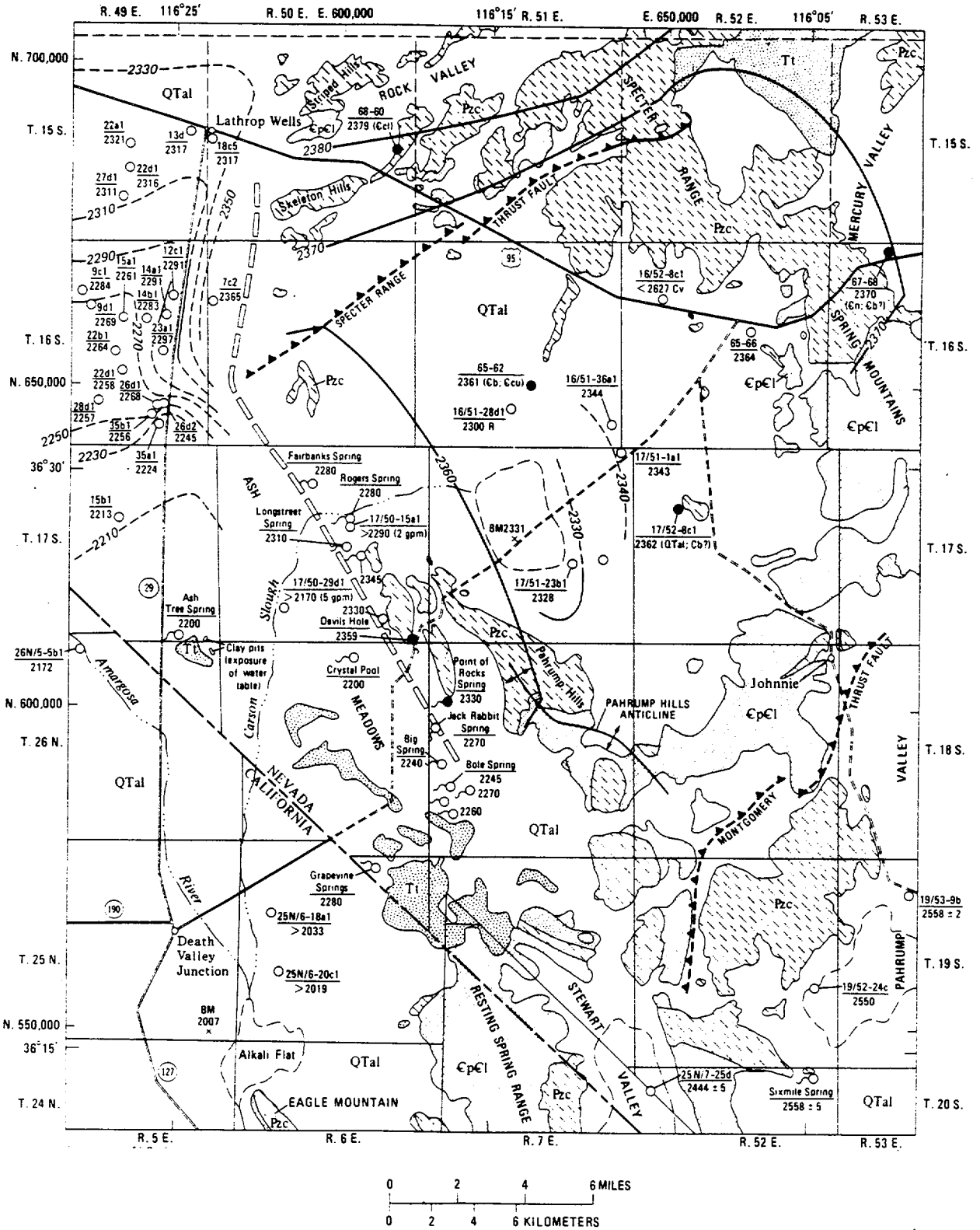

Configuration of water table in Amargosa Desert (discharge area of the Death Valley groundwater system). From Winograd and Thordarson, 1975.

QTal

Valley-fill aquifer

Alluvial fan, fluvial, fanglomerate, mudflow, playa, lake, and spring deposits; an aquitard in Ash Meadows

TERTIARY AND QUATERNARY

Tt

Tuff aquitard

Tuffaceous, fluvial, and lacustrine strata; Rocks of Paviits Spring and the Horse Spring Formation in north-northeastern part of map; sandstone, claystone, conglomerate, and tuff in southern part of map

TERTIARY

Pzc

Lower carbonate aquifer

Dolomite and limestone; minor shale and quartzite

CAMBRIAN TO DEVONIAN

€p€l

Lower clastic aquitard

Quartzite, siltstone, shale, and minor limestone

PRECAMBRIAN AND CAMBRIAN

Contact

Anticline

Thrust fault

Sawteeth on upper plate; dashed where inferred

HYDROGEOLOGIC AND GEOLOGIC UNITS

SYMBOL	GEOLOGIC UNIT	HYDROGEOLOGIC UNIT
€n	Nopah Formation	Lower carbonate aquifer
€b	Bonanza King Formation	Lower carbonate aquifer
€cu	Carrara Formation, upper part	Lower carbonate aquifer
€cl	Carrara Formation, lower part	Lower clastic aquitard

HYDRAULIC SYMBOLS

NOTE: All altitudes and contours in feet; datum is mean sea level. Areas of significant evapotranspiration are at Ash Meadows and at Alkali Flat and vicinity

07-08 / 2370 (€n; €b?)

Test well

Well tapping pre-Tertiary hydrogeologic units; upper number is well number; lower number is altitude of static water level; symbols in parentheses are formations tapped

17/52-6c1 / 2362 (QTal; €b?)

Water well

Well tapping valley-fill aquifer and lower carbonate aquifer; upper number is well number; lower number is altitude of composite static water level of both hydrogeologic units; symbols in parentheses are formations tapped

17/50-29d1 / >2170 (5 gpm)

Water well

Well tapping valley-fill aquifer; upper number is well number; lower number is altitude of static water level; R, reported water level; Cv, caved well; symbol > denotes well was flowing; flow rate is in parentheses

Devils Hole / 2350

Spring or cavern

Spring or cavern in lower carbonate aquifer (Bonanza King Formation); number is altitude of spring or of water level in cavern

Crystal Pool / 2200

Spring

Spring in Quaternary lake beds and travertine deposits; number is altitude of spring

2380

Potentiometric contour, inferred

Shows altitude of potentiometric surface in lower carbonate aquifer and lower clastic aquitard; contour interval, 10 feet

2330

Potentiometric contour

Shows altitude of potentiometric surface in valley-fill aquifer; dashed where inferred; contour interval, 20 feet; contours for southwest quadrant given on plate 1

Inferred ground-water barrier

Width of symbol not intended to represent width of hydraulic barrier, which may range from several tens to a few thousand feet

Dry lakebed

BM × 2087

BM, bench mark, showing altitude of land surface

Explanation of symbols used on Plate 4.2.3.-4. From Winograd and Thordarson, 1975.

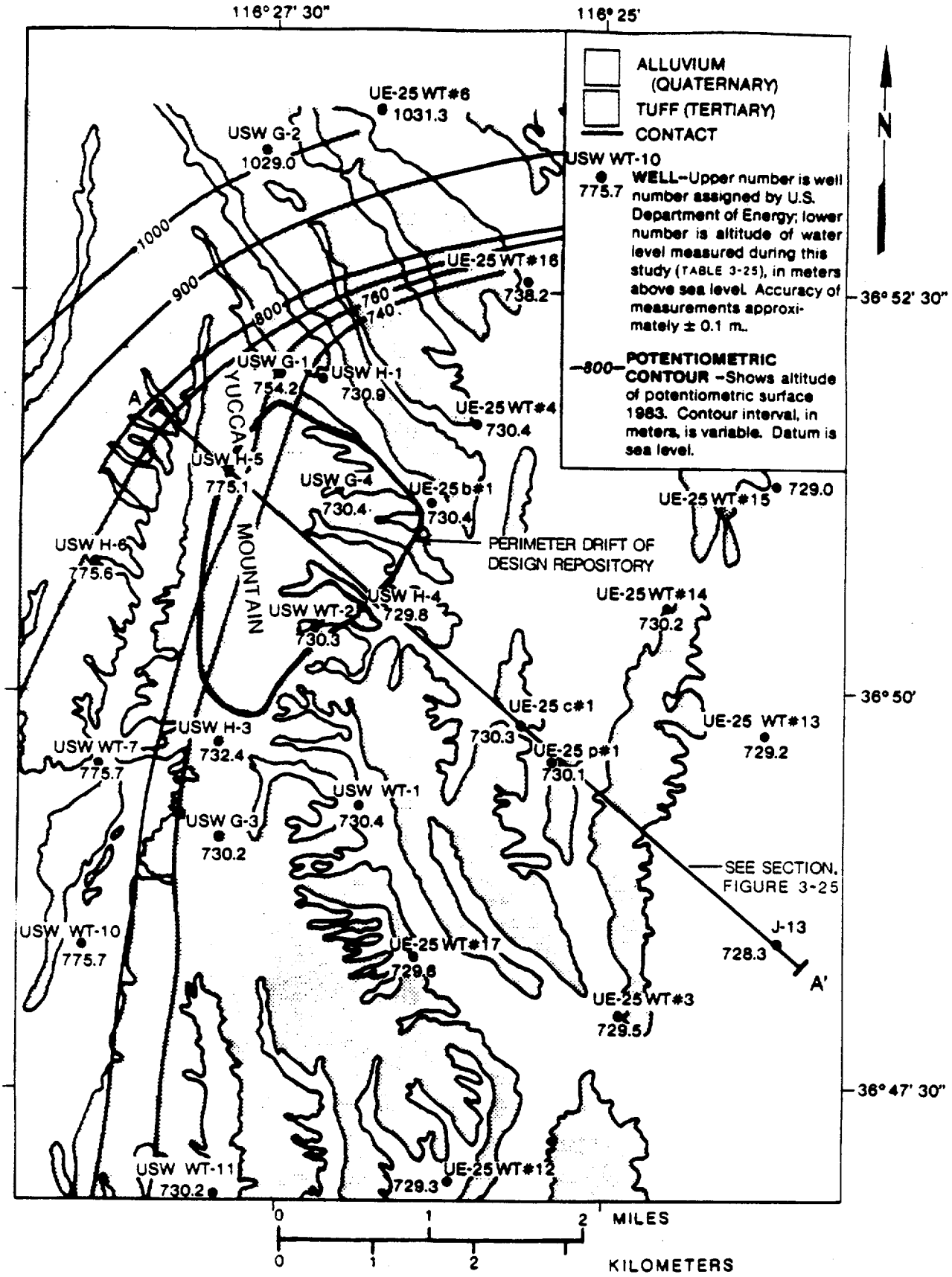

Configuration of water table at Yucca Mountain. Modified from Robison, 1986.

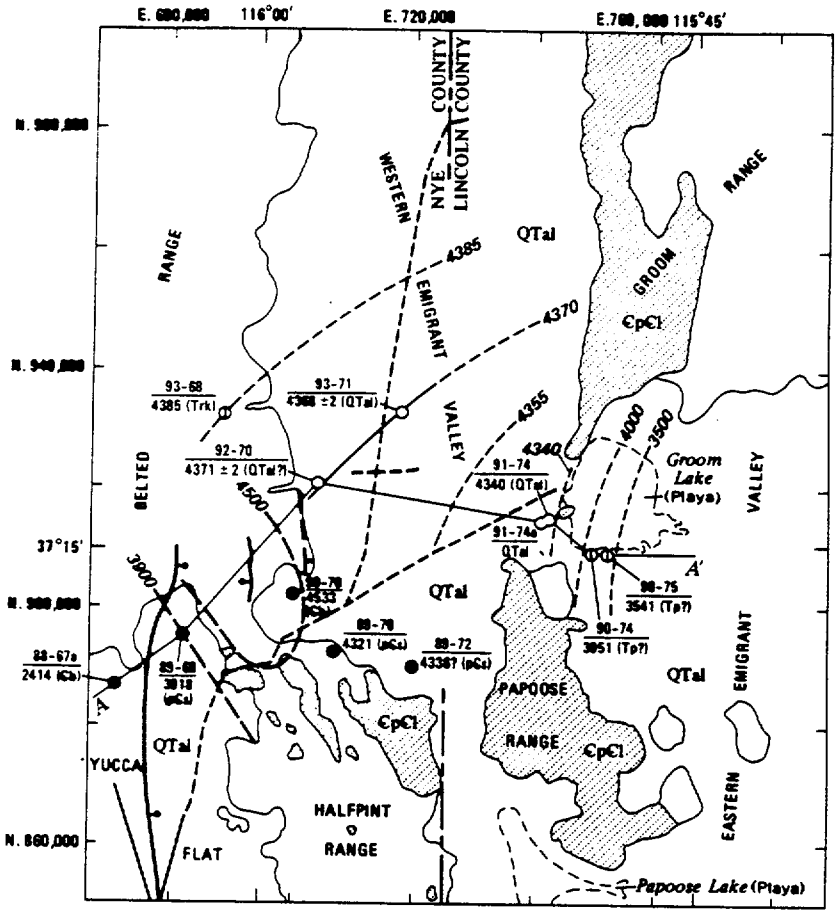

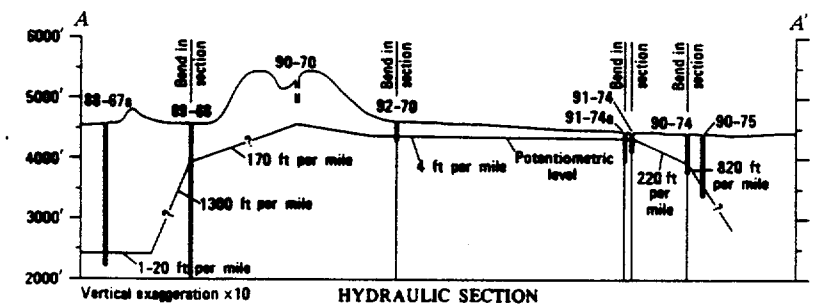

Configuration of water table in Yucca Flat and Emigrant Valley. From Winograd and Thordarson, 1975.

QTal

Valley-fill aquifer

TERTIARY AND QUATERNARY

€p€l

Lower clastic aquitard

Mostly Stirling Quartzite and Johnnie Formation but also includes lower part of Carrara Formation, Zabriskie Quartzite, and Wood Canyon Formation

PRECAMBRIAN AND CAMBRIAN

Upland area

Contact

Fault

Dashed where inferred. Bar and ball on downthrown side. Arrows indicate direction of relative movement

HYDROGEOLOGIC AND GEOLOGIC UNITS

SYMBOL	GEOLOGIC UNIT	HYDROGEOLOGIC UNIT
QTal	Quaternary and Tertiary valley fill	Valley-fill aquifer
Tpi	Piapi Canyon Group and Indian Trail Formation undifferentiated	Tuff aquifer and aquitard
Tp	Ash-fall(?) tuff of Piapi Canyon(?) Group	
Trk	Rhyolite of Kawich Valley	
Pzc	Paleozoic carbonate rocks	Lower carbonate aquifer
€b	Bonanza King Formation	
€p€l	Lower Cambrian and Precambrian clastic rocks	Lower clastic aquitard
p€s	Stirling Quartzite and Precambrian clastic and carbonate rocks	
p€n	Noonday(?) Dolomite	

HYDRAULIC SYMBOLS

Note: All altitudes and contours in feet; datum is mean sea level

89-68 / 3918 (p€s)

Test well

Well tapping pre-Tertiary hydrogeologic units: upper number is well number; lower number is altitude of static water level; symbol in parentheses is formation tapped

90-74 / 3951 (Tp?)

Test well

Well tapping Tertiary tuff aquifer; upper number is well number; lower number is altitude of static water level; symbol in parentheses is formation tapped

93-71 / 4388 ±2 (QTal)

Test well

Well tapping Quaternary and Tertiary valley-fill aquifer; upper number is well number; lower number is altitude of static water level; symbol in parentheses is formation tapped.

4370

Potentiometric contour

Shows altitude of potentiometric surface in Cenozoic hydrogeologic units; dashed where inferred; contour interval variable

4500

Potentiometric contour

Shows altitude of potentiometric surface in pre-Tertiary hydrogeologic units; dashed where inferred; contour interval variable

96-70

Test well, dashed where projected

Explanation of symbols used on Plate 4.2.3-6. From Winograd and Thordarson, 1975.

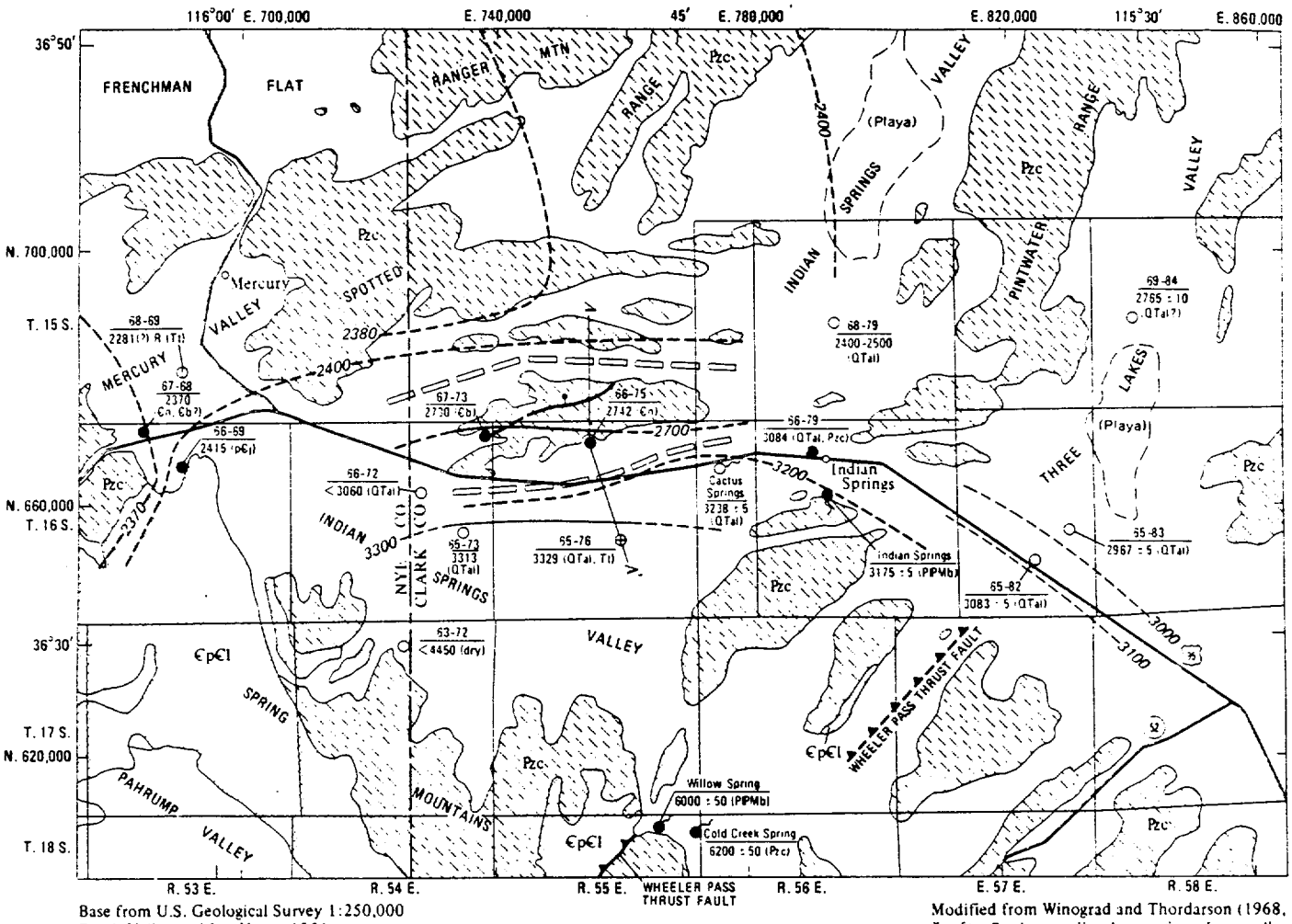

Base from U.S. Geological Survey 1:250,000
Death Valley and Las Vegas, 1954
40,000-foot grid based on Nevada
coordinate system, central zone

0 2 4 6 8 10 MILES
0 2 4 6 8 10 KILOMETERS

Modified from Winograd and Thordarson (1968, fig. 6). Rock type distribution from Longwell, Pampeyan, Bowyer, and Roberts (1965) and R. L. Christiansen, R. H. Moench, and M. W. Reynolds (written commun., Mar. 1965)

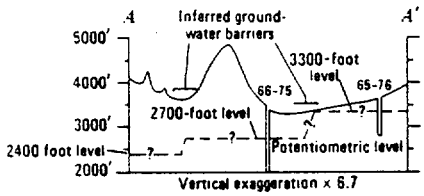

HYDRAULIC SECTION

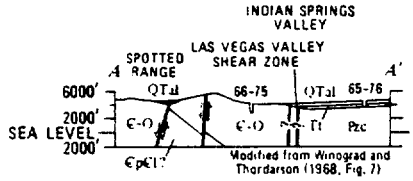

GEOLOGIC SECTION

Configuration of the water table in southern Indian Springs Valley. From Winograd and Thordarson, 1975.

Pzc

Lower carbonate aquifer

Dolomite and limestone; minor shale and quartzite; chiefly Middle Cambrian through Devonian age; in Spotted Range includes thin clastic strata, possible equivalents of Eleana Formation; in southeastern part of map includes Monte Cristo Limestone and Bird Spring Formation

CAMBRIAN TO PERMIAN

€pCl

Lower clastic aquitard

Quartzite, siltstone, shale, and minor limestone

PRECAMBRIAN AND CAMBRIAN

Contact

Fault

Dashed where inferred. Bar and ball on downthrown side. Arrows indicate direction of relative movement

Thrust fault

Sawteeth on upper plate; dashed where inferred

HYDROGEOLOGIC AND GEOLOGIC UNITS

SYMBOL	GEOLOGIC UNIT	HYDROGEOLOGIC UNIT
QTal	Valley fill	Valley-fill aquifer
Tt	Tertiary tuff, probably pre-Piapi(?) Canyon Group	Tuff aquitard
Pzc	Paleozoic carbonate rocks	Lower carbonate aquifer
PIPMb	Bird Spring Formation	
€-O	Cambrian and Ordovician carbonate rocks	
€n	Nopah Formation	
€b	Bonanza King Formation	
€pCl	Early Cambrian and Precambrian clastic rocks	Lower clastic aquitard
p€j	Johnnie Formation	

HYDRAULIC SYMBOLS

NOTE: All altitudes and contours in feet; datum is mean sea level

66-69 / 2415 (p€j)

Test well

Well tapping pre-Tertiary hydrogeologic units; upper number is well number; lower number is altitude of static water level; symbol in parentheses is formation tapped

66-79 / 3084 (QTal; Pzc)

Water well

Well tapping valley-fill and lower carbonate aquifer; upper number is well number; lower number is altitude of composite static water level of both hydrogeologic units; symbols in parentheses are formations tapped

68-69 / 2281(?) R (Tt)

Test well

Well tapping tuff aquitard; upper number is well number; lower number is altitude of static water level; R, water level reported; symbol in parentheses is formation tapped; water level reported for well 68-69 is probably inaccurate but given for completeness

66-72 / <3060 (QTal)

Test well

Well tapping valley-fill aquifer; upper number is well number; lower number is altitude of static water level; symbol < denotes dry well; symbol in parentheses is formation tapped

65-76 / 3329 (QTal; Tt)

Test well

Well tapping both valley-fill aquifer and tuff aquitard; upper number is well number; lower number is altitude of static water level; symbols in parentheses are formations tapped

Indian Springs / 3175 ± 5 (PIPMb)

Spring

Spring in, or near outcrop of, lower carbonate aquifer; above line, name of spring; below line, altitude of land surface; symbol in parentheses is formation supplying spring

Cactus Springs / 3238 ± 5 (QTal)

Spring

Spring in valley-fill aquifer; above line, name of spring; below line, altitude of land surface; symbol in parentheses is formation supplying spring

2700

Potentiometric contour

Shows altitude of potentiometric surface in lower carbonate aquifer; contour interval variable; dashed where inferred

3300

Potentiometric contour

Shows altitude of potentiometric surface in valley-fill aquifer; contour interval variable; dashed where inferred

Inferred ground water barrier along concealed fault zone

Width of symbol not intended to represent width of hydraulic barrier, which may range from several tens to a few thousand feet

Dry lakebed

66-75

Test well

Number is well number

Explanation of symbols used on Plate 4.2.3-7. From Winograd and Thordarson, 1975.

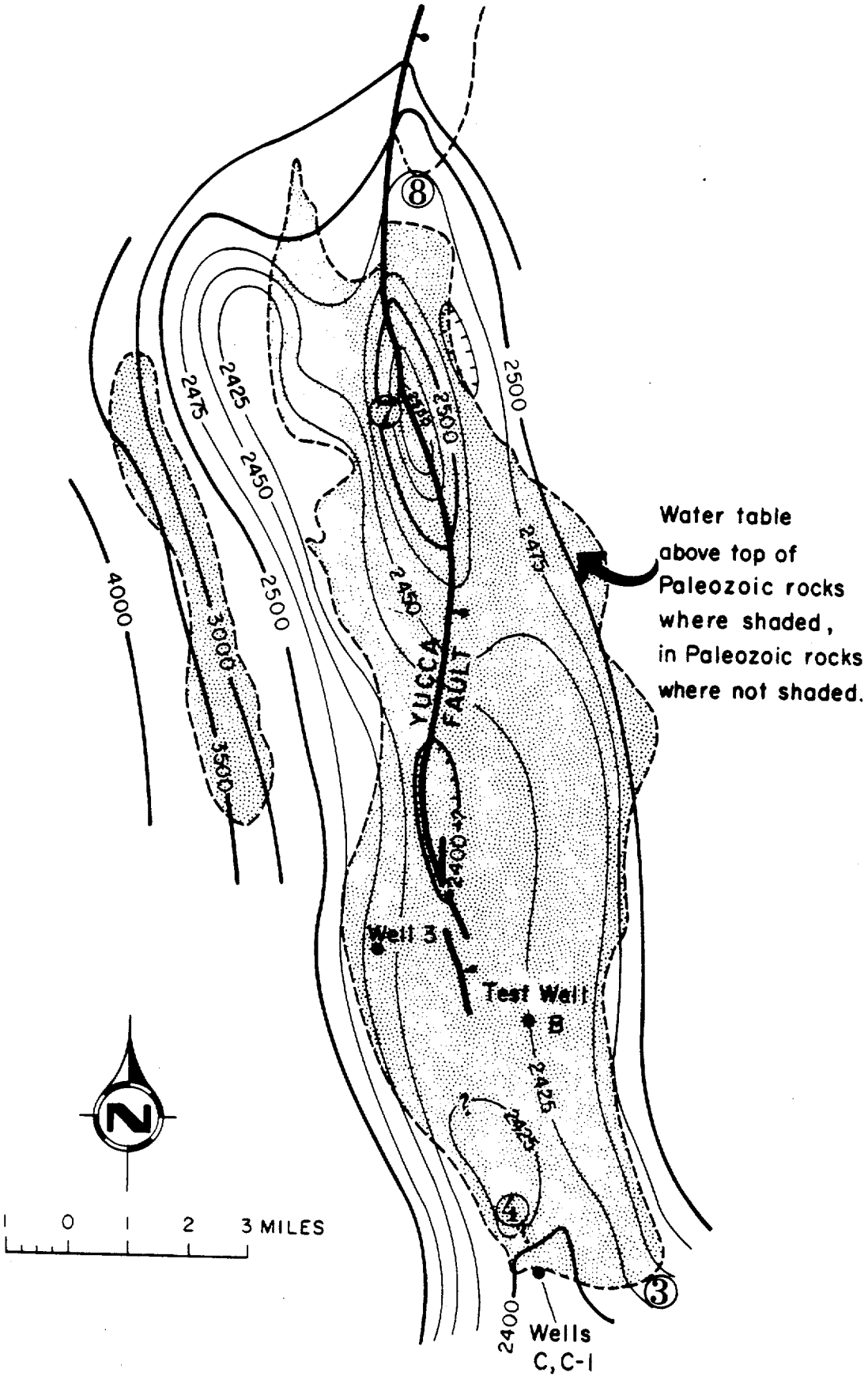

Configuration of water table in Yucca Flat. From Corchary and Dinwiddie, 1976.

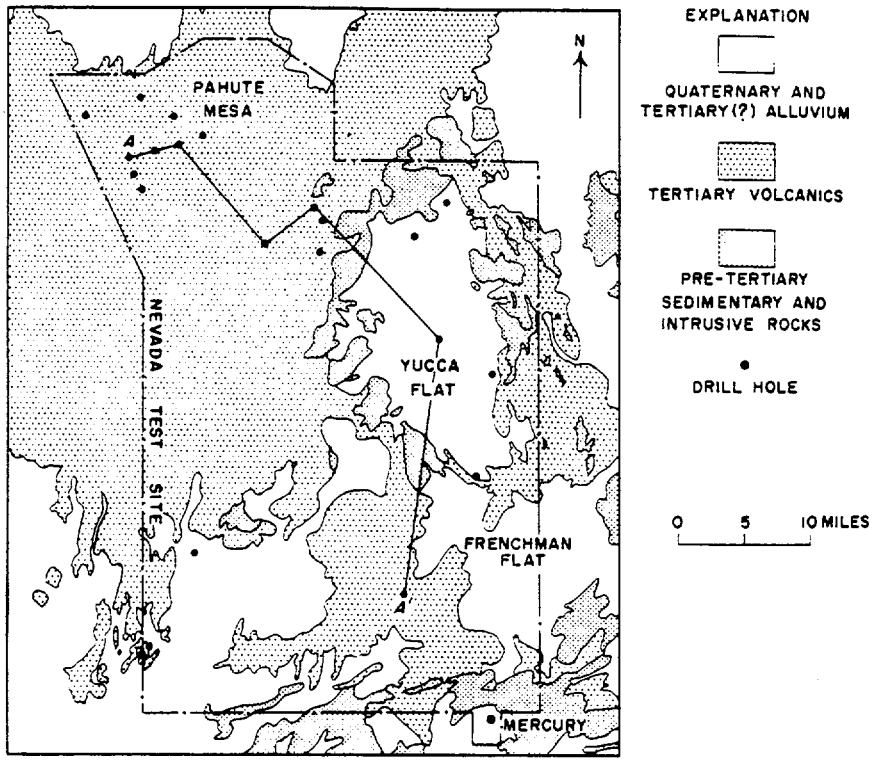

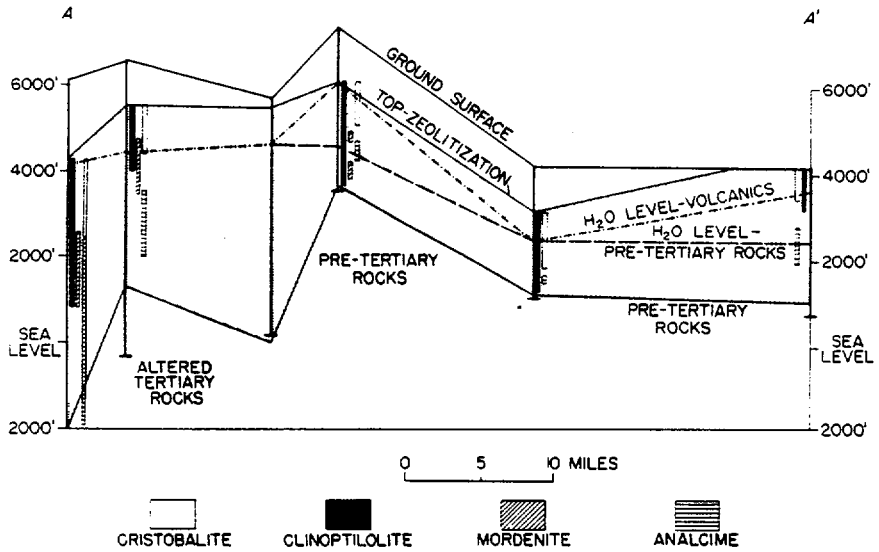

General hydrology of Yucca Flat. From Hoover, 1968.

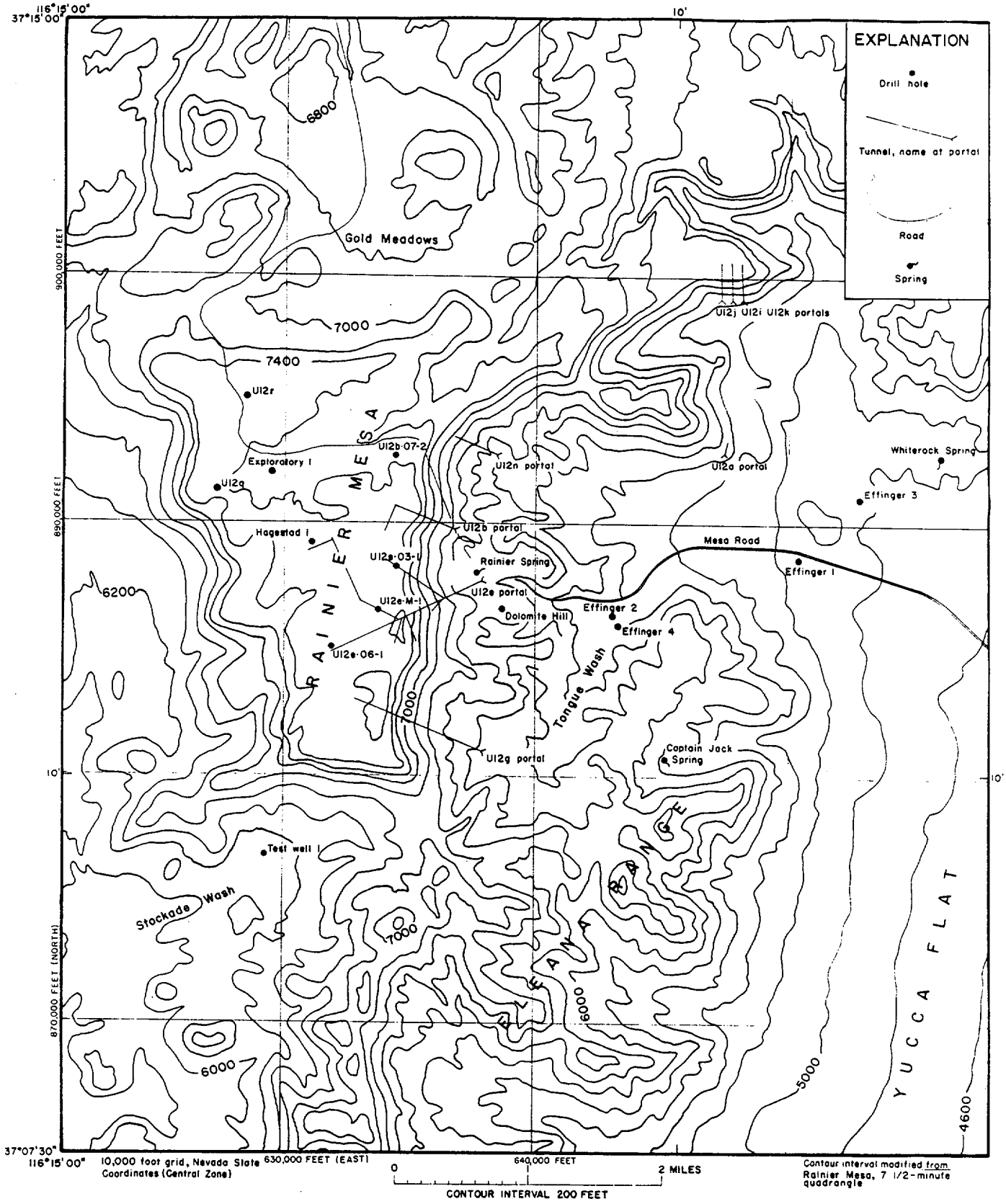

Generalized topographic map of the Rainier Mesa quadrangle, showing locations of wells: U12e.03-1; U12e.M-S; Hagestad #1; and Test Well #1. From Thordarson, 1965.

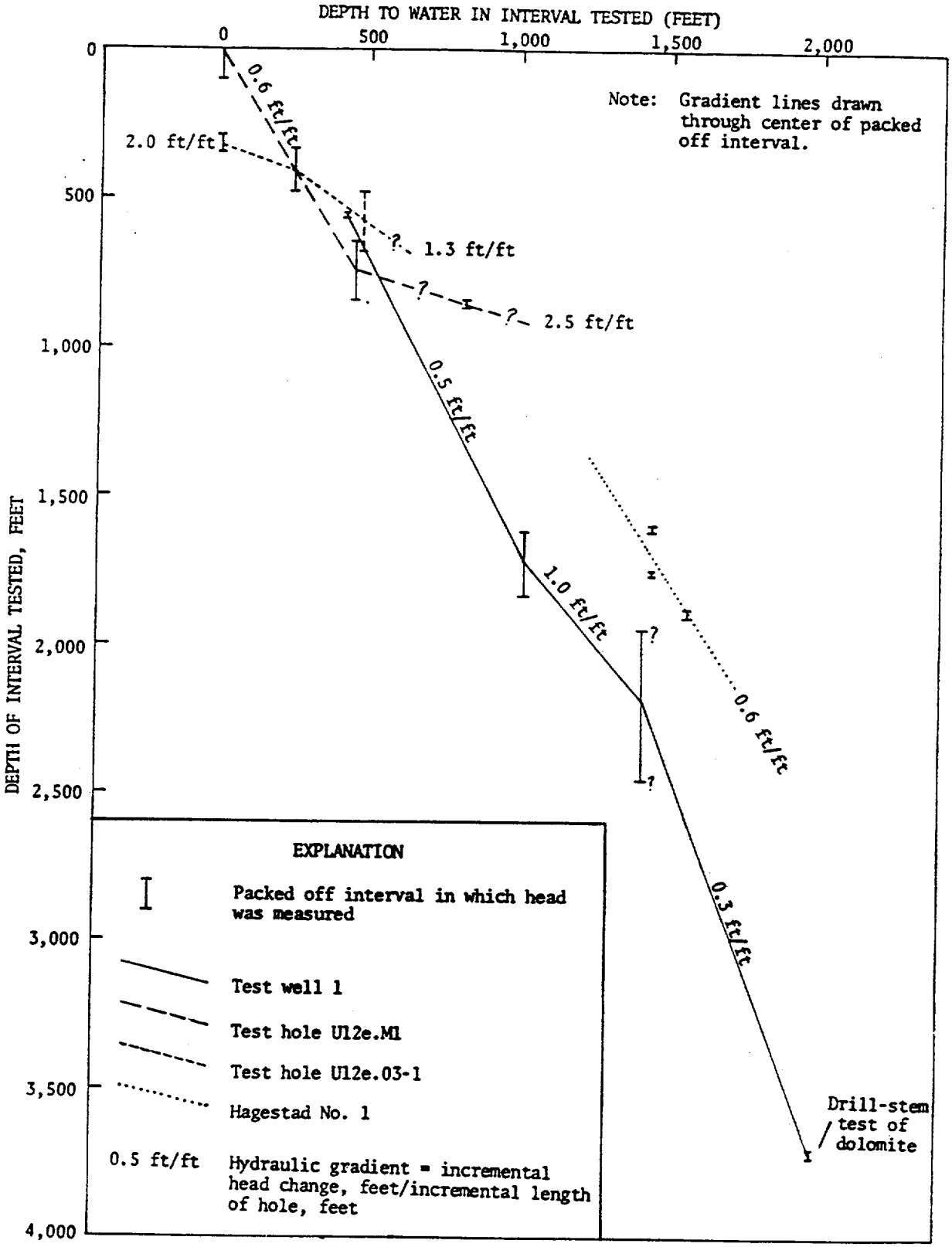

Vertical hydraulic gradients in four test wells from the area of Rainier Mesa. From Thordarson, 1965.

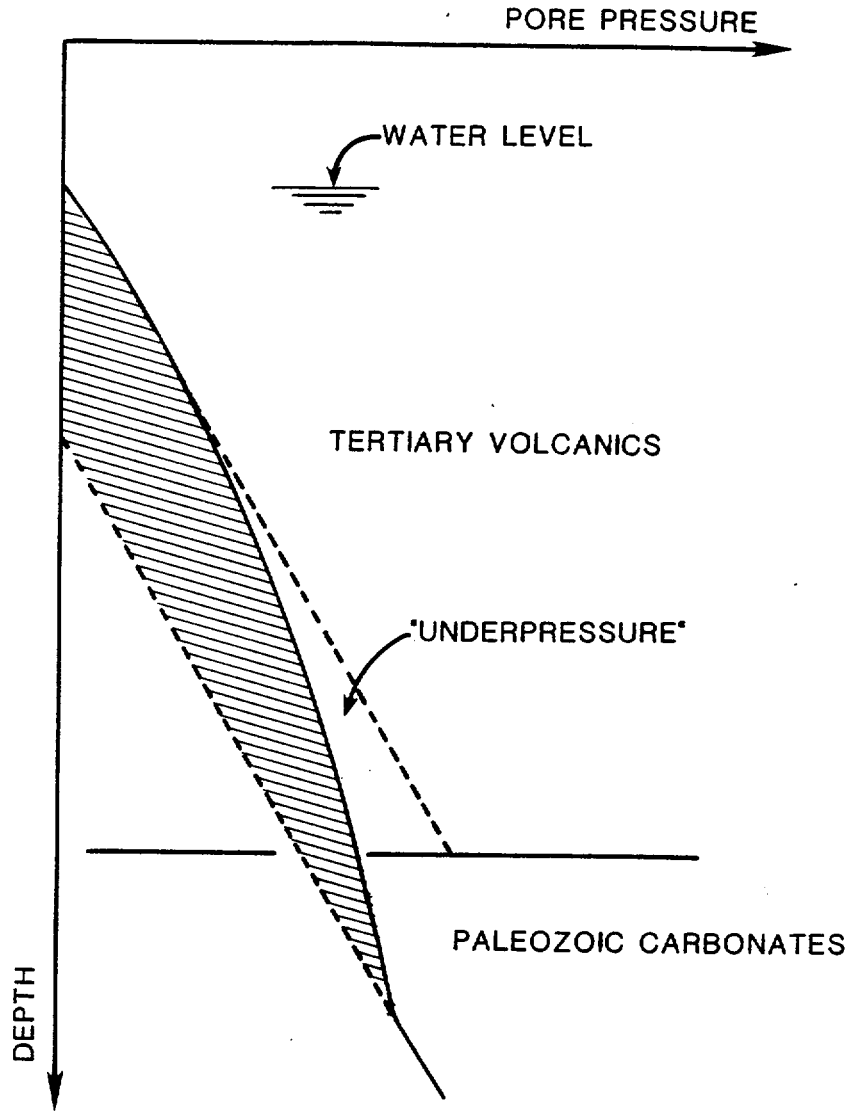

Idealized changes in pore pressure with depth. Rainier Mesa and Yucca Flat.

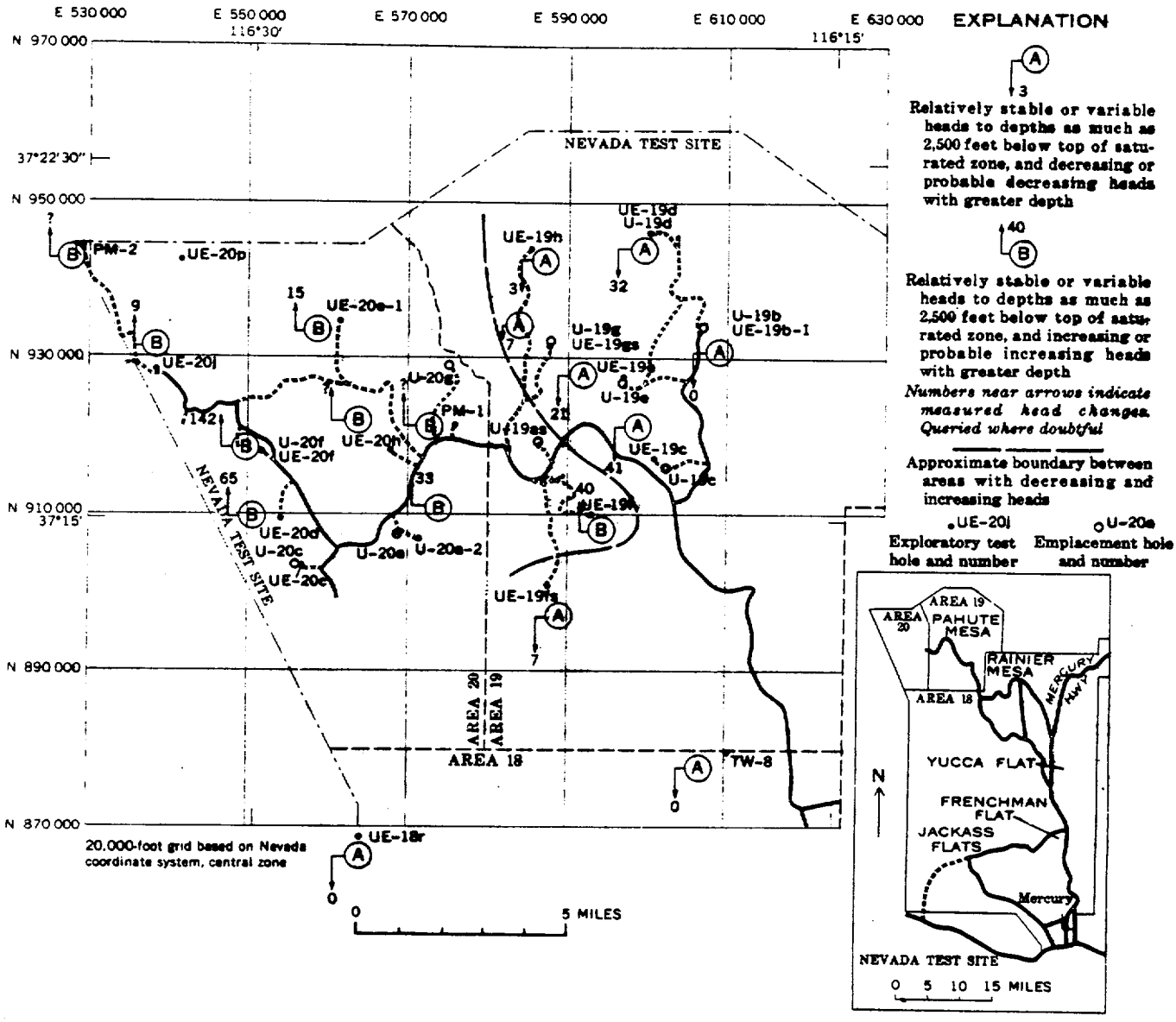

Vertical components of flow in the area of Pahute Mesa. From Blankennagel and Weir, 1973.

[All depths in feet below land surface. Intervals isolated with packers in PM-1 and PM-2 were too impermeable to yield data on head changes]

Exploratory hole	Depth to water in open hole	Interval(s) isolated with packers	Depth to water for isolated interval(s)	Principal rock types in isolated interval(s)	Depth of interval(s) with highest permeability
UE-19b-1	2,117	2,176–4,060	2,117	Rhyolite	2,610–2,640, 2,720–2,760
UE-19c	2,345	2,319–2,874	2,319(?)	Rhyolite and rhyolite breccia.	3,050–3,075
		2,884–3,284	2,348	do	
		4,033–4,231	2,360	Rhyolite	
UE-19d	2,177	2,500–3,483	2,177	Rhyolite	3,300–3,350
		3,472–3,852	2,186	do	
		3,844–4,042	2,178	do	
		4,626–4,784	2,180	do	
		4,810–4,968	2,200	do	
		5,823–6,583	2,210	do	
UE-19e	2,240	2,619–2,779	2,232	Welded tuff and zeolitized tuff.	2,650–2,690, 4,970–4,990
		4,802–6,004	2,253	do	
UE-19fs	2,305	2,750–3,218	2,302	Rhyolite	2,880–2,950, 3,150–3,160
		3,520–3,838	2,304	do	
		4,146–4,480	2,309	Rhyolite and tuff	
UE-19gs	2,045	2,802–2,970	2,043	Rhyolite	2,940–2,970, 4,786–4,790
		4,636–4,834	2,050	Welded tuff	
		6,920–7,118	2,049	Tuffaceous sandstone	
UE-19h	2,112	2,200–2,396	2,109	Rhyolite and welded tuff	2,378–2,388 (est.)
		2,408–3,705	2,112	do	
UE-19i	2,258	2,910–3,068	2,220	do	3,400–3,470, 3,750–3,765
		3,460–3,618	2,258	do	
		4,100–4,258	2,218	do	
U-20a-2	2,066	2,067–2,608	2,064	Rhyolite	2,400–2,682, 2,895–3,085, 3,648–3,838
		2,492–2,682	2,066	do	
		2,895–3,085	2,065	do	
		3,090–3,280	2,064	do	
		3,648–3,838	2,042	do	
		4,048–4,238	2,051	do	
		4,355–4,500	2,033	do	
UE-20d	2,075	2,578–2,776	2,078	Rhyolite	2,578–2,730
		4,118–4,316	2,018	do	
UE-20e-1	1,822	2,774–2,972	1,828	Rhyolite	3,550–3,660
		3,480–3,678	1,825	Rhyolite and vitrophyre	
		4,020–4,218	1,828	Zeolitized bedded tuff and welded tuff.	
		4,540–6,395	1,820	do	
UE-20f	[1]1,954	2,598–2,796	1,946	Rhyolite and vitrophyre	3,150–3,348, 4,568–4,766
		3,150–3,348	1,988	do	
		3,338–3,536	1,954	do	
		4,350–5,249	1,857	do	
		8,972–9,170	1,846	do	
UE-20h	2,116	2,575–2,743	2,111	Rhyolite	3,042–3,170, 4,040–4,060
		2,741–3,210	2,116	do	
		3,350–3,518	2,111	Zeolitized bedded tuff	
		3,705–3,873	2,114	do	
		3,892–4,060	2,116	Rhyolite breccia	
		4,070–4,238	2,117	do	
UE-20j	1,270	1,858–2,056	1,245	Welded tuff	2,060–2,150, 2,957–3,557
		2,051–2,249	1,247	do	
		2,253–2,461	1,249	do	
		2,670–2,868	1,261	do	
		2,957–3,155	1,270	do	
		3,359–3,832	1,273	do	
		4,023–5,690	1,264	Rhyolite and tuff	
UE-18r[2]	1,372	1,440–5,004	1,372	Welded tuff	1,660–1,675
				do	2,350–2,360
				Rhyolite	3,550–3,560
TW-8[2]	1,068	1,320–5,490	1,068	Rhyolite and welded tuff	1,290–2,010

[1]Depth to water when hole was drilled to 4,543 ft. After hole was cased to 4,490 ft and drilled to 13,696 ft, depth to water was 1,772 ft.
[2]South of Pahute Mesa.

Results of downhole measurements of distribution of hydraulic potentials, Pahute Mesa. From Blankennagel and Weir, 1973.

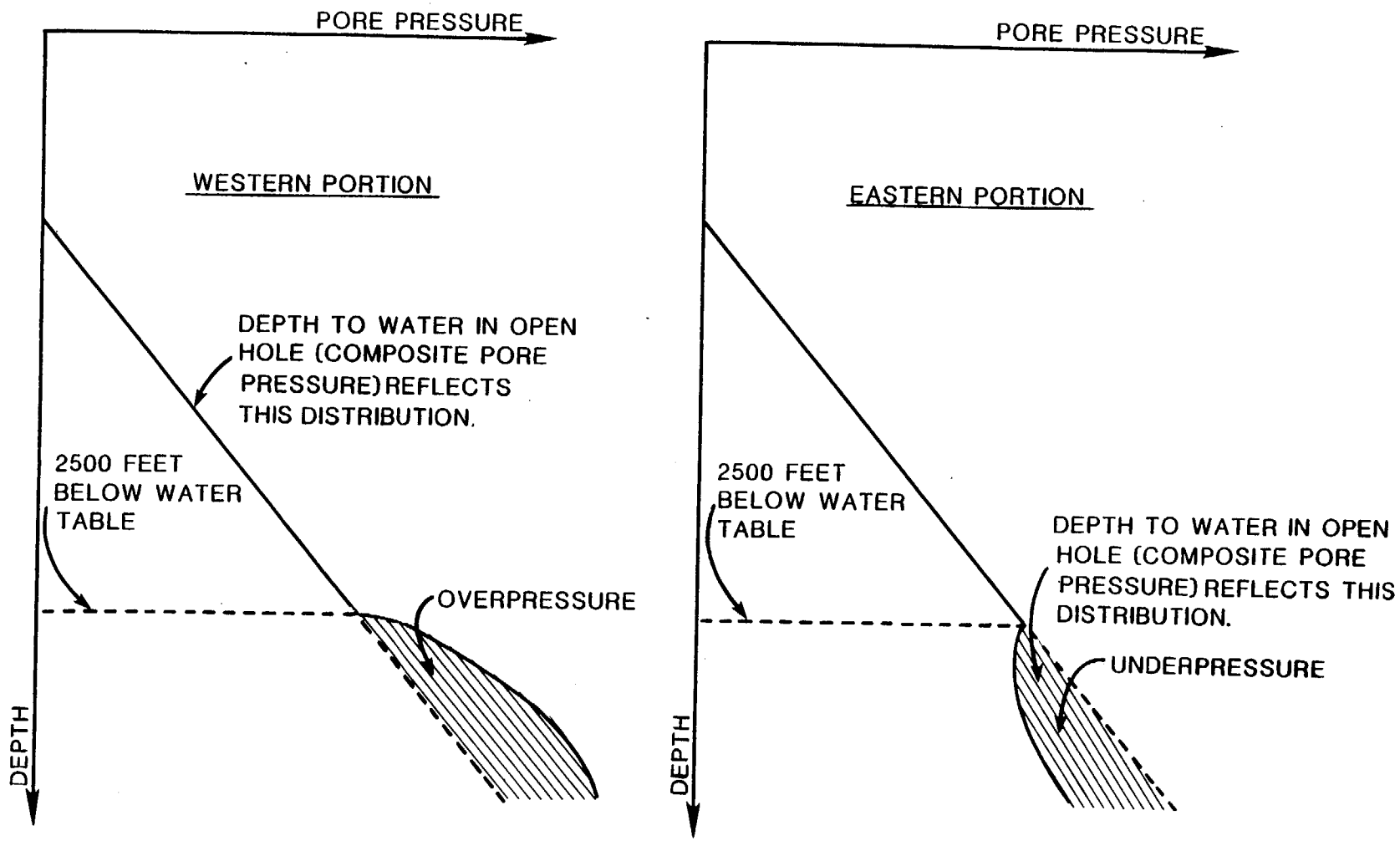

Idealized changes in hydraulic potentials in Pahute Mesa.

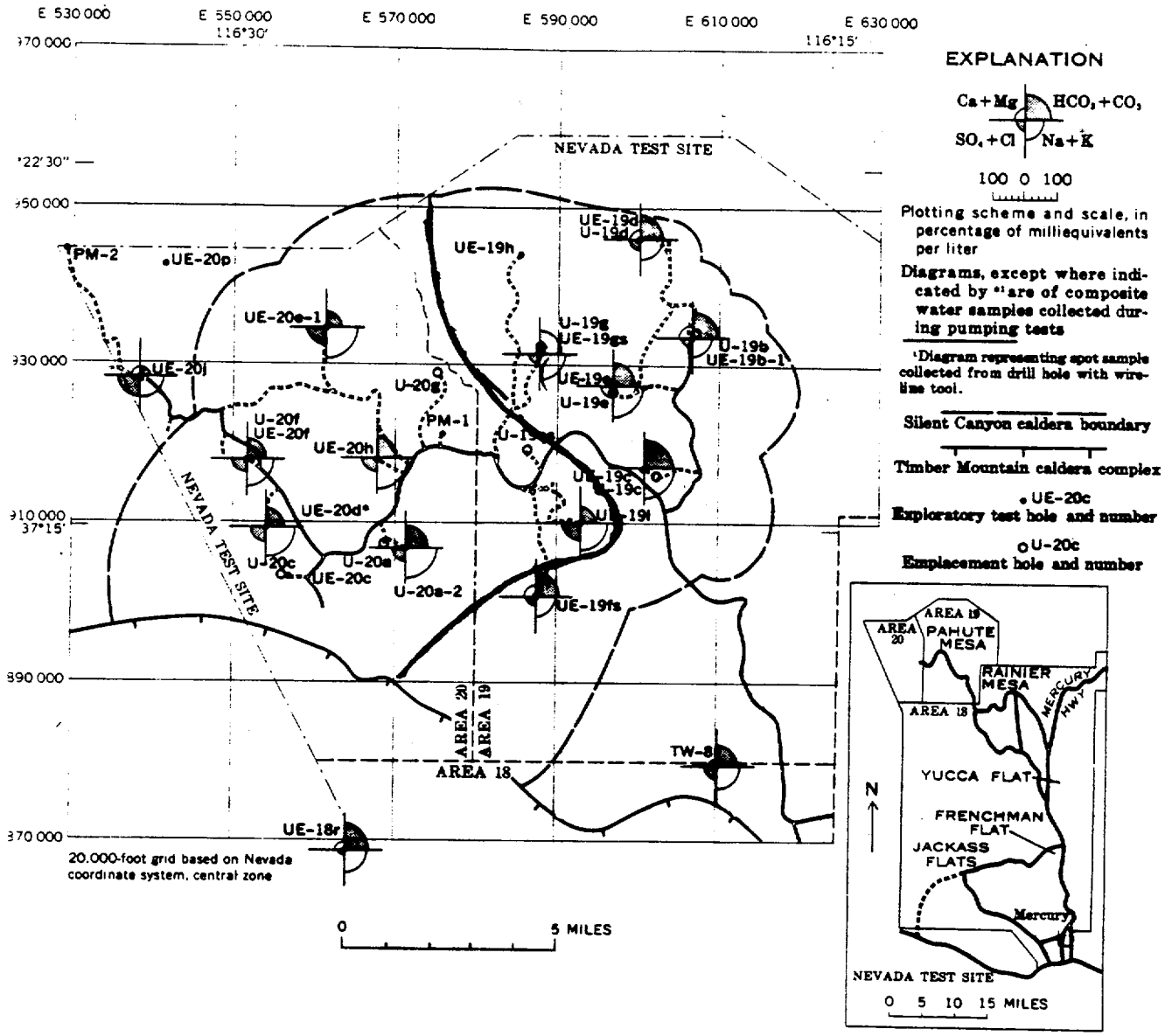

Water chemistry map for Pahute Mesa. From Blankennagel and Weir, 1973.

TABLE 10. — *Selected chemical analyses of water*

[Chemical analyses in milligrams

Hole	Date of sample collection	Interval sampled (ft)	Major producing zone(s) (ft)	Temperature (°C)	Silica (SiO_2)	Aluminum[1] (Al)	Iron[1] (Fe)	Manganese[1] (Mn)	Calcium (Ca)	Magnesium (Mg)	Strontium (Sr)	Sodium (Na)
UE-18r[2]	1-29-68	1,629-5,004	.....	32.2	45	<0.1	0.08	<0.01	26	1.0	0.18	81
U-19as	6- 7-65	3,195	.....	.....	66	.04	.03	<.02	2.0	.1	<.02	200
	6- 7-65	3,195	.....	.....	66	.09	.14	<.02	1.2	<.1	<.02	189
	6- 7-65	3,195	.....	.....	84	.08	.03	<.02	1.6	<.1	<.02	263
UE-19b-1	6-21-64	2,190-4,500	2,740	31.6	47	.03	.35	.05	20	1.7	.....	43
	10-13-64	2,190-4,500	2,740	30.0	41	.04	.41	1.2	24	2.4	.....	42
UE-19c	5- 7-64	2,421-4,520	3,040-3,075	38.3	41	<.01	.04	.01	1.0	.1	.05	29
	3- 9-66	3,050	3,040-3,075	31.1	30	<.01	.04	.90	13	.1	.09	141
UE-19d	3-24-64	724-4,500	3,300-3,480	32.2	28	.03	.59	.03	29	2.9	.29	173
	6-27-64	2,560-7,689	3,300-3,480	45.0	58	.02	.06	<.01	44	5.0	.....	150
	6-27-64	2,560-7,689	3,300-3,480	45.6	49	.06	.06	<.01	29	1.4	.....	148
	3- 9-66	3,280	3,300-3,480	34.4	55	<.01	<.01	.58	58	2.8	.19	158
	3- 9-66	4,200	3,300-3,480	34.4	55	<.01	.02	.56	57	2.8	.19	158
UE-19e	4-22-65	2,475-6,005	2,650-2,690; 4,970-4,990	.....	50	.52	.09	.02	.5	<.1	.....	50
	8- 1-66	2,475-6,005	2,650-2,690; 4,970-4,990	35.0	54	<.01	.02	.02	3.7	<.1	.02	43
UE-19fs	8-18-65	2,565-4,779	.....	37.7	56	.02	<.01	.03	11	1.6	.02	29
UE-19gs	3-27-65	2,650-4,503	2,940; 3,970; 4,270	41.6	46	.04	.07	.01	12	<.1	.....	68
	8- 2-66	2,650-7,500	2,940; 3,970; 4,270	41.6	50	.01	<.01	.01	2.8	<.1	.02	84
UE-19i	9- 2-65	2,896-8,000	3,460-3,618	47.2	39	.03	<.01	.05	5.0	<.1	.04	75
U-20a-2	10-14-64	2,066-4,500	.....	26.6	41	.05	.13	<.01	5.9	<.1	.....	58
	3-10-66	2,066-4,500	.....	.....	48	<.01	.09	.01	6.1	.1	.03	55
UE-20d	3- 8-66	2,920	2,570-2,720; 4,250-4,460	.....	37	<.01	.06	.01	1.4	<.1	.03	81
	3- 8-66	3,200	2,570-2,720; 4,250-4,460	41.6	46	.04	.07	.01	1.4	<.1	.03	83
	7-27-66	2,446-4,500	2,570-2,720; 4,250-4,460	40.0	47	<.01	<.01	<.01	4.2	.1	.07	88
	7-28-66	2,446-4,500	2,570-2,720; 4,250-4,460	40.0	52	<.01	<.01	.02	21	.1	.13	68
	8-12-66	2,446-4,500	2,570-2,720; 4,250-4,460	.....	45	.09	<.01	.39	8.5	.1	<.01	107
UE-20e-1	6- 5-64	1,825-6,395	3,550-3,660	47.2	44	.82	.13	<.01	.4	<.1	.....	112
	3- 8-66	2,600	3,550-3,660	32.8	36	.01	.02	<.01	.2	<.1	.03	82
UE-20f	8-11-64	4,456-13,636	4,570-4,650	48.3	47	.07	.56	.14	4.8	<.1	.....	113
U-20f	3-28-66	4,026	4,030	41.1	36	.04	<.01	.01	.8	.1	<.01	69
	5-27-66	4,025	4,025	41.6	39	.05	<.01	.02	.4	<.1	<.01	69
UE-20h	8-26-65	2,566-7,207	4,000-4,070	32.2	49	.02	<.01	.03	.6	<.1	<.02	64
UE-20j	10-21-64	1,740-5,690	2,050-2,250; 2,960-3,330	38.9	44	.01	4.8	<.01	46	1.2	.....	138
TW-8[2]	10-15-64	1,068-1,860	1,300-1,730	26.1	45	<.01	<.01	<.01	8.8	.9	.....	30

[1]In solution at time of analysis or collection.
[2]South of Pahute Mesa.

Results of chemical analyses of water samples from Pahute Mesa. From Blankennagel and Weir, 1973.

Hole	Date of sample collection	Interval sampled (ft)	Major producing zone(s) (ft)	Lithium (Li)	Selenium (Se)	Carbonate (CO_3)	Bicarbonate (HCO_3)	Sulfate (SO_4)	Chloride (Cl)	Fluoride (F)	Nitrate (NO_3)	Phosphate (PO_4)	Dissolved solids (residue on evaporation at 180°C)	Hardness as $CaCO_3$: Calcium, magnesium	Hardness as $CaCO_3$: Noncarbonate	Specific conductance (micromhos per cm at 25°C)	pH
UE-18r[2]	1-29-68	1,629-5,004	.....	0.10	0.11	0	252	24	7.8	2.9	0.6	<0.01	313	69	0	449	8.0
U-19as	6- 7-65	3,195	.....	.61	.06	39	174	26	19	80	1.0	<.01	526	6	0	889	9.3
	6- 7-65	3,195	.....	.62	.07	8	205	27	11	80	2.5	<.01	491	3	0	828	8.4
	6- 7-65	3,195	.....	.85	.04	82	261	51	12	70	12	<.01	723	4	0	1,150	9.3
UE-19b-1	6-21-64	2,190-4,500	2,740	.....	.03	0	130	24	13	3.2	.1	<.01	242	57	0	316	6.7
	10-13-64	2,190-4,500	2,740	.....	.03	0	150	21	6.8	3.2	.4	<.01	229	70	0	314	7.4
UE-19c	5- 7-64	2,421-4,520	3,040-3,075	.04	.05	0	66	4.6	2.6	1.2	1.8	<.01	117	3	0	124	7.6
	3- 9-66	3,050	3,040-3,075	.28	.....	0	400	<.1	7.7	4.3	.2	<.01	390	33	0	644	7.9
UE-19d	3-24-64	724-4,500	3,300-3,480	.20	.04	0	424	63	39	4.4	30.0	<.01	560	85	0	889	7.5
	6-27-64	2,560-7,689	3,300-3,480	.....	.....	0	380	80	33	6.9	.1	<.01	572	131	0	851	7.9
	6-27-64	2,560-7,689	3,300-3,480	.....	.....	0	320	66	30	7.5	<.1	<.01	525	79	0	777	7.6
	3- 9-66	3,380	3,300-3,480	.38	.....	0	481	60	19	5.0	.5	<.01	581	156	0	911	7.9
	3- 9-66	4,200	3,300-3,480	.38	.....	0	489	57	20	4.9	.6	<.01	578	154	0	906	7.9
UE-19e	4-22-65	2,475-6,005	2,650-2,690; 4,970-4,990	.15	.....	0	86	20	11	1.2	3.4	.01	190	1	0	232	7.4
	8- 1-66	2,475-6,005	2,650-2,690; 4,970-4,990	.06	.01	0	80	16	3.7	5.3	1.7	<.01	169	9	0	204	8.2
UE-19fs	8-18-65	2,565-4,779	.....	.02	....	0	86	9.0	6.3	3.6	2.2	<.01	186	34	0	202	8.1
UE-19gs	3-27-65	2,650-4,508	2,940; 3,970; 4,270	.....	.....	0	146	36	9.0	2.0	1.3	<.01	248	30	0	345	8.2
	8- 2-66	2,650-7,500	2,940; 3,970; 4,270	.04	.01	0	123	43	22	3.0	.6	<.01	270	7	0	388	8.2
UE-19i	9- 2-65	2,896-8,000	3,460-3,618	.05	.01	0	98	70	7.0	5.5	.2	<.01	230	13	0	228	7.7
U-20a-2	10-14-64	2,066-4,500	.....	.....	.01	0	108	28	11	2.6	1.2	<.01	206	15	0	285	6.9
	3-10-66	2,066-4,500	.....	.06	.....	0	106	27	11	2.7	1.4	<.01	201	16	0	286	7.7
UE-20d	3- 8-66	2,920	2,570-2,720; 4,250-4,460	.08	.....	0	122	40	23	3.1	1.3	<.01	252	4	0	384	8.3
	3- 8-66	3,200	2,570-2,720; 4,250-4,460	.08	.....	0	120	42	24	3.1	1.7	<.01	282	4	0	351	8.3
	7-27-66	2,446-4,500	2,570-2,720; 4,250-4,460	.00	.01	0	137	44	23	2.8	<.1	<.01	286	11	0	405	7.8
	7-28-66	2,446-4,500	2,570-2,720; 4,250-4,460	.00	.01	5	143	53	8.8	2.4	.3	<.01	281	53	0	394	8.4
	8-12-66	2,446-4,500	2,570-2,720; 4,250-4,460	.08	.01	4	192	40	24	3.0	<.1	<.01	327	22	0	487	8.5
UE-20e-1	6- 5-64	1,825-6,395	3,550-3,660	.....	.....	0	130	43	57	4.6	1.0	<.01	336	1	0	515	7.7
	3- 8-66	2,600	3,550-3,660	.07	.....	2	119	42	20	4.5	.5	<.01	245	1	0	352	8.5
UE-20f	8-11-64	4,456-13,686	4,570-4,680	.....	.....	0	164	48	40	5.0	.1	.02	368	12	0	519	7.2
U-20f	3-28-66	4,026	4,030	.02	.01	10	103	30	6.6	3.9	<.1	.07	240	3	0	296	8.9
	5-27-66	4,025	4,025	.00	.01	14	98	23	7.0	3.7	.7	.12	194	1	0	297	9.1
UE-20h	8-26-65	2,506-7,207	4,000-4,070	.08	<.1	0	107	30	15	2.7	1.3	<.01	231	2	0	301	8.1
UE-20j	10-21-64	1,740-5,690	2,050-2,250; 2,960-3,830	.....	.....	0	150	135	115	2.2	.9	<.01	588	120	0	904	7.0
TW-8[2]	10-15-64	1,068-1,860	1,300-1,780	.....	.....	0	78	16	7.8	.7	3.6	.01	149	26	0	197	6.8

[1]In solution at time of analysis or collection.
[2]South of Pahute Mesa.

Results of chemical analyses of water samples from Pahute Mesa (continued). From Blankennagel and Weir, 1973.

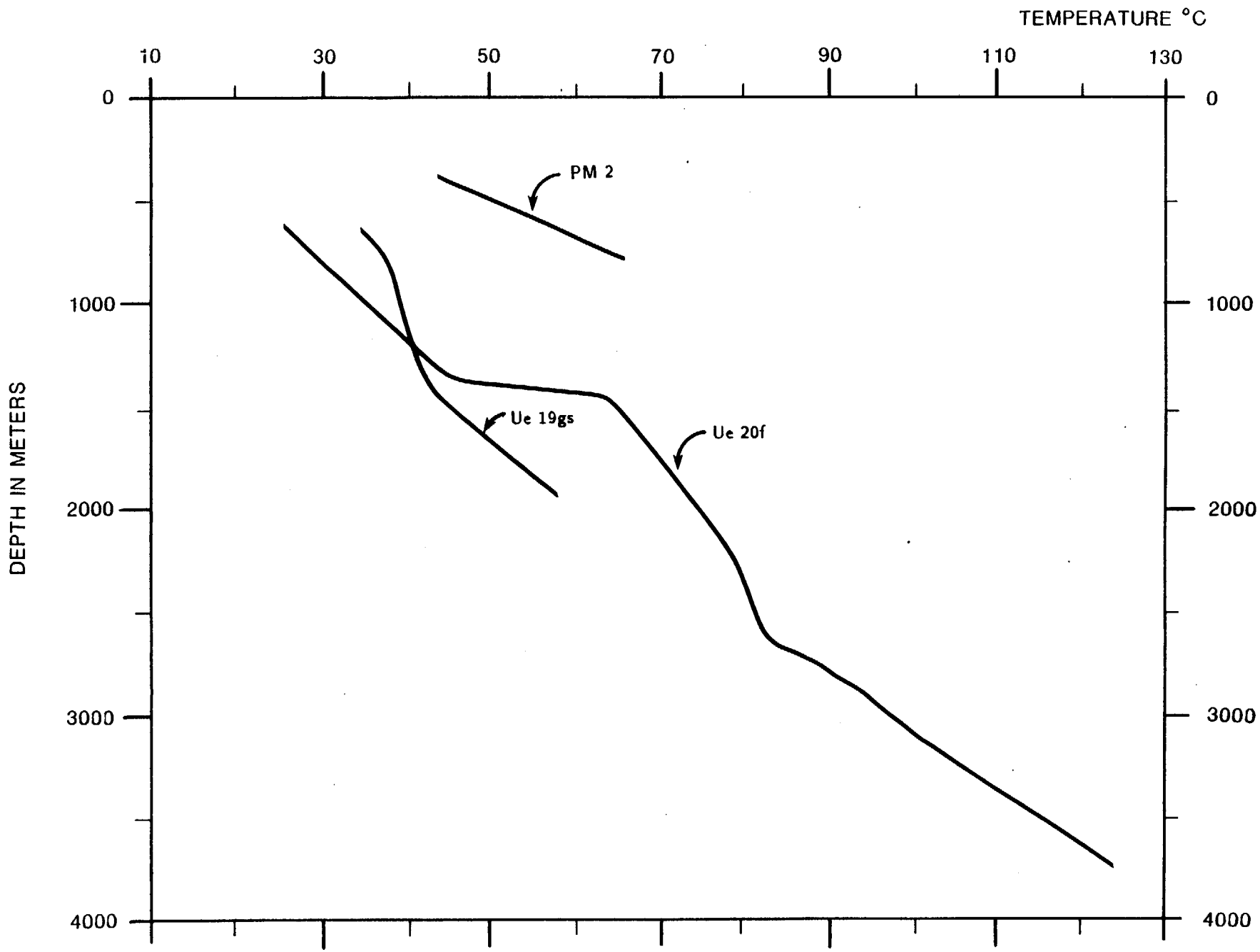

Downhole temperature for three boreholes in Pahute Mesa. From Sass and Lachenbruch, 1982.

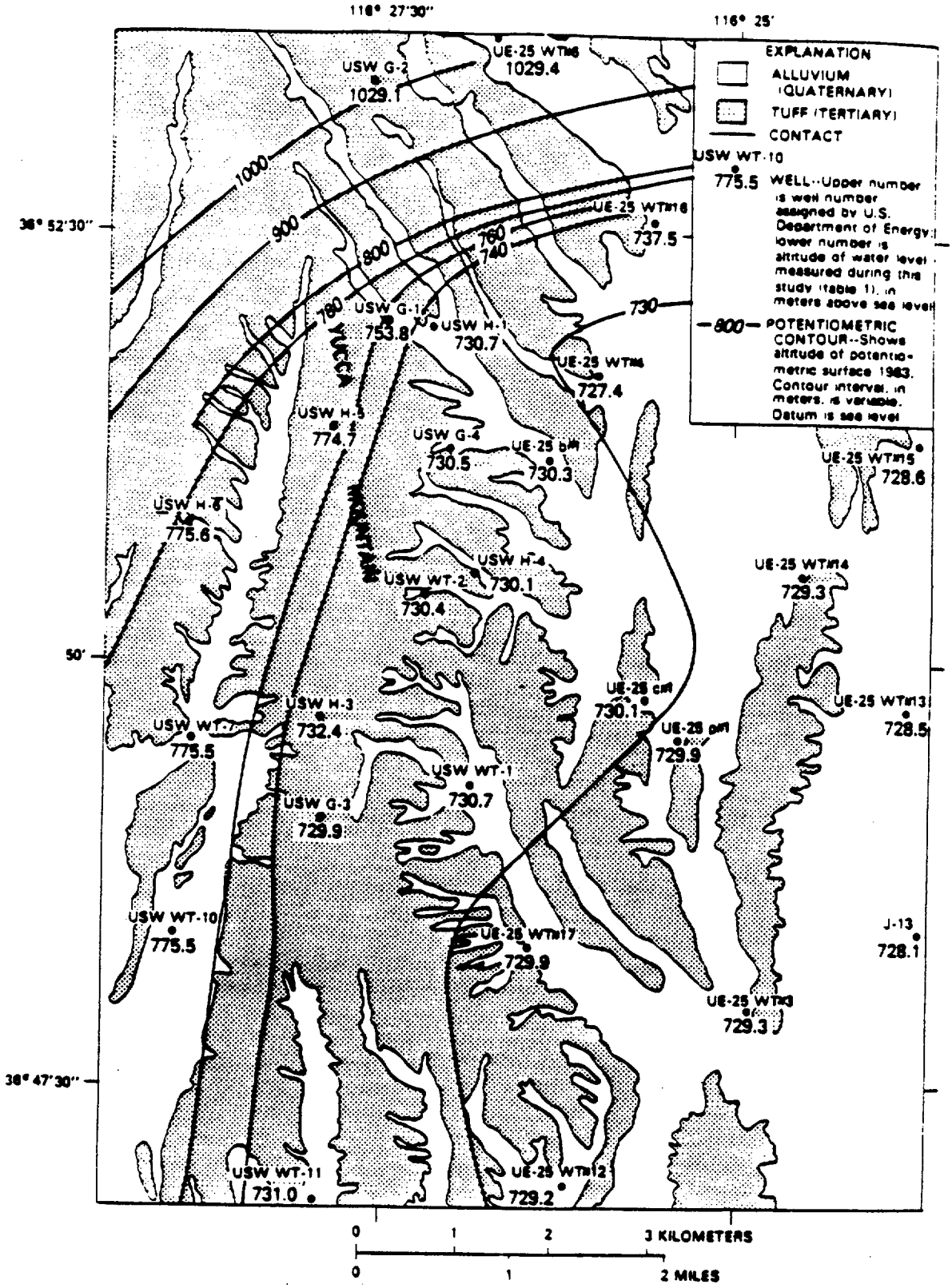

Location map for deep wells at Yucca Mountain. From Robison, 1984.

Hole or well number: Designation assigned by U.S. Department of Energy.
Location: Nevada State Coordinate System Central Zone (feet).
Hole Depth: Total depth drilled.
Land-surface altitude: Altitude above National Geodetic Vertical Datum of 1929 at well, reported by Holmes & Narver, Inc., contractor to U.S. Department of Energy.
Depth correction: Correction needed to adjust measured depth or altitude to true value because of hole deviation from vertical. The correction is computed for a depth approximately equal to the depth of the measured water level; this correction is obtained from a down-hole gyroscopic survey.
Date measured: Date of a water-level measurement.

Interval: Depth interval of the hole represented by the water-level measurement. Composite levels represent mixed hydraulic heads of the entire interval between the water table or lower end of the casing and the bottom of the hole. Where a specific interval is indicated, the zone was isolated, using inflatable packers for the straddled interval during permeability testing, or using a single packer installed to determine hydraulic head differences above and below the packer.
Depth to water: Depth based on direct measurements of water levels using down-hole wireline equipment, adjusted for depth correction (where available), except where noted.
Altitude: Computed altitude of water level above National Geodetic Vertical Datum of 1929, based on land-surface altitude and measured depth to water (corrected).

Hole or well number	Location (feet) North	Location (feet) East	Hole depth (meters)	Land-surface altitude (meters)	Depth correction (meters)	Date measured	Water level (corrected)[1] Interval (meters)	Depth to water (meters)	Altitude (meters)
UE-25b#1	765,243	566,416	1220	1200.6	0.25	12/03/83	Composite	470.6	730.8
						08/01/83	471-1199	470.3	730.3
						do.	1199-1220	472.2	728.4
UE-25c#1	757,095	569,680	914	1130.4	.06	11/07/83	Composite	400.3	730.1
UE-25p#1	756,171	571,485	1805	1114	.02	Feb. 1983	383- 500	383.9	729.9
						do.	500- 550	383.5	730.4
						do.	739- 789	383.3	730.6
						do.	764- 834	383.1	730.8
						do.	834- 904	381.1	732.7
						do.	904- 974	382.2	731.7
						do.	974-1044	380.9	733.0
						do.	1044-1114	379.4	734.5
						do.	1110-1180	361.7	[2]752.2
						do.	1117-1301	360.5	[2]753.4
						do.	1180-1301	355.0	[2]758.9
						May 1983	1297-1308	362.0	751.9
						do.	1297-1338	362.3	751.6
						do.	1341-1381	362.3	751.6
						do.	1381-1420	362.4	751.5
						do.	1423-1463	362.5	751.4
						do.	1463-1509	362.4	751.5
						do.	1509-1585	362.5	751.4
						do.	1597-1643	362.7	751.2
						do.	1643-1689	360.0	750.9
						do.	1734-1780	363.1	750.8
						do.	1780-1805	363.0	750.9
						11/07/83	1297-1805	364.7	[3]749.2

Water levels - Yucca Mountain. From Robison, 1984.

Hole or well number	Location (feet) North	Location (feet) East	Hole depth (meters)	Land-surface altitude (meters)	Depth correction (meters)	Date measured	Water level (corrected)[1] Interval (meters)	Depth to-- water (meters)	Altitude (meters)
USW G-1	770,500	561,000	1829	1325.5	0.67	03/23/82	Composite	571.7	753.8
USW-G-2	778,824	560,504	1831	1554.0	.16	09/17/82	Composite	524.9	1029.1
USW G-3	752,780	558,483	1533	1480.2	.57	11/30/83	Composite	750.3	729.9
USW G-4	765,807	563,082	915	1269.6	1.53	04/27/83	Composite	539.5	730.1
USW H-1	770,254	562,388	1829	1302.8	.19	02/25/82	Composite	572.1	730.7
						11/01/83	572- 673	572.4	730.5
						do.	716- 765	572.4	730.5
						do.	1097-1123	571.7	731.2
						do.	1783-1814	518.2	784.7
USW H-3	756,542	558,452	1219	1483.3	.08	11/19/82	Composite	750.8	732.5
						11/03/83	751-1190	750.9	732.4
						do.	1190-1219	729.0	754.1
USW H-4	761,643	563,911	1219	1248.6	.45	12/30/82	Composite	518.7	730.1
						06/16/83	518-1181	518.2	730.8
						do.	1181-1219	518.1	730.9
USW H-5	766,634	558,909	1219	1478.5	0.08	12/22/83	Composite	704.2	774.3
						11/07/83	704-1091	703.8	774.7
						do.	1091-1219	703.8	774.7
USW H-6	763,299	554,075	1220	1301.7	.05	12/15/82	Composite	526.6	775.1
						10/24/83	526-1187	526.1	775.6
						do.	1187-1220	524.7	777.0
USW WT-1	753,941	563,739	515	1201.7	.33	10/31/83	Composite	471.0	730.7
USW WT-2	760,661	561,924	628	1301.4	.53	11/01/83	Composite	571.0	730.4
UE-25 WT#3	745,995	573,384	348	1029.8	.27	10/31/83	Composite	300.5	729.3
UE-25 WT#4	768,512	568,040	482	1167.1	.46	11/01/83	Composite	438.9	728.2
UE-25 WT#6	780,576	567,524	383	1312.9	.24	10/31/83	Composite	283.9	1029.4
USW WT-7	755,570	553,891	491	1197.0	.03	10/24/83	Composite	421.2	775.9
USW WT-10	748,771	553,302	430	1123.2	.03	10/24/83	Composite	347.7	775.5
USW WT-11	739,070	558,377	441	1094.4	.12	10/24/83	Composite	363.9	730.5
UE-25 WT#12	739,726	567,011	399	1074.6	.20	10/31/83	Composite	345.4	729.2
UE-25 WT#13	756,884	578,843	352	1031.8	.01	10/31/83	Composite	303.3	728.5
UE-25 WT#14	761,651	575,210	399	1076.1	.09	11/07/83	Composite	346.2	729.9
UE-25 WT#15	766,116	579,806	415	1082.8	.19	12/01/83	Composite	354.2	728.6
UE-25 WT#16	774,420	570,395	519	1210.5	.06	12/01/83	Composite	472.7	737.8
UE-25 WT#17	748,420	566,212	443	1124.5	.48	11/07/83	Composite	394.6	729.9
J-11	740,968	611,764	405	1050	--	03/22/73	Composite	317.4	732.6
J-12	733,509	581,011	347	953.5	--	12/05/83	Composite	226.2	727.3
J-13	749,209	579,651	1063	1011.3	--	10/31/83	Composite	283.2	728.1
USW VH-1	743,356	533,626	762	963.5	--	02/12/81	Composite	184.2	779.3
USW VH-2	748,320	526,264	1219	974.4	--	04/23/83	Composite	164.0	[4]810.4

[1]Where more than one water-level altitude is reported for a well, the value shown on the map is underscored in the table.
[2]Water level probably not stabilized.
[3]Composite of interval open to rocks of Paleozoic age.
[4]Water level estimated from geophysical logs.

Water levels - Yucca Mountain (continued). From Robison, 1984.

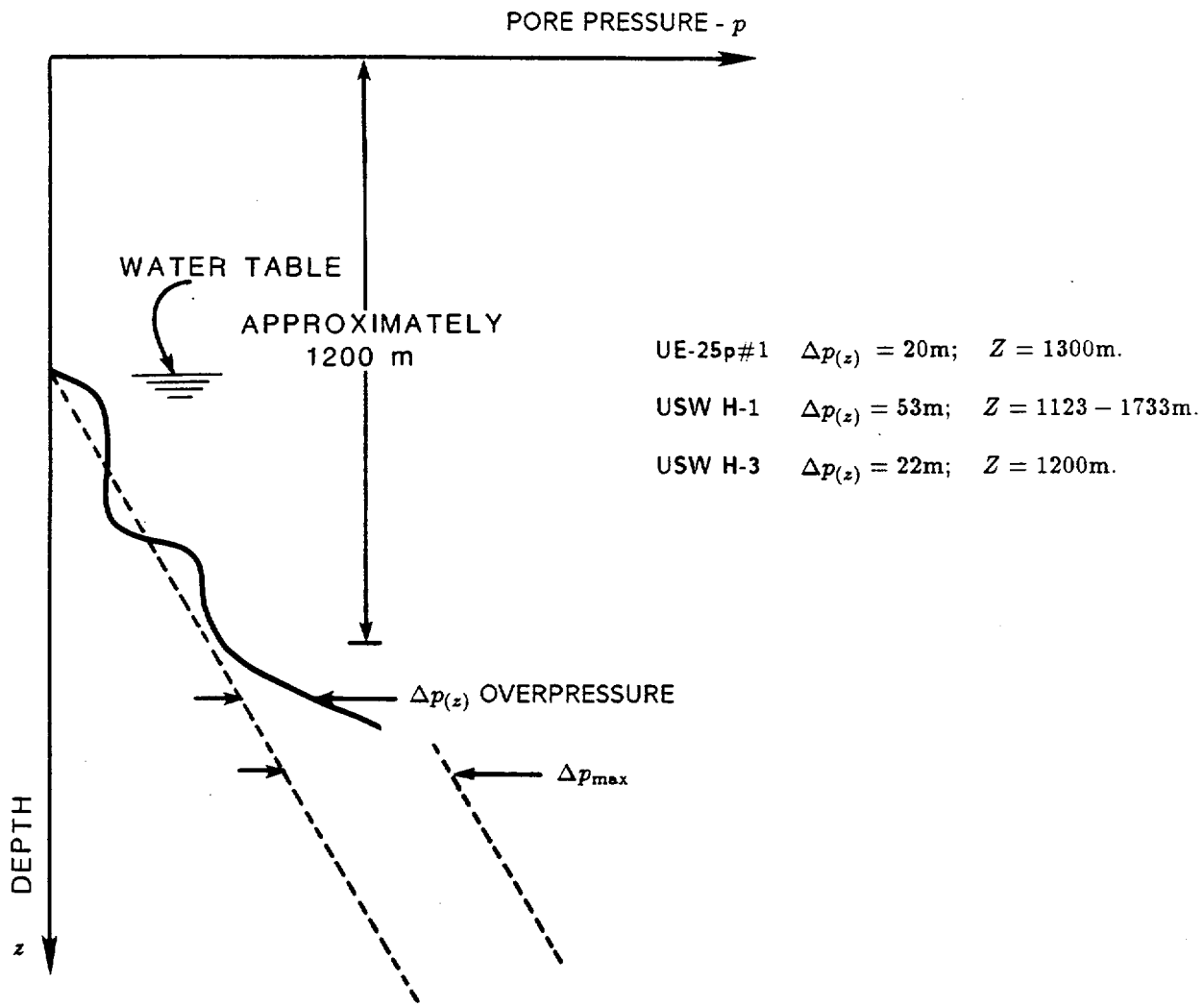

Idealized changes of pore pressure with depth at Yucca Mountain.

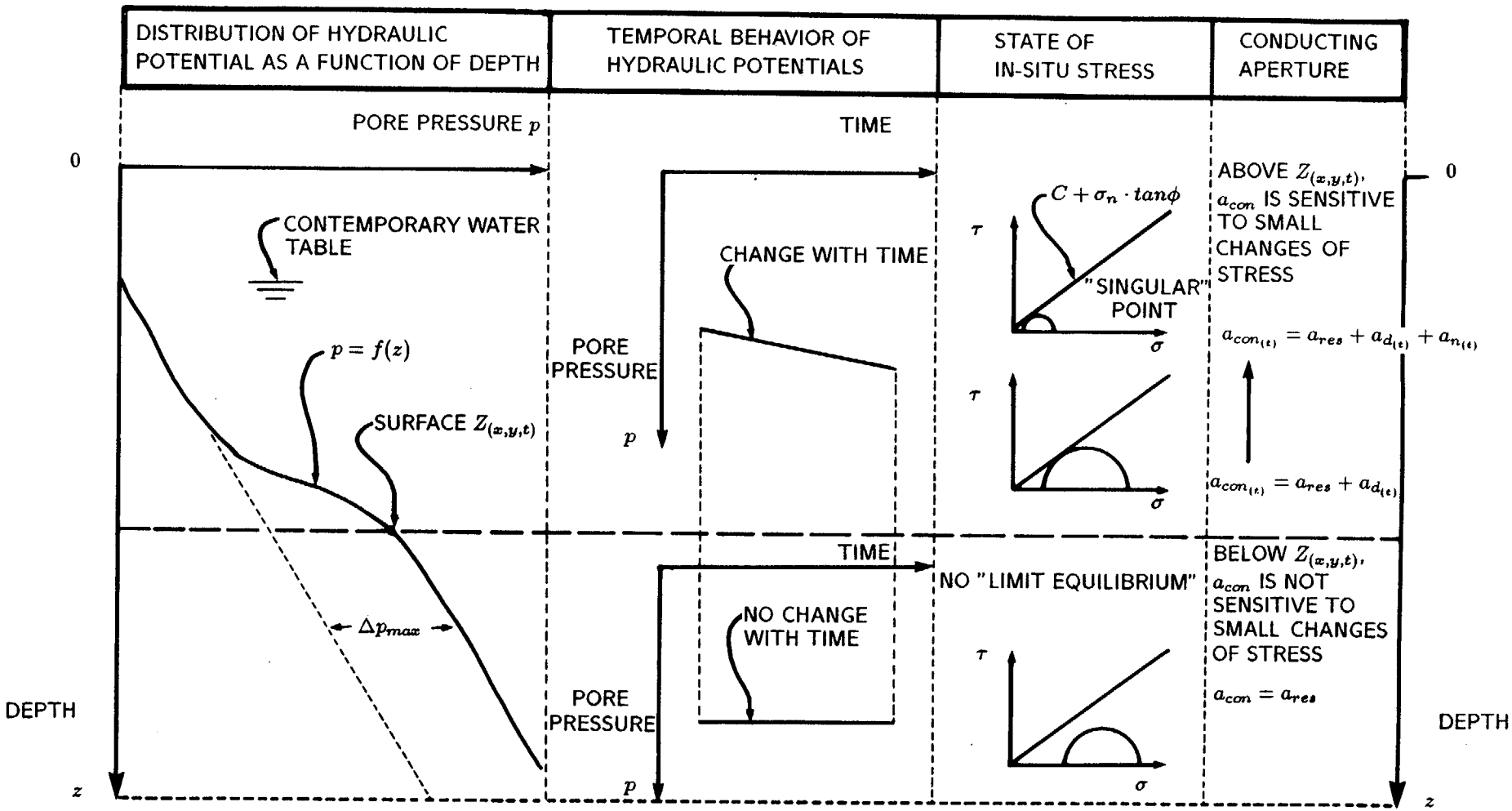

Schematic representation of depth-dependence of: a) pore pressure; b) temporal behavior of the hydraulic potentials; c) in situ stress state; and d) conducting aperture for a single borehole penetrating the deforming fractured medium.

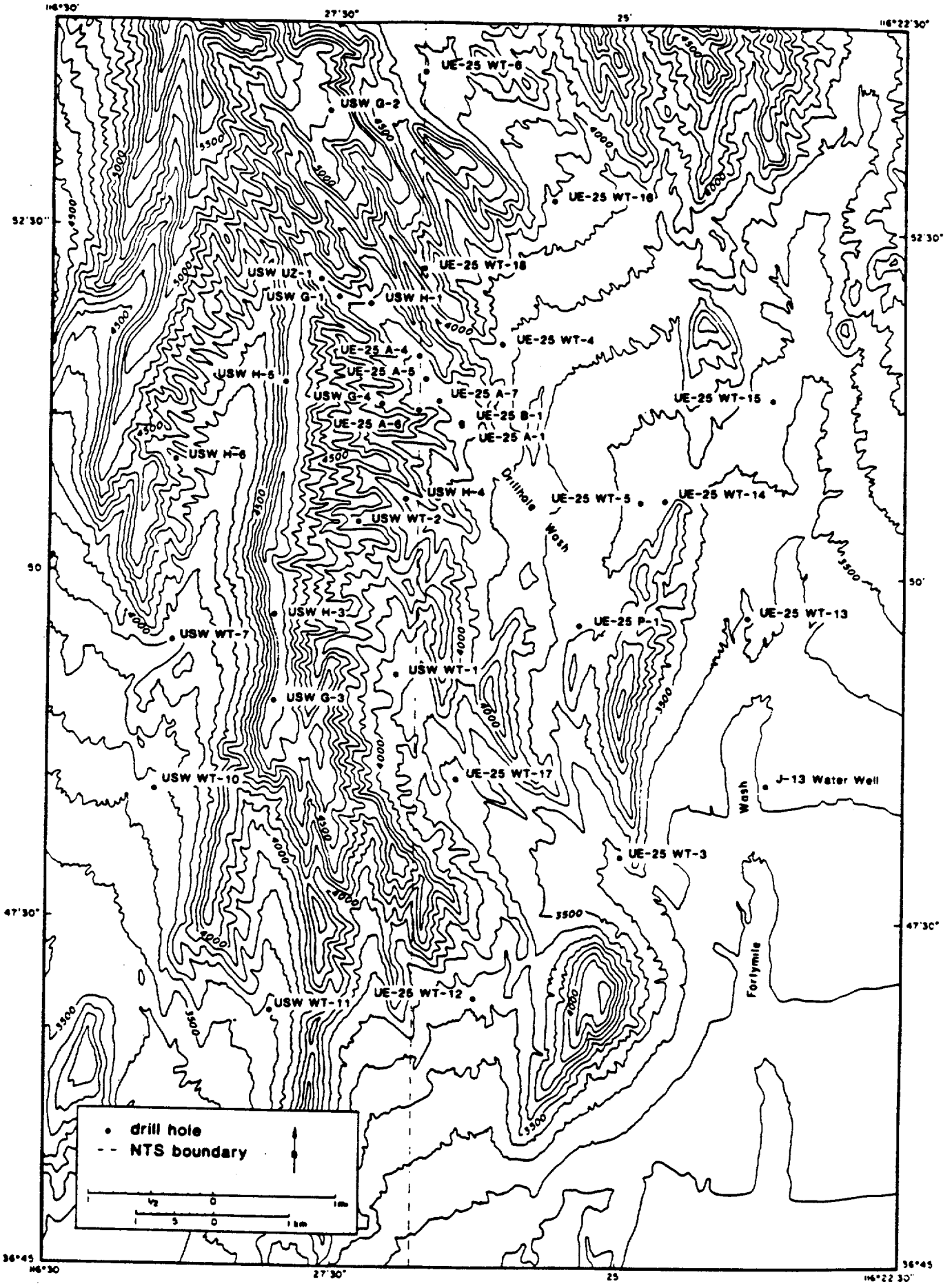

Map showing location of wells from which hydrographs shown on plates 4.2.4.4-6 through 4.2.4.4-21 were obtained. From Sass et al., 1987.

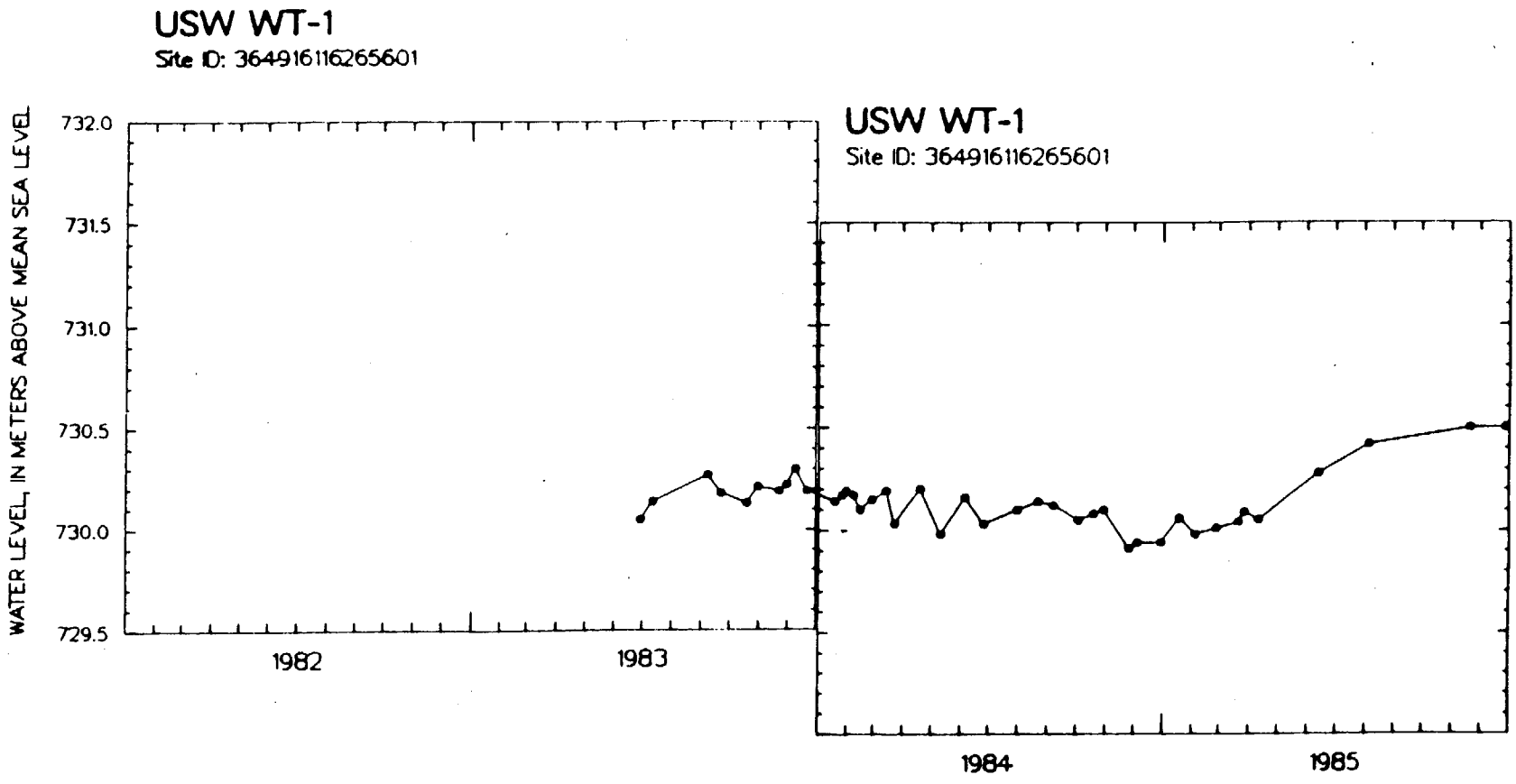

Hydrograph - Well USW WT-1. From Robison et al., 1988.

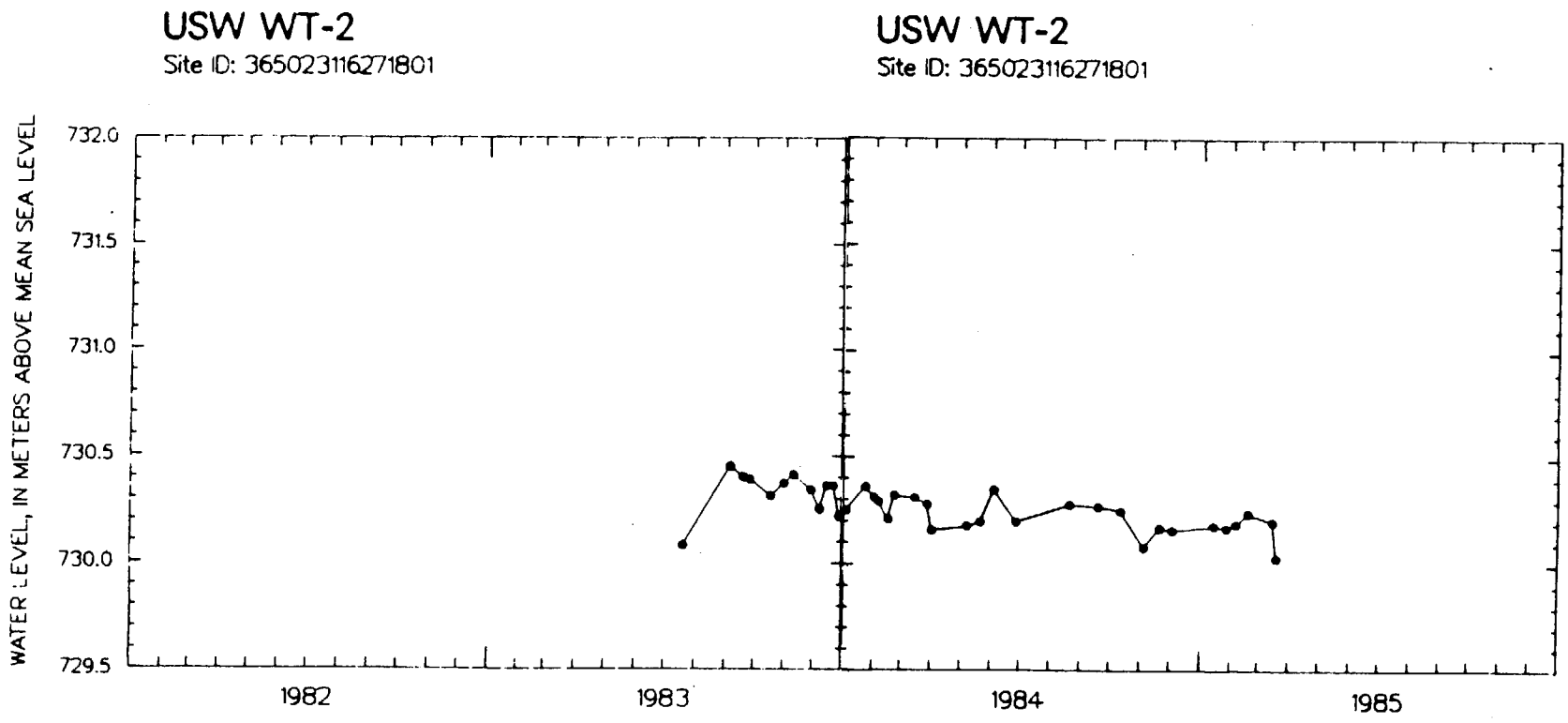

Hydrograph - Well USW WT-2. From Robison et al., 1988.

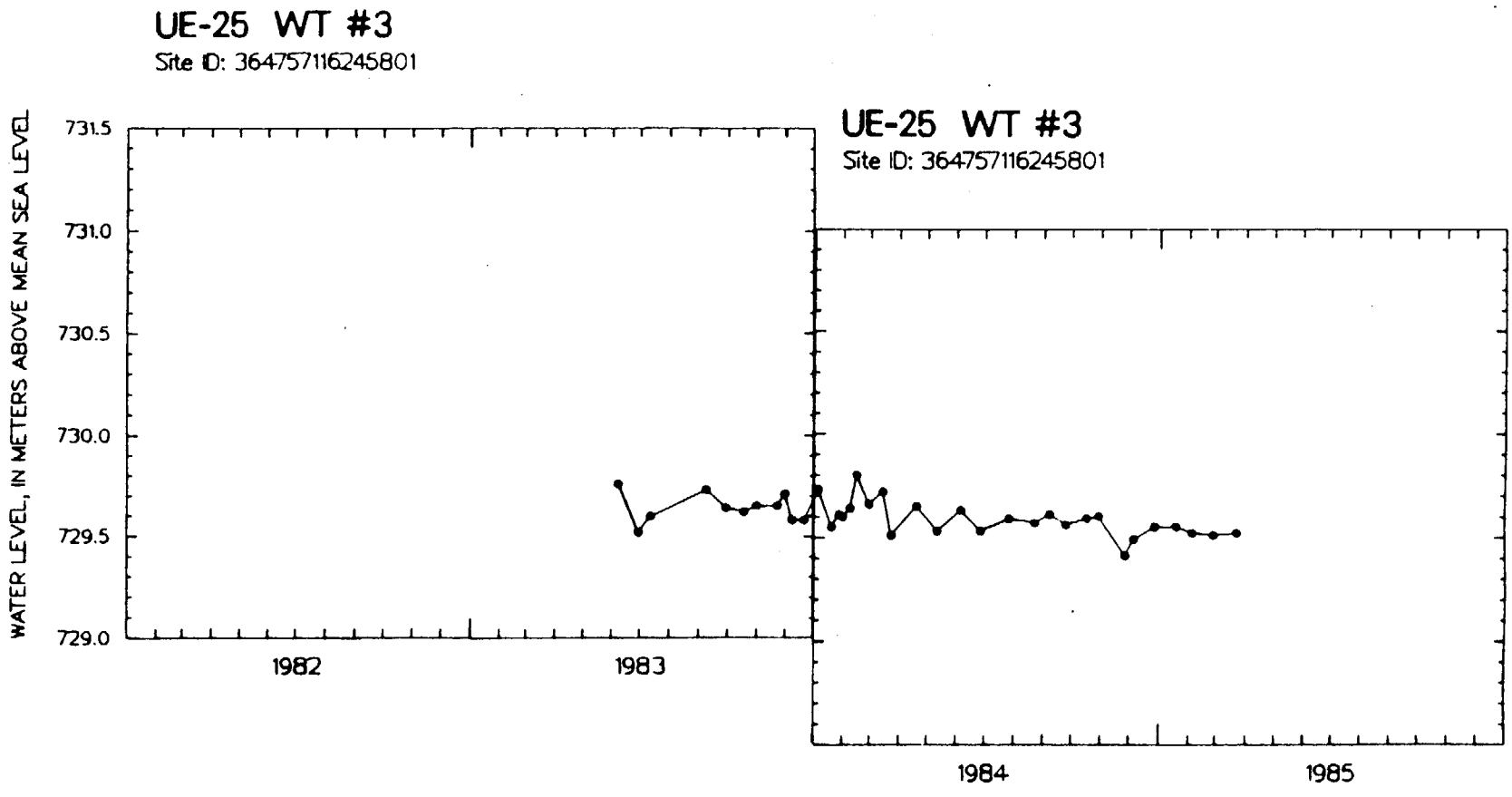

Hydrograph - Well UE-25 WT-3. From Robison et al., 1988.

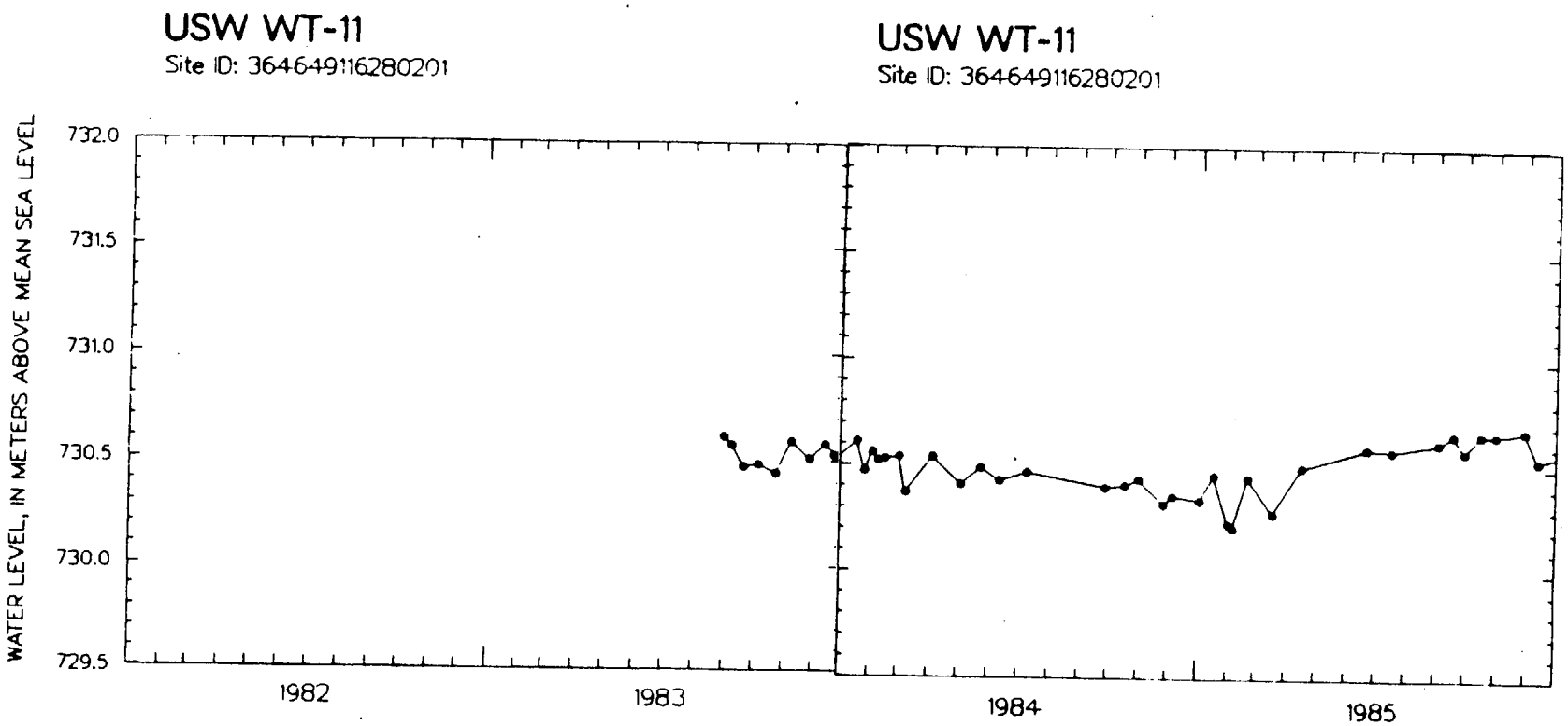

Hydrograph - Well WT-11. From Robison et al., 1988.

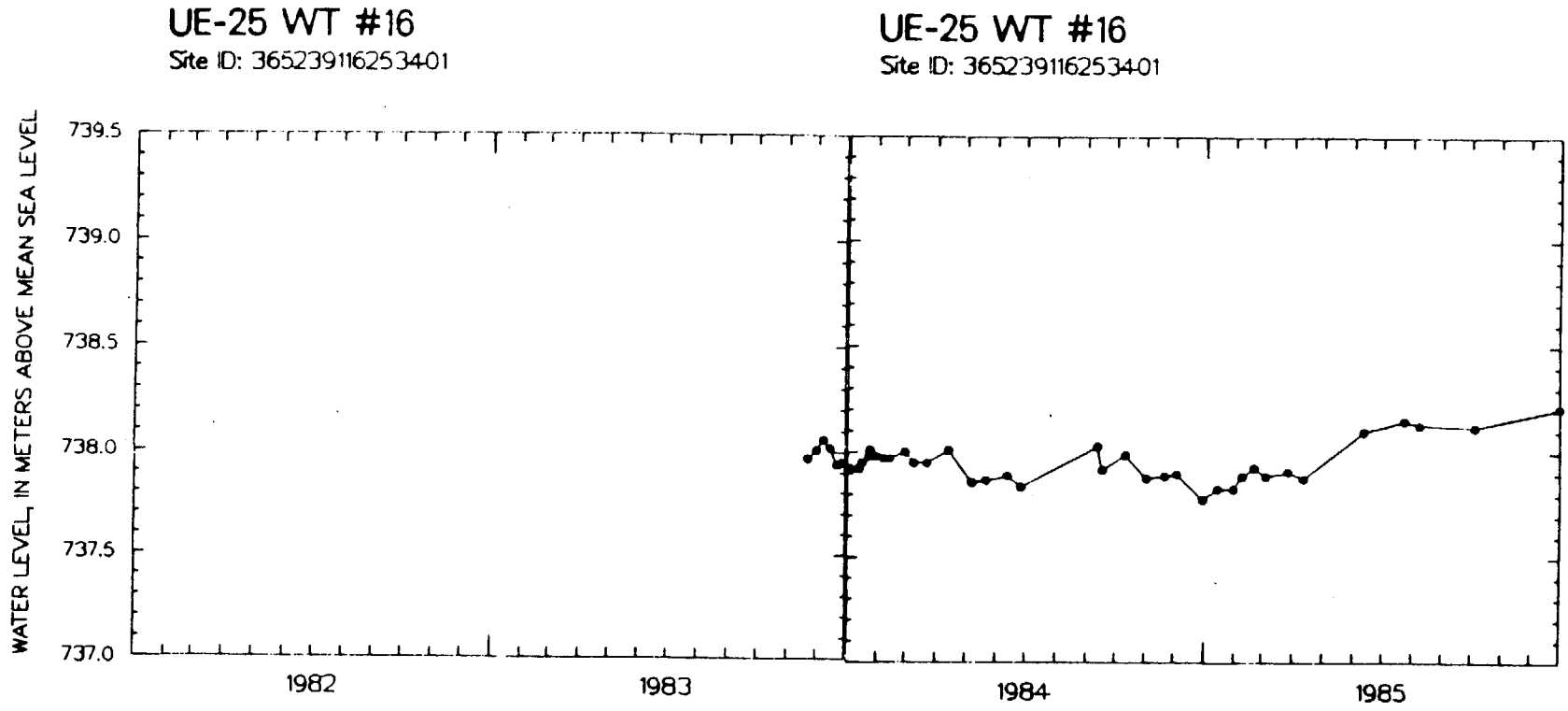

Hydrograph - Well UE-25 WT #16. From Robison et al., 1988.

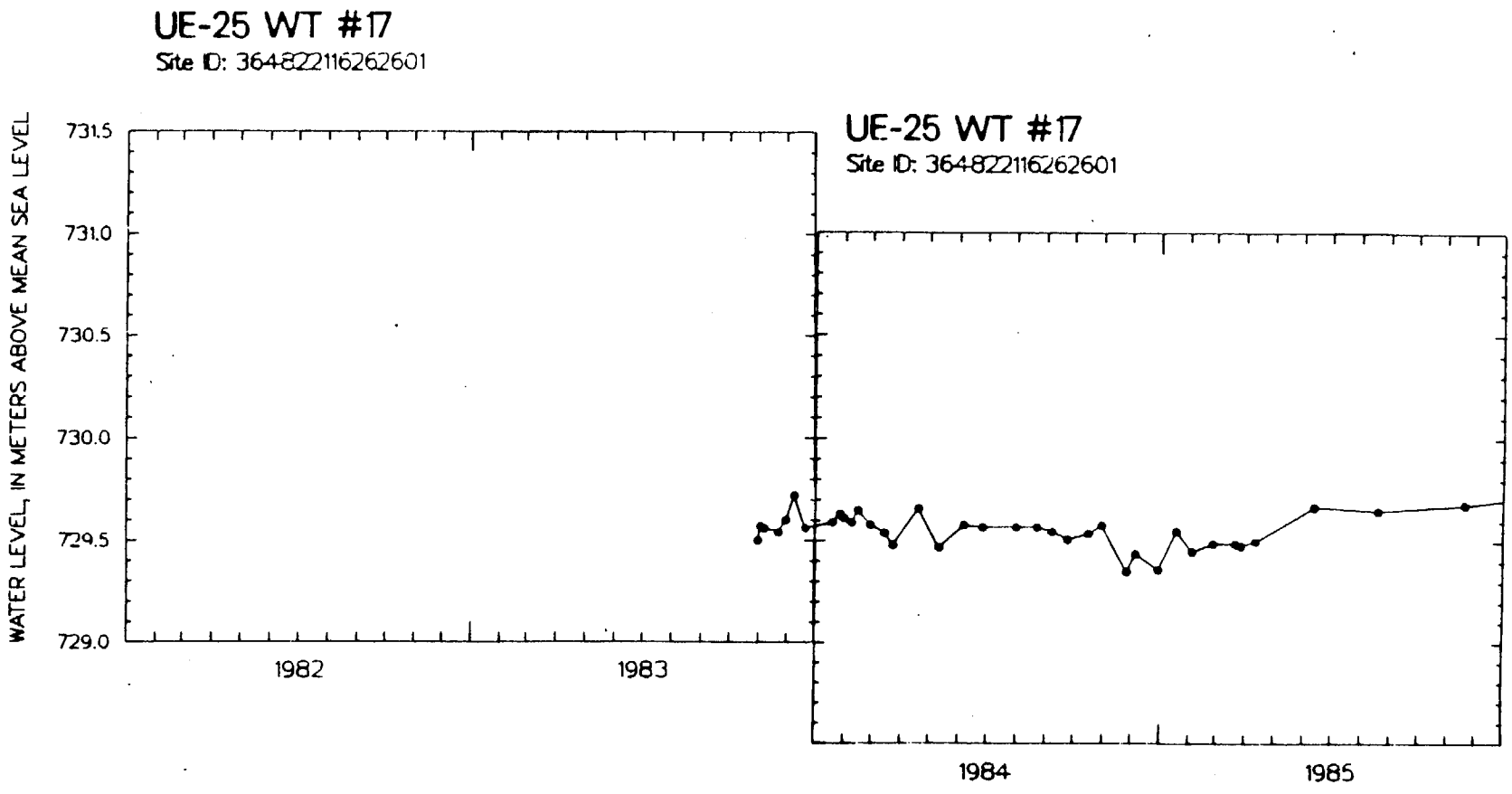

Hydrograph - Well UE-25 WT #17. From Robison et al., 1988.

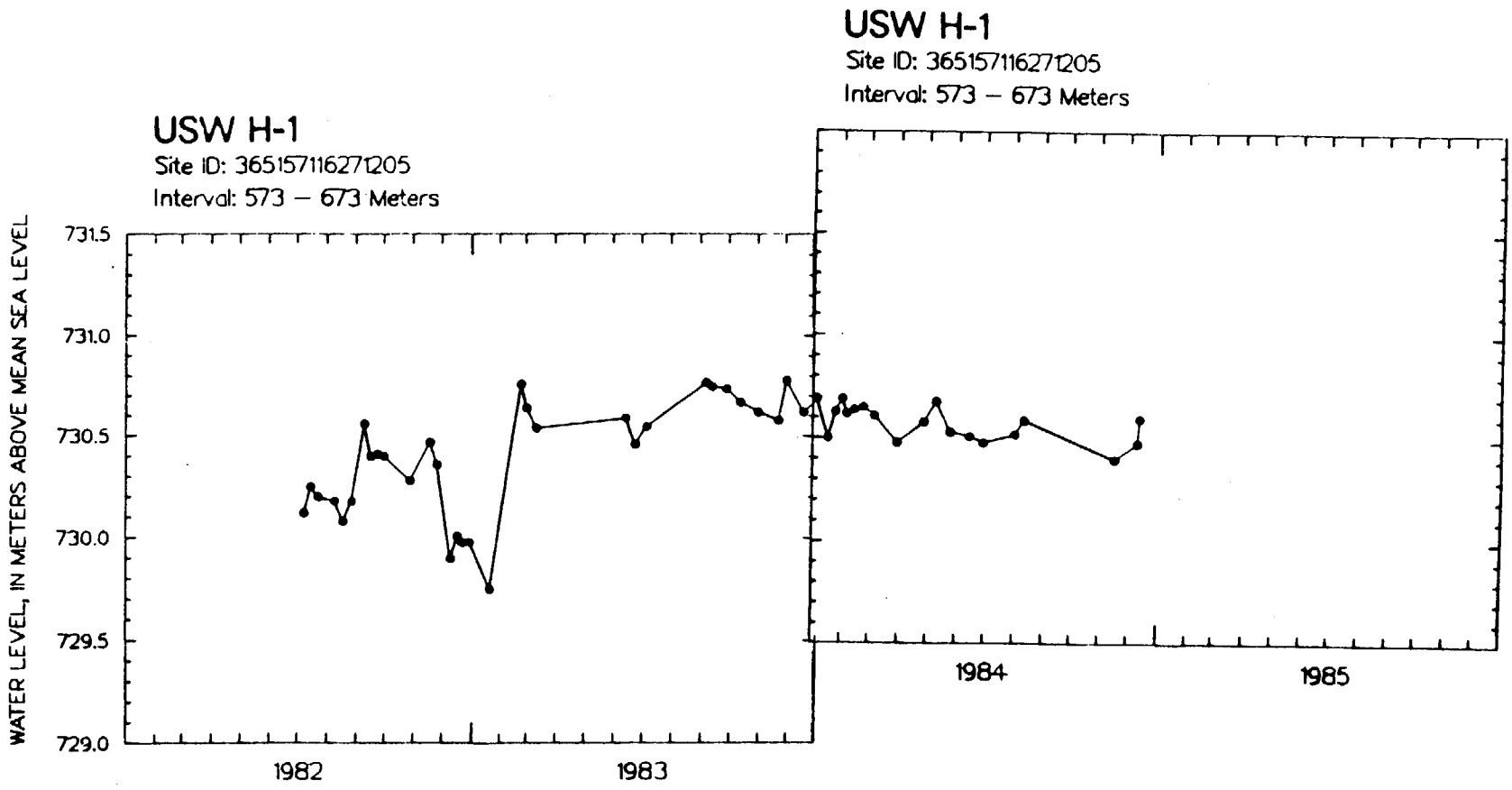

Hydrograph - Well USW H-1. From Robison et al., 1988.

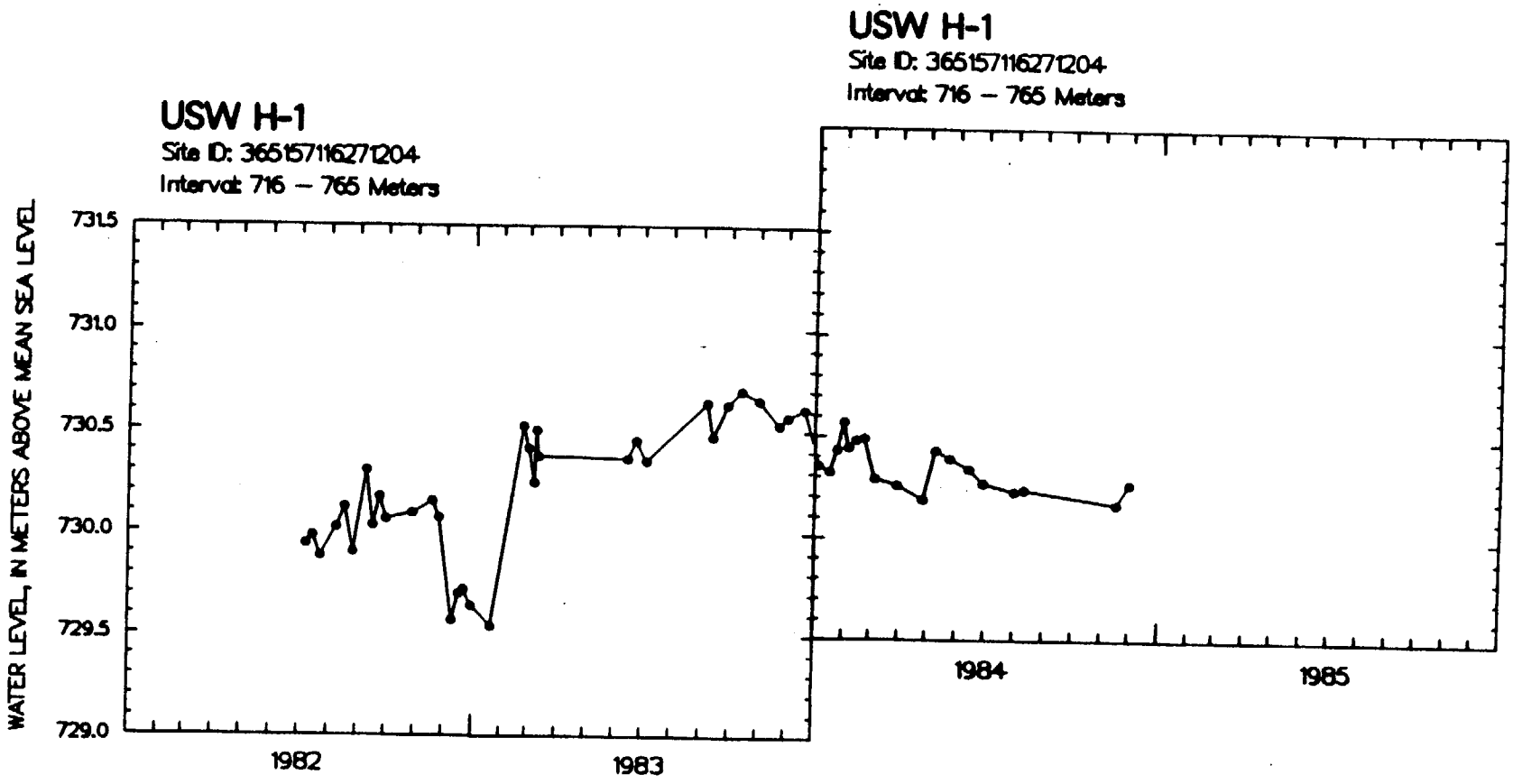

Hydrograph - Well USW H-1. From Robison et al., 1988.

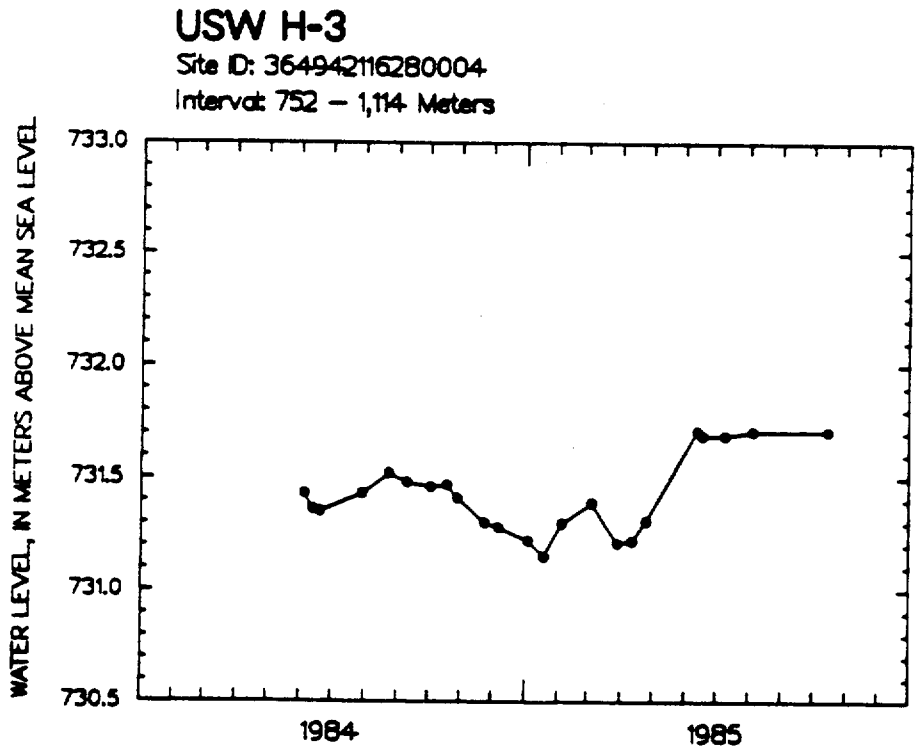

Hydrograph - Well USW H-3. From Robison et al., 1988.

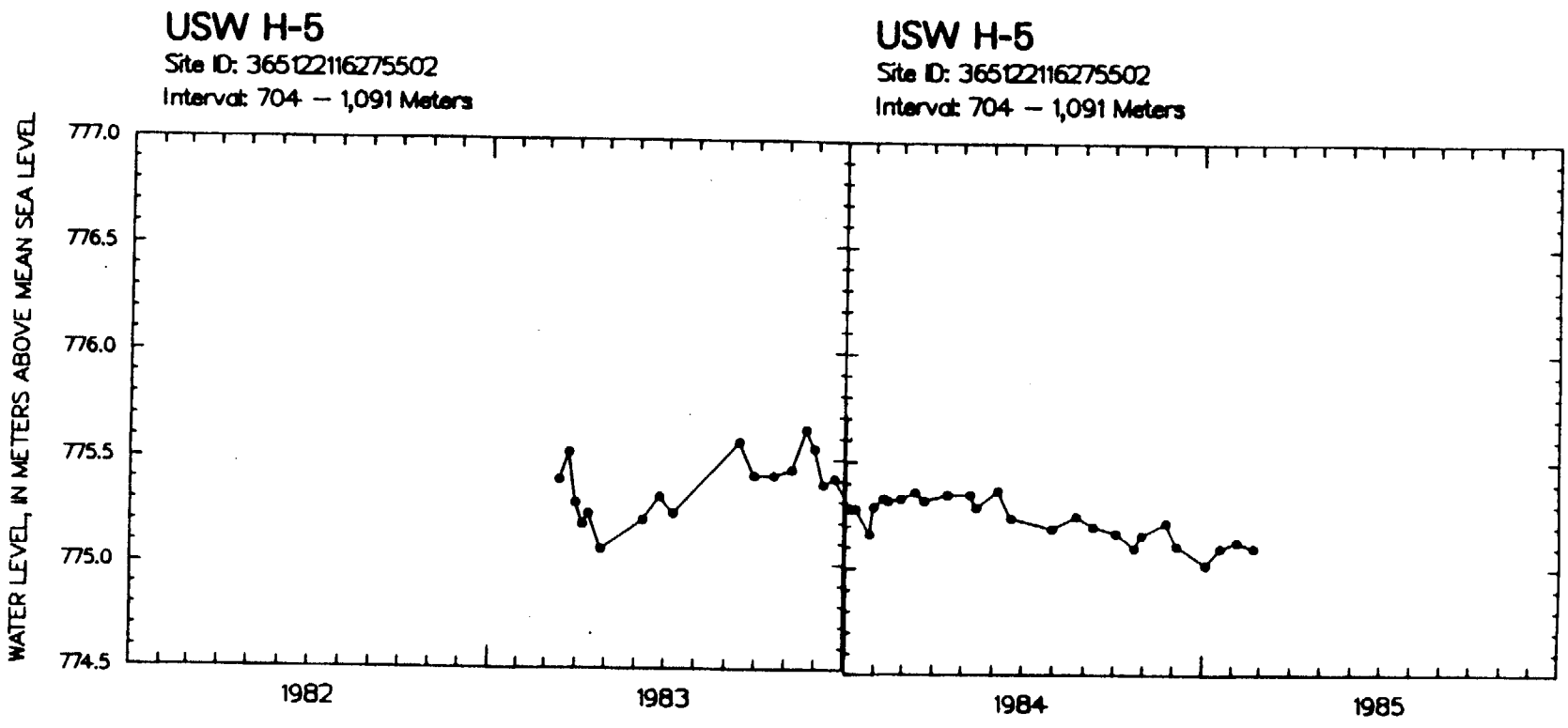

Hydrograph - Well USW H-5. From Robison et al., 1988.

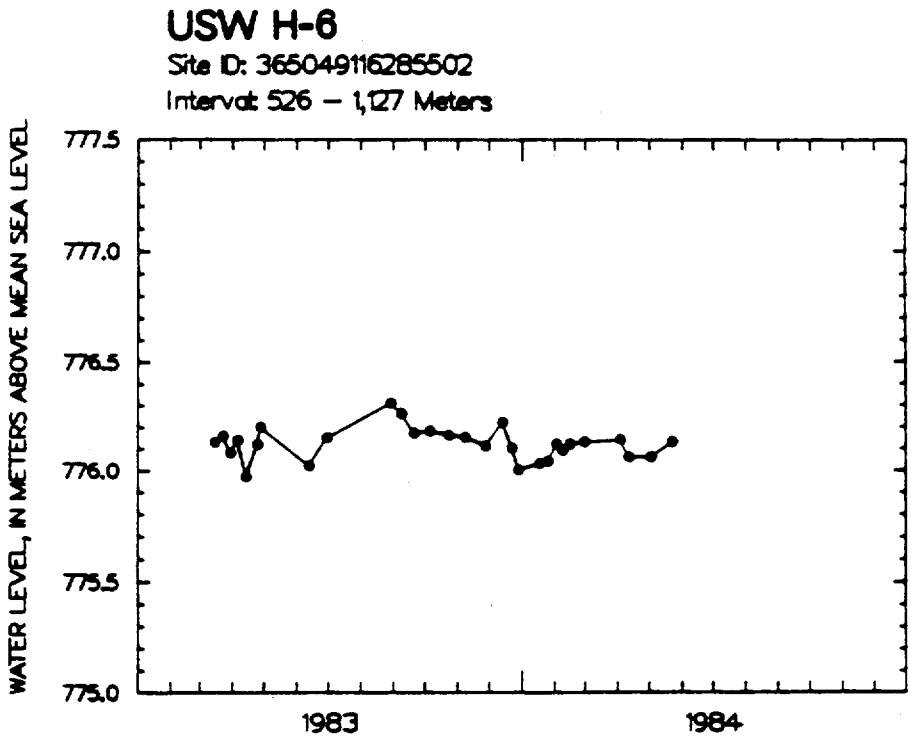

Hydrograph - Well USW H-6. From Robison et al., 1988.

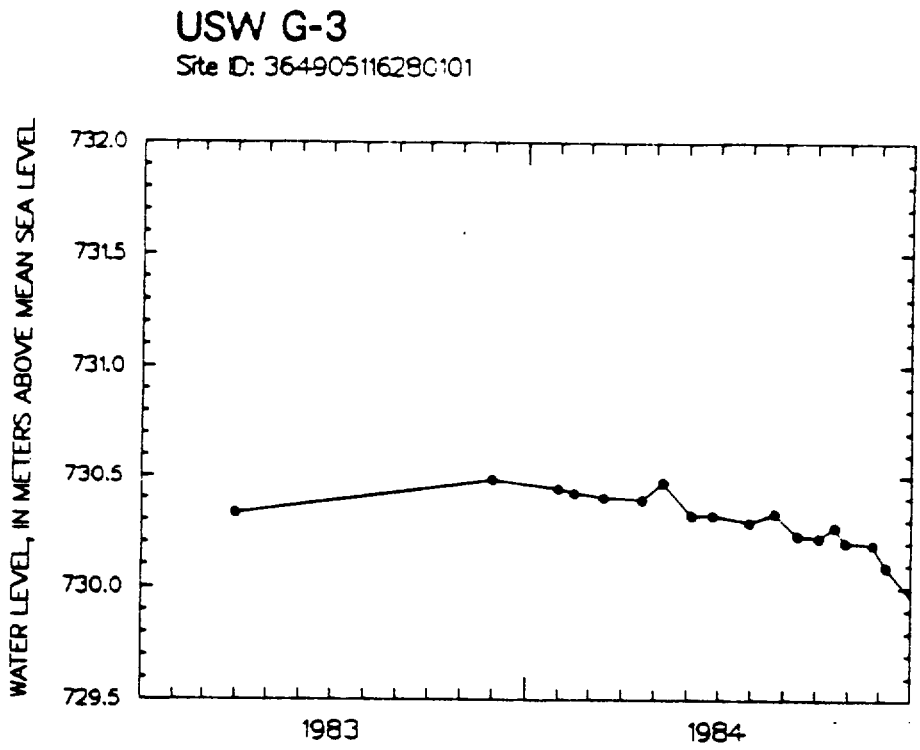

Hydrograph - Well USW G-3. From Robison et al., 1988.

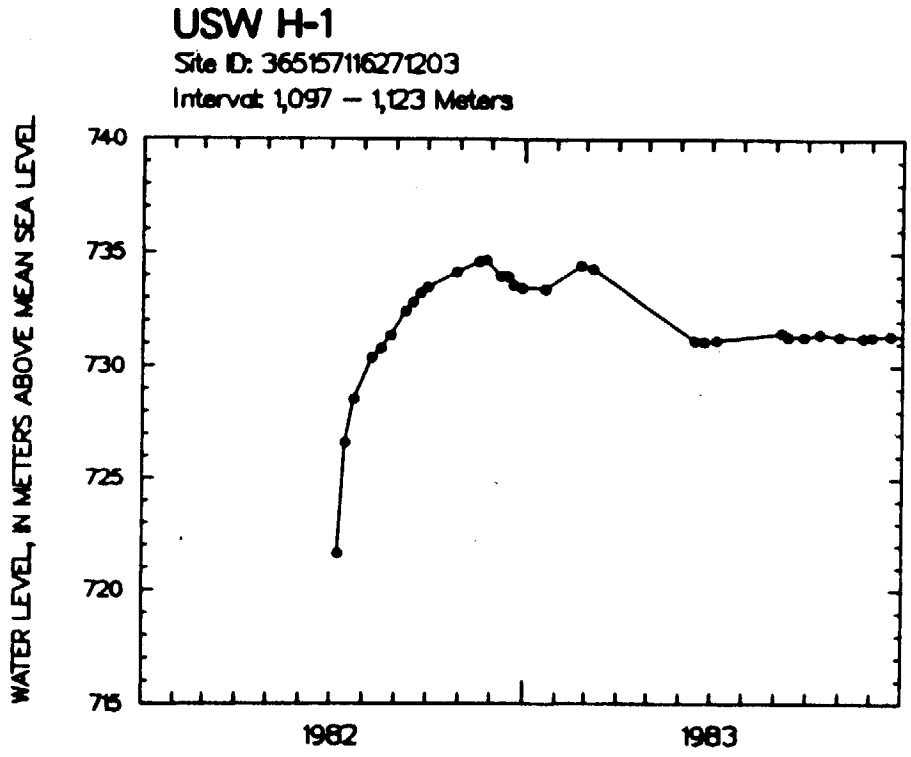

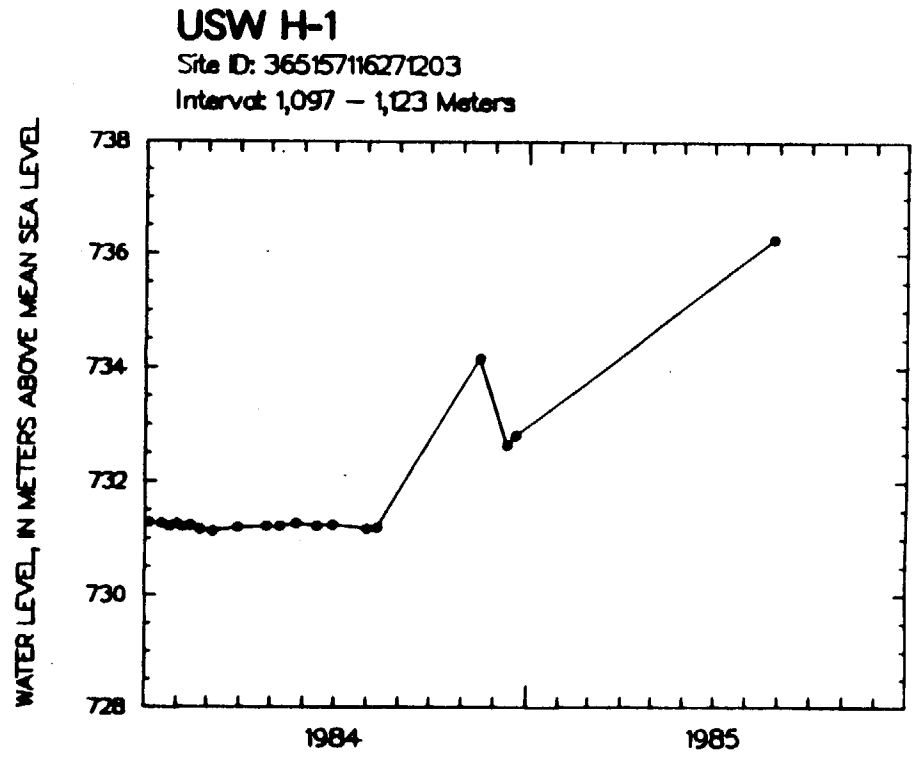

Hydrograph - Well USW H-1. From Robison et al., 1988.

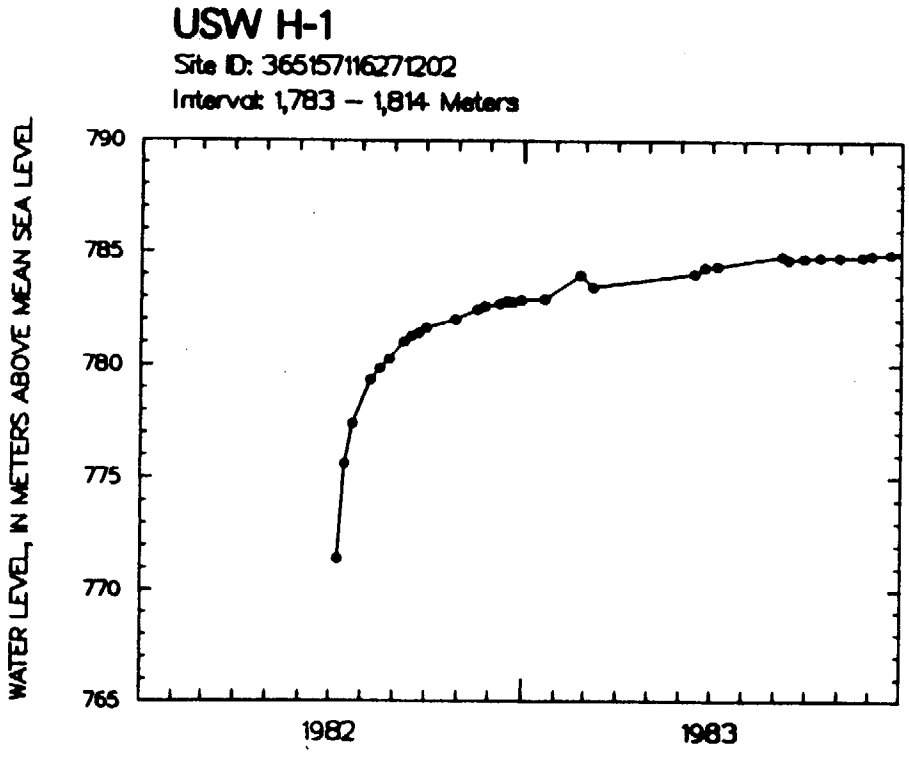

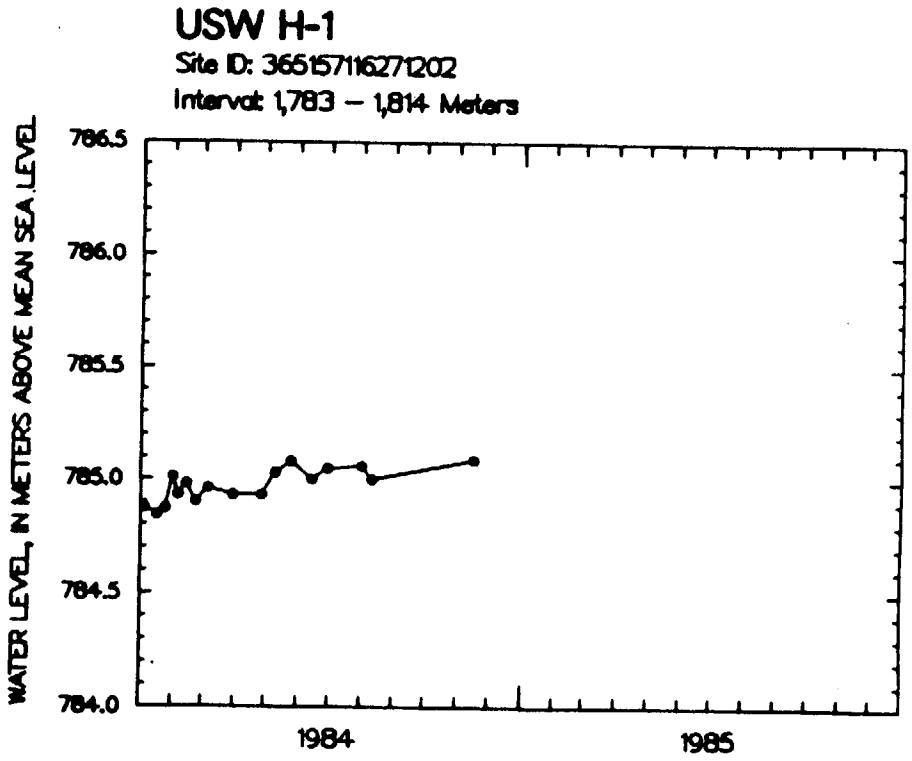

Hydrograph - Well USW H-1. Robison et al., 1988.

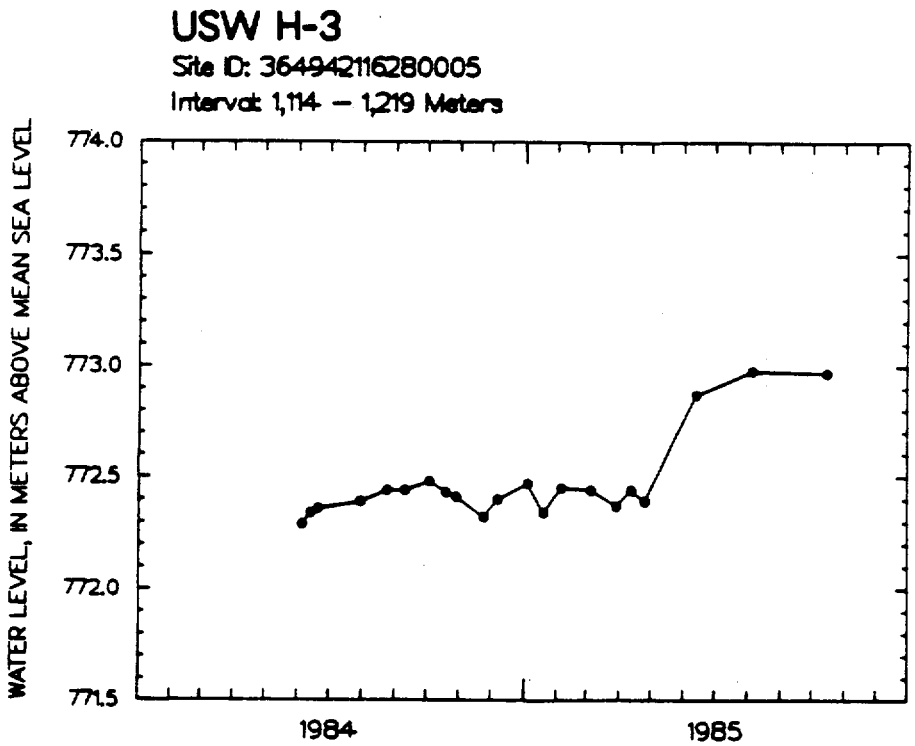

Hydrograph - Well USW H-3. From Robison et al., 1988.

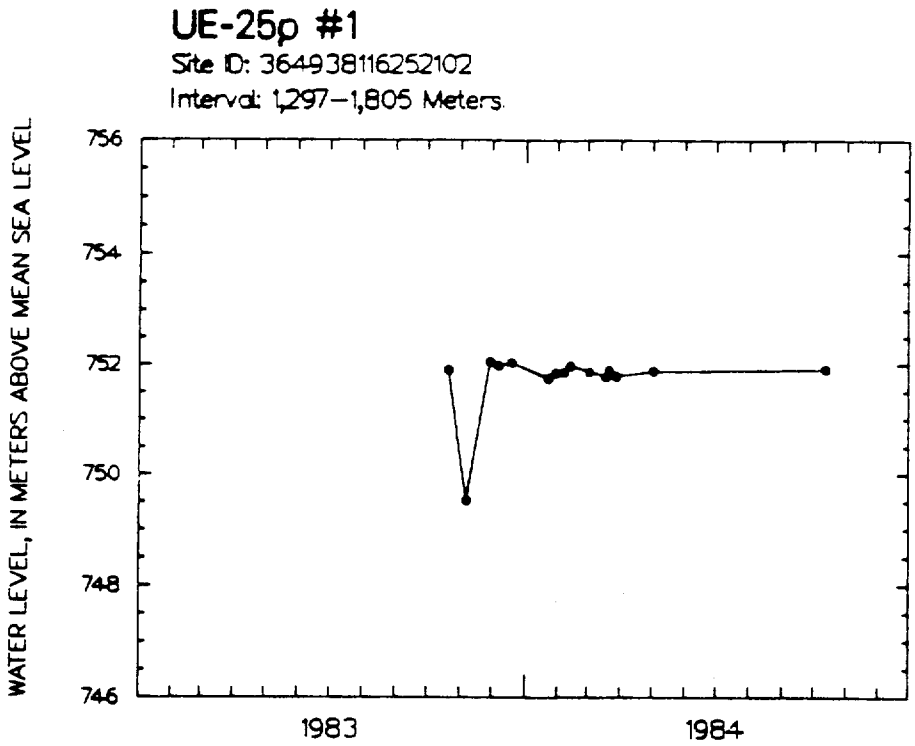

Hydrograph - Well UE-25p#1. From Robison et al., 1988.

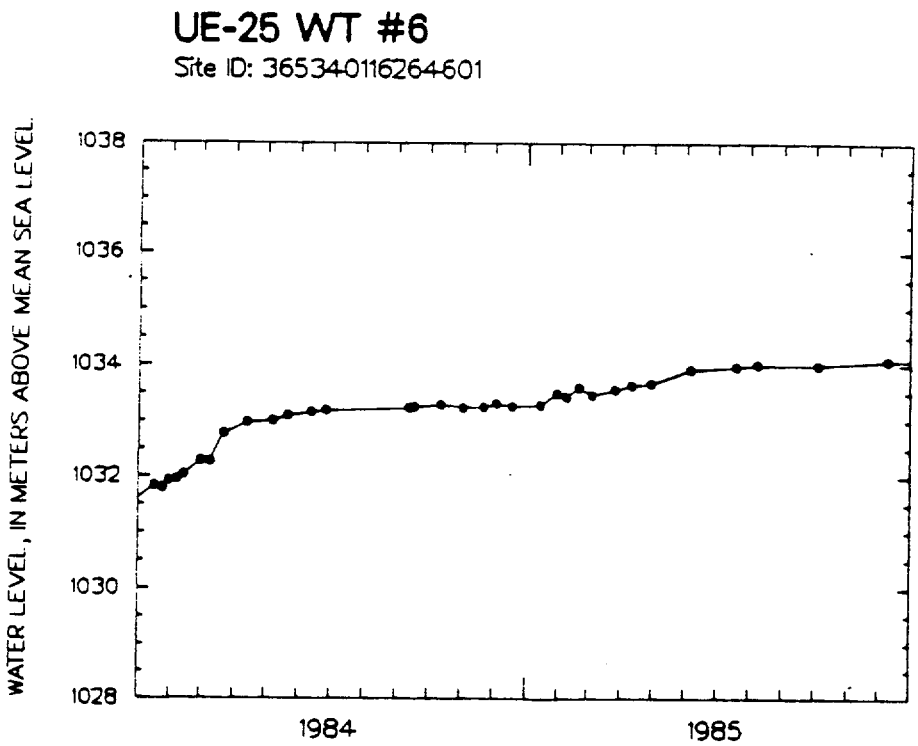

Hydrograph - Well UE-25 WT #6. From Robison et al., 1988.

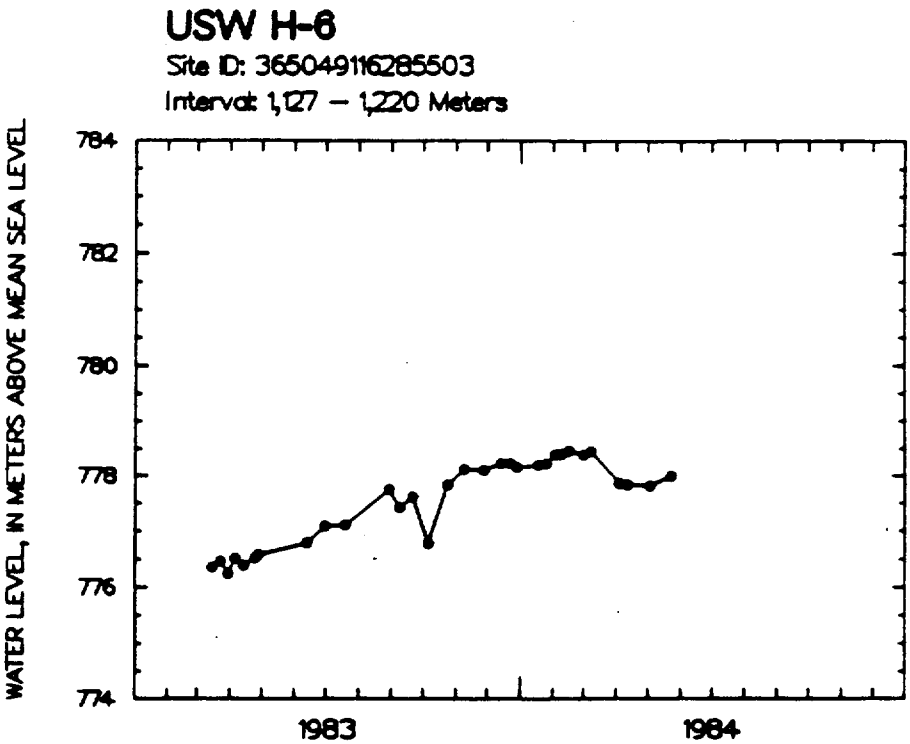

Hydrograph - Well USW H-6. From Robison et al., 1988.

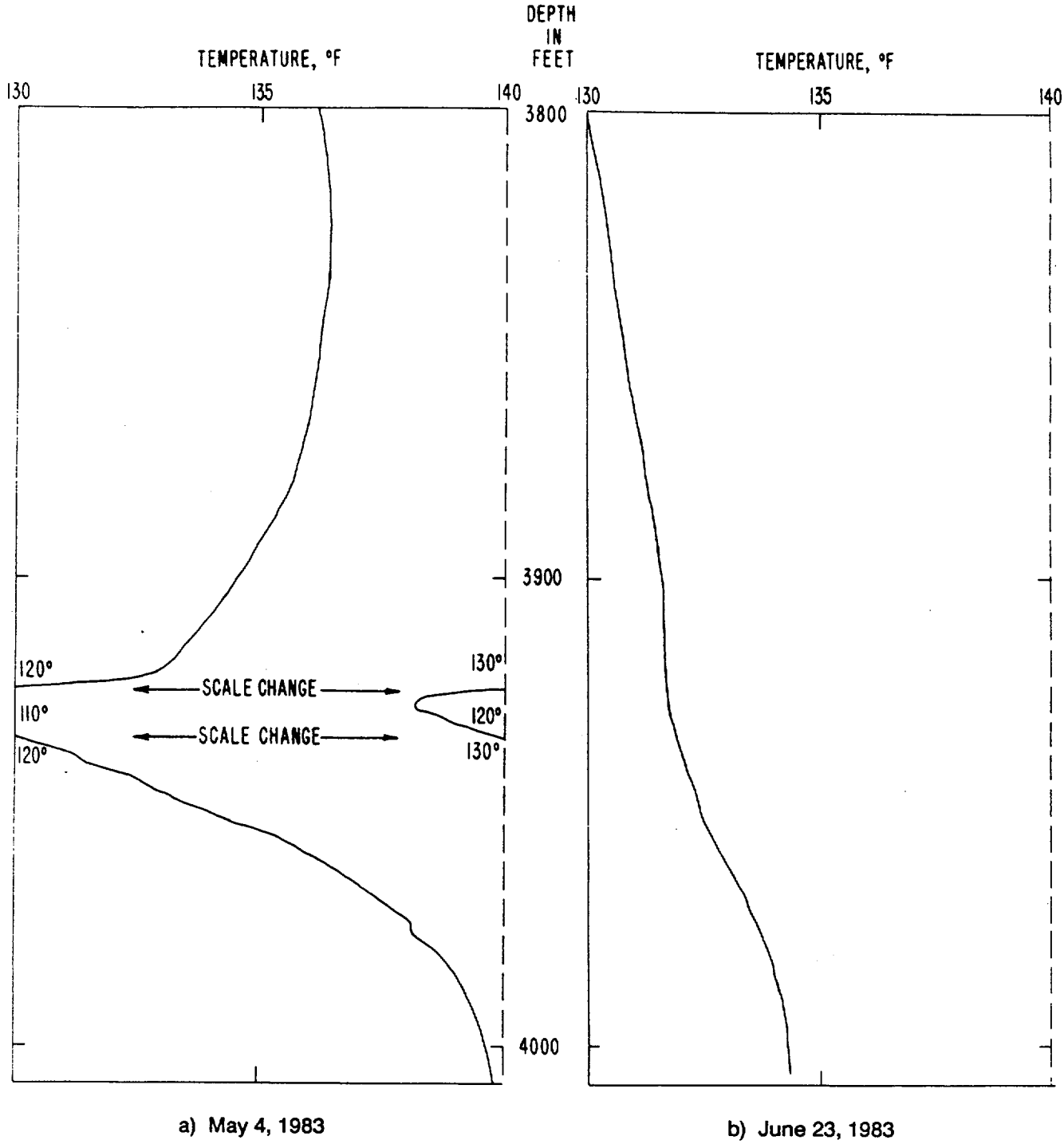

Temperature logs obtained during and shortly after completion of borehole UE-25p#1 in the vicinity of fault contact between the Paleozoic carbonates and the tuff "pile". From Carr et al., 1986.

[All units are milligrams per liter unless otherwise indicated]

Date of collection	02/09/83	05/12/83
Depth interval (meters)	1/381-1,197	1,297-1,805
Temperature (degrees Celsius)	44	56
pH, field (units)	6.8	6.6
pH, laboratory (units)	7.7	7.2
Potassium (K)	5.6	12
Calcium (Ca)	37	100
Magnesium (Mg)	10	39
Sodium (Na)	92	150
Strontium (Sr, micrograms per liter)	180	450
Lithium (Li, micrograms per liter)	230	590
Chloride (Cl)	13	28
Bicarbonate (HCO_3), field	330	710
Fluoride (F)	3.4	4.7
Sulfate (SO_4)	38	160
Silica (SiO_2)	49	41
Specific conductance, laboratory (microsiemens per centimeter at 25° Celsius)	639	1,330
Dissolved solids (sum)	418	878
Tritium (picocuries per liter)	0±10	0±10
Oxygen-18/oxygen-16 ($\delta^{18}O$)2/	-13.5	-13.8
Deuterium/hydrogen ($\delta^{2}H$)3/	-106.0	-106.0
Carbon-13/carbon-12 ($\delta^{13}C$)4/	-4.2	-2.2
Carbon-14 (percent of modern standard)	3.40	2.31

1/Borehole-flow survey indicated that about 28 percent of pumping production was from below 1,197 meters; see borehole-flow survey section for explanation.

2/Deviation of oxygen-18/oxygen-16 ratio of sample from standard mean ocean water (SMOW) relative to SMOW, in parts per thousand.

3/Deviation of deuterium/hydrogen ratio of sample from standard mean ocean water (SMOW) relative to SMOW, in parts per thousand.

4/Deviation of carbon-13/carbon-12 ratio of sample from Peedee belemnite standard (PDB) relative to PDB, in parts per thousand.

Comparison of the results of chemical analyses of water samples from the tuff "pile" and from the Paleozoic carbonates. From Craig and Johnson, 1984.

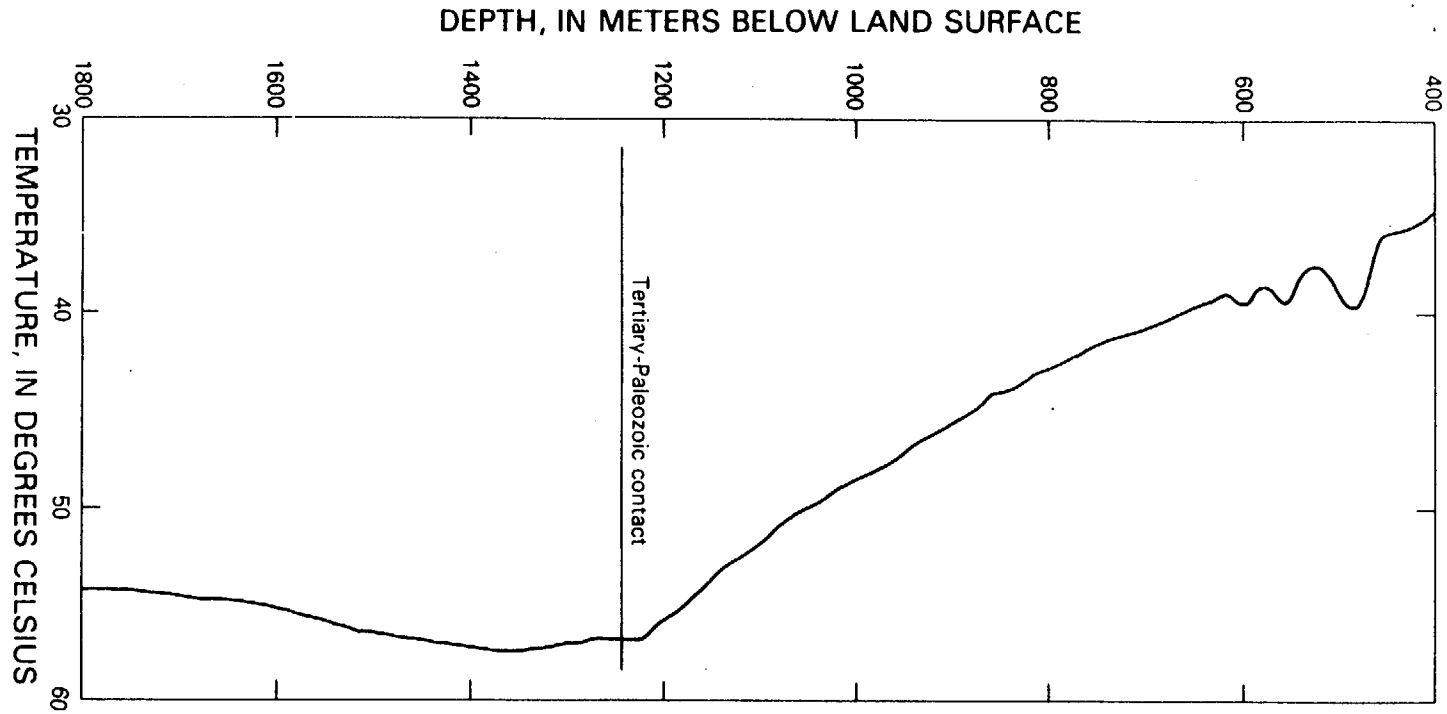

Borehole temperature log - Well UE-25p#1. From Craig and Johnson, 1984.

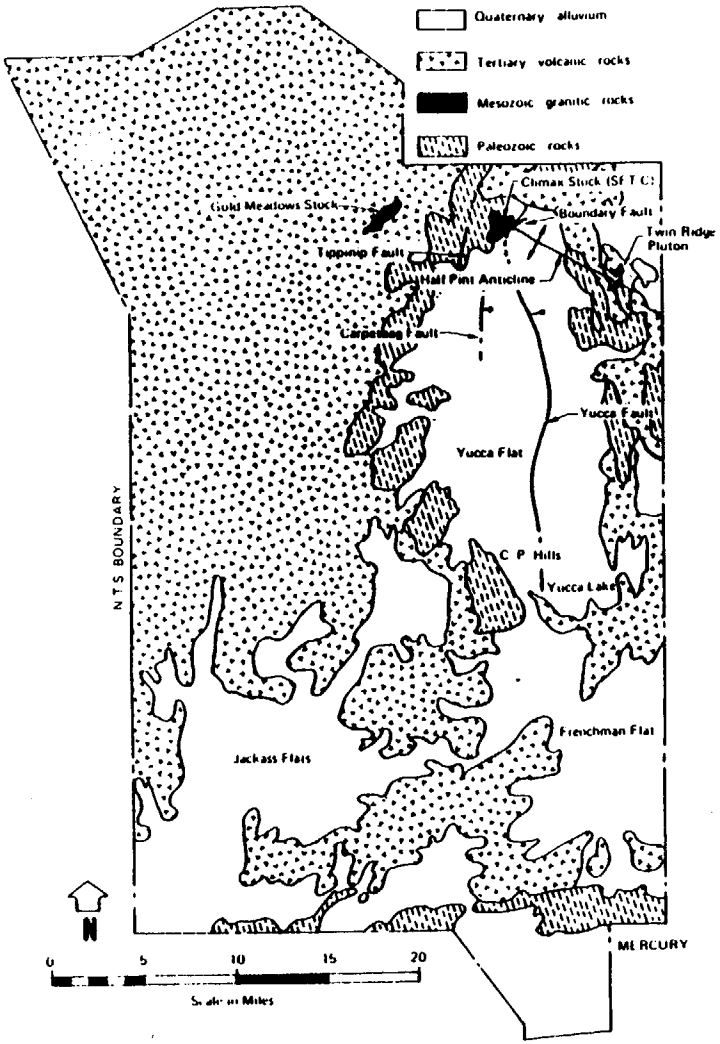

a) LOCATION MAP

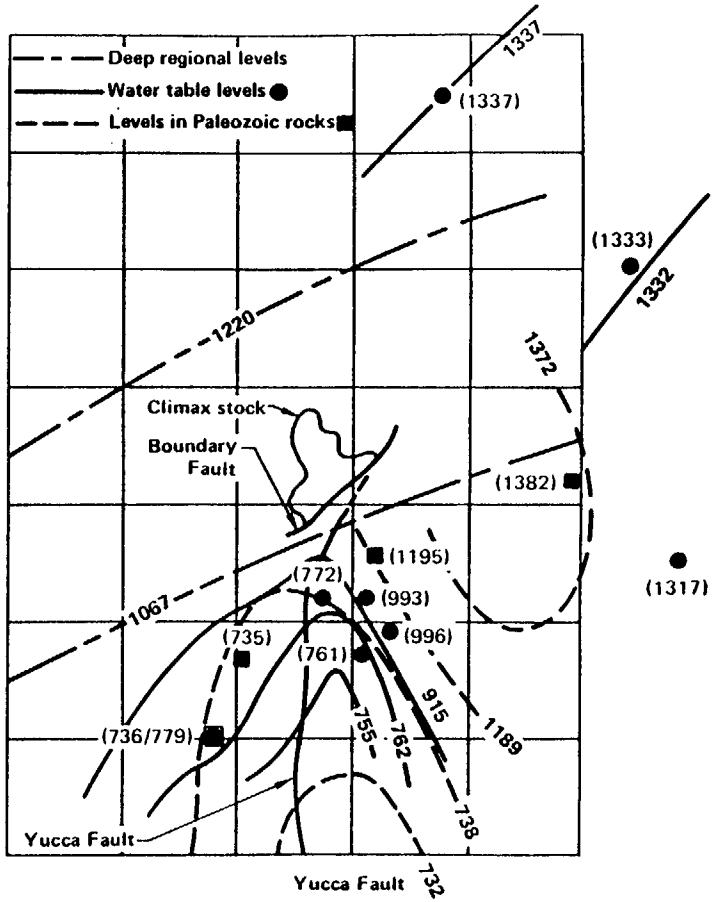

b) POTENTIOMETRIC MAP

Location map and geohydrologic setting. Climax Stock. From Murray, 1981.

	Stress magnitude	Standard deviation	Bearing	Inclination
	MPa	MPa		+ degrees above horizontal - degrees below horizontal
Principal stresses				
	(+, compression)			
S_1 (maximum)	+11.56	±1.05	N. 56° E.	-29°
S_2 (intermediate)	+7.13	±0.81	N. 26° E.	+57°
S_3 (minimum)	+2.75	±0.65	N. 42° W.	-14°
Normal stress components in X, Y, Z (east, north, vertical) coordinate system				
	(+, compression)			
σ_x	+7.64	±0.63	East	Horizontal
σ_y	+5.87	±0.81	North	Horizontal
σ_z	+7.92	±0.67	---	Vertical
Shear stress components in X, Y, Z coordinate system[1]				
τ_{xy}	+3.61	±0.50	---	---
τ_{yz}	-0.28	±0.72	---	---
τ_{zx}	-2.24	±0.54	---	---

[1]Positive or negative sign on shear stress magnitude indicates direction of shear stress with respect to X, Y, Z coordinate system.

State of in situ stress. South heater drift, STC-C. Climax Stock. From Ellis and Magner, 1982.

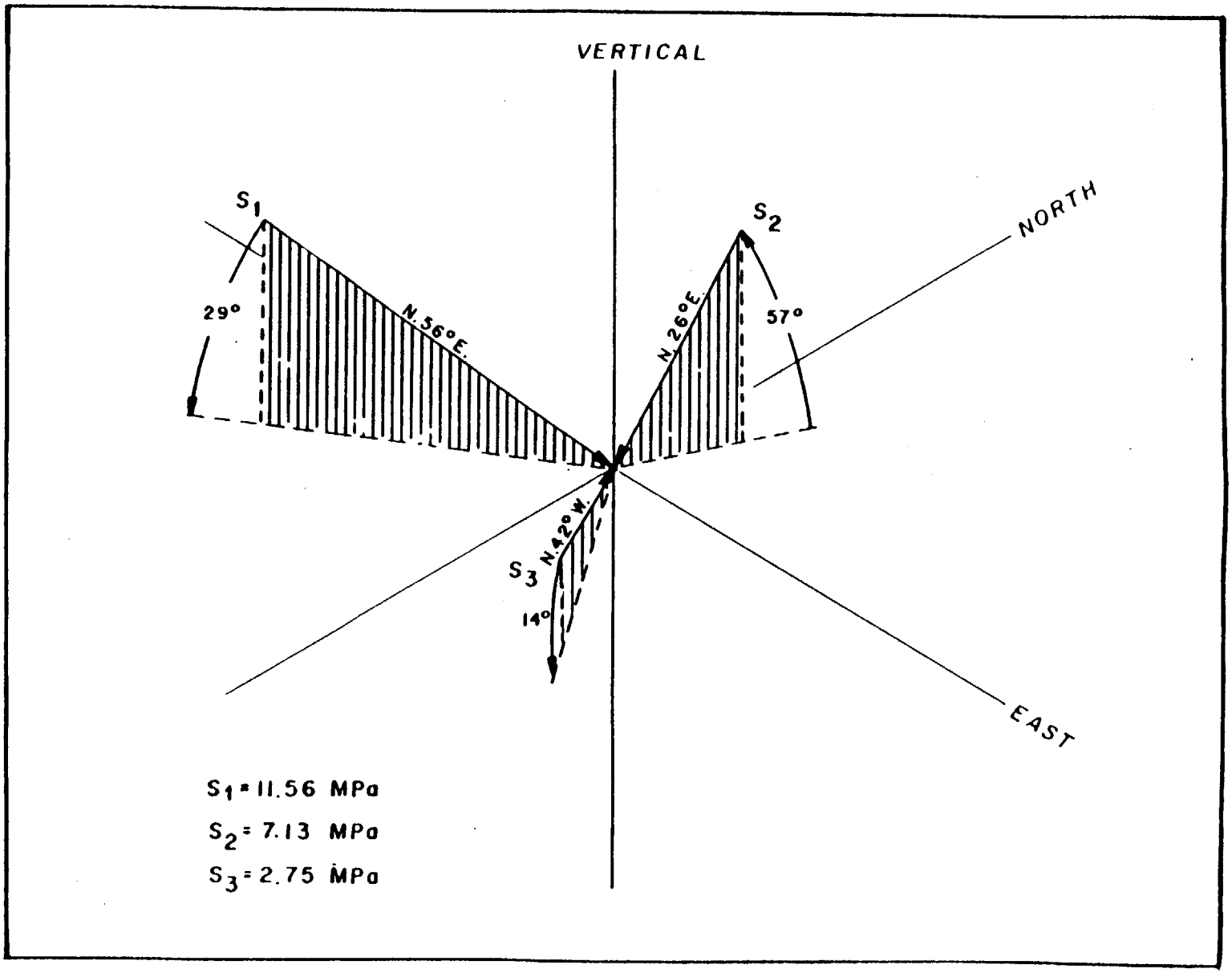

Graphical representation of principal stresses. South heater drift. Climax Stock. From Ellis and Magner, 1982.

	Stress magnitude	Standard deviation	Bearing	Inclination
	MPa	MPa		+ degrees above horizontal - degrees below horizontal
Principal stresses				
	(+, compression)			
S_1 (maximum)	+13.92	±0.77	N. 36° W.	+55°
S_2 (intermediate)	+9.07	±0.74	N. 59° E.	+4°
S_3 (minimum)	+4.28	±0.80	N. 28° W.	-35°
Normal stress components in X, Y, Z (east, north, vertical) coordinate system				
	(+, compression)			
σ_x	+8.89	±0.76	East	Horizontal
σ_y	+7.60	±0.76	North	Horizontal
σ_z	+10.78	±0.68	---	Vertical
Shear stress components in X, Y, Z coordinate system[1]				
τ_{xy}	+0.60	±0.44	---	---
τ_{yz}	+3.81	±0.56	---	---
τ_{zx}	-2.41	±0.56	---	---

[1]Positive or negative sign on shear stress magnitude indicates direction of shear stress with respect to X, Y, Z coordinate system.

State of in situ stress. Hard hat tunnel. Climax Stock. From Ellis and Magner, 1982.

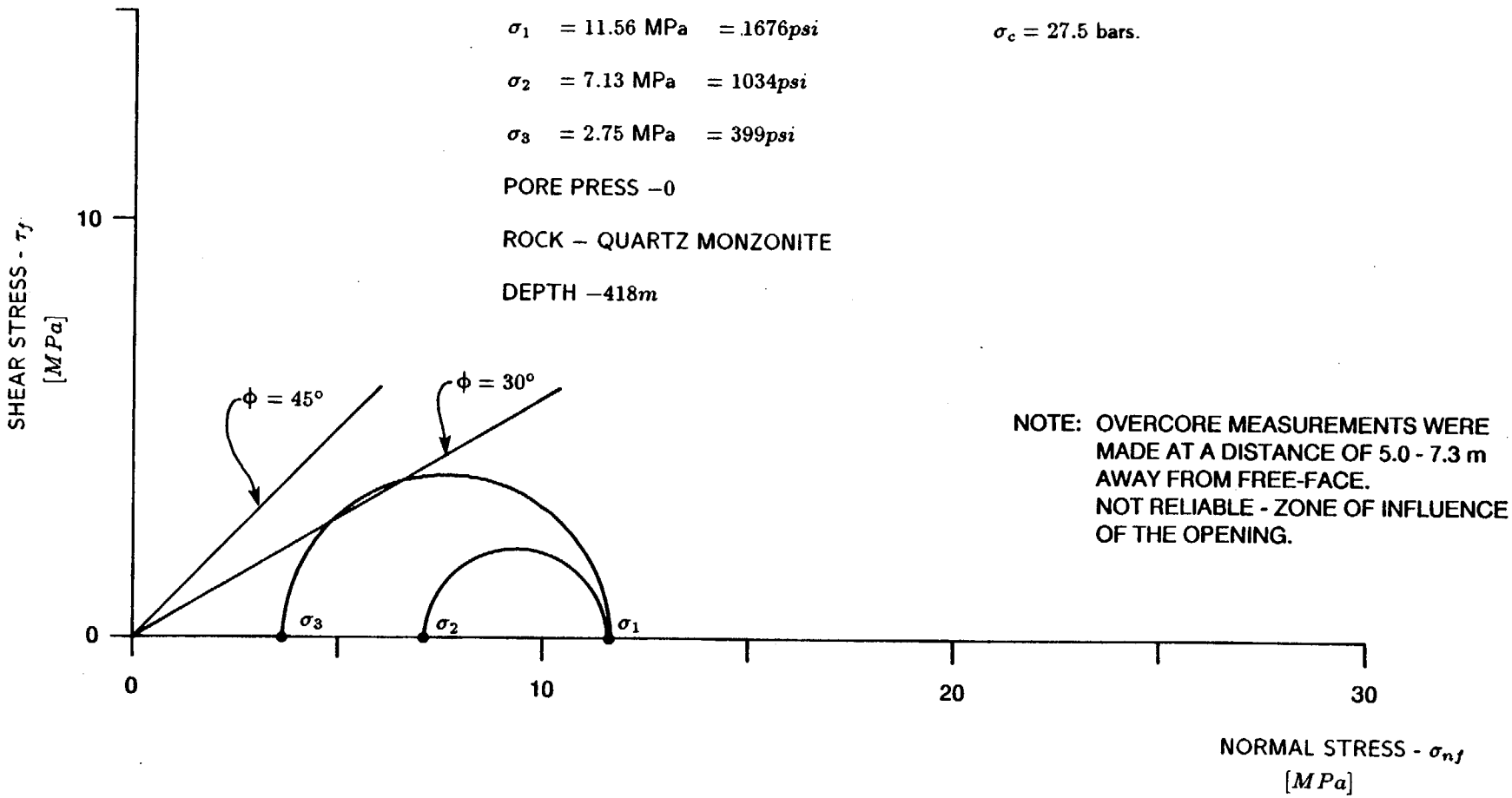

Mohr representation of in situ stress. South heater drift, STC-C. Climax Stock.

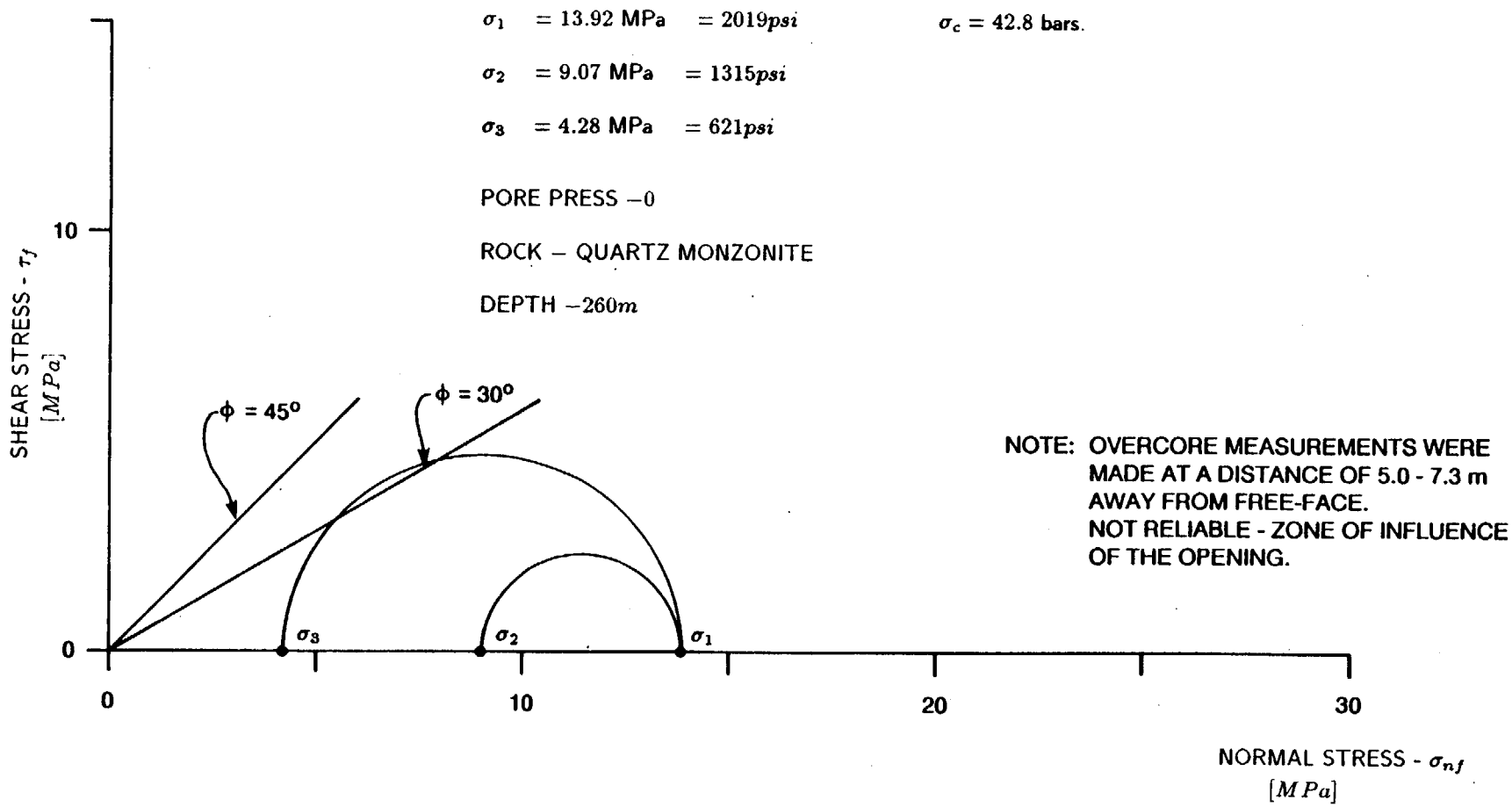

Mohr representation of in situ stress. Hard hat tunnel. Climax Stock.

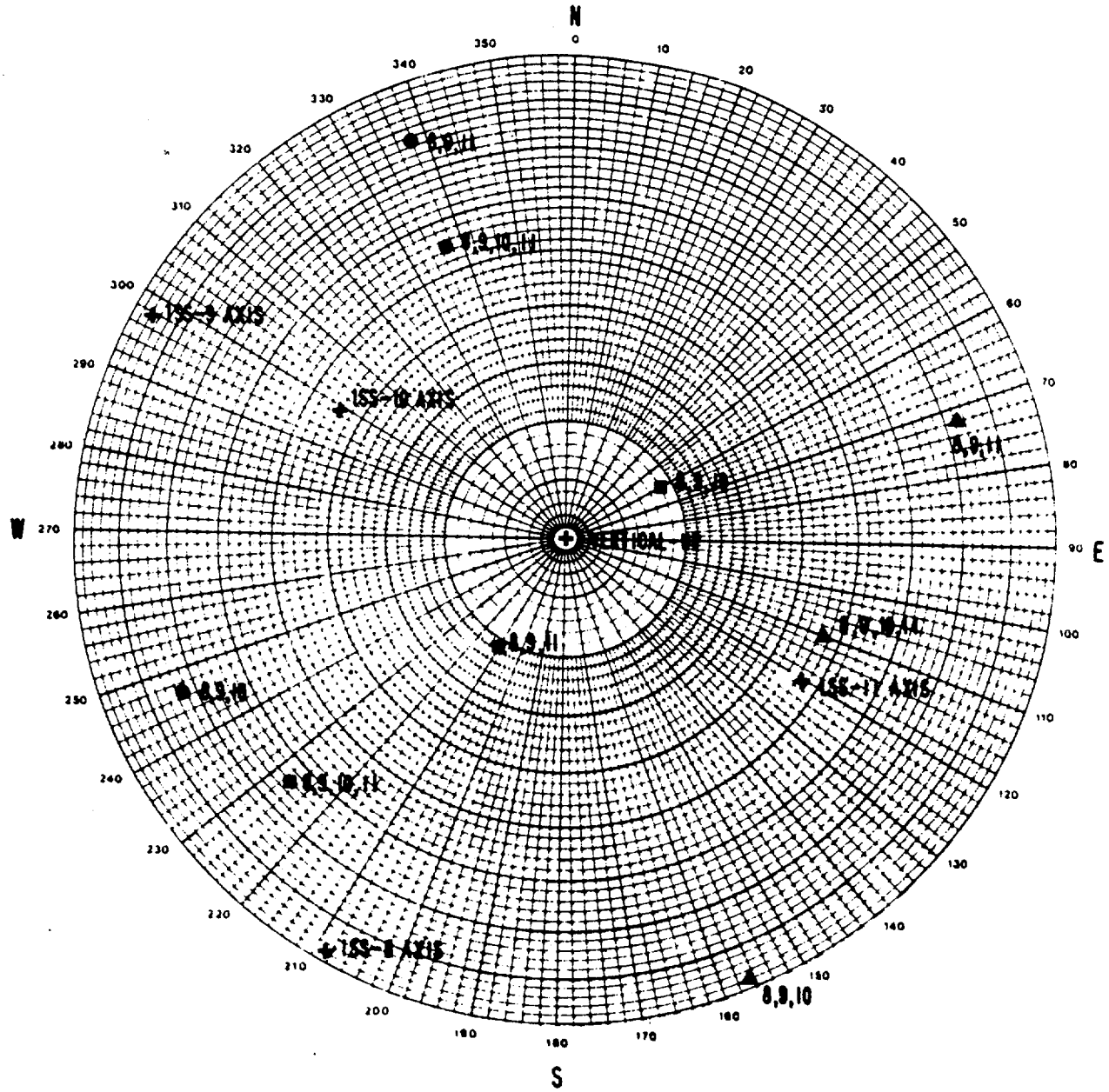

Principal Stresses, psi

Borehole Combinations	● σ_1	■ σ_2	▲ σ_3
ISS-8,9,10	1,795	1,081	714
ISS-8,9,11	1,844	1,287	557
ISS-8,9,10,11	1,654	1,195	992

Note: All stresses compressive

Borehole ISS-8 includes all USBM gage tests beyond depth 60 ft.

State of in situ stress (USBM gage). Spent fuel test facility. Boreholes ISS-8, 9, 10, and 11. Climax Stock. From Creveling et al., 1984.

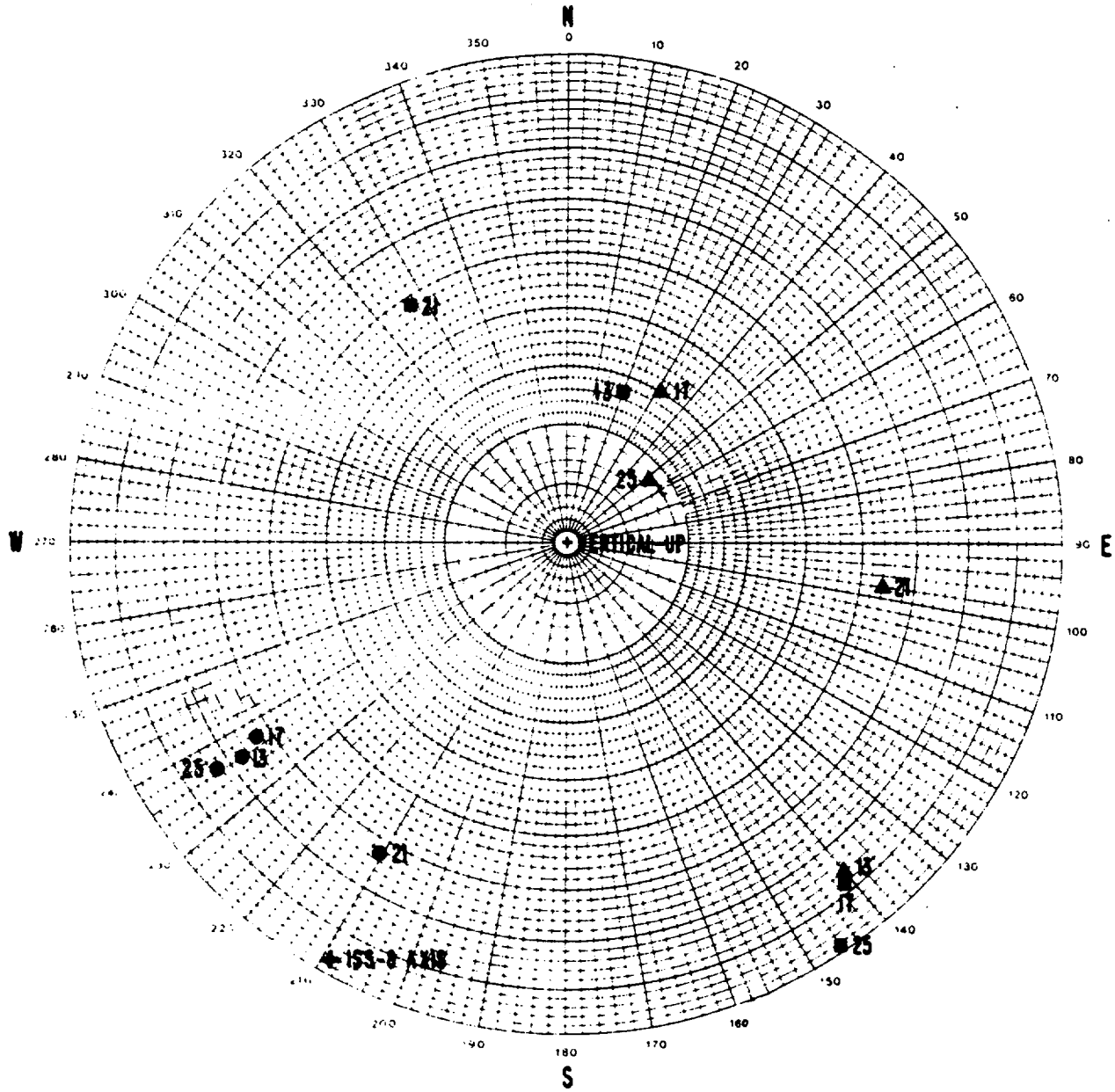

Principal Stresses, psi

ISS-8 Test No.	Depth, ft	● σ_1	■ σ_2	▲ σ_3
13	67.8	1,263	1,058	649
17	81.0	1,304	724	589
21	96.7	903	577	397
25	109.4	1,828	1,271	515

State of in situ stress (CSIRO cell). Spent fuel test facility. Borehole ISS-8. Climax Stock. From Creveling et al., 1984.

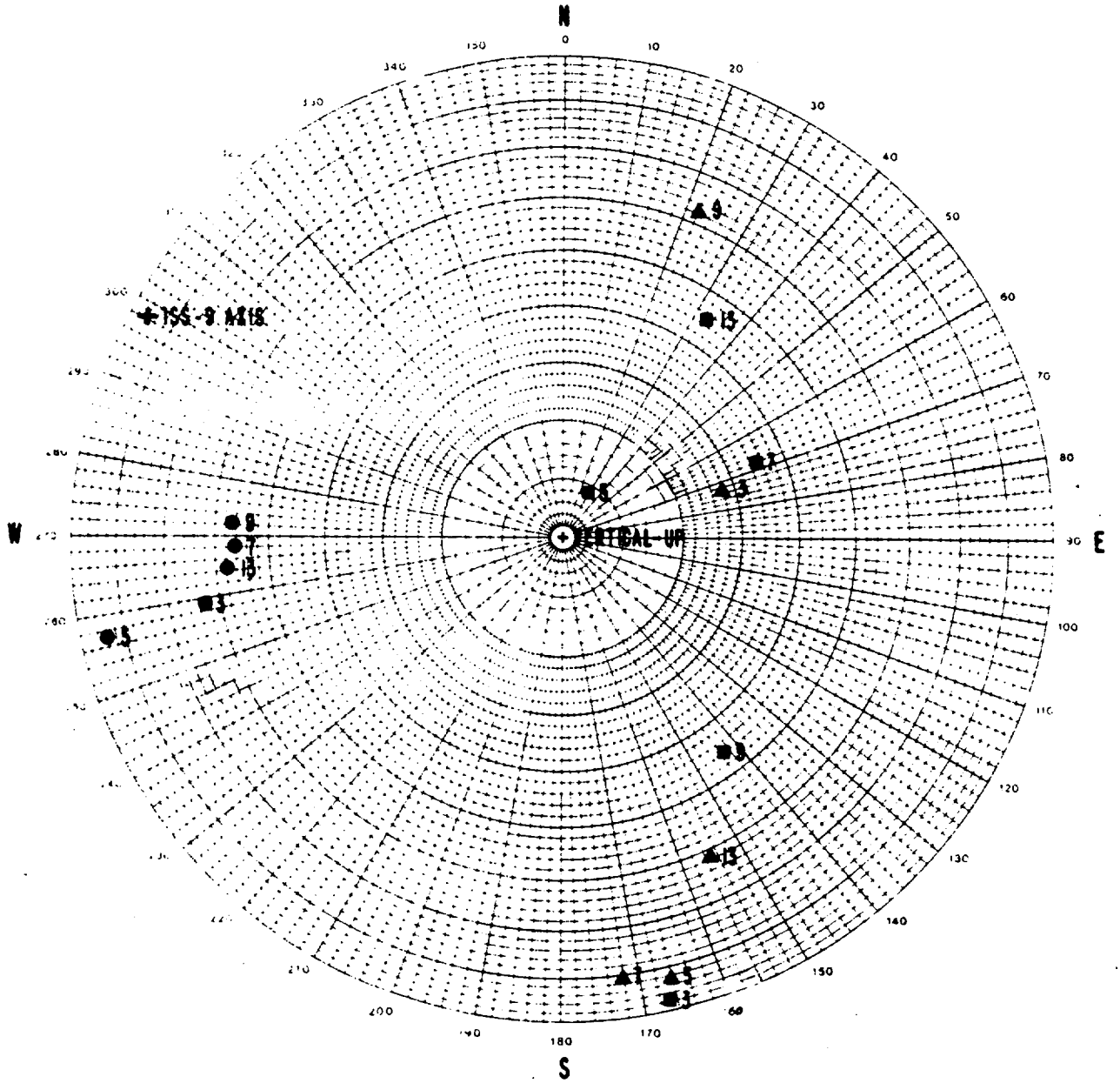

Principal Stresses, psi

ISS-9 Test No.	Depth, ft	● σ_1	■ σ_2	▲ σ_3
3	39.1	1,275	781	555
5	42.6	925	591	394
7	46.9	1,083	432	99
9	50.5	1,178	841	673
13	59.2	1,494	782	549

State of in situ stress (CSIRO cell). Spent fuel test facility. Borehole ISS-9. Climax Stock. From Creveling et al., 1984.

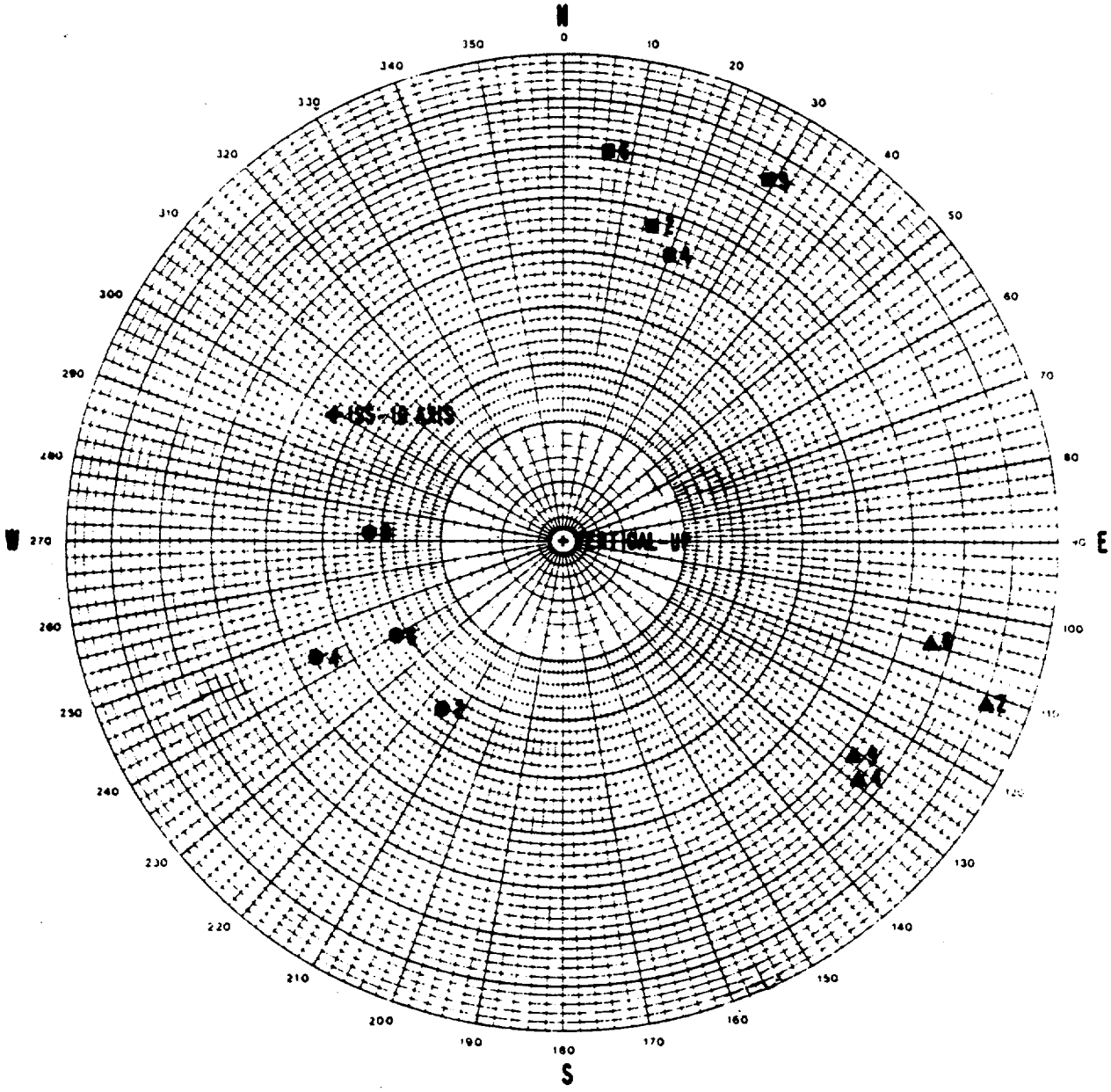

Principal Stresses, psi

ISS-10 Test No.	Depth, ft	● σ_1	■ σ_2	▲ σ_3
2	64.4	1,670	1,105	348
4	67.8	2,773	1,697	585
6	73.1	1,772	1,433	799
9	80.4	1,658	1,273	693

State of in situ stress (CSIRO cell). Spent fuel test facility. Borehole ISS-10. Climax Stock. From Creveling et al., 1984.

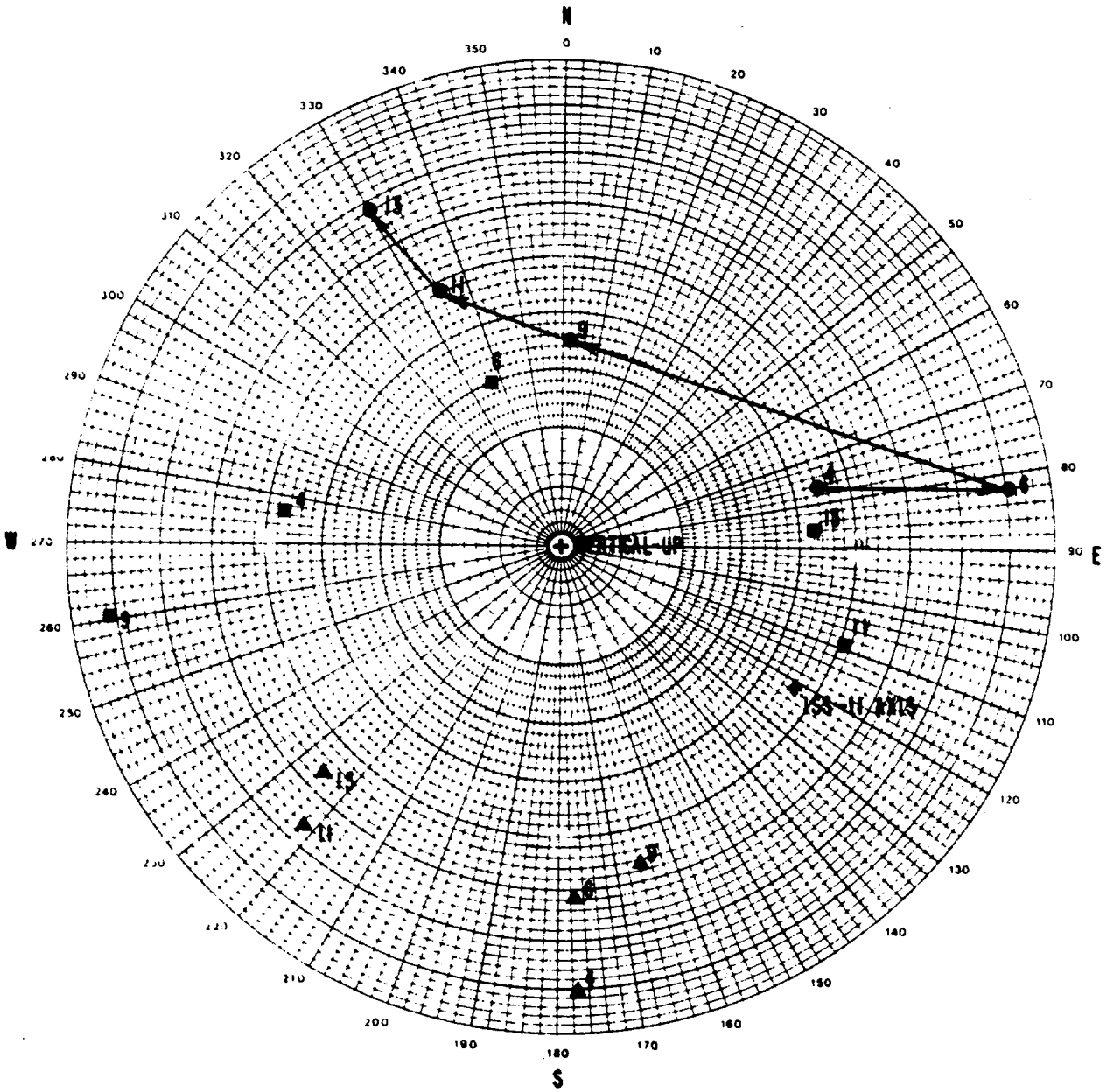

Principal Stresses, psi

ISS-11 Test No.	Depth, ft	● σ_1	■ σ_2	▲ σ_3
4	70.6	1,020	863	586
6	75.5	1,651	1,357	956
9	84.3	2,228	1,448	1,320
11	89.4	2,080	1,234	939
13	94.5	2,668	1,118	708

State of in situ stress (CSIRO cell). Spent fuel test facility. Borehole ISS-11. Climax Stock. From Creveling et al., 1984

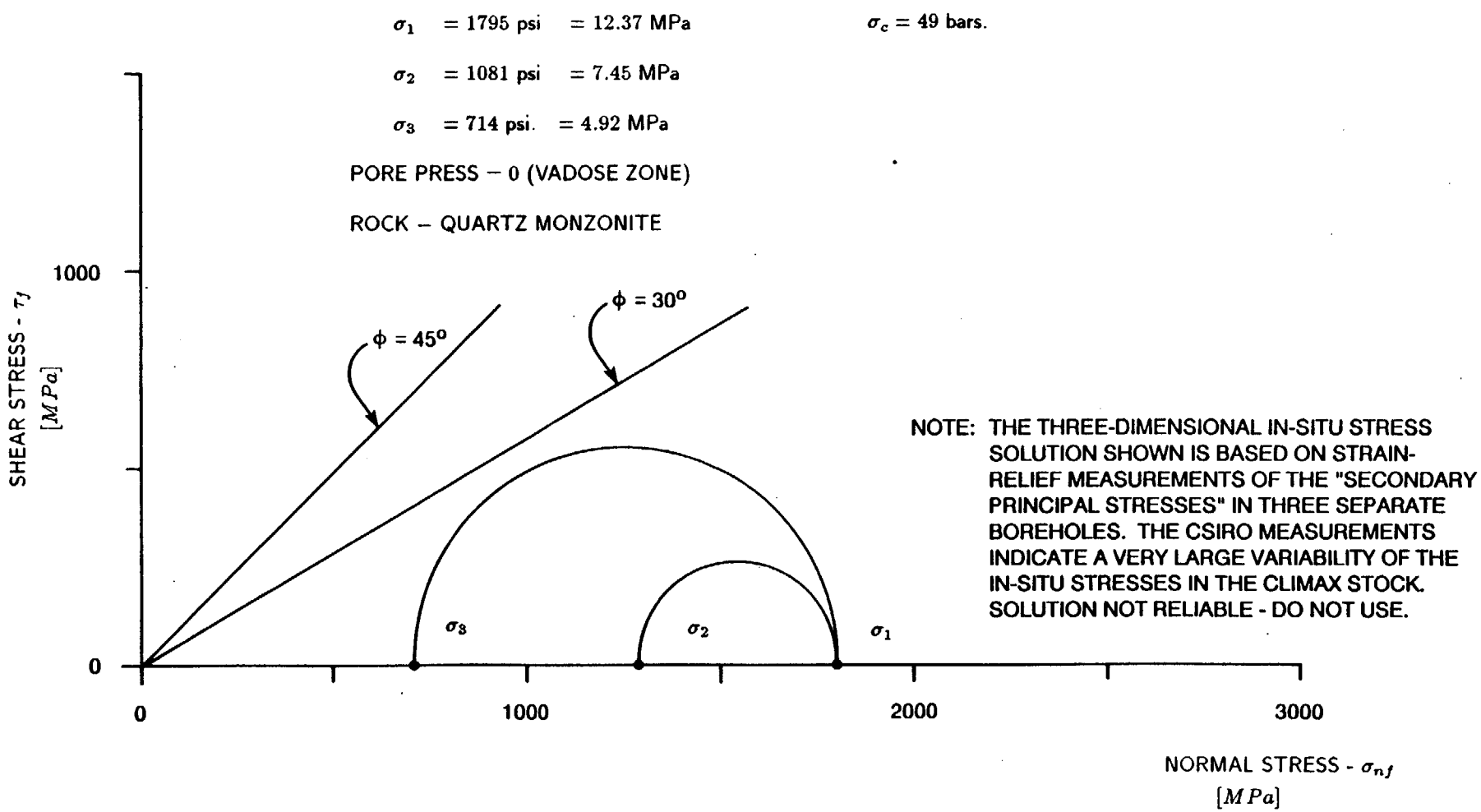

Mohr representation of in situ stress. Spent fuel test facility. Boreholes ISS-8, 9, 10, borehole depth > 60 feet. Climax Stock.

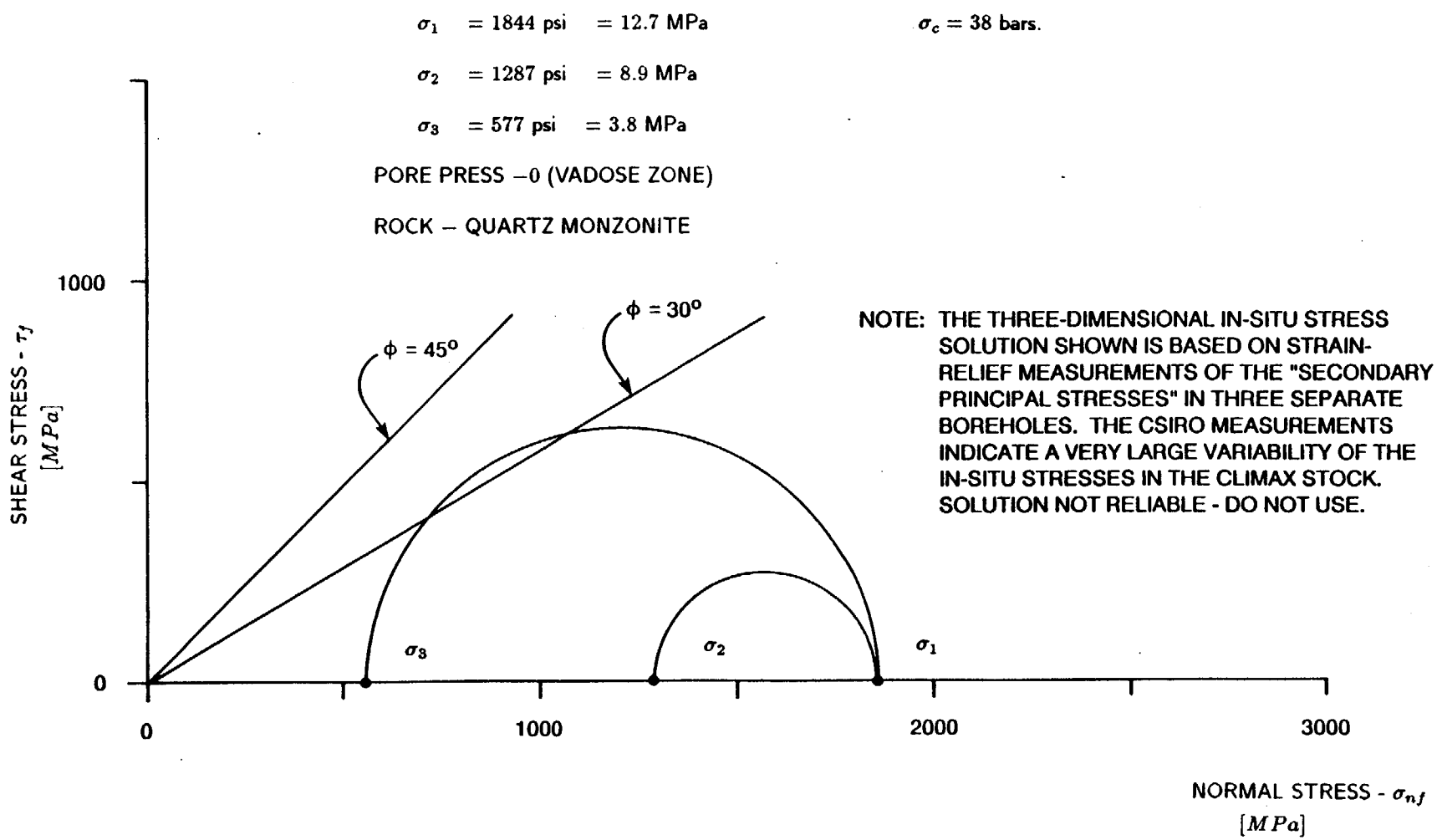

Mohr representation of in situ stress. Spent fuel test facility. Boreholes ISS-8, 9, 10, borehole depth > 60 feet. Climax Stock.

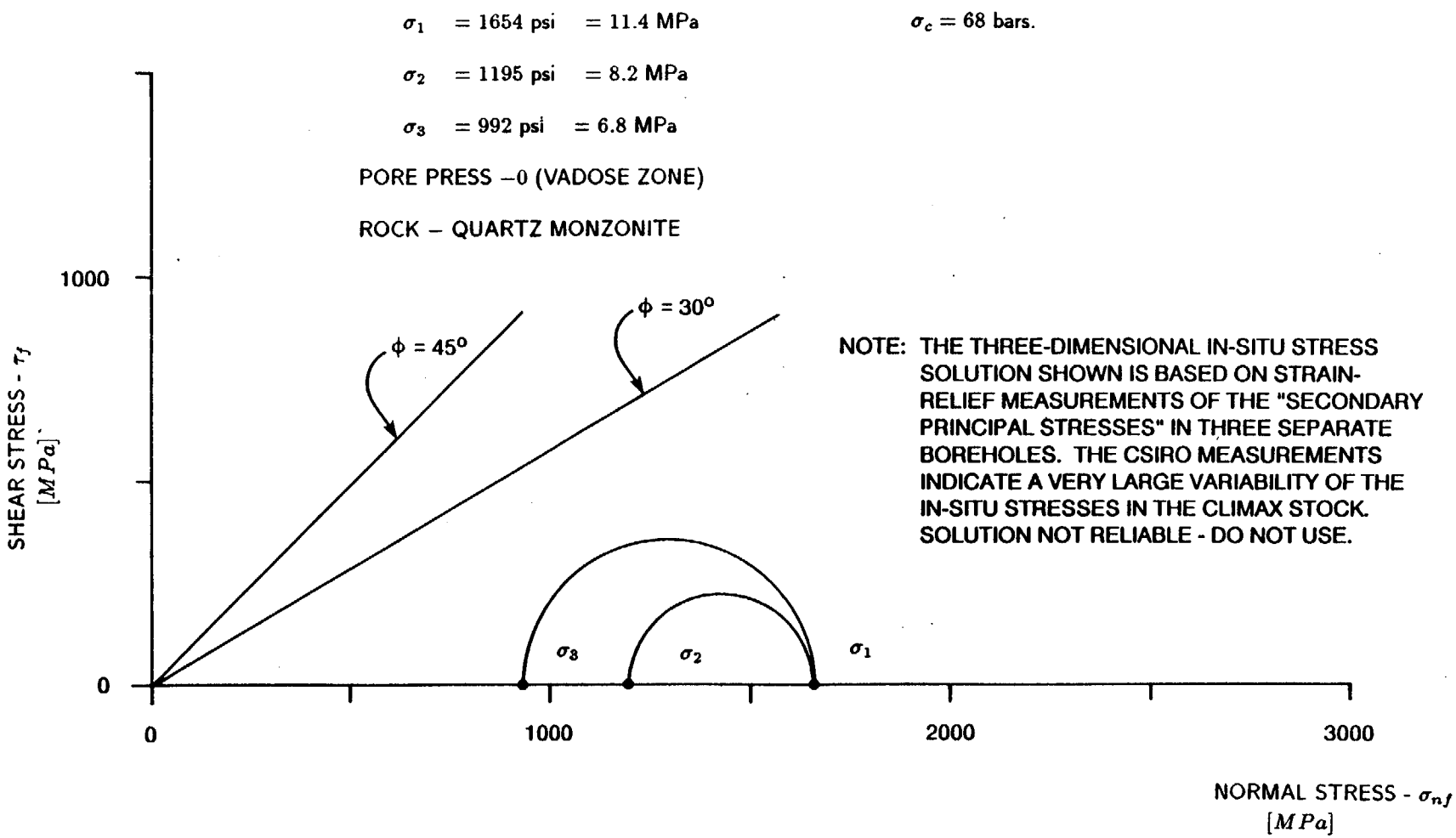

Mohr representation of in situ stress. Spent fuel test facility. Boreholes ISS-8, 9, 10, borehole depth > 60 feet. Climax Stock.

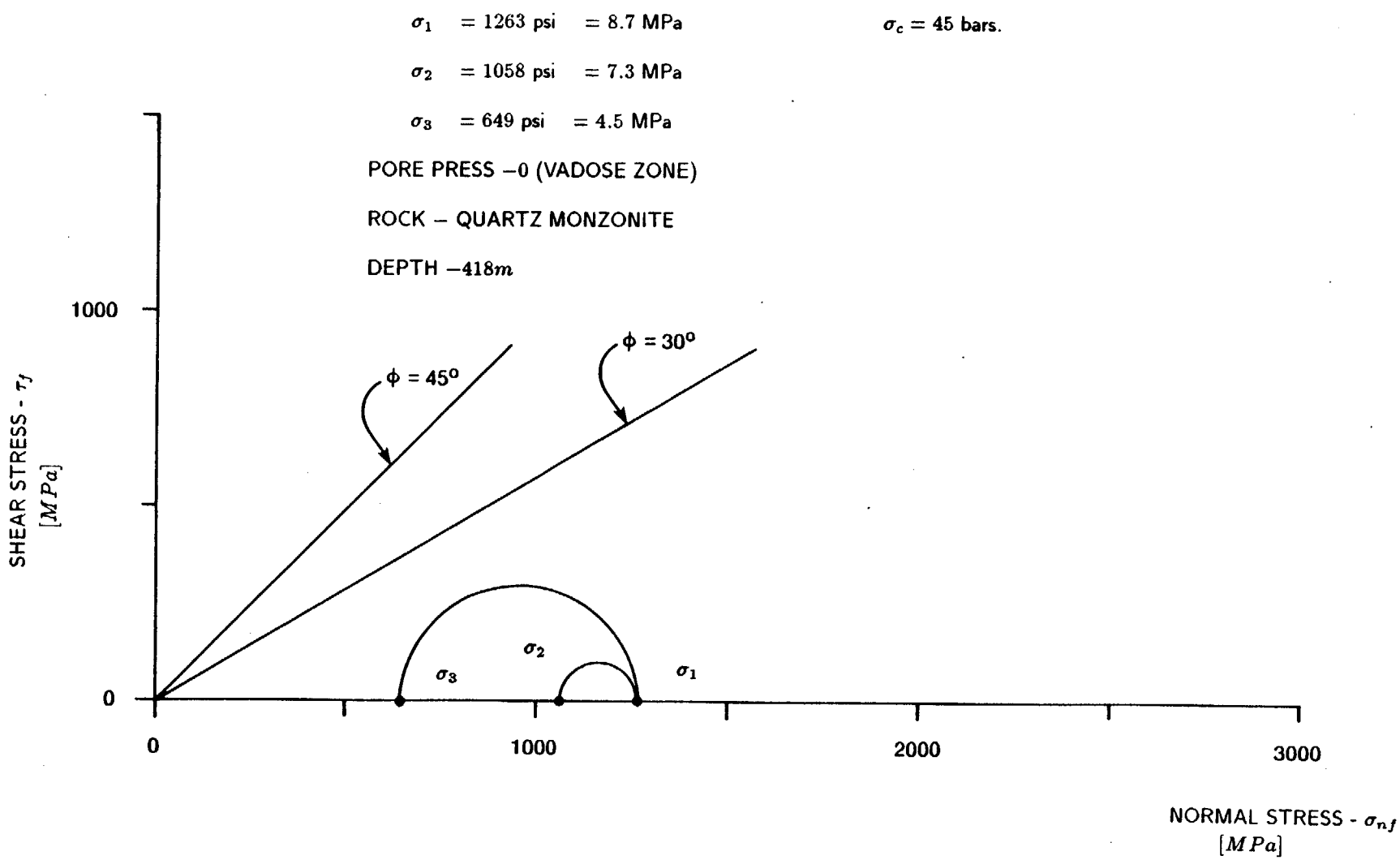

Mohr representation of in situ stress. Spent fuel test facility. Borehole ISS-8, Borehole depth 67.8 feet. Climax Stock.

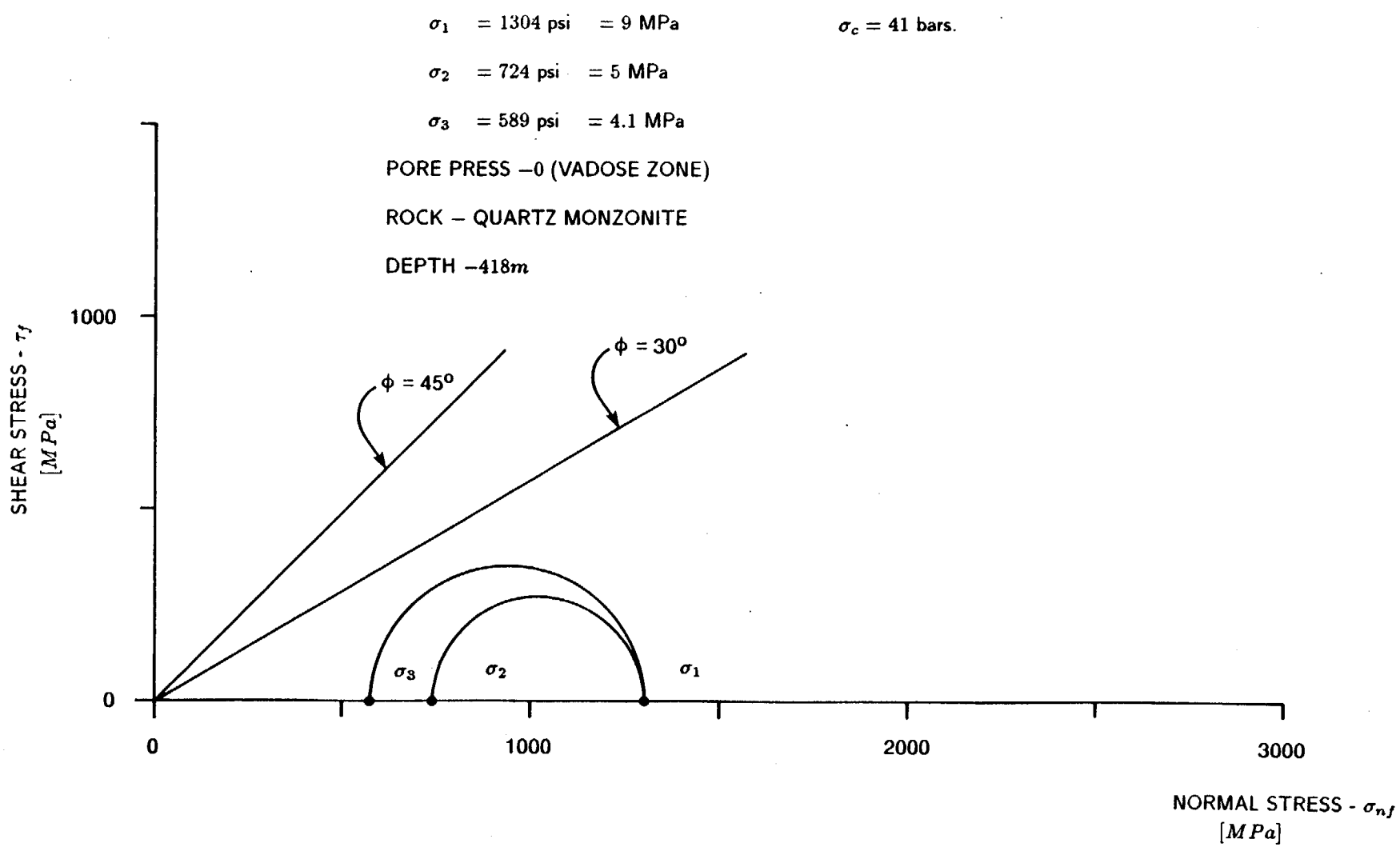

Mohr representation of in situ stress. Spent fuel test facility. Borehole ISS-8, borehole depth 81 feet. Climax Stock.

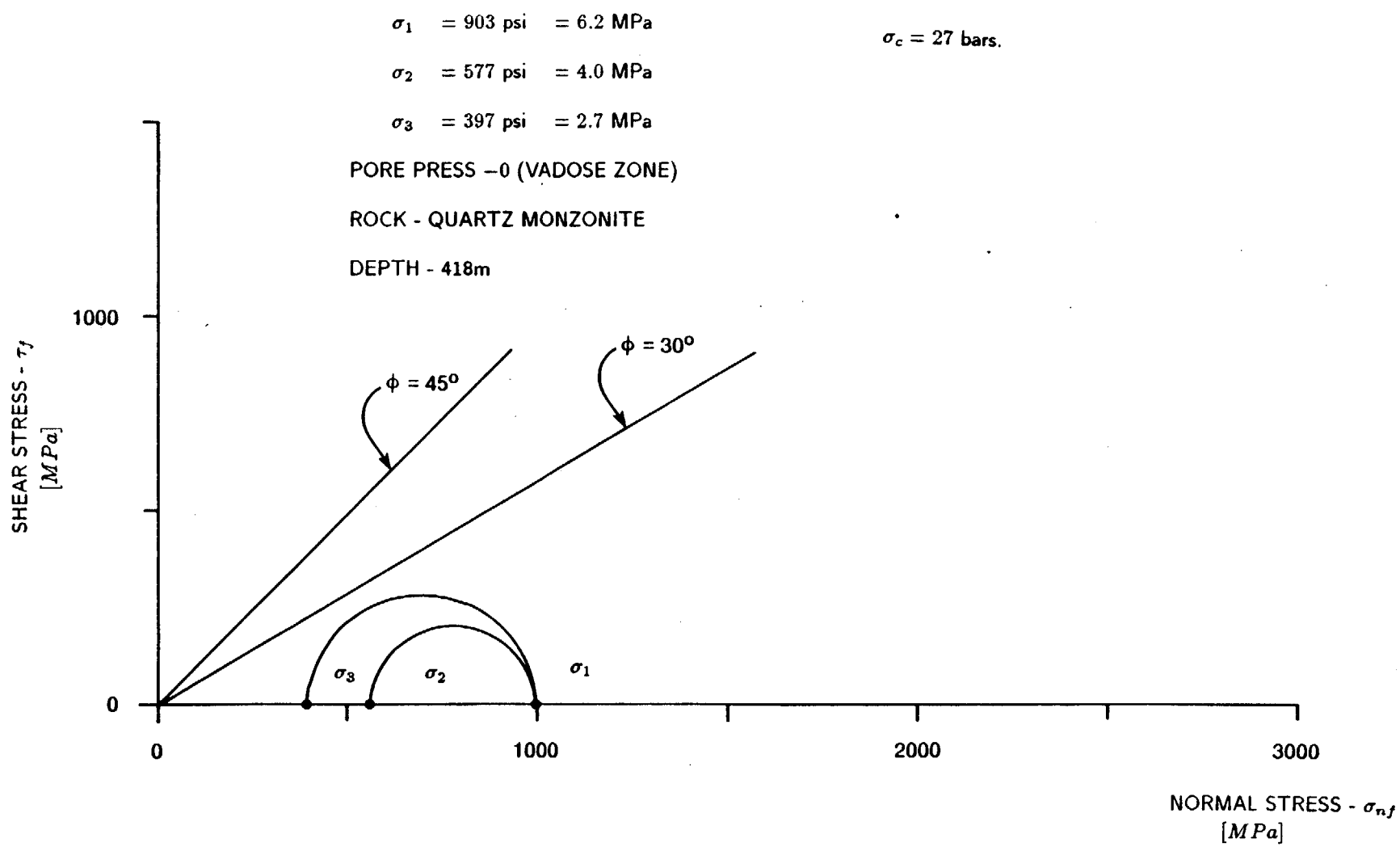

Mohr representation of in situ stress. Spent fuel test facility. Borehole ISS-8, borehole depth 96.7 feet. Climax Stock.

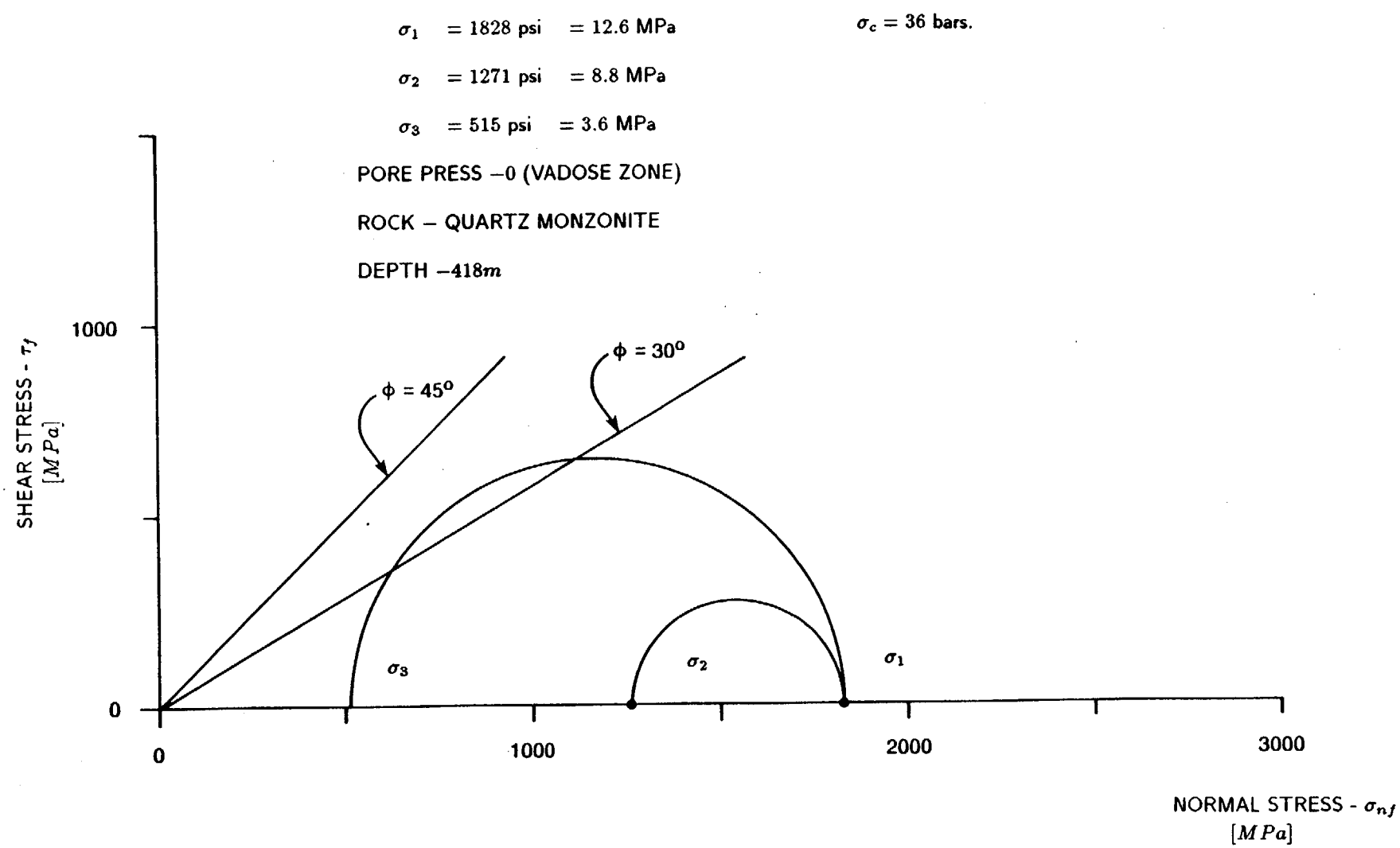

Mohr representation of in situ stress. Spent fuel test facility. Borehole ISS-8, borehole depth 109.4 feet. Climax Stock.

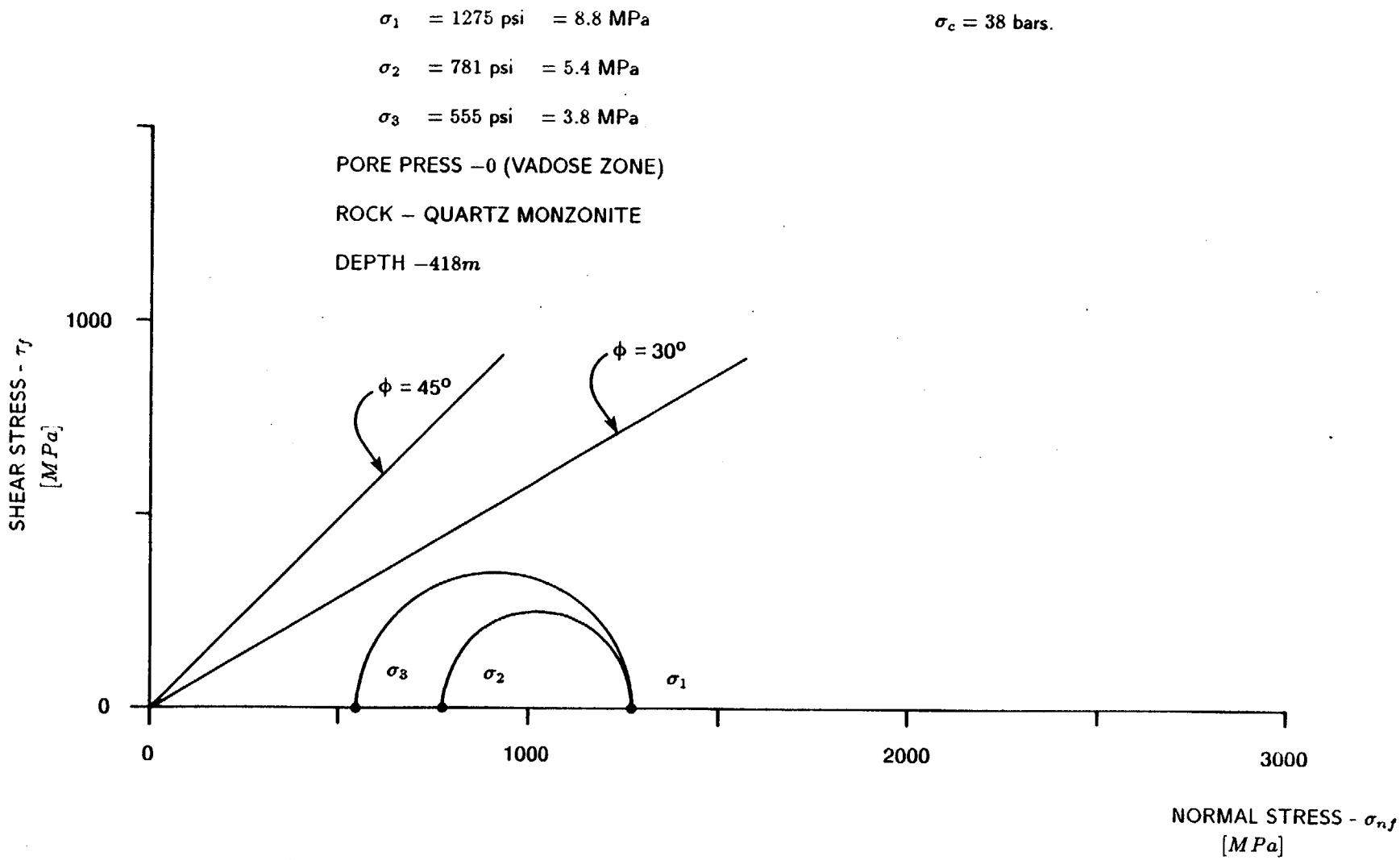

Mohr representation of in situ stress. Spent fuel test facility. Borehole ISS-9, borehole depth 39.1 feet. Climax Stock.

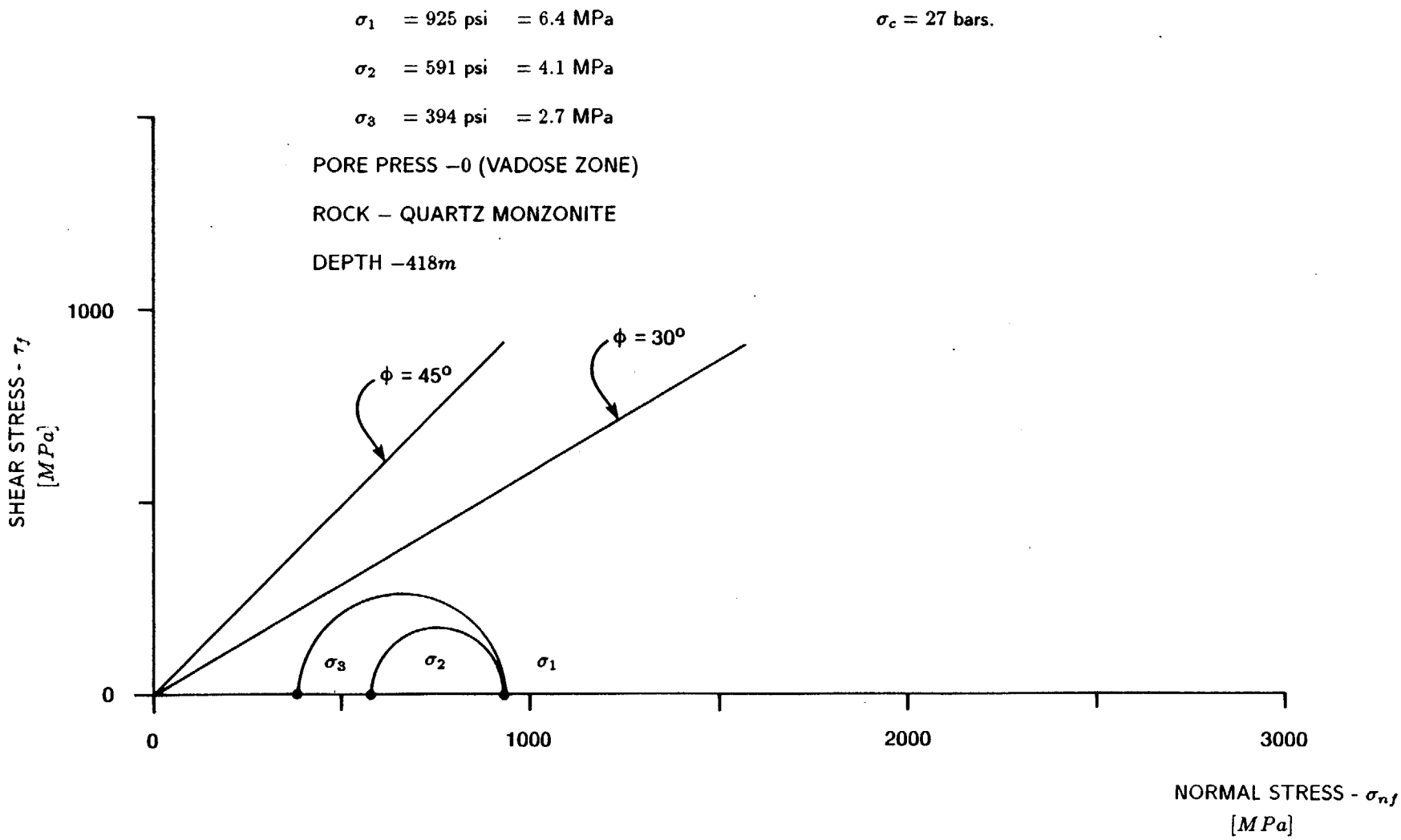

Mohr representation of in situ stress. Spent fuel test facility. Borehole ISS-9, borehole depth 42.6 feet. Climax Stock.

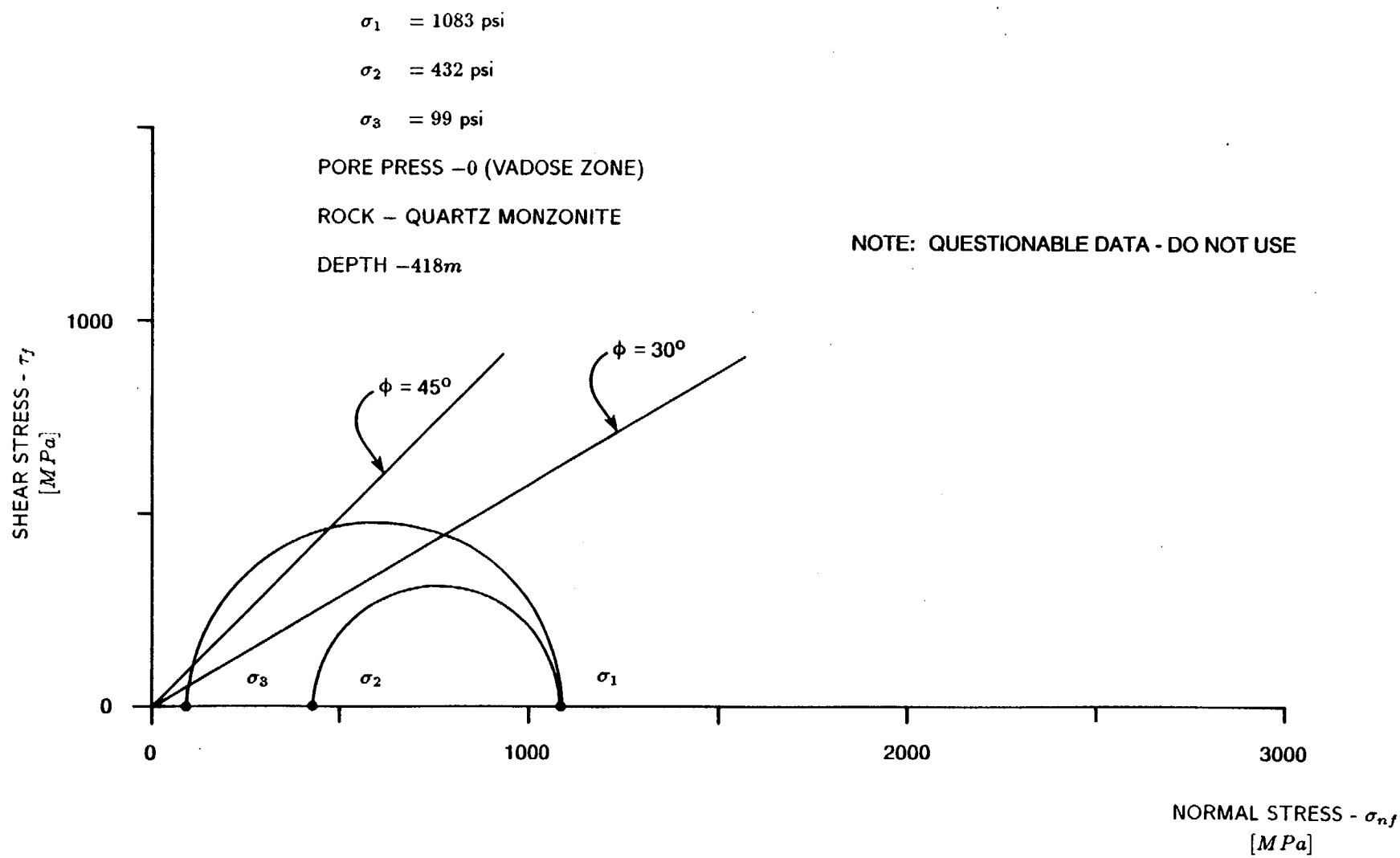

Mohr representation of in situ stress. Spent fuel test facility. Borehole ISS-9, borehole depth 46.9 feet. Climax Stock.

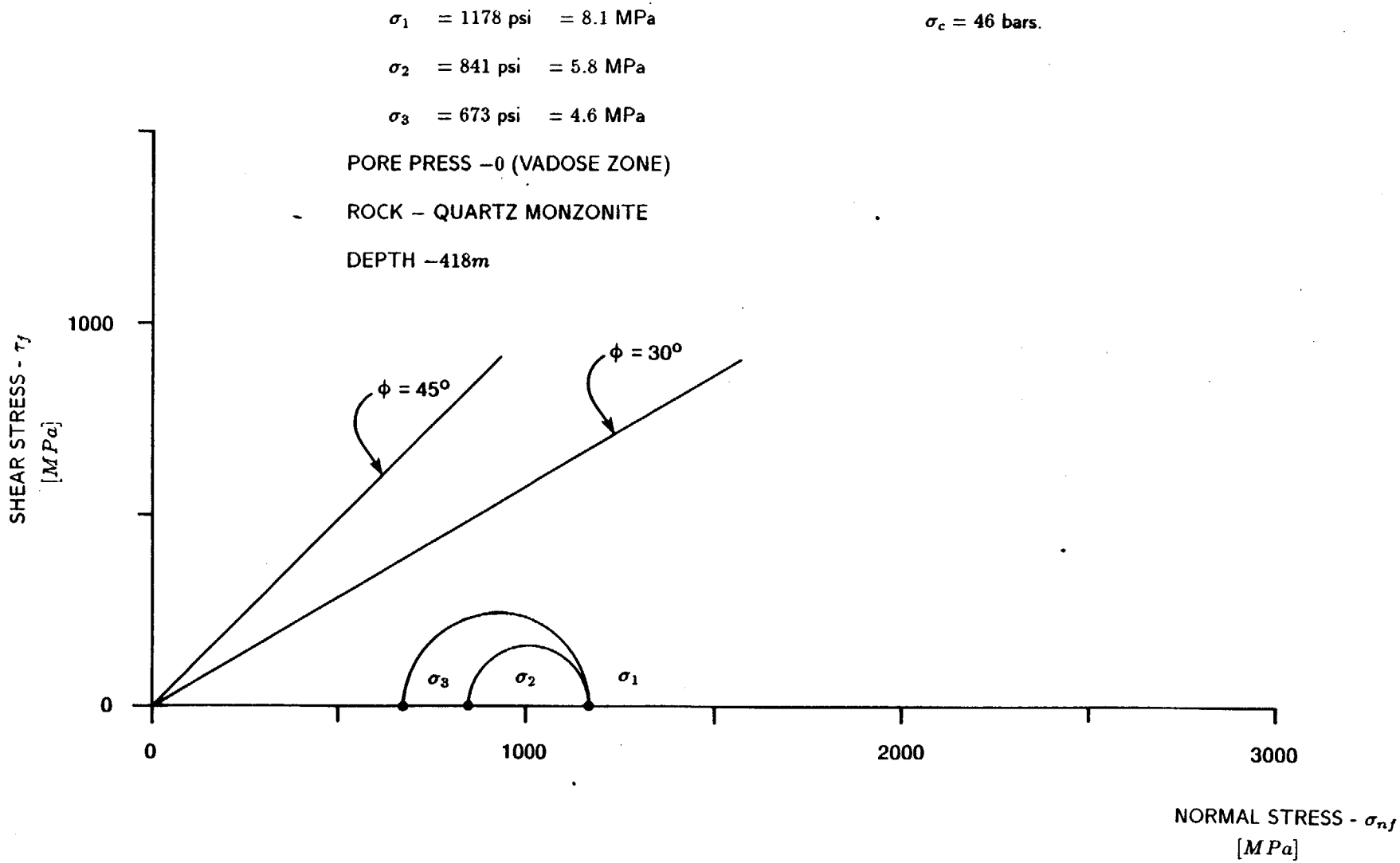

Mohr representation of in situ stress. Spent fuel test facility. Borehole ISS-9, borehole depth 50.5 feet. Climax Stock.

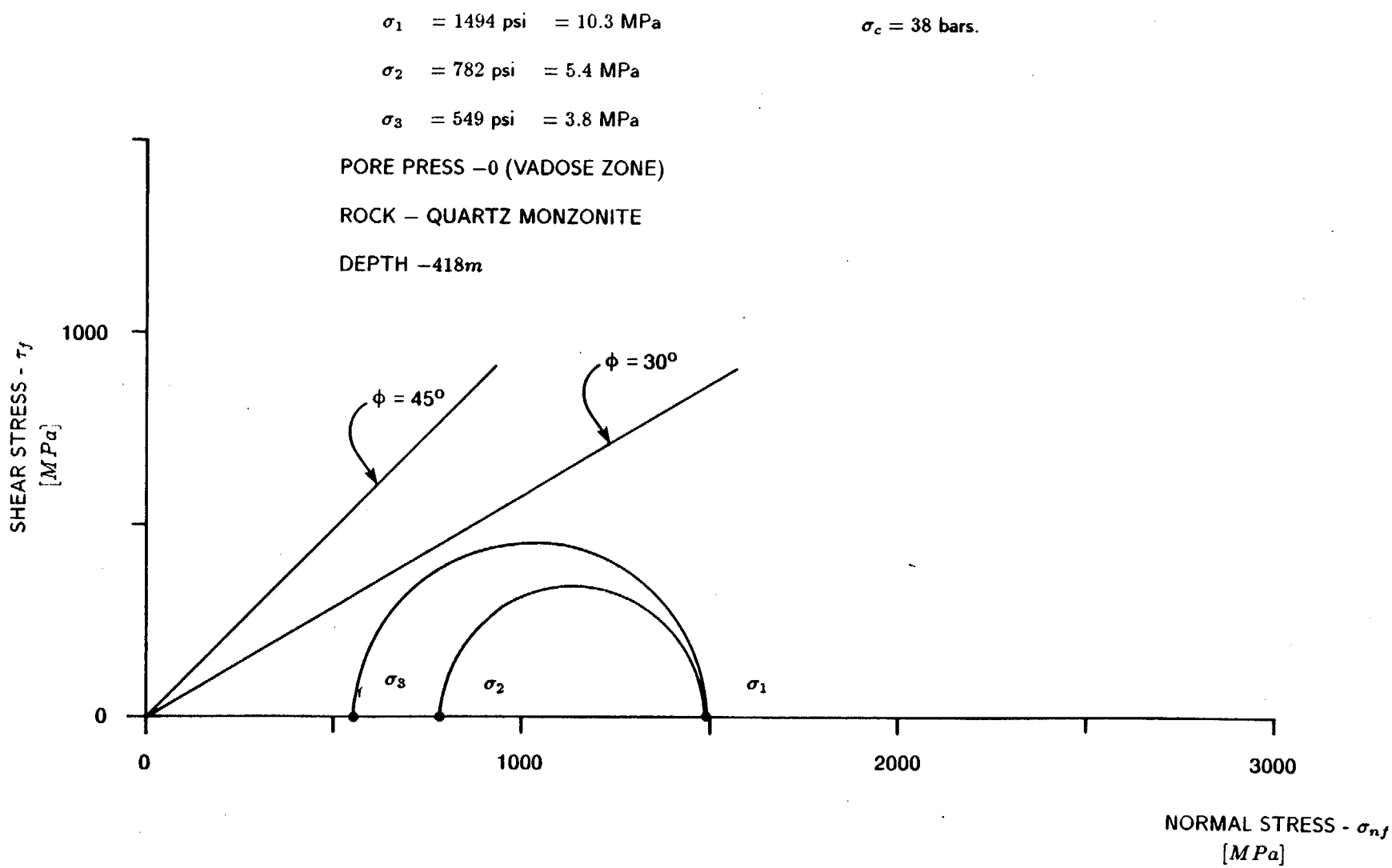

Mohr representation of in situ stress. Spent fuel test facility. Borehole ISS-9, borehole depth 59.2 feet. Climax Stock.

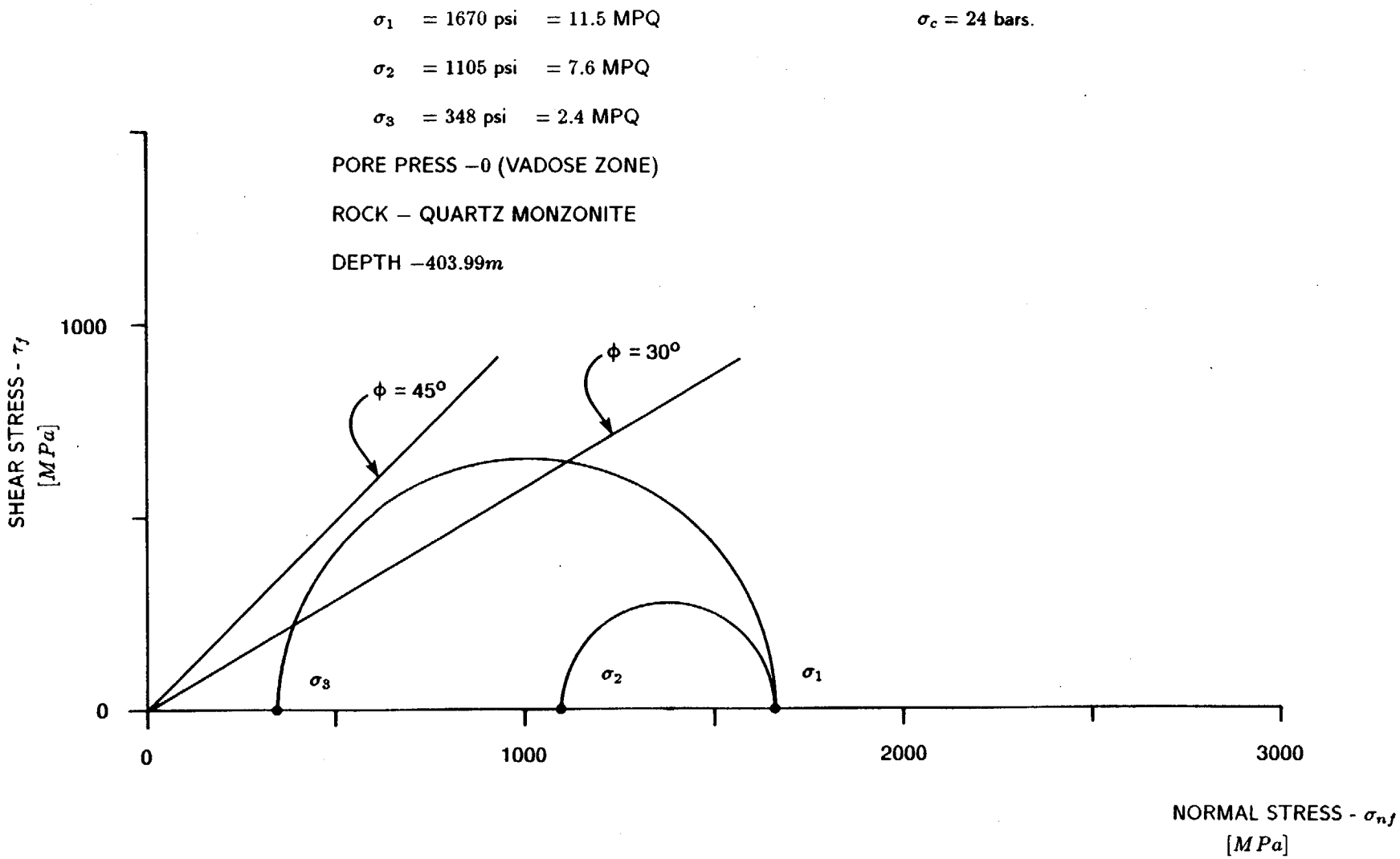

Mohr representation of in situ stress. Spent fuel test facility. Borehole ISS-10, borehole depth 64.4 feet. Climax Stock.

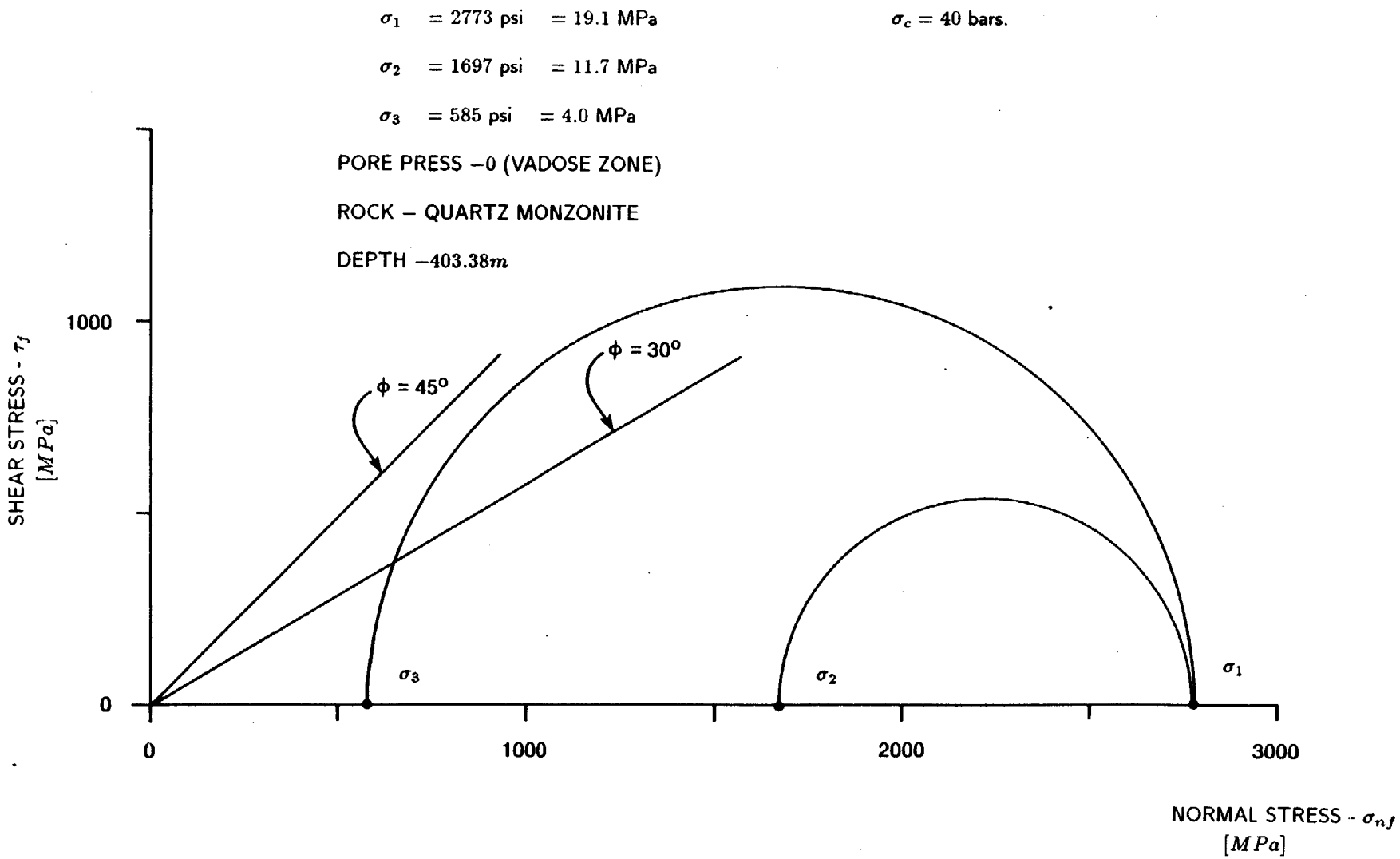

Mohr representation of in situ stress. Spent fuel test facility. Borehole ISS-10, borehole depth 67.8 feet. Climax Stock.

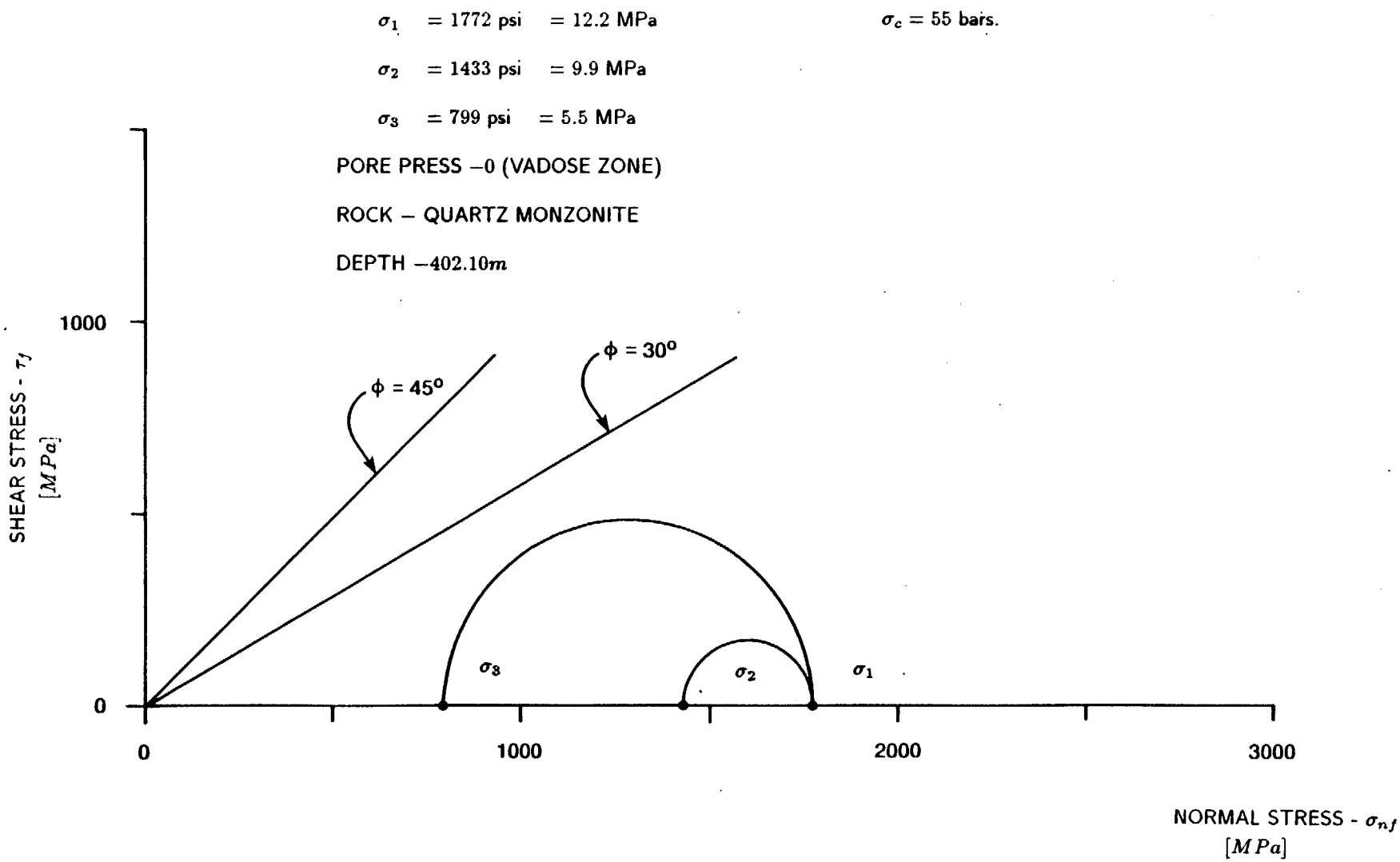

Mohr representation of in situ stress. Spent fuel test facility. Borehole ISS-10, borehole depth 73.1 feet. Climax Stock.

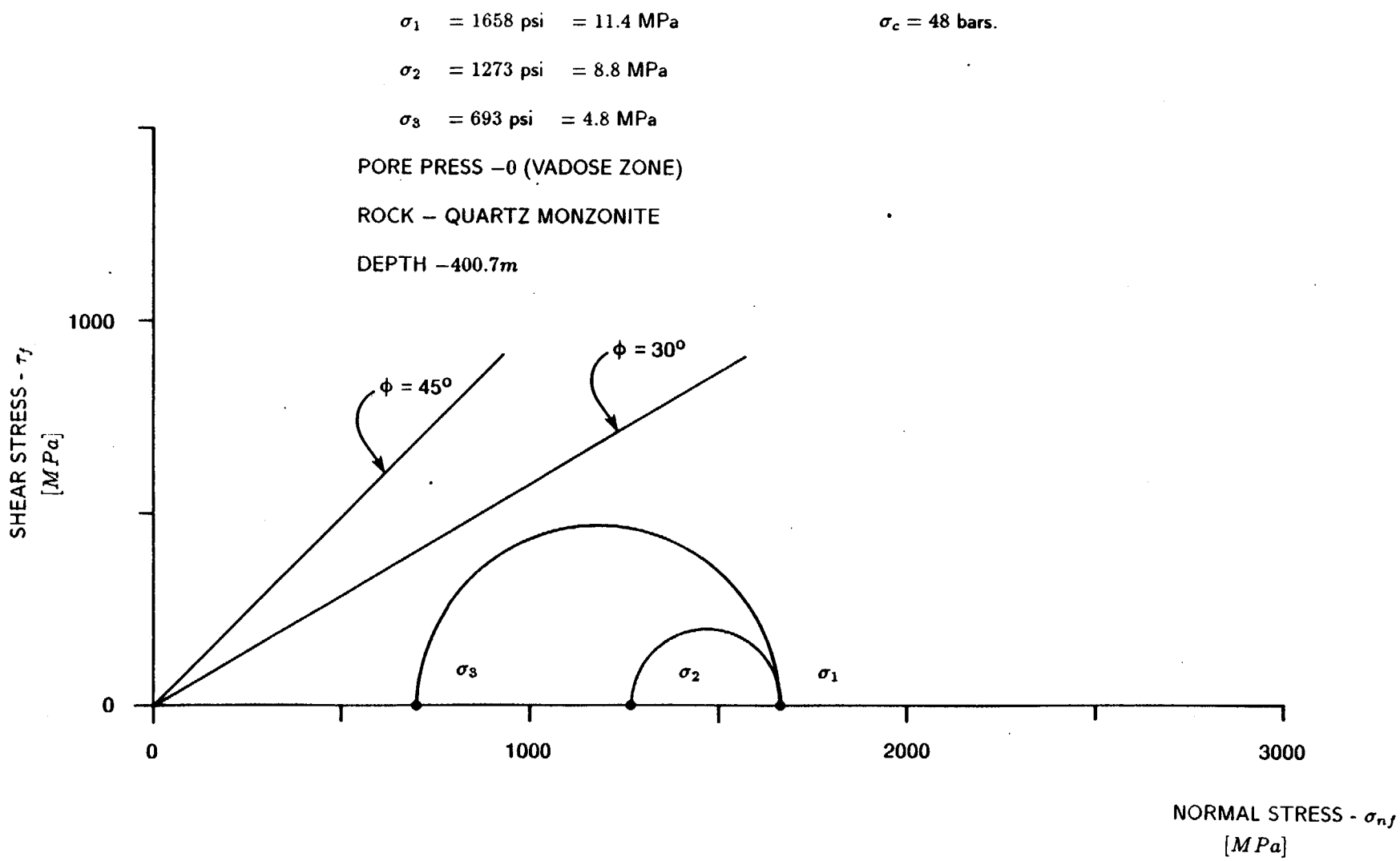

Mohr representation of in situ stress. Spent fuel test facility. Borehole ISS-10, borehole depth 80.4 feet. Climax Stock.

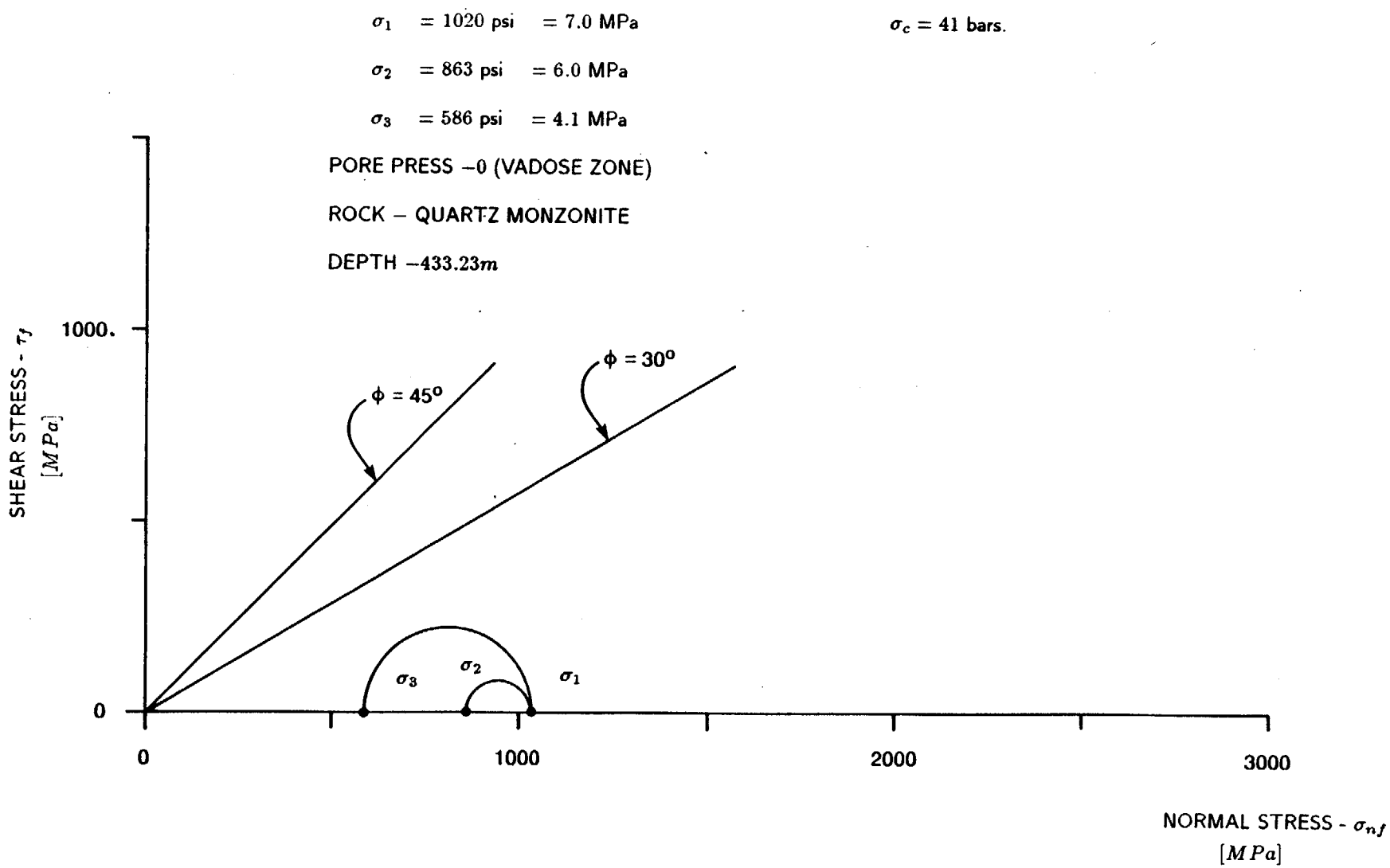

Mohr representation of in situ stress. Spent fuel test facility. Borehole ISS-11, borehole depth 70.6 feet. Climax Stock.

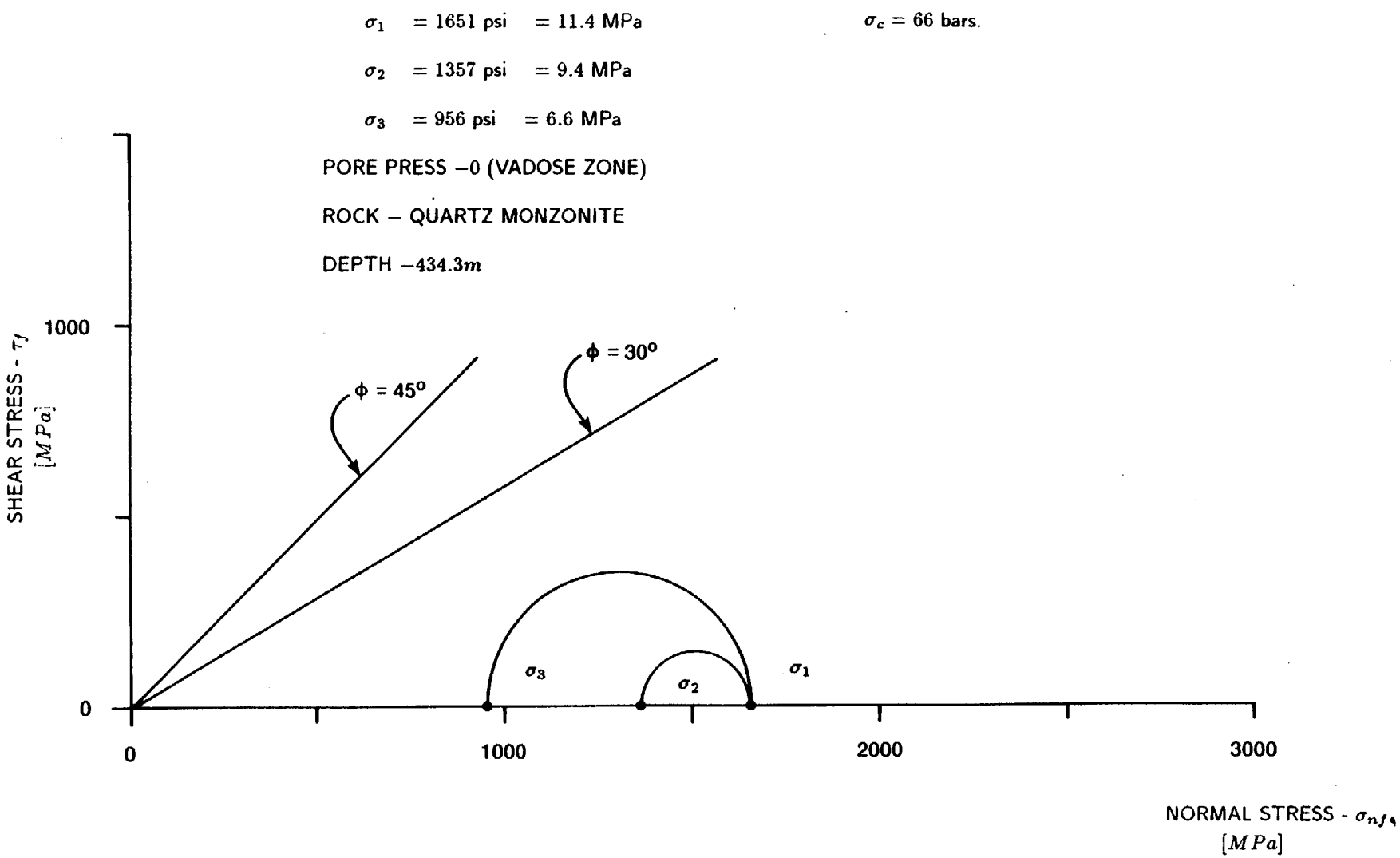

Mohr representation of in situ stress. Spent fuel test facility. Borehole ISS-11, borehole depth 75.5 feet. Climax Stock.

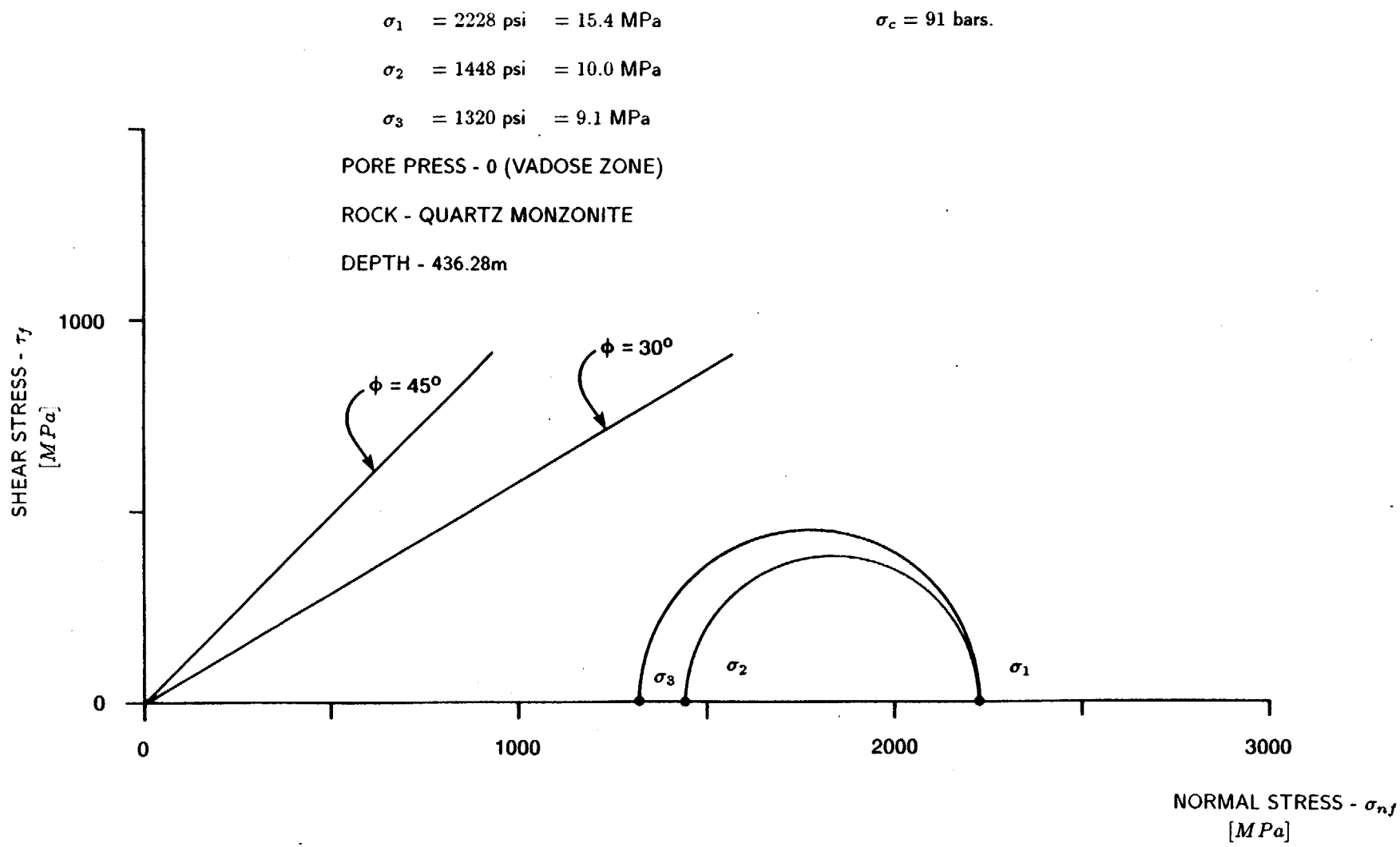

Mohr representation of in situ stress. Spent fuel test facility. Borehole ISS-11, borehole depth 84.3 feet. Climax Stock.

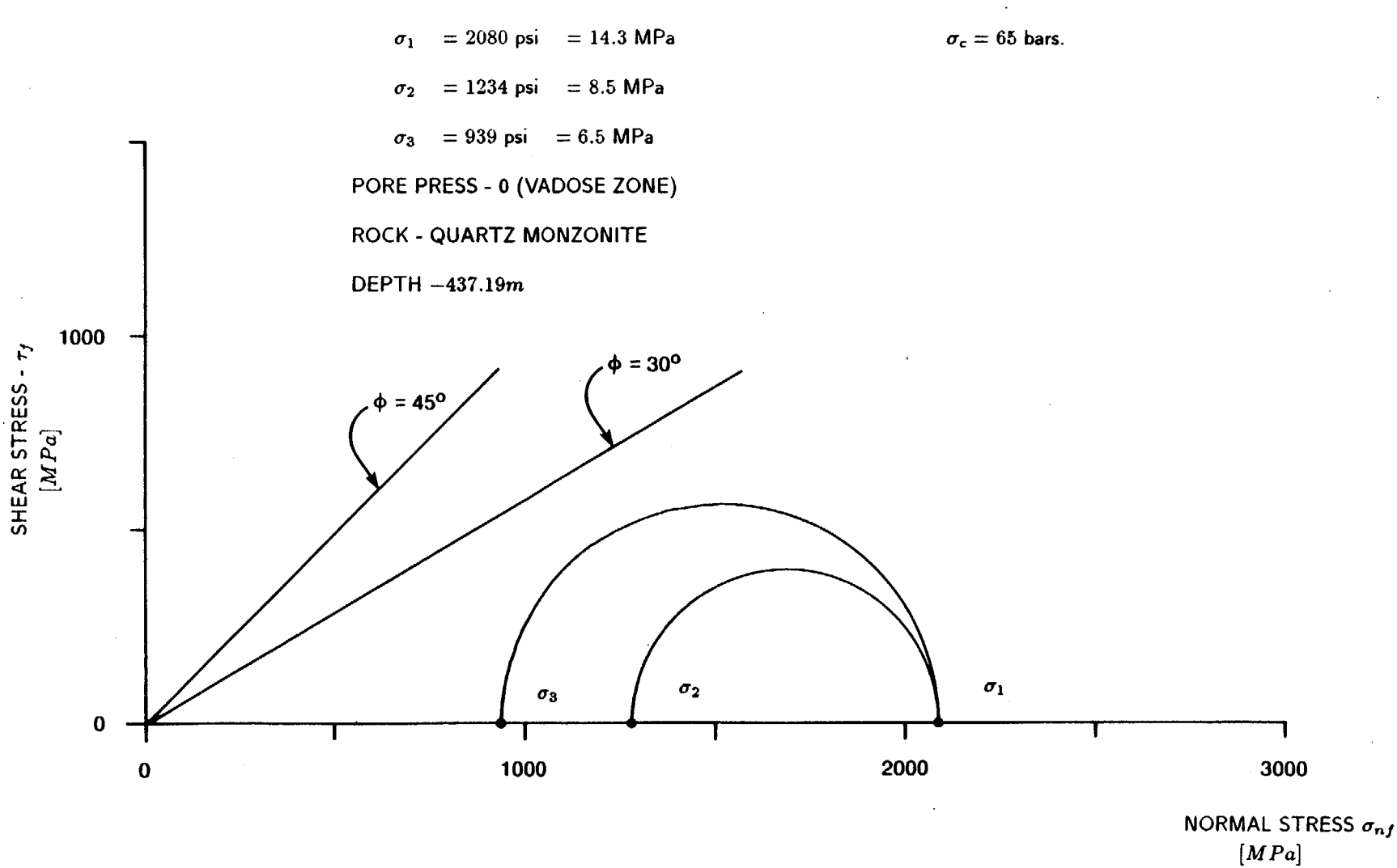

Mohr representation of in situ stress. Spent fuel test facility. Borehole ISS-11, borehole depth 89.4 feet. Climax Stock.

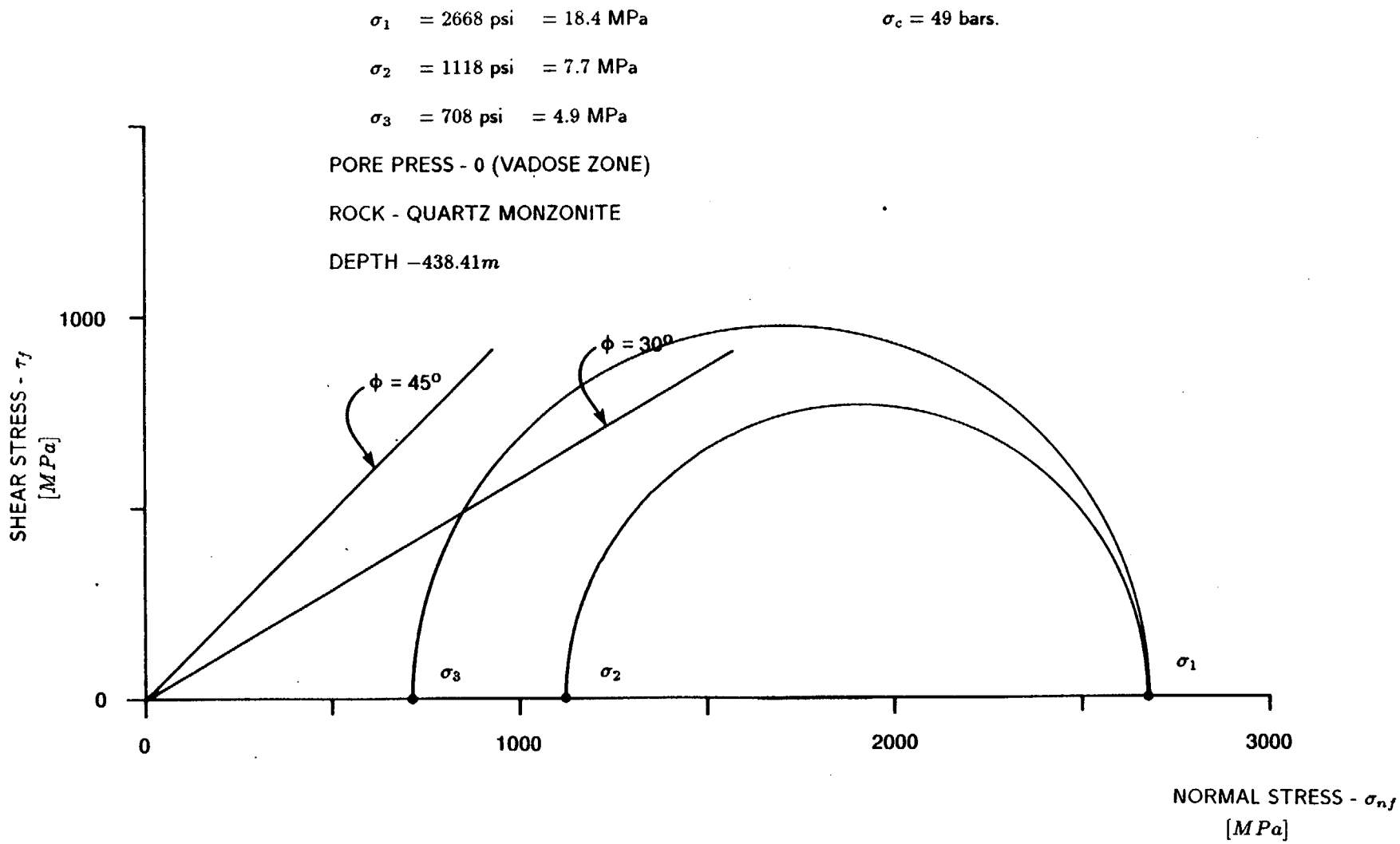

Mohr representation of in situ stress. Spent fuel test facility. Borehole ISS-11, borehole depth 94.5 feet. Climax Stock.

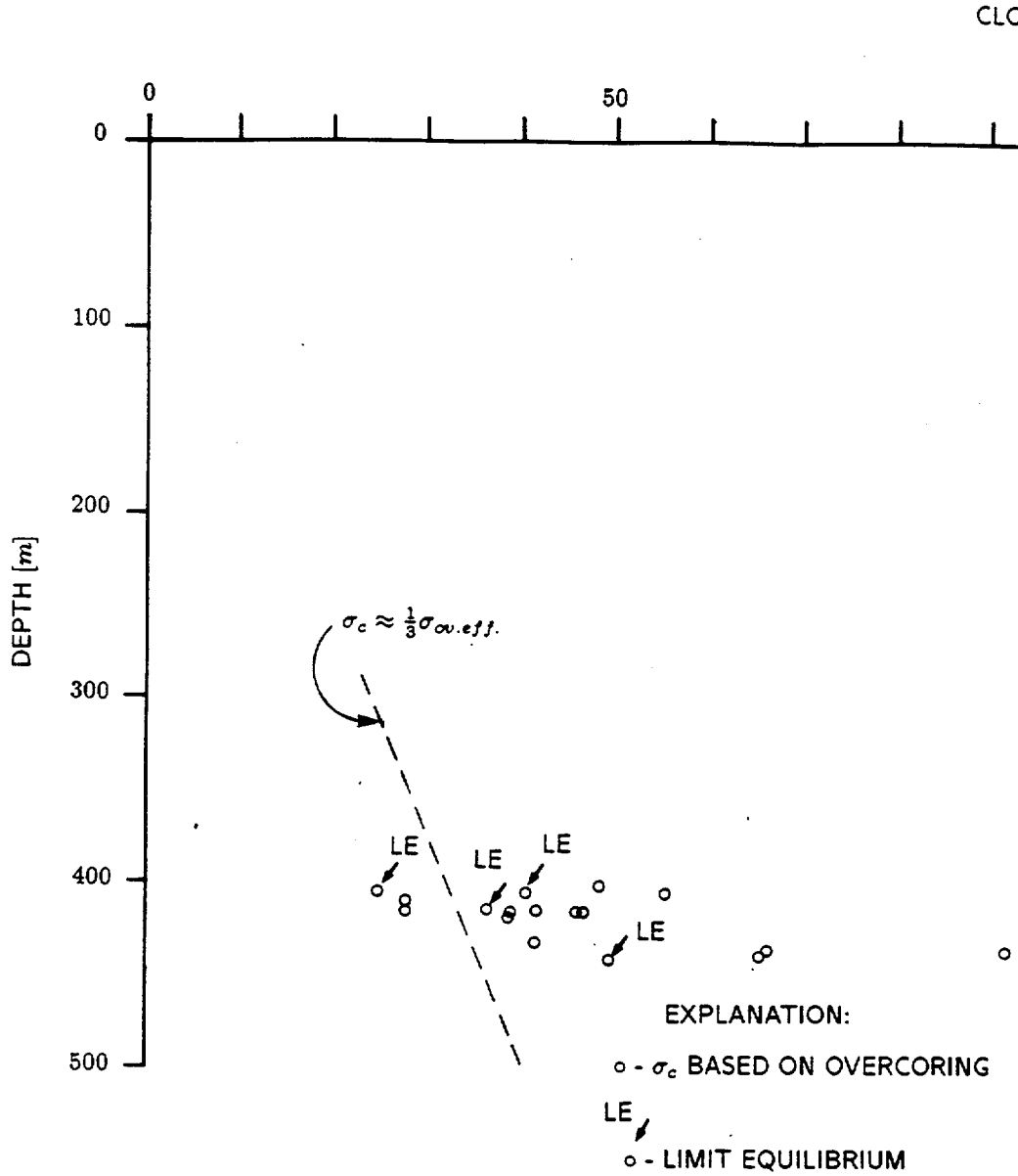

Hole	Depth	σ c	Stress Conditions
ISS - 8	418	45	nLE
- 8	418	41	nLE
- 8	418	27	nLE
- 8	418	36	LE
ISS - 9	418	38	nLE
- 9	418	27	nLE
- 9	418	46	nLE
- 9	418	38	nLE
ISS - 10	404	24	LE
- 10	403.4	40	LE
- 10	402.1	55	nLE
- 10	400.7	48	nLE
ISS - 11	433.2	41	nLE
- 11	434.3	66	nLE
- 11	436.3	91	nLE
- 11	437.2	65	nLE
- 11	438.4	49	LE

R.S.C

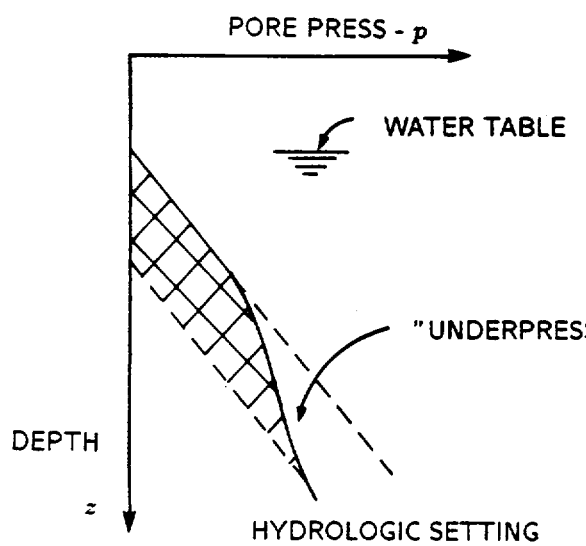

NOTE:

LIMIT EQUILIBRIUM IN-SITU STRESS CONDITIONS OCCUR FOR WIDE RANGE OF CLOSURE PRESSURE (σ_c — 24-49 bars). IT IS LIKELY THAT, WITH EXCEPTION OF BOREHOLE ISS-10 AT 404m, THESE CONDITIONS ARE CAUSED BY "REMNANT" STRESS CONCENTRATIONS IN ROCKS WITH VERY HIGH STIFFENESS

State of in situ stress. Summary. Climax Stock.